Investigating the Functional and Metabolic Role of Carnitine in the Diabetic Heart using Hyperpolarized MRI



Dragana Savic

Linacre College

Department of Physiology Anatomy & Genetics

University of Oxford

A thesis submitted for the degree of

Doctor of Philosophy

Michaelmas 2018

This thesis is dedicated to my family,
Mirjana, Ranko and Tamara Savic.
Volim Vas.

Imagination is more important than knowledge.
Knowledge is limited.
Imagination encircles the world.
- Albert Einstein

Acknowledgements

Though this is an individual Doctoral Thesis, a piece of work like this, it can never be completed without the help, support and guidance of many people, for which I am forever grateful.

First and foremost, I would like to give my sincerest thanks to Professor **Damian J. Tyler** for welcoming me to his research group and opening the door to a lot of amazing opportunities. I have treasured our meetings, where he shared his extensive knowledge and insight. He always supported me and trusted my judgement, allowing me to grow and improve on my abilities. I am profoundly grateful and hope we continue our collaborations for many more years.

I would also like to thank my co-supervisor Associate Professor **Lisa C. Heather** who has supported and taught me everything about metabolism throughout my studies. She has a unique abilities to make any topic fascinating, and I am deeply grateful that she was my co-supervisor.

A special thank you goes to Professor **Kieran Clarke** who has been my role-model, and who has always been available for questions and great advice whether it was for my thesis or my entrepreneurial ventures. She has always inspired me.

I am grateful to have been working together with all the outstanding researchers and colleagues at CMRG. They have made my past three years fly by a bit too fast. **Vicky Ball** has been a tremendous help and great support to me for the past three years, she has helped me during hard times and been there for the good, and I could not have done this without her. **Kate Curtis** and **Kerstin Timm** were always ready to help me when I was in need, and for that, I am very grateful. I would also like to thank Professor **Carolyn Carr**, who has helped me with scanning when nobody was around, and who was a great support throughout. I feel privileged to have had the honour to work with and learn from **Jack Miller**. His patience, willingness to help every single person in our laboratory (including me), and his kind heart will evermore be inspiring. **Michael Dodd** has taught me a lot throughout the past couple of years, and I feel lucky to have had his support, expertise and inputs.

A big thank you goes to everyone else in the laboratory who have made coming to work every day, fun; **Yvonne Green**, **Nicola Dixon**, **Cher-Rin Chong**, **Brianna Stubbs**, **Lucia Giles**, **Angus Lau**, **Justin Lau**, **David Dearlove**,

Andy Lewis, **Anna James-Bott**, **Lorenz Holzner**, **Claudia M. Aparicio**, **Javier G. Jaramillo**, **Adrian Soto-Mota**, **Heba Al-Siddiqi**, **Rita Alonaizan**, **Azrul Kadir**, and **Tony Zhou**, their help and support have been invaluable. A very special thanks go to my friends from the laboratory with whom I have made a bond that will last for a very long time. Their friendship, support and encouragement have made me feel very lucky. A sincerest thank you goes to **Sophia Malandraki-Miller**, **Colleen Lopez**, **Maria da Luz Sousa Fialho**, and **Matthew Kerr** for making hard work feel like a piece of cake. Being surrounded by intelligent, creative, compassionate and fun friends, have made three years feel like a few months.

I would also like to express my deepest gratitude to Dr. **Maria Rohm** with whom I enjoyed working with, and Professor **Frances Ashcroft**, who gave me the opportunity to undertake great work on her K_{ATP} mouse model together with Maria. A special thanks goes to Professor **Jules Griffin**, Dr. **James West** and Dr. **David Hauton** for their kind help and support with metabolomics.

I also feel highly privileged to have worked with great staff at the BSB; **Carol**, **Debbie**, **Courtney**, **Nick**, and **Lee**. Without their professional and productive work ethic, I could not have done the work I did.

My deepest appreciation goes out to collaborators and friends all over the world and of course my funding body DNP-Life from the Danish Council for Strategic Research. A special thanks goes to Professor **Stødkilde-Jørgensen**, Dr. **Laustsen** and of course Professor **Jan Henrik Ardenkjær-Larsen** for the great meetings and valuable inputs throughout the years. I would never have started a doctorate had it not been for Professor **Stuart Campbell** at Yale University who believed in me and Assistant Professor **Andrea Kwaczala** and Dr. **Yasser Aboelkassem** who have taught, inspired and encouraged me. I also want to express my deepest gratitude, and a huge thank you to Professor **Sharmila Majumdar**, Dr. **Rahul Prasad**, and Professor **Dan Vigneron** who opened up their door for me in San Francisco and who always included and inspired me! They have an exceptional ability to draw the best from people, and I would like to recognise how important they individually have been in my career! And a warm thank you goes to my friends all over the world.

Finally my greatest and warmest gratitude goes to my sister **Tamara Savic** and my parents **Mirjana** & **Ranko Savic** for being the greatest support one could ask for. I love you!

Abstract

Diabetes increases the incidence of myocardial infarction and heart failure, which are leading causes of mortality in diabetic patients. L-carnitine levels are decreased in the plasma of diabetic patients and L-carnitine supplementation has been shown to have protective effects. L-carnitine transports fatty acids into the mitochondria allowing for subsequent β-oxidation, but it can also export acetyl-CoA from the mitochondria through acetylcarnitine and thereby relieve PDH-flux.

The aim of this thesis was to explore the effects of modulating L-carnitine levels on *in vivo* metabolism and function in the diabetic heart. Hyperpolarized MRI was used to assess metabolism, while CINE MRI was used for the assessment of cardiac function. A Langendorff method was used to determine the *ex vivo* effect of L-carnitine on functional recovery post-ischemia.

Different diabetic models were initially investigated to find the most appropriate model in which to modulate L-carnitine levels. A neonatal model of diabetes showed decreased aerobic to anaerobic metabolism (50 %) in conjunction with functional impairment, which could be reversed with Glibenclamide treatment. A fasted streptozotocin induced rat model showed superior SNR on MRI and was pursued further. PDH-flux and alanine metabolism were decreased (>60%) with diabetes which coincided with functional impairments. Sustained hyperglycaemia for four weeks led to an elevation in lactate and alanine (>140 %), while also elevating stroke volume.

L-carnitine treatment (3 g/kg/day, i.p.) elevated acetylcarnitine (AC) levels (219 %) and slowed down the progression of hyperglycaemia in diabetes, while elevating PDH-flux (51 %), allowing for improved diastolic function (16 %) *in vivo*, and improved functional recovery post-ischemia *ex vivo* (270 %). However detrimental effects were observed in control animals treated with L-carnitine.

Daily Mildronate treatment, which inhibits L-carnitine uptake, reduced AC levels (52 %) and elevated PDH-flux (214 %) in the diabetics. These metabolic changes were not accompanied by functional changes. However, improved *ex vivo* functional recovery post-ischemia (34 %) was observed, but did not reach the level of recovery that L-carnitine had on the *ex vivo* heart.

This work has clarified that the use of L-carnitine treatment in diabetes can enhance carbohydrate metabolism and is more beneficial than decreasing L-carnitine levels with Mildronate. This work has shown the potential for using hyperpolarized and CINE MRI in better understanding the mechanism of L-carnitine's effect on the diabetic heart, and it may provide new insights into novel therapeutics.

Research Outcomes

Part of the work in **Chapter 3** regarding the neonatal genetic mouse model was published in April 2018 as "Cardiac Dysfunction and Metabolic Inflexibility in a Mouse Model of Diabetes without Dyslipidemia" *M. Rohm, **D. Savic**, V. Ball, M. K. Curtis, S. Bonham, R. Fischer, N. Legrave, J. I. MacRae, D. J. Tyler and F. M. Ashcroft* in the Journal of Diabetes.

Five abstracts were presented from Chapter 3 at conferences:

- "Type 1 Diabetic Hearts show Unexpected Biphasic Metabolic and Functional Progression as Evaluated with Hyperpolarised [1-13C]Pyruvate and CINE MR." ***D. Savic**, V. Ball, C. Carr, L. Heather, & D. Tyler.* International Society for Magnetic Resonance in Medicine (ISMRM), Hawaii, USA 2017.
- "Temporal Effects of STZ Induced Diabetes on Cardiac Metabolism and Function using Hyperpolarized 13C MRS and CINE MRI."***D. Savic**, V. Ball, C. Carr, L. Heather & D. Tyler.* Diabetes. Manchester, UK 2017.
- "Temporal Effects of Type 1 Diabetes on Cardiac Metabolism and Function using Hyperpolarized 13C MRS." ***D. Savic**, V. Ball, L. Heather & D. Tyler.* British Heart Foundation Centre of Research Excellence (BHF CRE) Annual Research Symposium. Oxford, UK 2016.
- "Assessment of the Progression of Type 1 Diabetes on Cardiac Metabolism and Function: A Hyperpolarized 13C MRS and CINE MRI Study. "***D. Savic**, V. Ball, L. Heather and D. Tyler.* British Chapter International Society for Magnetic Resonance in Medicine (BC-ISMRM), Leeds, UK 2016. Accepted as an oral presentation.
- "The Effects of Type 1 Diabetes Progression on Cardiac Metabolism and Function Assessed with Hyperpolarized 13C MRS and CINE MRI. "***D. Savic**, V. Ball, C. Carr, L. Heather & D. Tyler.* 2nd year DPhil day, Oxford, UK 2016.

Six abstracts were presented from Chapter 5 at conferences:

- "L-carnitine show Beneficial Effects on Cardiac Metabolism and Function: A Hyperpolarized MRS and Langendorff Perfusion Study." ***D. Savic**, V. Ball, K. Timm, L. Heather & D. Tyler.* ISMRM, Paris, France 2018. Selected for a prestigious oral power pitch.
- "Effects of Carnitine Supplementation in the Type 1 Diabetic Heart: an In Vivo Hyperpolarized MRS Study." ***D. Savic**, K. Timm, V. Ball, L. Heather, and D. Tyler.* British Society for Cardiovascular Research (BSCR), Oxford, UK 2017.

- "Improved Cardiac Pyruvate Metabolism with Carnitine Supplementation in the Type 1 Diabetic Heart: an In Vivo Hyperpolarized MRS Study." ***D. Savic****, K. N. Timm, V. Ball, L. Heather, and D. Tyler.* Society for Heart and Vascular Metabolism (SHVM), Weimar, Germany 2017.
- "In Vivo Hyperpolarized MRS Study Showing Improved Cardiac Metabolism in Type 1 Diabetes with Daily L-Carnitine Treatment." ***D. Savic****, K. Timm, V. Ball, L. Heather, and D. Tyler.*, ISMRM, Hawaii, USA 2017. Selected for a prestigious oral power pitch.
- "In Vivo Hyperpolarized MRS Study Showing Improved Cardiac Metabolism in Type 1 Diabetes with Daily L-Carnitine Treatment." ***D. Savic****, K. Timm, V. Ball, L. Heather, and D. Tyler.* ISMRM, Hawaii, USA 2017.
- "Effect of Carnitine Supplementation on Cardiac Function and Metabolism Assessed using CINE MRI and Hyperpolarised MRS." ***D. Savic****, V. Ball, L. Heather and D. Tyler.* British society for Cardiovascular Research (BSCR), Leeds, UK 2016.

One abstract was presented from Chapter 6 at ISMRM 2018:

- "In Vivo Hyperpolarized MRI Reveal Metabolic Changes Following Treatment with Mildronate in the Control and Diabetic Heart." ***D. Savic****, L. Holzner, V. Ball, K. Curtis, L. Heather & D. Tyler.* ISMRM, Paris, France 2018.

D. Savic received, in addition, a number of relevant awards and prizes:

- Winner of Magna Cum Laude Award for abstract "L-carnitine show Beneficial Effects on Cardiac Metabolism and Function: A Hyperpolarized MRS and Langendorff Perfusion Study." ISMRM, Paris, France 2018.
- Winner of the 2016 British Chapter Prize for *in vivo* MRI and MRS for outstanding research.
- Runner-up winner for Department of Physiology, Anatomy and genetics (DPAG) poster day: "A year of progress". Oxford, UK.
- 1st place for the hyperpolarization methods and equipment for targeting biological mechanisms study group abstract award
- Finalist at EIT Health Transition fellowship 2017
- Finalist at EIT Health Transition fellowship 2018

Contents

List of Figures **xix**

List of Abbreviations **xxiii**

1 Introduction **1**

1.1 Overview and Motivation 1
1.2 Diabetes and Cardiovascular Disease 3
1.3 Metabolism in the Healthy Heart 6
1.4 Metabolism in the Diabetic Heart 11
1.5 L-Carnitine in the Healthy Heart 12
1.6 L-Carnitine in the Diseased Heart 15
1.7 Cardiac Effects of Mildronate: Lowering L-Carnitine Levels 20
1.8 Technologies for Cardiac Assessment 22
1.8.1 Echocardiography 22
1.8.2 Computed Tomography (CT) 23
1.8.3 Positron Emission Tomography (PET) 23
1.8.4 Magnetic Resonance Imaging (MRI) 24
1.8.4.1 A Brief Introduction to MRI 25
1.8.4.2 A Brief Introduction to MR Spectroscopy (MRS) . 28
1.8.5 Cardiac MR Spectroscopy (MRS) 29
1.8.6 A Brief Introduction to Dynamic Nuclear Polarisation 30
1.8.7 Hyperpolarized ^{13}C MRS using Dynamic Nuclear Polarisation 33
1.9 Aims 35
1.9.1 Summary of Chapters 37

2 General Methods **39**

2.1 Animal Protocol 40
2.2 Induction of Diabetes using Streptozotocin 40
2.3 Reagents 41
2.4 Imaging Technologies 41
2.4.1 CINE MRI for Assessment of Cardiac Structure and Function in the Rat 41

2.4.1.1 Analysis of CINE MRI 43
2.4.2 CINE MRI for Assessment of Cardiac Structure and Function in the Mouse 45
2.4.3 Hyperpolarized ^{13}C MRS for Assessment of Cardiac *In Vivo* Metabolism 45
2.4.4 Echocardiography for Assessment of Cardiac Function . . . 49
2.5 Langendorff Perfusions 49
2.5.1 Krebs-Henseleit and Albumin Buffer Preparation 49
2.5.2 Palmitate Stock Preparation 50
2.5.3 Radioactive ^{3}H Palmitate Albumin Krebs-Henseleit Buffer Preparation 51
2.5.4 Langendorff Ischemia Reperfusion Protocol 51
2.5.5 Assessment of Cardiac Function 54
2.5.6 Measurement of Myocardial Palmitate Oxidation 55
2.6 Tissue Collection 57
2.7 Extractions for Metabolomics 57
2.8 Blood Analysis 58
2.9 Biochemical Analysis 58
2.9.1 Non-Esterified Fatty Acid Assay 58
2.9.2 Insulin ELISAs 59
2.9.3 L-Carnitine ELISAs 59
2.9.4 Western Blotting 60
2.10 Statistical Analysis 61

3 Functional and Metabolic Characterisation of the Diabetic Heart 63
3.1 Chapter Overview 64
3.2 Background 65
3.3 Neonatal Diabetes Mellitus (NDM) 66
3.3.1 Mouse Model of NDM 68
3.4 Streptozotocin (STZ)-Induced Type 1 Diabetes 69
3.5 Progression of Diabetes and Early Metabolic Changes 70
3.6 Chapter Aims 70
3.7 Methods 71
3.7.1 Mouse Model of Neonatal Diabetes Mellitus (NDM) 71
3.7.2 Establishing an Appropriate Model of STZ-Induced Type 1 Diabetes 72
3.7.3 Statistical Analysis 74
3.8 Results 74
3.8.1 Cardiac Metabolism and Function in a Mouse Model of NDM 74

3.8.1.1 Group 1: Reversibility of NDM with Glibenclamide 74
3.8.1.2 Group 2: Progression of NDM 78
3.8.2 Cardiac Metabolism and Function in STZ-Induced Models of Type 1 Diabetes 80
3.8.2.1 Weight and Blood Profile 80
3.8.2.2 Cardiac *In Vivo* Function 83
3.8.2.3 Cardiac *In Vivo* Metabolism 85
3.8.3 Exploration of the Temporal Effects of STZ-Induced Diabetes on Cardiac Metabolism and Function using Hyperpolarized ^{13}C MRS and CINE MRI 87
3.8.3.1 Blood Profile 87
3.8.3.2 Cardiac *In Vivo* Function 88
3.8.3.3 Cardiac *In Vivo* Metabolism 91
3.9 Discussion 94
3.9.1 Cardiac Metabolism and Function in a Mouse Model of NDM 94
3.9.2 Cardiac Metabolism and Function in STZ-Induced Models of Type 1 Diabetes 96
3.9.2.1 Weight and Blood Profile 96
3.9.2.2 Cardiac *In Vivo* Metabolism and Function 97
3.9.3 Temporal Effects of STZ-Induced Diabetes on Cardiac Metabolism and Function 98
3.9.4 Conclusion and Future Perspective 99

4 Feasibility Studies: Establishing Therapeutic Effects on Metabolism and Function in Healthy Hearts 101
4.1 Chapter Overview 102
4.2 Background 102
4.3 Chapter Aims 105
4.4 Methods 106
4.4.1 Langendorff Perfused Healthy Hearts 106
4.4.2 Daily L-Carnitine and Mildronate Treatment in the Healthy Heart 106
4.5 Results 108
4.5.1 Langendorff Perfused Healthy Hearts 108
4.5.1.1 Establishing a Low-flow Ischemic Rate for Langendorff Perfused Hearts 108
4.5.1.2 The Effects of L-Carnitine on Langendorff Perfused Control Hearts 111
4.5.2 Daily L-Carnitine Treatment in the Healthy Heart 117

4.5.3 Daily Mildronate Treatment in the Healthy Heart 120
4.6 Discussion 122
4.6.1 Langendorff Perfused Healthy Hearts 122
4.6.1.1 Establishing a Low-flow Ischemic Rate for Langendorff Perfused Hearts 122
4.6.1.2 L-Carnitine Effects on Langendorff Perfused Control Hearts 122
4.6.2 Daily L-Carnitine Treatment in the Healthy Heart 123
4.6.3 Daily Mildronate Treatment in the Healthy Heart 124
4.6.4 Conclusion and Future Perspective 124

5 Effects of L-Carnitine Supplementation on the Diabetic Heart 127
5.1 Chapter Overview 128
5.2 Background 129
5.3 Chapter Aims 133
5.4 Methods 133
5.5 Results 138
5.5.1 Weight and Blood Profile 138
5.5.2 Cardiac *In Vivo* Function 145
5.5.3 Cardiac *In Vivo* Metabolism 148
5.5.4 Tissue Analysis 152
5.5.5 Cardiac *Ex Vivo* Function 157
5.5.6 Cardiac *Ex Vivo* Fatty Acid Metabolism 163
5.6 Discussion 167
5.6.1 Summary of Key Findings 167
5.6.2 Daily L-Carnitine Treatment in the *In Vivo* Type 1 Diabetic Heart 168
5.6.3 Effects of L-Carnitine on Functional and Metabolic Recovery Post-Ischemia 172
5.6.4 Daily L-Carnitine Treatment in the *In Vivo* Healthy Heart . 174
5.6.5 Conclusion and Future Perspective 176

6 Effects of Reducing L-Carnitine in the Diabetic Heart using Mildronate 177
6.1 Chapter Overview 178
6.2 Background 179
6.3 Chapter Aims 181
6.4 Methods 181
6.5 Results 184
6.5.1 Weight and Blood Profile 184

6.5.2 L-Carnitine and Mildronate Levels 189
6.5.3 Cardiac *In Vivo* Function 191
6.5.4 Cardiac *In Vivo* Metabolism 193
6.5.5 Cardiac *Ex Vivo* Function 196
6.5.6 Cardiac *Ex Vivo* Fatty Acid Metabolism 203
6.5.7 Tissue Analysis 205
6.6 Discussion 206
6.6.1 Summary of Key Findings 206
6.6.2 Daily Mildronate Treatment in the *In Vivo* Type 1 Diabetic Heart 206
6.6.3 Conclusion and Future Perspective 210

7 General Discussion **211**
7.1 Overview 211
7.2 Effects of Diabetes on the Heart 212
7.3 L-Carnitine/Mildronate Effects on the Diabetic Heart 215

8 Conclusion, Limitations, and Future Work **219**

9 Bibliography **221**

List of Figures

1.1 Glucose stimulates insulin release in a normal β-cell 4
1.2 Brief overview of metabolism 9
1.3 The Randle cycle 10
1.4 L-carnitine biosynthesis 13
1.5 L-carnitine transport 15
1.6 Rodrigues *et al.*: L-carnitine's effect on the diabetic heart *ex vivo* . 18
1.7 Spin and precession 25
1.8 Example of relaxation times T_1 and T_2 27
1.9 Spectrum of ^{13}C in a urea sample 31
1.10 Polarizer and dissolution equipment 32

2.1 Left ventricle chamber views for MRI 42
2.2 CINE short axis slices of the heart 43
2.3 Freehand draw function for CINE 44
2.4 Example of C_1 or C_2 spectra 48
2.5 Echocardiography views 49
2.6 Langendorff perfusion apparatus 52
2.7 Langendorff perfusion protocol 53
2.8 Timeline for Langendorff perfusion protocol 54
2.9 Example of Langendorff functional trace 55
2.10 Palmitate transport into a cardiomyocyte 56

3.1 K_{ATP} channels and their subunits 66
3.2 K_{ATP} channel regulation of insulin release 67
3.3 K_{ATP} channels in a NDM mouse model 68
3.4 Experimental design for NDM mouse model study 72
3.5 Experimental design for STZ-induced models study 73
3.6 Blood glucose levels and body weight in the NDM mouse model . . 75
3.7 Cardiac function in treated NDM mice 76
3.8 Pyruvate infusion in NDM mice at baseline, diabetes, and treatment 77
3.9 Body weight in the NDM mouse model 78
3.10 Progression of cardiac function in NDM mice 79

3.11 Weight of fed/fasted STZ-induced rats 80
3.12 Low dose (LowD) STZ glucose levels 81
3.13 High dose (HighD) STZ glucose levels 82
3.14 Food and water intake in fasted HighD STZ group 83
3.15 CINE MRI in LowD and HighD STZ groups at two weeks 84
3.16 Cardiac metabolism in LowD and HighD STZ groups 86
3.17 Progression of blood glucose in fasted HighD STZ group 87
3.18 Echocardiography in fasted HighD STZ group 89
3.19 Progression of cardiac function in fasted HighD STZ group 90
3.20 Progression of cardiac metabolism in fasted HighD STZ 92
3.21 Metabolic correlations with glucose levels and stroke volume 93
3.22 SNR comparison between mouse and rat spectra 95

4.1 Experimental setup for Langendorff perfusions 107
4.2 Pilot study: Two weeks of L-carnitine/Mildronate supplementation 108
4.3 Healthy tissue characteristic 109
4.4 Langendorff perfusions in controls with different low-flow rates . . . 110
4.5 Reperfusion traces in L-carnitine and control groups 112
4.6 Langendorff perfusions with L-carnitine in healthy heart: RPP . . . 113
4.7 Langendorff perfusions with L-carnitine in healthy heart: HR 113
4.8 Langendorff perfusions with L-carnitine in healthy heart: DevP . . 114
4.9 Langendorff perfusions with L-carnitine in healthy heart: SysP . . . 114
4.10 Langendorff perfusions with L-carnitine in healthy heart: DiaP . . . 115
4.11 FAO rates in control and L-carnitine treated hearts 116
4.12 Effect of L-carnitine supplementation on body weight 117
4.13 Effect of L-carnitine supplementation on cardiac function 118
4.14 Two weeks of daily L-carnitine effects on *in vivo* metabolism 118
4.15 Two weeks of daily Mildronate treatment on body weight 120
4.16 Free L-carnitine detected in plasma from metabolomics 121
4.17 L-carnitine levels after two weeks of daily Mildronate treatment . . 121

5.1 Animal numbers 134
5.2 Experimental design for L-carnitine diabetes study 137
5.3 L-carnitine effects on body weight 138
5.4 L-carnitine effects on fat, tibia and kidneys 139
5.5 L-carnitine effects on blood glucose levels 140
5.6 L-carnitine effects on insulin levels 141
5.7 L-carnitine effects on insulin resistance 141
5.8 L-carnitine effects on fasted ketone bodies 142
5.9 L-carnitine effects on fed plasma profile 143

5.10 Example of M-mode in a control and a diabetic heart 145
5.11 L-carnitine effects on cardiac function: CINE MRI 147
5.12 L-carnitine effects on *in vivo* metabolism: $^{13}C_1$ HP MRI 150
5.13 L-carnitine effects on *in vivo* metabolism: $^{13}C_2$ HP MRI 151
5.14 L-carnitine effects on cardiac protein expression 153
5.15 L-carnitine effects on free L-carnitine in heart tissue 153
5.16 L-carnitine effect on short, medium and long-chain acyl-carnitines . 155
5.17 L-carnitine effect on the TriCarboxylic Acid (TCA) cycle intermediates 156
5.18 L-carnitine effects on *ex vivo* rate pressure product: RPP 158
5.19 L-carnitine effects on *ex vivo* developed pressure: DevP 159
5.20 L-carnitine effects on *ex vivo* diastolic pressure: DiaP 160
5.21 L-carnitine effects on *ex vivo* systolic pressure: SysP 161
5.22 L-carnitine effects on *ex vivo* heart rate: HR 162
5.23 L-carnitine effects on functional recovery pre- and post-ischemia . . 164
5.24 L-carnitine effects on FAO rates 165
5.25 L-carnitine effects on FAO rates normalized to work (RPP) 166

6.1 Experimental design for Mildronate study 183
6.2 Effects of Mildronate on body weight 184
6.3 Mildronate effects on tissue 185
6.4 Effects of Mildronate on food and water intake 186
6.5 Effects of Mildronate on fasted blood glucose 186
6.6 Mildronate effect on fed plasma profile 188
6.7 Mildronate effects on free L-carnitine in plasma 189
6.8 Mildronate effects on free L-carnitine measured with metabolomics . 190
6.9 Mildronate effects on free L-carnitine in plasma 190
6.10 Mildronate effects on cardiac function: CINE MRI 192
6.11 Mildronate effects on *in vivo* metabolism: $^{13}C_1$ HP MRI 194
6.12 Mildronate effects on *in vivo* metabolism: $^{13}C_2$ HP MRI 195
6.13 Mildronate effects on *ex vivo* rate pressure product: RPP 197
6.14 Mildronate effects on *ex vivo* heart rate: HR 198
6.15 Mildronate effects on *ex vivo* systolic pressure: SysP 199
6.16 Mildronate effect on *ex vivo* diastolic pressure: DiaP 200
6.17 Mildronate effects on *ex vivo* developed pressure: DevP 201
6.18 Example of LV pressures in the Mildronate treated groups 202
6.19 Mildronate effects on FAO 204
6.20 Mildronate effects on cardiac protein expression 205

7.1 Summary of cardiac function for the STZ studies 214
7.2 Summary of blood glucose levels and PDH-flux for the STZ studies 214
7.3 Summary of the effects of treatments on control and diabetes 217

List of Abbreviations

AC . . . . . Acetylcarnitine
ACC . . . . . Acetyl-CoA Decarboxylase
ADP . . . . . Adenosine Diphosphate
ALT . . . . . Alanine Aminotransferase
AMPK . . . . . AMP-Activated Protein Kinase
ANOVA . . . . . Analysis of Variance
ATP . . . . . Adenosine Triphosphate
BBOX . . . . . γ-Butyrobetaine Hydroxylase
BPM . . . . . Beats Per Minute
BW . . . . . Body Weight
cAMP . . . . . Cyclic Adenosine Monophosphate
CAT . . . . . Carnitine AcylTransferase
CACT . . . . . Carnitine Acylcarnitine Translocase
CAD . . . . . Coronary Artery Disease
CrAT . . . . . Carnitine AcetylTransferase
CDI . . . . . Color Doppler Imaging
CHD . . . . . Coronary Heart Disease
CI . . . . . Cardiac Index
CO . . . . . Cardiac Output
CT . . . . . Computed Tomography
CTR . . . . . Control
CVD . . . . . Cardiovascular Disease
CPT . . . . . Carnitine Palmitoyltransferase/ Carnitine Acyltransferase
DevP . . . . . Developed Pressure
DiaP . . . . . Diastolic Pressure
DNP . . . . . Dynamic Nuclear Polarisation
ECG . . . . . Electrocardiogram
EDP . . . . . End Diastolic Pressure
EDV . . . . . End Diastolic Volume
EF . . . . . Ejection Fraction
ELISA . . . . . Enzyme-Linked Immunosorbent Assay
EMA . . . . . European Medicines Agency
ESV . . . . . End Systolic Volume
ESP . . . . . End Systolic Pressure
FA . . . . . Fatty Acid
FACS . . . . . Fatty Acyl-CoA Synthetase
FAO . . . . . Fatty Acid Oxidation
FDA . . . . . Food and Drug Administration

FDG . . . . . Fluorodeoxyglucose
FFA . . . . . Free Fatty Acid
FP . . . . . Fat Pads
FS . . . . . Fractional Shortening
F6P Fructose-6-Phosphate
GIP . . . . . Gastric Inhibitory Polypeptide/Glucose Dependent Insulinotropic Polypeptide
GK . . . . . Glucokinase
GLB . . . . . Glibenclamide
GLP1 . . . . . Glucagon-Like Peptide-1
GLUT . . . . . Glucose Transporter Type
GWW . . . . . Gram Wet Weight
G6P Glucose-6-Phosphate
HDL . . . . . High-Density Lipoprotein
HOMA-IR . . . . . Homeostasis Model Assessment of Insulin Resistance
HP . . . . . Hyperpolarized
HR . . . . . HR
HTML . . . . . Trimethyllysine hydroxylase
IDF . . . . . International Diabetes Federation
IR . . . . . Insulin Resistance
I.P. . . . . . Intra Peritoneal
KH . . . . . Krebs-Henseleit
KHB . . . . . Krebs-Henseleit Buffer
LDH . . . . . Lactate Dehydrogenase
LDL . . . . . Low-Density Lipoprotein
LV . . . . . Left Ventricle
LVM . . . . . Left Ventricular Mass
LVDP . . . . . Left Ventricular Developed Pressure
LW . . . . . Lateral Wall
MCAD . . . . . Medium-Chain Acyl-CoA Dehydrogenase
MCD . . . . . Malonyl-CoA Decarboxylase
MI . . . . . Myocardial Infarction
MR . . . . . Magnetic Resonance
MRI . . . . . Magnetic Resonance Imaging
MRS . . . . . Magnetic Resonance Spectroscopy
NDM . . . . . Neonatal Diabetes Mellitus
NEFA . . . . . Non-Esterified Fatty Acids
NMR . . . . . Nuclear Magnetic Resonance
OCTN2 . . . . . Organic Cation/ Carnitine Transporter 2 (SLC22A5)
PAGE . . . . . PolyacrylAmide Gel Electrophoresis
PCD . . . . . Primary Carnitine Deficiency
PDH . . . . . Pyruvate Dehydrogenase
PDK . . . . . Pyruvate Dehydrogenase Kinase
PET . . . . . Positron Emission Tomography
PFK1 . . . . . Phosphofructokinase-1
PPAR . . . . . Peroxisome Proliferator-Activated Receptor
PPM . . . . . Parts Per Million

PPP . . . . . Pentose Phosphate Pathway
PVC . . . . . Polyvinyl Chloride
PWD . . . . . Pulse Wave Doppler
RB . . . . . Recirculating Buffer
RF . . . . . Radiowave Frequency
RPP . . . . . Rate Pressure Product
SA . . . . . Specific Activity
SD . . . . . Standard Deviation
SDS . . . . . Sodium Dodecyl Sulfate
SI . . . . . Stroke Index
SNR . . . . . Signal to Noise Ratio
SV . . . . . Stroke Volume
STZ . . . . . Streptozotocin
SysP . . . . . Systolic Pressure
TAG . . . . . Triglycerides
TCA . . . . . Tricarboxylic acid
TBS . . . . . Tris-Buffered Saline
TD . . . . . Tissue Doppler
TTE . . . . . Transthoracic Echocardiography
TCA . . . . . Tricarboxylic Acid
TMA . . . . . TriMethylAmine
TMA . . . . . TriMethylAmine-N-Oxide
TMB . . . . . Tetramethylbenzidine
TMBA . . . . . Trimethylaminobutyraldehyde
TML . . . . . Trimethyllysine
TMLH . . . . . Trimethyllysine Hydroxylase
T1D . . . . . Type 1 Diabetes Mellitus
T2D . . . . . Type 2 Diabetes Mellitus
UCP . . . . . UnCoupling Protein
WADA . . . . . World Anti-Doping Agency
WB . . . . . Western Blot
αKG . . . . . α-KetoGlutarate

3-OHB . . . . . β-Hydroxybutyrate

It was six men of Hindostan,

To learning much inclined,

Who went to see the elephant

(Though all of them were blind)

That each by observation

Might satisfy his mind. — J.G. Saxe (to be continued)

1 Introduction

Contents

1.1 Overview and Motivation 1
1.2 Diabetes and Cardiovascular Disease 3
1.3 Metabolism in the Healthy Heart 6
1.4 Metabolism in the Diabetic Heart 11
1.5 L-Carnitine in the Healthy Heart 12
1.6 L-Carnitine in the Diseased Heart 15
1.7 Cardiac Effects of Mildronate: Lowering L-Carnitine Levels 20
1.8 Technologies for Cardiac Assessment 22
1.8.1 Echocardiography 22
1.8.2 Computed Tomography (CT) 23
1.8.3 Positron Emission Tomography (PET) 23
1.8.4 Magnetic Resonance Imaging (MRI) 24
1.8.5 Cardiac MR Spectroscopy (MRS) 29
1.8.6 A Brief Introduction to Dynamic Nuclear Polarisation . 30
1.8.7 Hyperpolarized ^{13}C MRS using Dynamic Nuclear Polarisation 33
1.9 Aims 35
1.9.1 Summary of Chapters 37

1.1 Overview and Motivation

Diabetes mellitus is a metabolic disorder and one of the major endocrine diseases involving the islet cell hormones. The global prevalence of diabetes has risen from

108 million people in 1980 to 425 million in 2014 [279], of which 5-15 % of diabetic patients have type 1 diabetes (T1D) [182]. T1D patients are insulin deficient due to an autoimmune response that destroys the insulin-producing islet β-cells in the pancreas and they, therefore, require insulin therapy. Diabetes is associated with an elevated risk of cardiovascular diseases (CVD) such as cardiomyopathy, myocardial infarction, coronary heart disease (CHD), arrhythmias, and hearts valve problems [247, 58]. CVD are the major causes of premature death in diabetic patients, and their incidence continues to rise in the diabetic population, despite advances in diabetes care [243]. Even though diabetes increases the incidence of heart disease and is the leading cause of mortality in diabetic patients, the underlying link between heart disease and diabetes is not entirely understood [226].

Improving our understanding of the metabolic changes that occur in the diabetic heart may be vital to understanding the pathophysiology of diabetic heart disease. This could have significant implications not just for the health and survival rate of diabetic patients but may also relieve the major economic burden that it imposes on society. By understanding the basic metabolic pathways through advanced imaging technologies and diagnostics, therapies for the diabetic heart could be improved.

Magnetic resonance imaging (MRI) and magnetic resonance spectroscopy (MRS) make it possible to study *in vivo* metabolism in the heart, while it is also providing information about the morphology and function of the heart. MRI is advantageous to echocardiography because it does not make any assumption of the geometric shape of the heart, and it shows superior interstudy reproducibility. Finally, it is safe and uses no ionizing radiation compared to positron emission tomography (PET). A recent advance in MRI technology, called hyperpolarized ^{13}C MRS, makes it possible to study nuclei other than protons with more than $10,000$ times higher signal to noise ratio using a dynamic nuclear polarisation (DNP) technique, followed by a rapid dissolution process to create a non-harmful and injectable solution [7]. This technology allows for mapping of specific metabolic pathways, and can in contrast to PET, map both the injectable solution and its downstream substrates, providing chemical as well as spatial information.

Hyperpolarized ^{13}C MRS together with MRI can provide unique *in vivo* information regarding both metabolism and function in diabetic hearts, and could help elucidate the underlying pathophysiology of diabetic heart disease.

1.2 Diabetes and Cardiovascular Disease

The International Diabetes Federation (IDF) estimates that 425 million people had diabetes worldwide in 2017, and predicts that 642 million people will suffer from diabetes in 2040, resulting in a prevalence of one in ten people suffering from diabetes [102]. Most of these patients have type 2 diabetes (T2D). IDF also estimates that 1.1 million children between 0 and 19 years currently suffer from T1D, and every year 132,600 new cases are diagnosed. The worldwide prevalence of T1D is 5-15 % of the total diabetic population, resulting in approximately 64 million people suffering from T1D by 2040 [55, 116, 182]. However, this estimate is likely to be conservative since the distinction between T1D and T2D becomes less apparent in the later stages of life.

T1D is characterized by insulin deficiency, due to either an autoimmune or idiopathic destruction of pancreatic β-cells [65], resulting in hypoinsulinaemia and hyperglycaemia. Normal β-cells release insulin based on glucose stimulation (Fig. 1.1).

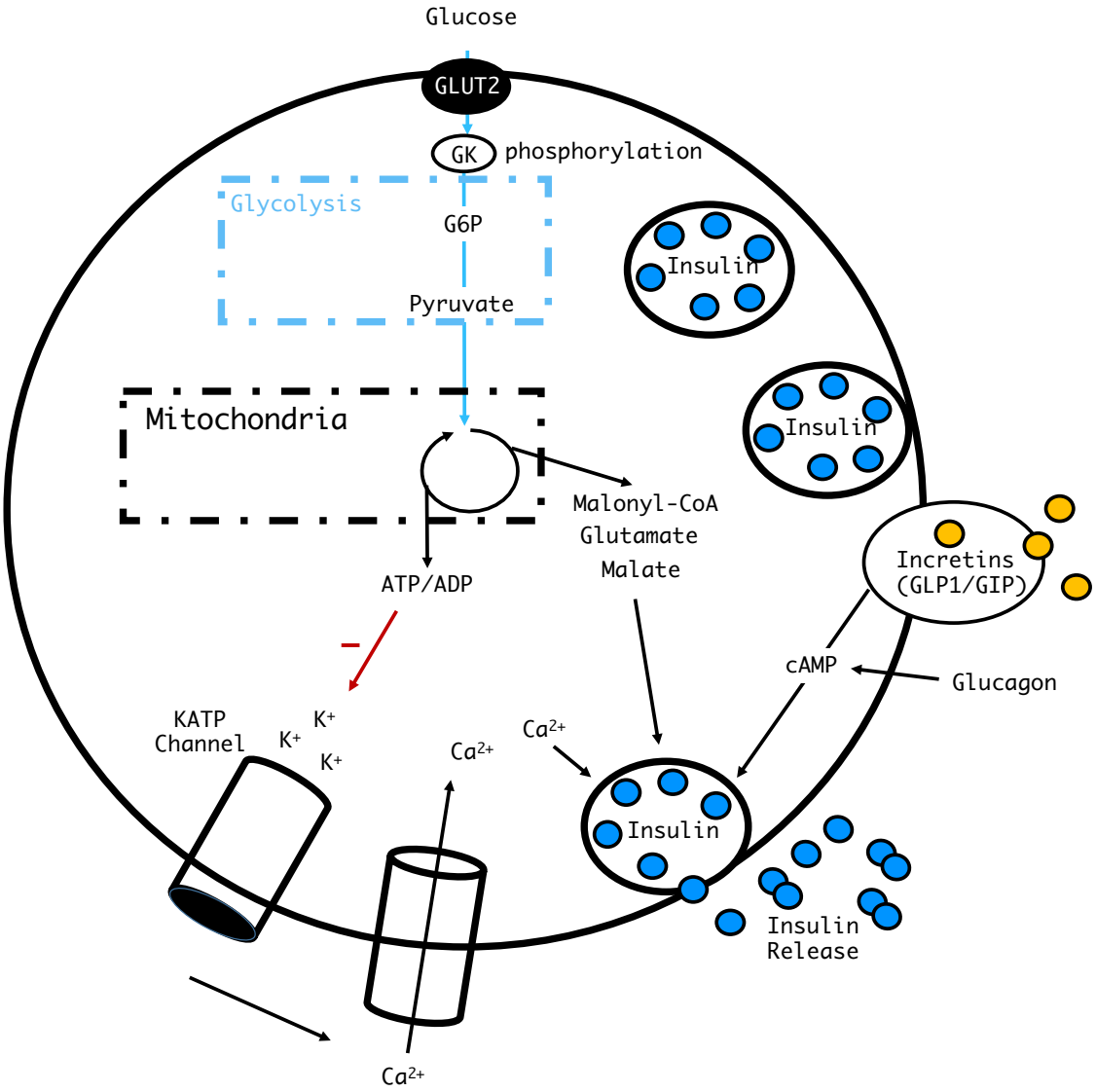

Figure 1.1: Glucose stimulated insulin release in a normal β-cell. Glucose phosphorylates via glucokinase (GK) to glucose-6-phosphate (G6P) that enters glycolysis and produces pyruvate. Pyruvate enters the mitochondria where it metabolizes. Intermediates produced from the TCA cycle stimulate insulin release. Increased ATP/ADP ratio closes the K_{ATP} channels which result in depolarization of the membrane, that opens the voltage-gated calcium channels and an influx of calcium stimulates insulin release. Increased influx of glucose into the TCA cycle results in an accumulation of intermediates in the cytosol that also lead to insulin release [204]. Finally, incretins such as glucagon-like peptide-1 (GLP1) and gastric inhibitory polypeptide (GIP) as well as glucagon can stimulate cAMP pathways that also results in insulin release. Adapted from [204].

The autoimmune response in T1D has a genetic component, but it is believed that an environmental trigger is also present such as a virus. The rate of β-cell destruction can vary, avoiding absolute insulin dependence for years after the onset of the disease [65]. The onset is most common in children and adolescents; therefore it used to be called "juvenile diabetes", however, it can occur in adulthood as well.

The typical symptoms are hyperglycaemia, polyuria, polydipsia, hyperlipidaemia, and weight loss. So even though life-long insulin treatment is necessary for survival, the prognosis is much better today, than before insulin treatments were available. Insulin treatment introduction to the clinic in the 1920s dramatically changed the life expectancy of the T1D population [180].

Cardiovascular disease is a long-term complication for T1D [247, 128]. People with diabetes are 2-3 times more likely to develop cardiovascular disease (CVD), and the prevalence of end-stage renal disease is ten times higher in people with diabetes [102]. Evidence of cardiovascular risk used to be based on risks extrapolated from the T2D population, however, more evidence suggest that these risk factors are present in T1D [128] especially with the life expectancy rising in these patients. T1D patients have been shown to develop cardiovascular diseases ten years earlier than in the matched non-T1D population, and the prevalence has been demonstrated to be mostly associated with elevated triglycerides and decreased HDL cholesterol levels [244, 116]. Hyperglycaemia leads to both micro and macrovascular complications that lead to cardiovascular disease [220]. Improved glycaemic control can significantly reduce the long-term complications of T1D, although insulin treatment can cause significant weight gain. Melin *et al.* have shown that increased abdominal fat in T1D is also associated with cardiovascular risk factors and complications [163].

Cardiovascular disease (CVD) can be divided into coronary heart disease (CHD), heart failure and cardiomyopathy. It is also divided into congenital heart disease, peripheral vascular disease and cerebrovascular disease, although these are not as relevant for this thesis.

CHD is also known as ischemic heart disease which leads to a blockage of the blood flow to the heart resulting in a heart attack (acute myocardial infarction),

damaging the cardiac muscle and function. CHD can also refer to angina, which temporarily blocks the supply of blood to the heart, causing short episodes of chest pain. Heart failure means that the heart cannot meet the body's demand for oxygenated blood resulting in chronic tiredness, shortness of breath and oedema. Cardiomyopathy impairs myocardial function either through dilation, hypertrophy or restrictive cardiomyopathy, all of which reduce the effectiveness of the myocardium. Cardiomyopathies have been described in T1D patients, but the information is not as robust as for other cardiovascular diseases in T1D [138, 166, 142]. Cardiac disease is associated with changes in metabolism, and understanding the balance between different energy sources, can be core to understanding the pathophysiology of cardiac diseases.

1.3 Metabolism in the Healthy Heart

The heart is a biological pump that converts chemical energy into mechanical energy. The heart requires ATP to sustain the necessary cardiac output for the body. In a healthy heart, ATP production comes from triglycerides (TAG), long-chain fatty acids (FA), glucose, glycogen, pyruvate, lactate, as well as ketone bodies, with the majority of ATP production coming from FA β-oxidation [254, 147]. FA reach the cardiomyocytes either as FA bound to albumin or as FA released from TAG. They are converted to long-chain acyl-CoA esters by fatty acyl-CoA synthetase (FACS) in the cytoplasm, and are either used for the production of intracellular lipid intermediates or transported by L-carnitine into the mitochondria, for β-oxidation into acetyl-CoA, allowing entrance into the TCA cycle (Fig. 1.2).

The heart is metabolically flexible and can utilise all classes of energy substrates, it changes substrate utilisation depending on the environment to maintain cardiac function [117]. FA can produce more ATP per mole than glucose and therefore have a higher energy density. However, FAs require more oxygen to generate ATP than glucose, as glucose is more oxygen efficient, making it a better fuel when oxygen is limited [58]. However, during a normal cardiac function, oxygen is not limited and the heart, therefore, prefers FA.

A rise in blood glucose stimulates β-cells in the pancreas to release insulin, which in turn increases glucose utilisation in the liver, adipose and muscle tissues. If blood glucose levels fall, the α-cells in the pancreas release glucagon, signalling to the liver to break down glycogen and thereby increase glucose levels in the blood. Even though glucose is not the primary energy provider to the heart, it is a critical substrate provider during increased workload, ischemia and hypertension. Basal glucose is taken up via a glucose transporter (GLUT1) to sustain respiration in all cells. The insulin-sensitive glucose transporter (GLUT4) also facilitates glucose uptake in the heart [1]. Once in the cell, glucose can be used for glycogenesis, the pentose phosphate pathway (PPP), lipogenesis and glycolysis. Glycolysis consists of 9-10 enzyme-catalysed steps, which convert glucose to pyruvate in the cytosol, whereby pyruvate can subsequently enter the mitochondrion. Glycolytic pyruvate is decarboxylated by pyruvate dehydrogenase (PDH) into acetyl-CoA, which can enter the TCA cycle for efficient energy transfer (Fig. 1.2). Pyruvate can also be metabolised by lactate dehydrogenase (LDH) creating lactate, malic enzyme forming malate, pyruvate carboxylase creating oxaloacetate or transaminated to alanine [53].

Increased production of acetyl-CoA stemming from β-oxidation inhibits glucose oxidation by activating pyruvate dehydrogenase kinase (PDK), which inhibits the regulatory enzyme PDH via phosphorylation [85]. There are four isoforms of PDK, that have different activity and phosphorylation rates, with the most active being PDK1. PDK1 is mostly expressed in heart tissue, PDK2 is expressed ubiquitously, PDK3 is primarily expressed in testis, and PDK4 is mainly expressed in skeletal muscle and heart tissue. In addition to an increased ratio of acetyl-CoA/CoA, increased β-oxidation activates PDK through an elevated ratio of $NADH/NAD^+$, suppressing PDH-flux. Peroxisome proliferator-activated receptor α (PPARα) also enhances protein expression of PDK4. PPARα is expressed in the heart and plays an essential role in lipid metabolism. The glucose fatty-acid cycle (Randle cycle) is fundamental to the control of blood glucose levels, fatty acid concentrations, as well as insulin sensitivity [207]. Increased production of acetyl-CoA stemming from pyruvate oxidation, inhibits FA β-oxidation via production of

malonyl-CoA, which inhibits the uptake of FAs into the mitochondria [147]. Fructose-6-phosphate and malonyl-CoA signals that carbohydrates are being oxidized and inhibits carnitine palmitoyltransferase (CPT1), the rate-limiting step, by inhibiting fatty acid uptake into the mitochondria (Fig. 1.2). Malonyl-CoA is the regulatory factor, if carbohydrates are oxidized, it will be used as a substrate for fatty acid synthesis and inhibit fatty acid oxidation [161].

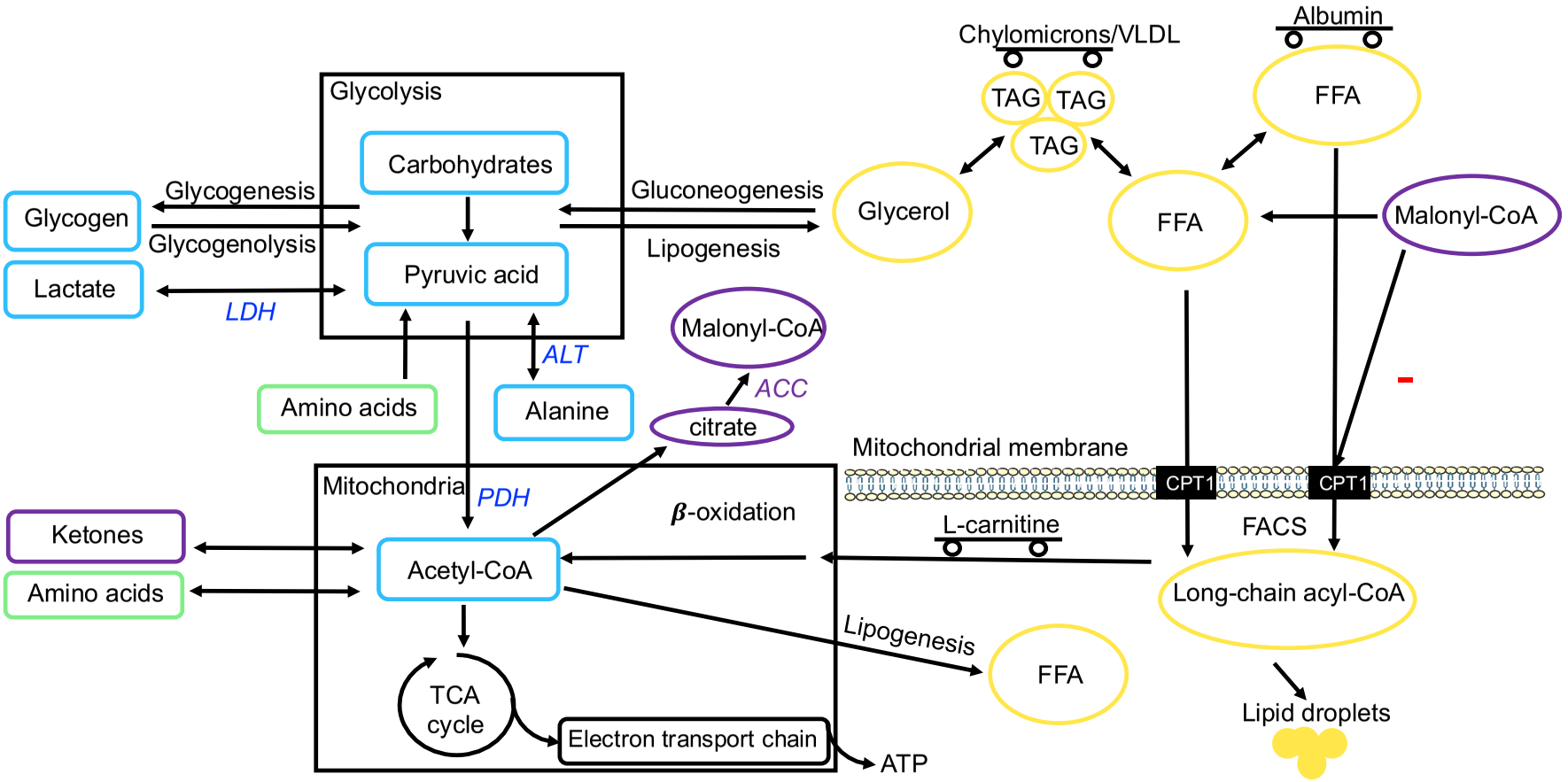

Figure 1.2: Brief overview of metabolism. Triglycerides (TAG) form from glycerol and free fatty acids (FFA). FFA are either released from triglycerides (TAG) or released from albumin before they enter through the myocardial cell membrane. In the cytoplasm fatty acyl-CoA synthetase (FACS) converts FFA into long-chain acyl-CoA, which then either produces lipid droplets or is transported by L-carnitine into the mitochondria for ATP production. Acetyl-CoA carboxylase (ACC) can catalyse carboxylation of acetyl-CoA to form malonyl-CoA, that can inhibit the rate-limiting step in FAO, CPT1, and therefore result in FA biosynthesis. Lipogenesis is the production of lipids but is mainly produced in the liver together with ketone bodies. Production of acetyl-CoA can also be made from some amino acids, ketone bodies and pyruvic acids by pyruvate dehydrogenase (PDH). Glycolysis is the anaerobic metabolic pathway that converts glucose into pyruvate in the cytosol. Pyruvate can also be converted to alanine by alanine aminotransferase (ALT) or to lactate by lactate dehydrogenase (LDH). Gluconeogenesis is the production of glucose from non-carbohydrates. Glycogenolysis is the breakdown of glycogen to glucose-6-phosphate. Glycogenesis is the process of glycogen synthesis.

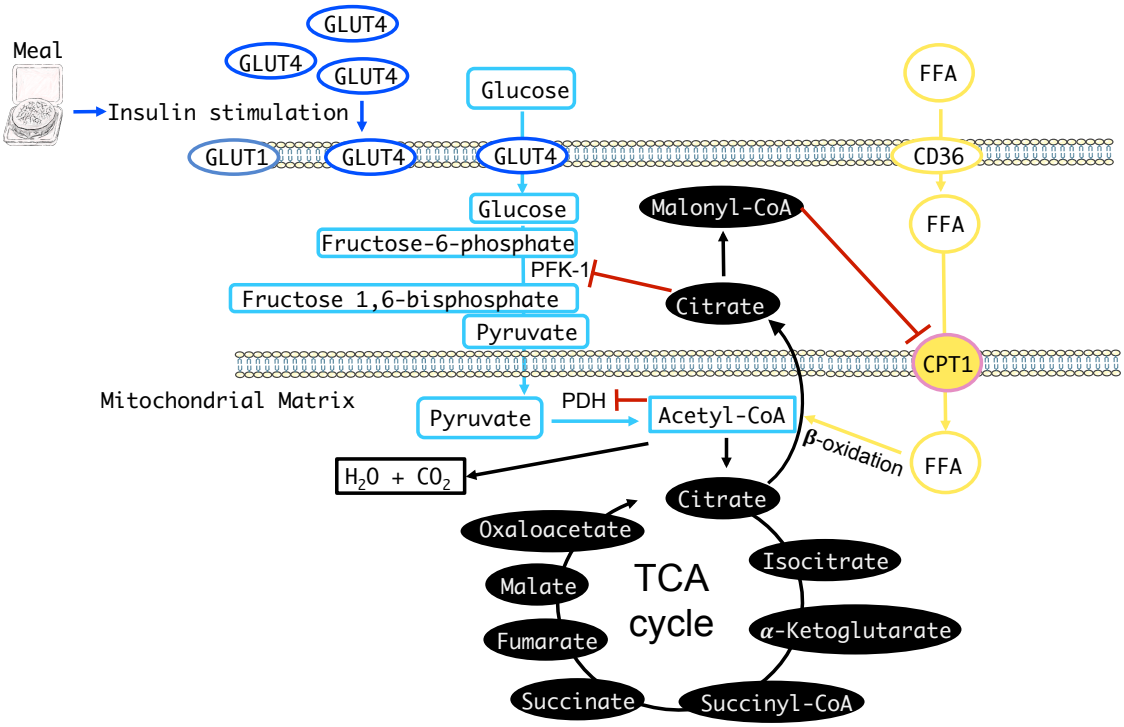

Figure 1.3: The Randle cycle. The Randle cycle describes the interaction between carbohydrate and fat metabolism. Fatty acid metabolism can inhibit glucose metabolism first through the production of acetyl-CoA, that increases the ratio of acetyl-CoA and CoA as well the ratio of NADH and NAD^+ which inhibits pyruvate dehydrogenase (PDH). An accumulation of citrate inhibits phosphofructokinase-1 (PFK1), which is an essential enzyme in the glycolysis pathway, this leads to an accumulation of fructose-6-phosphate (F6P). Malonyl-CoA signals that carbohydrates are oxidised, and therefore it inhibits carnitine palmitoyl transferase/ carnitine acyltransferase (CPT1/CAT1), which blocks the transport of fatty acids into the mitochondria.

1.4 Metabolism in the Diabetic Heart

In a healthy heart, almost 60-70 % of the ATP production comes from FAs, and the remaining 30-40 % comes from glucose and lactate. However, in many diseases such as diabetes, cardiac hypertrophy, and myocardial infarction, this balance is shifted [58, 12]. In fasting, obesity and diabetes, a high concentration of free FA increases expression of PDK4, which leads to inhibition of PDH-flux and therefore decreases pyruvate oxidation. In uncontrolled T1D, glucose utilisation is significantly reduced, and almost all cardiac energy supply arises from FA oxidation [147]. Even though glucose levels are high in T1D, there is a low uptake of glucose into the cardiomyocyte and other tissues by the insulin-dependent GLUT4 transporters [208], due to a lack of insulin. Even glycogen synthesis stops, due to the lack of insulin. As if this was not enough, the lack of insulin leads to an increased secretion of glucagon. Glucagon stimulates both the breakdown of glycogen (glycogenolysis) and the production of glucose from other fuels (gluconeogenesis), consequently elevating blood glucose levels even further.

Glycogen, fat and proteins are all metabolized to produce the required energy, leading to muscle atrophy and ketoacidosis [30]. As a consequence, fatty acid oxidation is accelerated by the lack of insulin. The activity of insulin on the adipocyte hormone-sensitive lipase is lost leading to elevated adipose lipolysis. This leads to a high release of non-esterified fatty acids (NEFA) from adipose tissue. An increased level of NEFAs results in increased production of ketone bodies and therefore ketogenesis, which can lead to a dangerous fall in blood pH levels called *diabetic ketoacidosis*. Furthermore, an elevation of NEFA results in higher VLDL-triacylglycerol concentrations, which are not cleared from the blood. So in addition to high glucose levels, there will also be high levels of triglycerides in the blood [71].

The elevated glucose levels result in an increased loss of glucose in the urine and consequently an elevation of urine volume (polyuria), thirst (polydipsia) and appetite (polyphagia). Sakamoto *et al.* have shown that the reduction in glucose oxidation in the T1D heart is not entirely caused by the lack of insulin or substrate utilisation [218]. They showed that in the streptozotocin induced diabetic perfused

heart insulin did not alter glucose oxidation whether they were perfused with low-fat/low-glucose or if they were perfused with high-fat/high glucose. This implies that the low glucose oxidation in the type 1 diabetic heart is not solely due to the circulating substrate or due to insulin. Moreover, while Sakamoto *et al.* found no changes in AMP-activated protein kinase (AMPK) or acetyl-CoA carboxylase (ACC), they found elevated malonyl-CoA decarboxylase (MCD) in type 1 diabetic hearts, suggesting a direct alteration in fatty acid oxidation and decreased levels of glucose oxidation [218].

1.5 L-Carnitine in the Healthy Heart

L-carnitine is mainly synthesised in the liver, kidneys, and the brain, from two amino acids; lysine and methionine, but the synthesis also needs vitamins, B_6, C, niacin and iron, and any shortage of these can result in reduced levels of L-carnitine. However, L-carnitine is also taken up through diet. The word *carnitine* comes from the word "carnis", which means flesh or meat. Red meats contain the highest levels of L-carnitine although smaller quantities are also found in vegetables and fruits like in avocados, asparagus and pears. L-carnitine is taken up by the heart and muscle tissue from the circulation (Fig. 1.4).

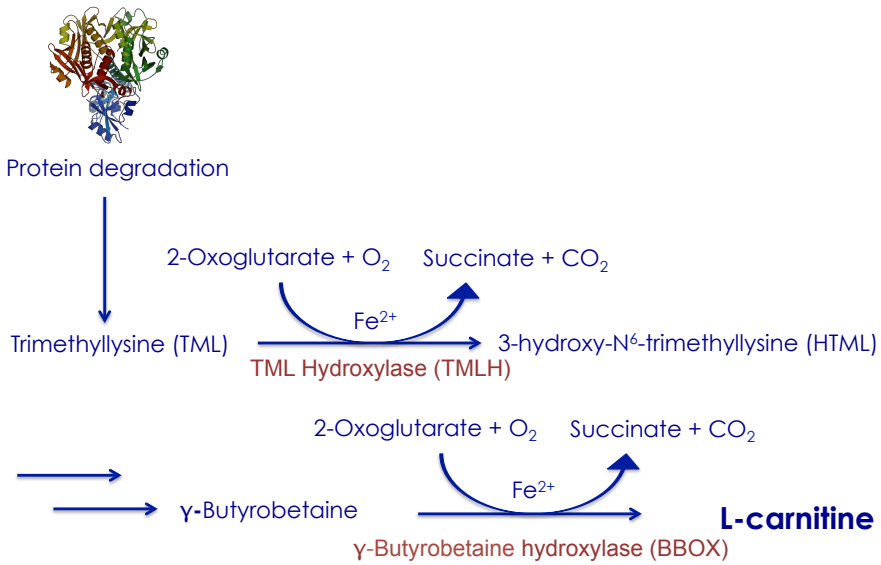

Figure 1.4: L-carnitine biosynthesis. L-carnitine is biosynthesized in the kidney, liver and the brain. Trimethyllysine (TML) is released from lysosomal protein degradation, where it is hydroxylated by trimethyl lysine hydroxylase (HTML) forming hydroxytrimethyl lysine (HTML). HTML is cleaved forming trimethylaminobutyraldehyde (TMABA) and glycine, whereafter TMABA is oxidized to form γ-butyrobetaine and which is finally hydroxylated by γ-butyrobetaine hydroxylase (BBOX) leading to L-carnitine

L-carnitine is critical for the transport of long-chain FAs into the mitochondria for energy production, but it also acts through acetylcarnitine as a buffer of excess acetyl-CoA units in the mitochondria from glucose metabolism [176, 143]. Long-chain acyl-CoA are found in the cytoplasm of cells, and cannot pass the mitochondrial membrane for further β-oxidation, without first binding to free L-carnitine via carnitine acyltransferase I (CAT1/CPT1), to pass through the outer mitochondrial membrane in the form of long-chain acylcarnitine (Fig. 1.5). The first step in the synthesis of FAs, malonyl CoA, is a crucial regulator of the conversion of long-chain acyl-CoA to long-chain acylcarnitine by inhibiting CAT1/CPT1 [70, 107, 238]. Carnitine acylcarnitine translocase (CACT) is required to transport the long-chain acylcarnitine through the inner mitochondrial membrane and simultaneously carries free L-carnitine back out from the mitochondrial matrix for new CAT1/CPT1 conversion (Fig. 1.5). Once acylcarnitine has entered the mitochondrial matrix, it can be cleaved by carnitine acyltransferase 2 (CAT2/CPT2), and the long-chain acyl-CoA released, can enter the mitochondria for β-oxidation. CAT2/CPT2 is not as sensitive to malonyl-CoA inhibition as CAT1/CPT1. If L-carnitine levels are low, long-chain FAs cannot be taken up into mitochondria and oxidized, and there is an accumulation of triglycerides in the cytosol of cardiomyocytes [143, 107].

It has been suggested in isolated mitochondria that acetylcarnitine reduces the acetyl-CoA/CoA ratio and, therefore, allows CoA to be utilized for other functions [150]. Acetyl-CoA rapidly cycles through the acetylcarnitine pool in the mitochondria and enables acetyl-CoA to be transported out of the mitochondria. Schroeder *et al.* have shown in healthy hearts using hyperpolarised $[2-^{13}C]$pyruvate MRS, that if the signal from acetylcarnitine is saturated, only 50 % of the TCA cycle intermediates are observed, meaning that almost 50 % of the acetyl-CoA that is produced from PDH-flux is buffered into acetylcarnitine before being converted back into acetyl-CoA and incorporated into the TCA cycle. L-carnitine, therefore, allows the heart to be able to adapt quickly to metabolic changes that require an elevated supply of acetyl-CoA, and can, in addition, reduce the inhibitory effects of the accumulation of acetyl-CoA [224].

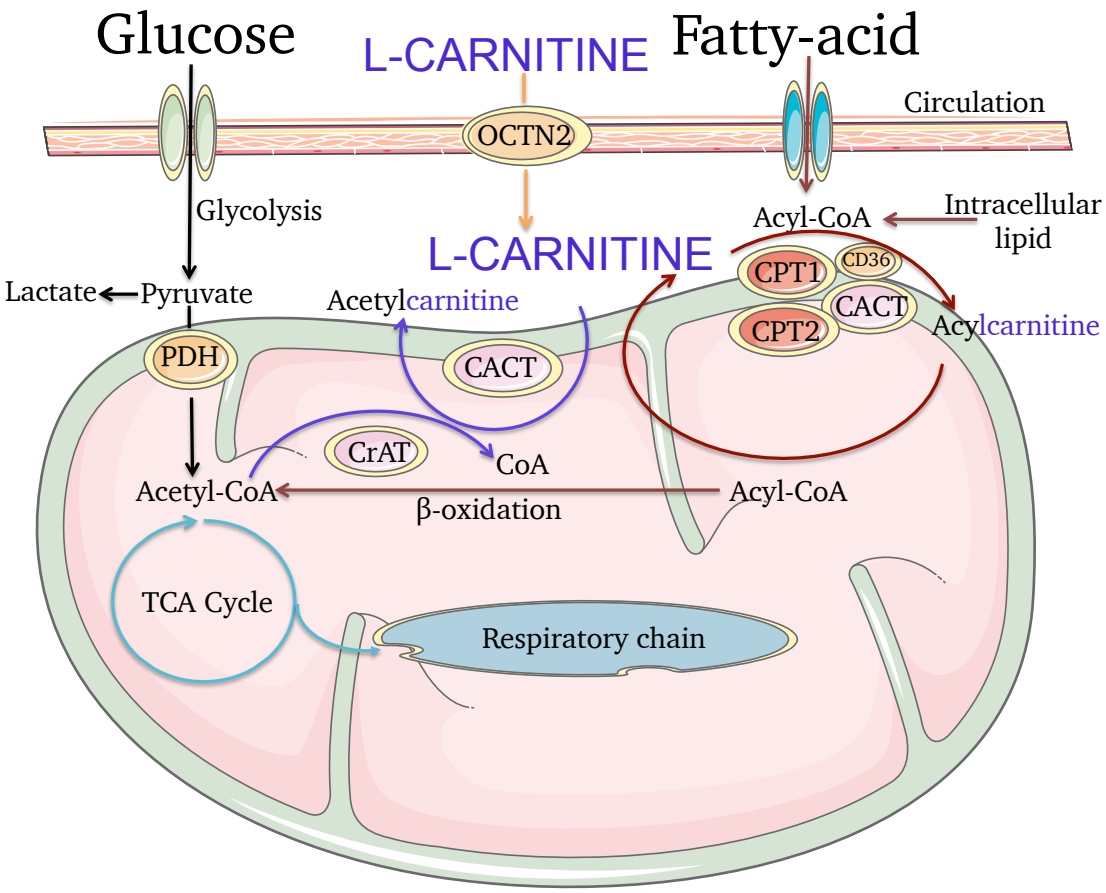

Figure 1.5: The L-carnitine dependent transport of activated long-chain fatty acids through the mitochondrial membrane. L-carnitine is taken up through the plasma membrane by the membrane transport protein; Organic Cation/Carnitine Transporter Type 2 (OCTN2). The outer mitochondrial membrane is containing Carnitine Palmitoyl Transferase/Carnitine AcylTransferase (CPT I/CAT I). The inner mitochondrial membrane is containing Carnitine AcylCarnitine Translocase (CACT) and Carnitine AcylTransferase I/Carnitine PalmitoylTransferase II (CPT II/CAT II) and the mitochondrial matrix is containing Carnitine AcetylTransferase (CrAT).

1.6 L-Carnitine in the Diseased Heart

Cardiac metabolism and function are inherently linked. It is therefore a clinical goal to find a way to alter metabolism that will lead to functional improvement pharmacologically. L-carnitine stores deplete with age and have been shown to be reduced in multiple disease states. Several studies report positive effects of L-carnitine supplementation on cardiac function in disease [213, 29, 194, 67, 165].

Primary Carnitine Deficiency (PCD), is an autosomal recessive disorder, which leads to defects in fatty acid oxidation and eventually results in pediatric cardiomy-

opathies [77]. Interestingly, and maybe not surprisingly, metabolic cardiomyopathies have been shown to be treatable with oral L-carnitine supplementation in PCD [72]. In a few cases, where L-carnitine supplementation was discontinued, sudden cardiac death resulted, demonstrating how critical continuation of L-carnitine treatment is [72]. L-carnitine deficiency does not only compromise cardiac energy metabolism by limiting fatty acid oxidation, but it has also been shown that it could compromise cardiac energy metabolism by also limiting glucose oxidation [224, 221]. Many studies have shown protective effects of L-carnitine supplementation, such as reduced blood pressure and a decline in inflammation associated with arterial hypertension [165, 100, 34]. A study was undertaken in patients with myocardial infarction, they were treated with L-carnitine orally for 12 months and showed an attenuated progression of left ventricular dilation already at three months post treatment [100]. Likewise, a study showed improved glucose tolerance in type 2 diabetes with L-carnitine supplementation [34].

The beneficial mechanism of L-carnitine is believed to be through improved oxidative metabolism by reducing intramitochondrial acetyl-CoA/CoA ratios relieving PDH inhibition, while at the same time transporting free fatty acids into the mitochondria for oxidation and thereby counteracting the toxic cytosolic effects of high levels of free fatty acids [67]. The Randle cycle explains the relationship between glucose and fatty acids, and theoretically, if L-carnitine transports free fatty acids for oxidation, glucose oxidation will be reduced. L-carnitine is an essential compound in keeping the balance between the utilisation of glucose and fatty acids, and its effects appear to be dependent on the experimental conditions, dosage, as well as, duration of treatment [56]. Diaz *et al.* showed that acute L-carnitine treatment in the Langendorff perfused hearts worsened tissue injury and recovery of function after transient ischemia and that a low dose of L-carnitine (1 mM) led to a decrease in glucose oxidation [56]. Thus suggests that L-carnitine is not always beneficial and could show favourable effects only under specific pathological conditions such as cardiovascular diseases or diabetes [68].

Nevertheless, in diabetes, L-carnitine supplementation has been shown to lead to full functional recovery following 60 minutes of low-flow ischemia with 30 minutes of subsequent aerobic reperfusion. Glucose oxidation has been shown to be stimulated during reperfusion in control rats as well as diabetic rats. However, glycolysis was only stimulated in the diabetic rats during ischemia [29, 194, 67, 27]. Rodrigues *et al.* studied T1D rat hearts and investigated what effect six weeks of daily intraperitoneal (i.p.) injections of L-carnitine had on cardiac function using the working heart mode. With L-carnitine treatment, blood glucose levels, and lipid levels (triglycerides, cholesterol and phospholipids) were shown to be restored to control levels independent of insulin treatment in a T1D rat model [213]. Full recovery of cardiac function were also observed in the diabetic rats (Fig. 1.6). This is supported by other studies [194, 201], but the underlying mechanisms are still being investigated.

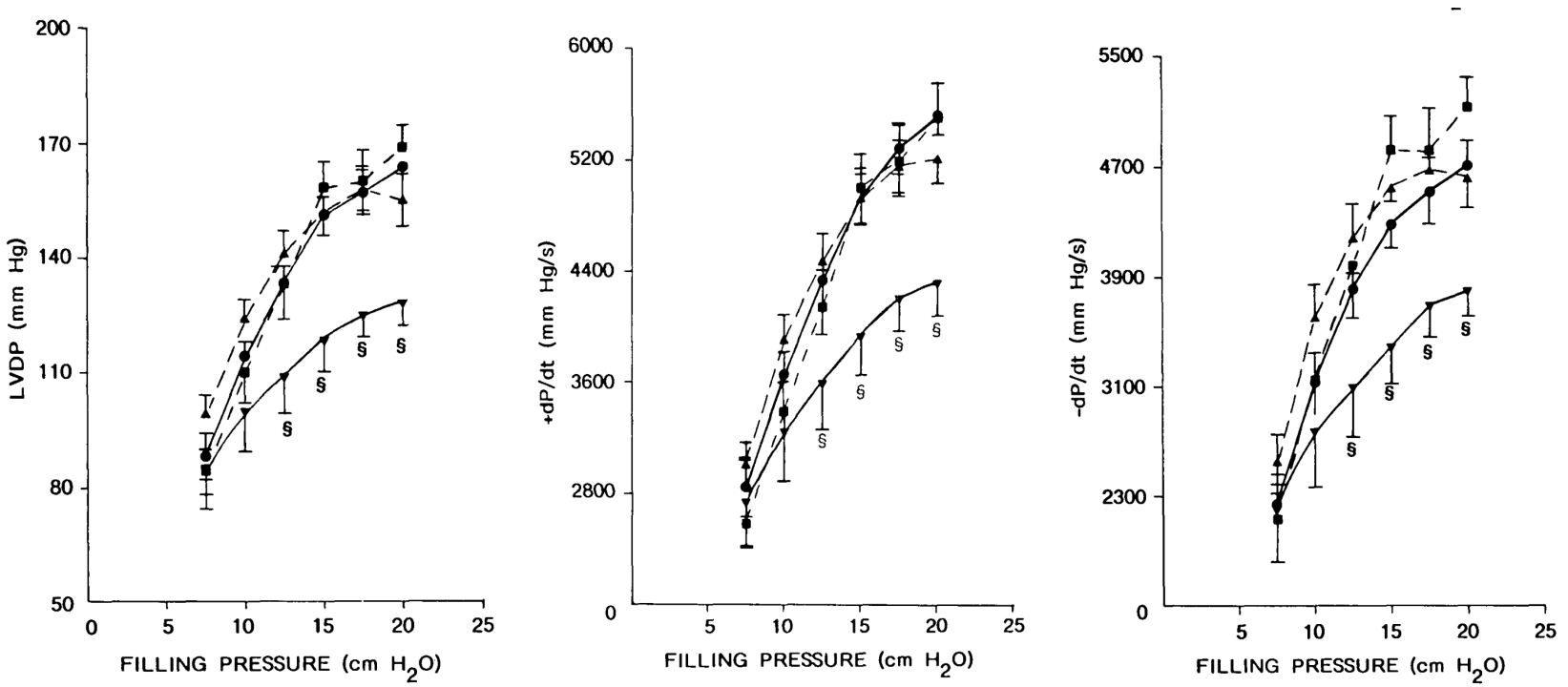

Figure 1.6: Effect of diabetes and L-carnitine treatment on left ventricular developed pressure (LVDP; left), cardiac contractility (+ dP/dt), and ventricular relaxation (-dP/df) of isolated perfused working hearts at various filling pressures. Hearts were isolated from 4 experimental groups 42 days after induction of diabetes with streptozocin (55mg/kg i.v.). Each point represents mean ± SE for n hearts. ●, Untreated control, n = 8; ■ , L-carnitine-treated control, n = 6; ▼ , untreated streptozocin-induced diabetic, n = 8; ▲ , L-carnitine-treated streptozocin-induced diabetic, n = 8. § Significantly different from other 3 groups ($P < .05$). Reprinted with permission [213]. American Diabetes Association, Effect of L-Carnitine Treatment on Lipid Metabolism and Cardiac Performance in Chronically Diabetic Rats, American Diabetes Association, 1988. Copyright and all rights reserved. Material from this publication has been used with the permission of the American Diabetes Association.

In contrast, diabetic rats treated with saline for six weeks have shown severe cardiac depression in both left ventricular pressure, contractility and relaxation [213, 29]. With treatment, free L-carnitine in the plasma was elevated similar to the control values. This also caused a reduction in the accumulation of fatty acid intermediates (acyl-CoA, long-chain acylcarnitine) in the heart, resulting in improved functional recovery with a lower level of acyl-CoA [213, 199]. Another reason for the improvement could have been an elevation in glucose oxidation via relief of PDH inhibition due to a reduced ratio of acetyl-CoA/CoA via acetylcarnitine buffering coming from restored levels of free L-carnitine [213, 33].

Even though 75 % of L-carnitine is obtained from the diet [68, 265], some studies on diabetes have failed to show alteration in *in vivo* metabolism with oral L-carnitine supplementation [212]. In the diseased state, L-carnitine requirement might exceed the dietary intake and a higher concentration is needed to increase uptake into tissues. L-carnitine has a poor absorption from oral treatments and has high renal clearance, which is why injections might prove more efficient. Many studies that have not shown beneficial effects with oral treatment have used a relatively low dose of L-carnitine [212], and it is known that muscle content of L-carnitine increases exponentially with higher dietary L-carnitine intake. Only a slight increase in muscle content has been shown with doses 40 to 600 mg/kg, hereafter it exponentially increases and levels off around 1100 mg/kg [187]. However, even if a sufficient oral dose of L-carnitine is given it might be detrimental to the cardiovascular system. Koeth *et al.* showed that if L-carnitine is taken up orally, it is metabolized in the gut by microbiota, where trimethylamine (TMA) is produced which is metabolized to trimethylamine-N-oxide (TMAO). TMAO has been shown to lead to atherosclerosis in mice and has been shown in humans to predict cardiovascular diseases and major cardiac adverse events. Therefore it may be a good idea to administer L-carnitine via an alternative route to bypass the gut microbiota [115].

1.7 Cardiac Effects of Mildronate: Lowering L-Carnitine Levels

Mildronate $(3-(2,2,2-trimethylhydrazinium)-propionate)$ also called Meldonium or MET-88 is an anti-ischemic drug used in the treatment of cardiovascular disease [49, 241]. Mildronate lowers the levels of L-carnitine in the body and therefore inhibits fatty acid oxidation. Mildronate has several mechanisms of actions, and not all are clearly understood. Mildronate inhibits L-carnitine biosynthesis by being a competitive inhibitor of γ-butyrobetaine hydroxylase (BBOX) (Fig. 1.4), which is located in the kidneys, the liver and in the brain [50, 251]. Mildronate also affects L-carnitine concentrations in tissues by inhibiting L-carnitine re-absorption in the kidneys through blockage of organic cation/carnitine transport type 2 protein (OCTN2) and thereby increases the clearance of L-carnitine via urine. Mildronate is a very weak inhibitor of Carnitine AcetylTransferase (CrAT), that regulates the ratio between acetyl-CoA and free CoA, as well as a weak inhibitor of Carnitine AcylCarnitine Translocase (CACT), which is responsible for the transport of acetylcarnitine in and out of the mitochondrial matrix (Fig. 1.5) [50].

Mildronate is used as an anti-ischemic drug in Eastern Europe, where it has been shown to precondition the heart to use more carbohydrates for energy production, by inhibiting L-carnitine biosynthesis and L-carnitine uptake. It reduces fatty acid oxidation which becomes useful in an ischemic event. Effects of long-term treatment with Mildronate on heart tissue have been shown to be dependent on the dose, and that extended treatment beyond four weeks shows no additional lowering of L-carnitine levels. Interestingly Mildronate has shown no positive nor negative effects on the healthy heart during ischemia reperfusion, proving its safety [137]. In a model of T2D, Mildronate has been shown to lower glucose levels after eight weeks of treatment without any effects on insulin levels. Mildronate treatment has been shown to reduce the necrotic area by 30 % in ischemia reperfused *ex vivo* hearts [137]. Vilskersts *et al.* showed that Mildronate decreased the necrotic area by 50 % after only 14 days of oral treatment in the ischemia reperfused *ex vivo* heart [270]. Mildronate leads to an accumulation of γ-butyrobetaine, showing an

association between γ-butyrobetaine accumulation and smaller infarcts size [134, 227]. The drug has also been shown to lower glucose levels as well as triglycerides in the streptozotocin-induced T1D rat model [245]. Diabetes reduces the expression of GLUT4, but Mildronate treatment has demonstrated increased expression of GLUT4 in the isolated mouse heart [135], suggesting a mechanism for the lowering of blood glucose levels [246].

In conclusion when considering the results from the studies investigating L-carnitine supplementation and also Mildronate supplementation, it is possible that both the elevated availability of L-carnitine but also the reduced availability of L-carnitine could both stimulate carbohydrate metabolism, depending on the specific physiological and pathological conditions, and therefore both can affect the overall metabolic state [137].

There is mixed evidence on what effect L-carnitine has on the heart. This is partly due to the *ex vivo* methodologies used in the investigation of metabolism and function. However recently more technology has become available that allows for *in vivo* imaging of cardiac function and metabolism, which might be able to elucidate some of the effects L-carnitine has on the heart.

1.8 Technologies for Cardiac Assessment

In vivo imaging of cardiac function and metabolism is of critical importance for both diagnosis and also for investigating treatment response.

Cardiac function can be assessed with several imaging technologies, like echocardiography, PET, cardiac computed tomography (CT) and MRI. Depending on the severity of the disease, required re-visits, location of the patient, and also a cost-benefit analysis prescribes the most suited imaging technology for every patient.

1.8.1 Echocardiography

The most widely used technology in cardiology is echocardiography, which uses ultrasound to create images. A transducer array emits acoustic pulses in a given direction, and the same transducer then records acoustic echoes that are transmitted by the different tissues along the specific direction [276]. It has evolved from simple Brightness mode (B-mode: imaging two dimensional images) and Motion mode (M-mode: imaging valve motion, wall size and cardiac function) into Pulse Wave Doppler (PWD: determining the velocity of blood), Colour Doppler Imaging (CDI: visualizing if blood is moving towards or away from the transducer), to Tissue Doppler (TD: imaging fast movement of tissue) and finally into transthoracic echocardiography (TTE: 3D imaging, by repositioning the transducer to obtain several different acquisitions for reconstruction). A combination of all these provides structural and functional information of the chambers, the pericardium, valves, as well as blood flow information. Echocardiography is used for detection of hypertrophied and dilated cardiomyopathies, in cases of suspected cardiac failure and the diagnosis of valve disease. Diabetes and high glucose levels can have an adverse effect on left ventricular function, and advanced echocardiography has proven a successful imaging modality for detecting cardiac abnormalities [197, 18]. Left ventricular dysfunction starts with a diastolic dysfunction as an early sign of heart failure in diabetic patients [190], the diastolic function can be measured well with echocardiography. Echocardiography is widely accessible and has a low cost in contrast to other imaging modalities. However it only offers a semi-quantitative assessment of the diastolic

function, poor visualisation of deeper lesions, the images have lower resolution than other modalities and the field of view is limited. Echocardiography is highly operator-dependent: the orientation of the probe is controlled by an operator's hand. Ultrasound needs a medium to propagate in, and structures can be hard to image if bone, air, or accumulation of fat, are in the way [250].

1.8.2 Computed Tomography (CT)

Cardiac computed tomography (CT) uses multiple x-ray measurements obtained 360 degrees around the patient. The images are reconstructed to generate 3D images. Usually, a coronary CT angiography is performed which requires the injection of a contrast agent (iodine), this has increasingly been used recently for detection of coronary heart disease especially in combination with a stress test [250]. In addition, it is good at imaging calcium in the arteries, to determine if they are blocked or narrowed by the buildup of plaque, which is a strong indication for atherosclerosis. The downside is that it requires a low heart rate due to motion artefacts and has little ability to distinguish normal from abnormal tissue. Furthermore, it exposes the patient to ionising radiation. Although there are discrepancies in the effective dose cardiac CT exposes to patients, it has shown to be almost five times higher than that of positron emission tomography [242, 236].

1.8.3 Positron Emission Tomography (PET)

Positron emission tomography (PET) is a functional imaging technology that detects radiation from the patient that has been injected with a radioactive tracer. The nuclei usually used, have a short half-life, because nuclei with longer half-life would expose the patient to unnecessary radiation. The nuclei are incorporated into a compound that the body usually uses. The most common PET tracer is fluorodeoxyglucose (FDG), an analogue of glucose, that is labelled with ^{18}F (half-life: 110 minutes) and is used to show altered areas of glucose uptake, where glucose uptake and glucose oxidation are not distinguished by imaging. Once distributed in the body, the nuclei emit a positron, which annihilates with an electron (typically

within 1 mm diameter from emission), and produces two gamma rays travelling in opposite directions [236]. These gamma rays are detected by the PET scanner allowing for visualisation of the FDG uptake in the body. Most PET scanners are combined with a CT scanner, and more recent advances have managed to merge them with MRI scanners allowing for co-registration of functional images on top of anatomical images. Cardiac PET has recently become more popular for imaging of several conditions like coronary artery disease, atherosclerosis and inflammation. FDG is taken up by the heart similar to glucose, hereafter it is phosphorylated to FDG-6-phosphate, and it stays trapped inside the myocardium because it is not a good substrate for glycogen synthesis nor glycolysis [152]. During an ischemic event, FDG shows decreased regional FDG uptake. However, exposure to radiation is an important concern and should be considered carefully, especially when repeated scans are necessary, or the patients are children or women in their reproductive age.

1.8.4 Magnetic Resonance Imaging (MRI)

Magnetic resonance imaging (MRI) does not use any form of ionising radiation and is completely safe for the patient. MR imaging is a medical application of NMR[1]. It uses strong magnetic fields, magnetic field gradients and radio waves to image hydrogen atoms in the body although it can also image other nuclei. Cardiac MRI is relatively new to the clinic and access to it can be limited due to cost. MRI is used often in adjunct to other imaging modalities if further information is needed. However it can provide precious information for several diagnostics and treatment responses while being harmless to the patient [250]. The guidelines (Task Force Report) for when cardiac MRI should be used in the clinic were divided into four classes in 1998 [196], and have continued to stay the same, even though cardiac MRI has advanced significantly since 1998. The lack of ionising radiation is why MRI has proven to be a superior imaging technology when evaluating treatment response, but also when imaging children and women in their reproductive age. It becomes the main imaging technology, when scar tissue, lungs or fat obstruct the field of

[1]The physics and chemistry fields refer to this technology as NMR, the imaging community has omitted "nuclear" due to its negative association to radiation.

view for echocardiography and is less operator dependent than echocardiography imaging. When compared to cardiac CT, cardiac MR can not image calcium, which is important for detecting calcifications in coronary arteries and are signs of atherosclerosis or coronary heart disease. However, despite lack of calcium imaging, cardiac MR allows for precise and accurate measurements of chamber size and volumes as well providing great information about soft tissues, blood flow, and even allows for metabolic imaging. All this makes it an excellent modality for imaging complex conditions [196].

1.8.4.1 A Brief Introduction to MRI

The first paper in nuclear magnetic resonance (NMR) was published in 1946, and the impact of it was already recognised in 1952 when the Nobel Prize in Physics was awarded to Bloch and Purcell [19, 16].

Nuclei (^{1}H, ^{13}C, ^{23}Na, and ^{31}P) are not only magnetic but also rotate around their own axis; this is called "spin" (Fig. 1.7), which makes the nuclei magnetic along the rotational axis, called precession. More precisely they possess an intrinsic form of angular momentum.

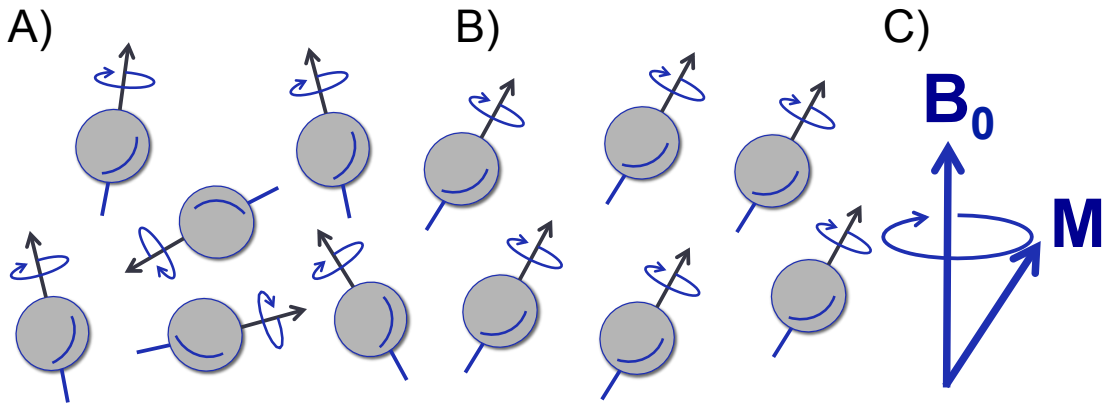

Figure 1.7: The spin of the nuclei (rotation) makes them magnetic. **A)** Nuclei that are pointing in different directions outside a magnetic field. **B)** Nuclei that are aligned in a magnetic field. **C)** A magnetization (M) that precess around the magnetic field (B_0) because of the spin (rotation around M).

The body contains mostly water, and therefore what is usually imaged with magnetic resonance imaging is hydrogen nuclei (^{1}H), also called protons. Once

a subject is put in an MR scanner, the protons will partially align in the field, and a net magnetization will form along the magnetic field of the scanner. The net magnetisation is temperature and field strength dependent since the nuclei will interact with each other in the body.

The net magnetisation can be pushed away from equilibrium, so it does not point along the magnetic field any more (B_0), it will precess around the field with a frequency proportional to the product of the external magnetic field and the gyromagnetic ratio (γ, an intrinsic property of each nucleus) and eventually return to equilibrium (relaxation). This precession frequency is called the Larmor frequency (Eq.1.1) [62].

$$f = \gamma B_0 \tag{1.1}$$

The application of a magnetic field (B_1) also know as radio waves (RF pulses) applied at the above frequency will rotate the net magnetisation away from its equilibrium. During the relaxation, radio waves will be emitted by the body, which can be measured. The relaxation happens at two time scales. The magnetisation that is perpendicular to the magnetic field, also called transverse magnetization (M_{xy}), decreases exponentially on a time scale called T_2 relaxation. And the magnetization that is parallel to the field, the longitudinal magnetization (M_z), recovers to equilibrium, M_0, on a time scale called T_1 relaxation. The Bloch equations (1.2) describe the relationship between the magnetisation and the relaxation times. Following a 90° RF pulse. Equation 1.3, 1.4, and 1.5 describe the solutions to the Bloch equations [62].

$$\frac{d\mathbf{M}}{dt} = \mathbf{M} \times \gamma \ \mathbf{B} - \frac{M_x \ \mathbf{i} + M_y \mathbf{j}}{T_2} \frac{(M_z - M_0)\mathbf{k}}{T_1} \tag{1.2}$$

$$M_x(t) = M_0 e^{-t/T_2} \sin(\omega t) \tag{1.3}$$

$$M_y(t) = M_0 e^{-t/T_2} \cos(\omega t) \tag{1.4}$$

$$M_z(t) = M_0(1 - e^{-t/T_1}) \tag{1.5}$$

where:

γ = Gyromagnetic ratio

T_1 = Longitudinal-z relaxation time constant

T_2 = Transverse-xy relaxation time constant

M_0 = Equilibrium magnetization due to B_0 field

i,j,k = Unit vectors in x,y,z- directions

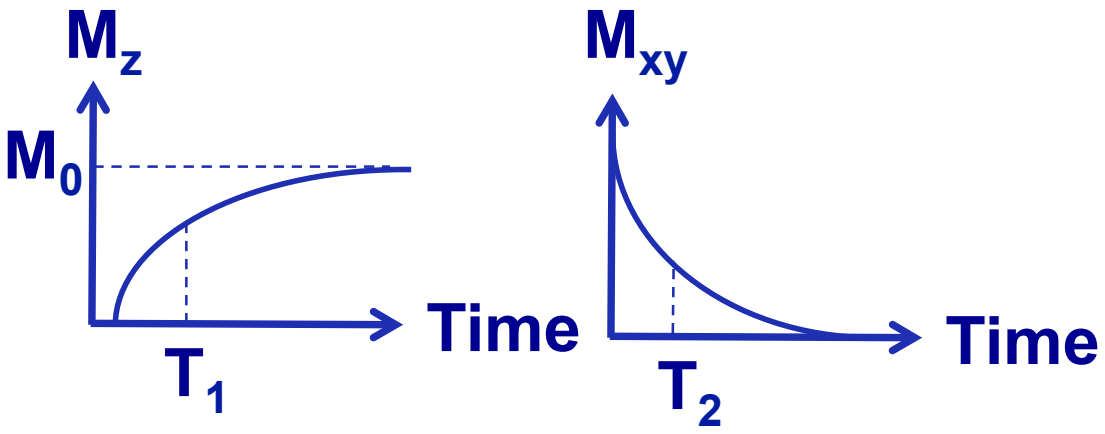

Figure 1.8: The longitudinal relaxation time (T_1) represents the time that is required for M_z to grow from zero to $(1 - 1/e)$. The transversal relaxation time (T_2) represents the time that is needed for (M_x or M_y) to decay down to $(1/e)$ magnetisation

MR scanners are equipped with gradient coils that vary the magnetic field linearly in addition to B_0. This field still leaves the combined magnetic field pointing in the z-direction, but the field strength will vary along the G_x or/and G_y or/and G_z direction. Gradient coils are therefore used for slice selection, k-space encoding, and a lot more.

Diseased and healthy tissues show significant differences in the relaxation times, and by designing pulse sequences with different characteristics, the differences in relaxation times can be exploited to generate high contrast for images [200].

Continued advances of magnetic resonance imaging (MRI) are fostering novel applications. One of the most new advances has been hyperpolarized MRS.

1.8.4.2 A Brief Introduction to MR Spectroscopy (MRS)

The application of ^{1}H, ^{23}Na, ^{31}P, and ^{13}C for MRS is dependent on their natural abundance but also on their concentrations in tissue. ^{1}H, ^{23}Na and ^{31}P all have a high natural abundance, but only ^{1}H is present in high concentrations in the body. In addition, ^{1}H also has the highest gyromagnetic ratio, which is why protons are also the basis for MRI [200]. Chemical shift provides the basis for MRS, that can map the spatial distribution of compounds with a different chemical shift. A small displacement of the resonance frequency caused by orbital motion of the electrons surrounding the nuclei (called shielding) is called a chemical shift. The chemical shift is defined with respect to a reference frequency and is displayed in parts per million (ppm). The amplitude illustrates the number of nuclei present at that specific frequency. In MR imaging the desire is to obtain the magnetisation distribution, and the combined contribution of the different chemical shifts are added in every image, $I(x, y)$. This is described by equation 1.6 . However in MRS, the desire is to obtain an image, $I(x, y, f)$, that gives both spatial localisation and separates chemical shift for the different components, obtaining a spectrum at each location [62].

$$I(x, y) = \int m(x, y, f)df \tag{1.6}$$

where:

$$\begin{aligned} I(x, y, f) &= \text{MRS image} \\ I(x, y) &= \text{MRI image} \\ m(x, y) &= \text{Magnetisation distribution} \\ f &= \text{Chemical shift} \end{aligned}$$

Each image point is equal to the integrated value of m(x,y) at that point over all chemical shift components [62].

1.8.5 Cardiac MR Spectroscopy (MRS)

Cardiac MR spectroscopy (MRS) offers a non-invasive and non radioactive imaging modality to study myocardial metabolism. Myocardial energetics have been investigated with several nuclei with a nuclear spin [257], the most common are ^{1}H, ^{23}Na, ^{31}P and ^{13}C. All nuclei have a lower sensitivity than ^{1}H, that is the nuclei most abundant in our bodies. ^{1}H can image all metabolites in the body, and compared to the other nuclei it has a good signal to noise ratio (SNR); however all ^{1}H spectra require suppression of the water (H_2O) resonance due to its high abundance in the body [257]. Despite a low sensitivity, studies have shown impairment in myocardial lipids, and creatine in patients with dilated cardiomyopathy [271] and other studies have supported ^{1}H MRS' value in monitoring myocardial metabolism especially lipids, which are more abundant than metabolites [260, 219].

The first cardiac ^{31}P MRS was obtained from an isolated rat heart [74], demonstrating almost a five hour stability of heart function, when perfused in a Langendorff mode. Resonances from the three phosphate groups of ATP, creatine phosphate (PCr) and inorganic phosphate (P_i) can be obtained, which otherwise are hard to measure in tissue samples due to their instability [179], giving ^{31}P MRS its advantages. The presence of diabetes accelerates heart failure in people with myocardial infarction. Myocardial infarction has shown to decrease the PCr/ATP ratio even in remote regions away from the infarction [174] and most studies showing a shift of balance in the energy state performed on the failing heart have been done with ^{31}P MRS. The PCr/ATP ratio has been shown to reduce in heart failure, in type 1 diabetes and with systolic and diastolic dysfunction [179, 123, 178, 234]. ATP is maintained throughout life, but PCr will decrease with age and disease. Many studies have shown altered energetics in both *ex vivo* and *in vivo* hearts, and the PCr/ATP ratio is an excellent index for assessment of the cardiac energy state.

Like the first cardiac ^{31}P MRS, the first cardiac ^{13}C MRS was also obtained in the isolated perfused rat heart [123]. This technique has made it possible to study myocardial biochemistry, where the incorporation of ^{13}C into glycogen and amino

acids have been demonstrated [232]. Cardiac ^{13}C MRS has shown in streptozotocin-induced diabetic rats that production of lactate and TCA intermediates is limited from glucose. However, with insulin plus dichloroacetate cardiac ^{13}C MRS has been demonstrated that pyruvate re-enters into the TCA cycle by increasing the incorporation of ^{13}C into glutamate and elevate glucose oxidation [37]. A major downside to cardiac ^{13}C MRS is that the natural abundance of ^{13}C is only 1.1 % and the resonance frequencies of the different metabolites are closely spaced, making it difficult to separate without heart tissue analysis [225]. ^{13}C MRS, therefore, has low sensitivity and requires long scan times, which is why most studies have been performed in the *ex vivo* heart. These studies have in addition high cost because they require ^{13}C labelled tracers.

This relatively low sensitivity of MRS has prevented cardiac MRS from becoming a standard clinical tool [257]. However, there have been recent advances in ^{13}C MRS called hyperpolarized ^{13}C MR technology using a dynamic nuclear polarisation technique, that might have what it takes for the clinic to adopt the technology.

1.8.6 A Brief Introduction to Dynamic Nuclear Polarisation

Dynamic Nuclear Polarisation (DNP) increases the polarisation of nuclear spins. One type of DNP was first described by Overhauser in 1953 [186]. Hyperpolarisation allows for the nuclear spins to be unequally distributed (Fig. 1.9CD). In MR, the signal strength is proportional to the degree of nuclear polarisation which is small for ^{13}C (Fig. 1.9AB). Figure 1.9A shows a thermal equilibrium spectrum of ^{13}C in a urea sample after a three hour acquisition. Figure 1.9C shows a hyperpolarized spectrum of ^{13}C in a urea sample after a one second acquisition illustrating the advantages of this technology in both acquisition time and SNR.

To obtain this very high SNR spectrum, a ^{13}C labelled compound is doped with a free radical (which allows for the presence of unpaired electrons) and is put into a high field magnet (> 3.35 T) at low temperature (< 1.2 K). DNP works on the principle that unpaired electrons are easily polarised (90 %) at low

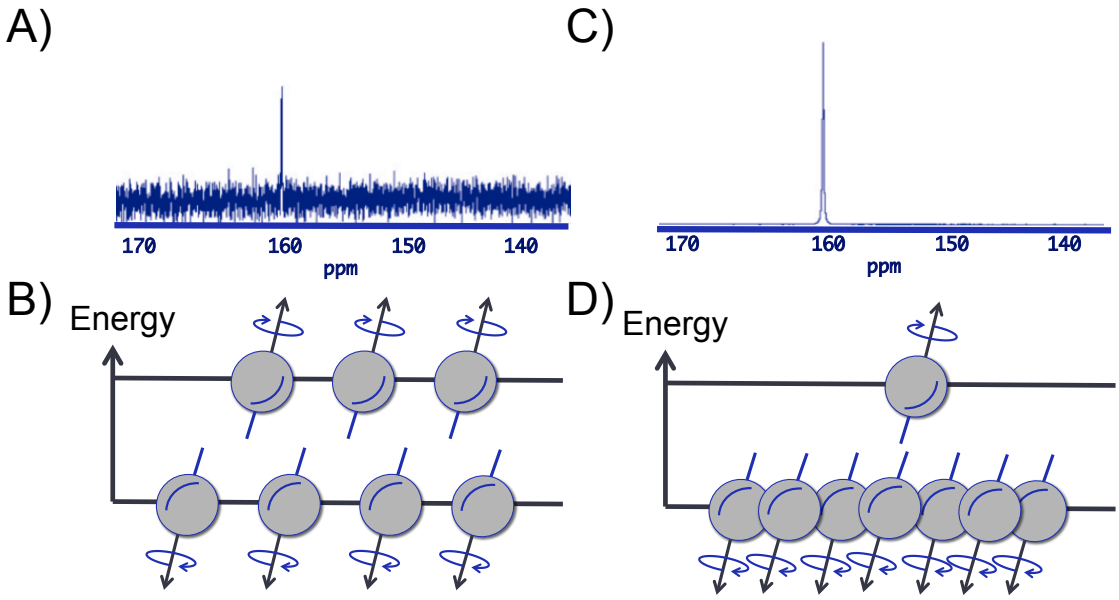

Figure 1.9: Thermal equilibrium of a 3 hour acquisition of ^{13}C (AB). Hyperpolarisation of a 1 second acquisition of ^{13}C (CD). Adapted from Ardenjaer-Larsen *et al.* [7] and Schroeder *et al.* [222]

temperatures in a magnetic field, while the ^{13}C nuclei are still polarized below 0.1 % [42, 80]. Microwave radiation applied to the sample with a frequency close to the Larmor frequency of the electron (Equation 1.7), induces a polarisation transfer from electron to the nuclei;

$$\omega_m = \omega_e - \omega_n \tag{1.7}$$

ω_e = Larmor frequency of the electron

ω_n = Larmor frequency of the nuclei

ω_m = Microwave irradiation frequency

The polarisation is only obtained at these low temperatures, which is why it was very hard to imagine how this technology could be used for *in vivo* imaging. However, the breakthrough came in 2003, when it was demonstrated how to maintain the high polarisation while transitioning from a solid state to a liquid state

(dissolution process) allowing for *in vivo* imaging in animals and humans (Fig. 1.10). The dissolution process is an engineering challenge, and Ardnekjaer-Larsen *et al.* described the first dissolution process in 2003 (Fig. 1.9AC) using hyperpolarized ^{13}C labelled urea, followed rapidly by the first *in vivo* hyperpolarized [1-^{13}C]pyruvate injection in rodents, where real-time metabolism was observed [79].

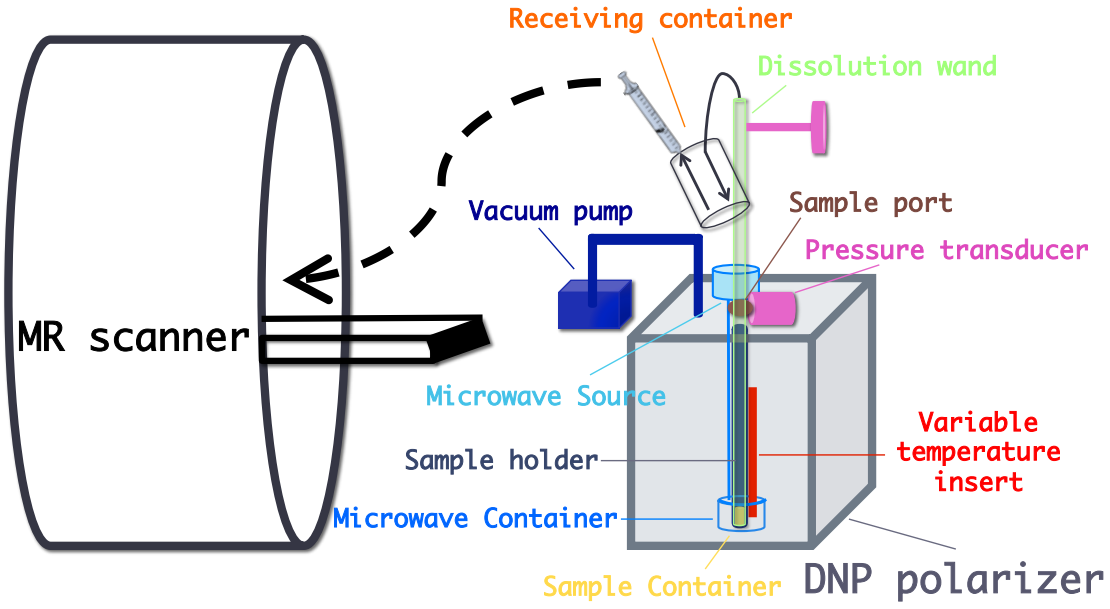

Figure 1.10: The polariser has a magnet of 3.35 T (modified Magnex, Oxford), it is adjusted to contain a stainless-steel tube that ends in a heat exchanger connected via a capillary tube to a liquid helium dewar, all this is called the variable temperature insert (red). A needle valve controls the flow of helium. A DNP insert is made from fibreglass to guide the sample into the cooled magnet bore. The fibreglass ends in a metal container for microwave irradiation; Microwave container (blue). The helium vapour is measured by a pressure transducer (pink), and a stepper motor controls the opening and closing of the needle valve. The vapour pressure is used to measure the temperature, and the vacuum pump (purple) is able to sustain the vapour pressure. A Teflon tube makes up the sample holder (grey) and is used to hold the sample container (dark yellow) in place and to enable elevation just prior to dissolution. The sample holder (grey) with the sample container (dark yellow) is loaded into the polariser through the sample port (brown), that is then closed off with a rubber piece. Microwave irradiation is started, and the sample is submerged in liquid helium. Before dissolution, microwaves are turned off, and the insert is pressurized with liquid helium. The sample holder and container are lifted out of the liquid helium 10 cm. The dissolution wand (green) is prepared with boiling buffer and is inserted into the sample holder and connected to the sample container. The buffer is injected rapidly through one tube in the dissolution wand, it is mixed with the sample and ejected through another tube in the dissolution wand into the receiving container (orange). Adapted from Ardenjaer-Larsen *et al.* [7]

1.8.7 Hyperpolarized ^{13}C MRS using Dynamic Nuclear Polarisation

Dynamic nuclear polarisation (DNP) allows for hyperpolarisation of ^{13}C labelled compounds, which leads to a $>$ 10,000 times higher SNR than previously available for ^{13}C. The advances in this technology allow for hyperpolarisation of ^{13}C in the solid state to be preserved and transferred into a liquid state that is ready for injection in subjects [7].

This technology has mainly been applied to ^{13}C labelled pyruvate, but research has been conducted on ^{13}C labelled lactate [40, 158], butyrate [172, 14, 11], acetate [69], acetylcarnitine [114] and many more. It allows for *in vivo* imaging of the myocardium, it can both produce an image but also high temporal resolution dynamic spectra of *in vivo* metabolism previously not visible with MRS and as such pre-clinical applications have been exponentially rising.

The first cardiac hyperpolarized [1-^{13}C]pyruvate image has been obtained from pigs in 2006 by Golman *et al.*, displaying the potential of this technology for cardiac applications [78]. Golman *et al.* have shown metabolic alterations in ischemic regions, that otherwise are not visible on MRI [78]. Ever since an increased amount of publications have demonstrated that cardiac metabolism is altered in heart diseases using hyperpolarized [1-^{13}C]pyruvate.

Atherton *et al.* have shown that in hyperthyroid induced hypertrophy, glucose oxidation is inhibited and that through stimulation of glucose oxidation, the hypertrophy can be reduced [10]. Seymour *et al.* have shown increased incorporation of ^{13}C into lactate [228], but there is a lack of change in pyruvate dehydrogenase flux in the hypertrophied rat heart. This suggests that the increase in lactate is caused by an elevation in glycolytic flux and therefore demonstrates an uncoupling between glucose oxidation and glycolysis [228].

Diabetes has been shown to affect myocardial metabolism using hyperpolarized [1-^{13}C]pyruvate. Le Page *et al.* showed that myocardial metabolism could be restored with dichloroacetate in a T2D model while also normalizing glucose levels and diastolic function [126]. In a streptozotocin-induced T1D rat model it has

been shown that there is an elevation of ^{13}C incorporation into lactate in the kidneys and liver [125, 171], and Schroeder *et al.* have shown decreased PDH-flux five days post STZ injection [223] but no studies have been investigating the metabolic and functional changes that occur *in vivo* in a T1D rat beyond five days or with therapeutic treatments.

A great deal of pre-clinical research has been conducted not just on cardiac metabolism but on prostate, liver, and renal cancers [177, 61, 110], gliomas [189, 39], and other diseases, such as spinal cord disease [188], using hyperpolarized [1-^{13}C]pyruvate. This technology proved to be a great tool for both diagnosis, evaluating progression and treatment response. All this led to the first-in-human trial conducted in prostate cancer patients. These patients had received a hyperpolarized [1-^{13}C]pyruvate injection and it (a) proved safe, (b) showed increased production of lactate in biopsy proved cancers, and (c) even managed to detect a lesion that would otherwise have been missed using the gold standard clinical practice. This technology could possibly revolutionise cancer treatment monitoring [177].

Cardiac clinical translation of this technology has shown great potential for imaging several cardiac diseases [211], and only a few years after this first-in-human scan (which was imaging the prostate with the technology), the first human hearts were imaged. These cardiac images show that ^{13}C incorporation into bicarbonate is confined to the myocardium and lactate is obtained from both the left ventricle and from the myocardium [48]. The first cardiovascular spectrum shows a 'second pass' of pyruvate that generally is not observed in rodents [6].

Hyperpolarized ^{13}C pre-clinical and clinical studies are exponentially growing. More pre-clinical research is emerging due to its fast clinical translation. A more thorough understanding of myocardial metabolism in pre-clinical models will allow for improved pharmacological studies and better targeted drugs for cardiovascular diseases in patients [59].

1.9 Aims

A better understanding of the effects of L-carnitine on the myocardium is needed to improve pharmacological studies and obtain targeted drugs for cardiovascular and diabetic diseases. The work in this thesis aims to elucidate our understanding of the metabolic and functional changes that occur in the diabetic myocardium over time when elevating or reducing L-carnitine levels.

Initially, this is accomplished by establishing and following the progression of an appropriate model of T1D with cardiac dysfunction. Both a neonatal model of diabetes, and four different streptozotocin-induced T1D models are investigated, to explore the functional and metabolic alterations in the heart, and to establish the best model that can be used for studying the treatment effects in subsequent chapters.

The treatment comprises of elevating or reducing L-carnitine levels in the plasma. Given the overview in the introduction, L-carnitine clearly has a prolonged effect on cardiac structure and metabolism. It is therefore vital to be able to understand the *in vivo* metabolic remodelling that occurs in the heart using hyperpolarized ^{13}C MRS. Likewise, and maybe, in contrast, Mildronate has shown improved functional and metabolic changes, although Mildronate inhibits L-carnitine synthesis, therefore investigating these effects in the *in vivo* myocardium could be crucial to our understanding of myocardial metabolism in diabetes and L-carnitine's role. Initially pilot studies aim to validate if L-carnitine and Mildronate could, in fact, be altered in the plasma of daily treated animals. Furthermore, an optimal ischemic low-flow rate is established so that the subsequent chapter can investigate metabolic and functional recovery post-ischemia.

The main chapter of this work aims to investigate the effects of L-carnitine supplementation on cardiac metabolism and function in the diabetic rat heart. Following two weeks of treatment, all animals are scanned with hyperpolarized [1$-^{13}$C]pyruvate and [2$-^{13}$C]pyruvate to investigate TCA cycle intermediates as well as acetylcarnitine levels. Cardiac function is assessed *in vivo* with both echocardiography and CINE MRI. Ischemia reperfusion Langendorff perfusions are

undertaken in a subgroup of animals to establish functional recovery and fatty acid oxidation rates post-ischemia. Subsequently, blood profile and metabolomics in the heart are assessed to validate the *in vivo* findings.

Finally, the aim is to explore the metabolic and functional alterations in the heart with daily Mildronate treatment, which reduces L-carnitine uptake. Following two weeks of treatment all animals are scanned with hyperpolarized [1$-^{13}$C] pyruvate and [2$-^{13}$C]pyruvate to investigate TCA cycle intermediates and acetylcarnitine levels *in vivo*. Cardiac function is assessed *in vivo* with both echocardiography and CINE MRI. Functional and metabolic changes are induced in all animals by ischemia reperfusion using a Langendorff method of the isolated heart to validate the *in vivo* findings.

The work undertaken for this thesis aims to understand the underlying mechanism of L-carnitine treatment on the diabetic heart to elucidate our understanding of the diabetic myocardium allowing for better targeted drug therapies in the future.

1.9.1 Summary of Chapters

(1) Chapter 3 describes a characterization of a genetic model of neonatal diabetes (NDM) and of a streptozotocin (STZ) induced rat model and the remodelling of myocardial metabolism and function over time.

(2) Chapter 4 establishes a Langendorff low-flow ischemic rate and explores the effects of L-carnitine added acutely to the perfusate buffer in healthy ischemia re-perfused hearts. Furthermore, it establishes the feasibility of daily i.p. injections on healthy animals using L-carnitine or Mildronate supplementation.

(3) Chapter 5 evaluates the *in vivo* and *ex vivo* effects of L-carnitine on myocardial metabolism and function.

(4) Chapter 6 assesses the *in vivo* and *ex vivo* effects of Mildronate on myocardial metabolism and function.

The first approached the elephant,
And happening to fall
Against his broad and sturdy side,
At once began to bawl,
"Bless me, it seems the elephant
Is very like a wall."

2 General Methods

Contents

2.1 Animal Protocol 40
2.2 Induction of Diabetes using Streptozotocin 40
2.3 Reagents 41
2.4 Imaging Technologies 41
2.4.1 CINE MRI for Assessment of Cardiac Structure and Function in the Rat 41
2.4.2 CINE MRI for Assessment of Cardiac Structure and Function in the Mouse 45
2.4.3 Hyperpolarized ^{13}C MRS for Assessment of Cardiac *In Vivo* Metabolism 45
2.4.4 Echocardiography for Assessment of Cardiac Function . 49
2.5 Langendorff Perfusions 49
2.5.1 Krebs-Henseleit and Albumin Buffer Preparation 49
2.5.2 Palmitate Stock Preparation 50
2.5.3 Radioactive ^{3}H Palmitate Albumin Krebs-Henseleit Buffer Preparation 51
2.5.4 Langendorff Ischemia Reperfusion Protocol 51
2.5.5 Assessment of Cardiac Function 54
2.5.6 Measurement of Myocardial Palmitate Oxidation 55
2.6 Tissue Collection 57
2.7 Extractions for Metabolomics 57
2.8 Blood Analysis 58
2.9 Biochemical Analysis 58
2.9.1 Non-Esterified Fatty Acid Assay 58
2.9.2 Insulin ELISAs 59
2.9.3 L-Carnitine ELISAs 59
2.9.4 Western Blotting 60
2.10 Statistical Analysis 61

This chapter gives a summary of the general methodology used throughout this thesis to avoid repetition. Specific methods are summarised in each experimental chapter.

2.1 Animal Protocol

All procedures were reviewed and approved under the Home Office Guidance on the Operation of the Animals (SCIENTIFIC PROCEDURES) ACT 1986 and were carried out by a personal license holder. All experiments were also approved by the University of Oxford ethics review board.

Animals were housed on a 12:12 hour light-dark cycle at animal facilities at the University of Oxford (Biomedical Sciences Services, University of Oxford, UK). All animals were fed standard chow and water (Harlan Laboratories, Kent, UK) *ad libitum*. When animals were fasted, the chow was taken away between 6-7 pm, and animals were re-fed before 12 pm on the following day.

All *in vivo* magnetic resonance imaging was performed in the fed state (between 6 am - 1 pm).

2.2 Induction of Diabetes using Streptozotocin

The induction of diabetes was done with a single i.p. injection of streptozotocin (STZ) in the conscious fasted state. STZ was purchased from Sigma-Aldrich (St. Louis, MO, USA) and was prepared fresh on the day (either 25 mg/kg or 55 mg/kg) in 0.1 M citrate buffer (pH = 4), and 300 μl was injected in each animal.

Animals were provided with a drink of 15 % D-glucose in water for the first two days post STZ injection in addition to their regular water. All diabetic animals were housed on absorbent bedding (alpha cellulose, which is a paper based material with high absorbency) (LBS Serving Biotechnology, UK). Animals were considered diabetic if a urine-glucose test was positive for two consecutive days post STZ injection and also had fasted blood glucose levels above 8.8 mmol/L one week

post STZ injection. Animals were also excluded from the study if blood glucose levels reached above 30 mmol/L and/or they looked sick. Weight was monitored daily if treated with a compound, otherwise weekly. All fasted blood glucose levels were taken with a hand-held Accu-Check Aviva blood glucose meter (Roche, Basel, Switzerland) and all fasted ketone levels were taken with a hand-held FreeStyle OptimumH meter(Abbott, Illinois, USA) under 2.5 % isoflurane vol:vol in 1 litre/min O_2. Urine glucose was measured with reagent strips for urinalysis (Dirui, Jilin, China) in the conscious fed state.

Animals that were treated with L-carnitine were treated with daily intraperitoneal (i.p.) injections of 3 g/kg/day L-carnitine in 600 μl of saline. Saline treated animals were matched and treated with the same 600 μl volume as L-carnitine treated animals. Animals that were treated with daily i.p. injection of Mildronate were treated with 100 mg/kg/day obtained in ampoules (Grindex, Riga, Latvia), and the volume injected corresponded to the body weight of the rat in μl. Saline treated animals were matched and treated with the same volume as Mildronate treated animals.

2.3 Reagents

All reagents were purchased from Sigma-Aldrich Company Ltd. (St. Louis, MO, USA) unless otherwise stated.

2.4 Imaging Technologies

2.4.1 CINE MRI for Assessment of Cardiac Structure and Function in the Rat

Rats were anaesthetised using 2.5 % isoflurane vol:vol in 1 litre/min O_2 and positioned in a 7T horizontal bore MR scanner interfaced to a Direct Drive console (Varian Medical Systems, U.K.), using a ^{1}H phased array 4-channel surface receive coil (RAPID Biomedical GmbH, Germany) and a 72 mm ^{1}H volume transmit coil.

A FLASH localizer was acquired to confirm the location of the heart with the following parameters: TR/TE, 3.22/1.34 ms; flip angle, 15 °; Averages, 4; slice thickness, 2 mm; matrix, 128 × 128; field of view, 12.8 × 12.8 mm [57].

Four axial slices were acquired with the following parameters: TR/TE, 3.33/1.45 ms; flip angle, 15 °; Averages, 4; slice thickness, 1.6 mm; matrix, 128 × 128; field of view, 12.8 × 12.8 mm in order to obtain sagittal slices of the heart. Sagittal slices were acquired with electrocardiogram gating (ECG) to define the axis of the heart. Initially, a slice was placed on the heart to obtain a long-axis acquisition of a two-chamber view, which was used for the subsequent acquisition of a four-chamber view, that then was subsequently used to ensure a correct plane of a short-axis view of the mid left ventricle to be acquired (Fig. 2.1).

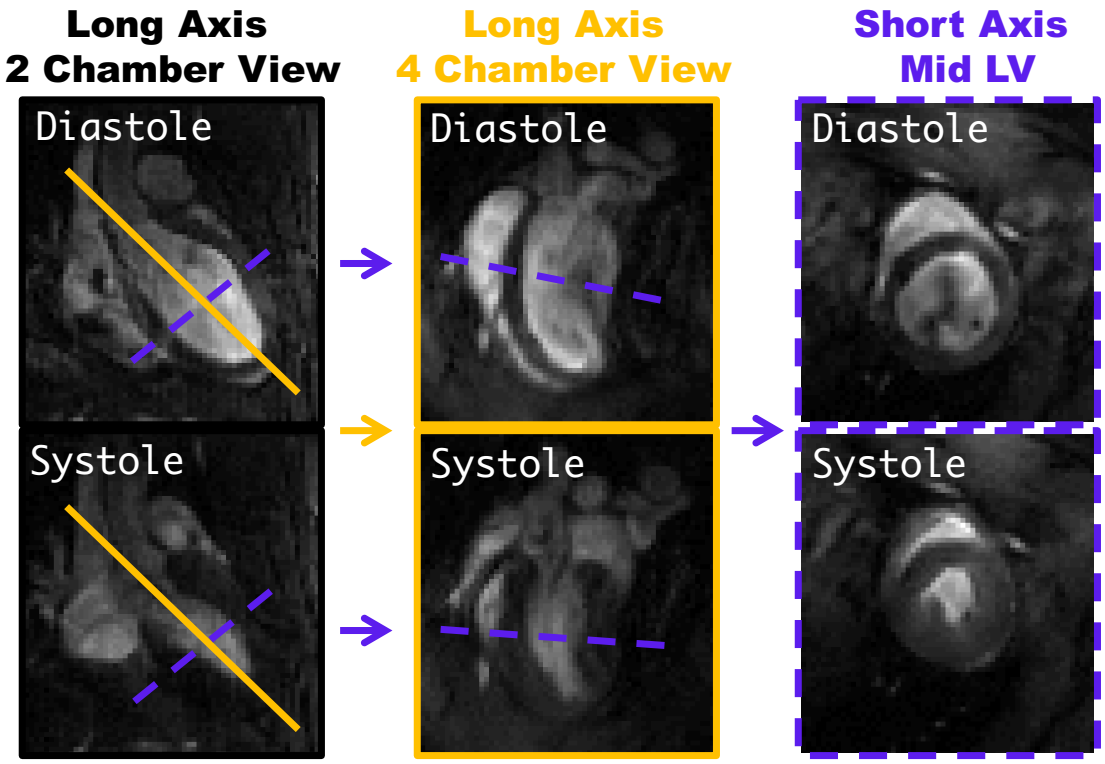

Figure 2.1: A schematic overview of a two-chamber and four-chamber long axis view of the heart and the respective slices that are prescribed in order to obtain a four-chamber view and a mid left ventricle (LV) short axis view.

Global shimming was applied with ECG gating to reduce the proton linewidth to < 250 Hz. The images were acquired with a CINE-FLASH sequence [89]. Imaging parameters were set as: slice thickness: 1.6 mm, matrix size: 128×128, TE/TR:

4.60/1.46 ms, flip angle: 18°, and number of averages: 4. The CINE-FLASH sequence was used to acquired eight-ten short-axis slices with around 30 frames per cycle, to cover the entire heart from base to apex (Fig. 2.2).

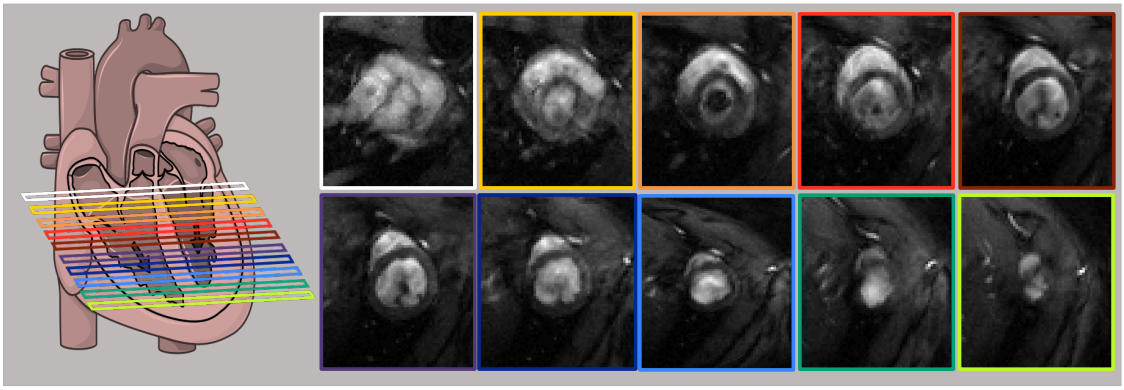

Figure 2.2: A schematic overview of the heart slices. The heart is shown in diastole and ten short axis slices acquired with CINE-FLASH. The slices are colour coded moving from the base of the heart (white) to the apex of the heart (light green)

2.4.1.1 Analysis of CINE MRI

For each heart, the end diastolic and end systolic frames were selected in accordance to maximum and minimum left ventricular volumes. Geometric and functional parameters were obtained through segmentation of these frames for every slice using the freehand draw function in ImageJ (NIH, USA) by drawing the epi- and endocardial borders (Fig. 2.3) to obtain volumes (i.e. area times slice thickness). The left ventricular volumes obtained were converted to left ventricular mass by multiplying the measured volume by the specific gravity for myocardial tissue (1.05 g/cm^3) [259]. The *in vivo* functional parameters were then subsequently calculated with the following equations.

Left Ventricular Mass (LVM) [mg]:

$$LVM = \frac{ESM + EDM}{2} \tag{2.1}$$

Stroke Volume (SV) [μl]:

$$SV = EDL - ESL \tag{2.2}$$

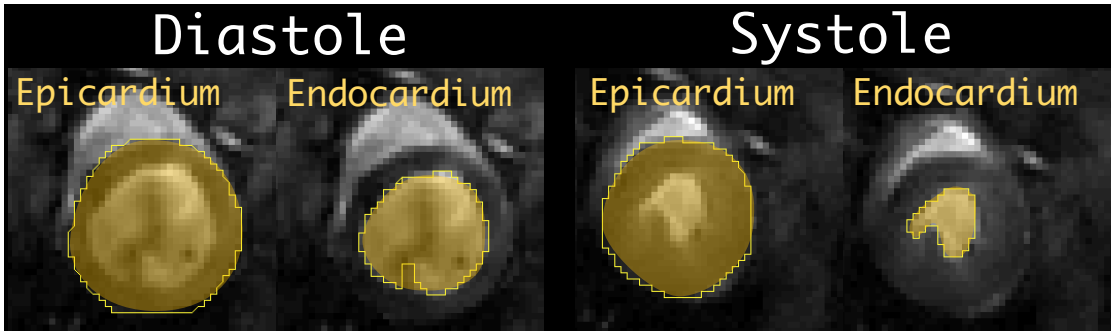

Figure 2.3: Short axis mid left ventricle slice in diastole (left) and systole (right). Yellow outline of the endocardium and epicardium using the freehand draw function in ImageJ. Schematic four yellow volumes show what is used for calculations of the left ventricular mass.

Stroke Index (SI) [μ/g]:

$$SI = \frac{SV}{BW} \tag{2.3}$$

Ejection Fraction (EF) [%]:

$$EF = \frac{SV}{EDL} \tag{2.4}$$

Cardiac Output (CO) [ml/min]:

$$CO = SV \times HR \tag{2.5}$$

Cardiac Index (CI) [ml/min/g]:

$$CI = \frac{CO}{BW} \tag{2.6}$$

where:

$$ESM = \text{End Systolic Mass [mg]}$$

$$EDM = \text{ End Diastolic Mass [mg]}$$

$$EDL = \text{ End Diastolic Lumen [}\mu\text{l]}$$

$$ESL = \text{End Systolic Lumen [}\mu\text{l]}$$

$$BW = \text{Body Weight [g]}$$

$$HR = \text{Heart Rate [bpm]}$$

2.4.2 CINE MRI for Assessment of Cardiac Structure and Function in the Mouse

Mice were anaesthetised using 2 % isoflurane vol:vol in 1 litre/min O_2 and positioned in an 11.7T vertical bore MRI system (Magnex Scientific, Oxon, UK) interfaced to a Bruker Avance console (Bruker Medical, Ettlingen, Germany) using a ^{1}H volume RF coil (Rapid Biomedical, Rimpar, Germany), and a shielded 500 mT/m gradient systems (Magnex Scientific, Oxon, UK). The images were acquired with a CINE-FLASH sequence [89] as described above, but only seven-eight ECG triggered slices were obtained with the following parameters: TE/TR: 1.43/4.6 ms; flip angle: 17.5°; Matrix size: 256 x 256; slice thickness: 1 mm, field of view: 2.56x2.56 cm, number of averages: 4. Left ventricular volumes were derived using the freehand draw function in ImageJ (NHI, USA). For each heart, left ventricular mass (LVM), ejection fraction (EF), stroke volume (SV) and cardiac output (CO) were calculated as described in the previous section.

2.4.3 Hyperpolarized ^{13}C MRS for Assessment of Cardiac *In Vivo* Metabolism

^{13}C pyruvate Preparation

Approximately 40 mg of [1−^{13}C] or [2−^{13}C] labelled pyruvic acid doped with 15 mM trityl radical (OXO63, GE Healthcare) and 3 μl Dotarem (for rat) and 2.5 μl Dotarem (for mouse) (1:50 dilution, Guerbet, Birmingham, UK), was hyperpolarized in a prototype polarizer (Oxford Instruments, UK). Microwave irradiation (94 GHz) was applied for approximately 30 min or 45 min, for [1-^{13}C]pyruvate or [2-^{13}C]pyruvate respectively at 1.2 K [7]. The sample was then dissolved in a pressurized and heated alkaline solution, containing 2.4 g/L sodium hydroxide and 100 mg/L EDTA dipotassium salt, to yield a solution of 80 mM hyperpolarized sodium [1−^{13}C]pyruvate or [2−^{13}C]pyruvate with a polarization of approximately 30 % or 20 % respectively, at physiological temperatures.

Hyperpolarized ^{13}C pyruvate MRS Acquisition

Before dissolution, a rat or a mouse was anaesthetised with respectively 2.5 % and 2 % isoflurane vol:vol in 1 litre/min O_2 and positioned in a 7T horizontal bore MR scanner interfaced to a Direct Drive console (Varian Medical Systems, U.K.). A home-built ^{13}C butterfly coil (loop diameter, 40 mm x 20 mm) was placed over the chest of the rat, and a home-built circular ^{13}C RF surface transmit/receive coil (radius 10 mm) was placed over the chest of the mouse to localise the signal from the heart [57]. The heart was placed at the isocenter of the magnet and positioning was confirmed with an axial proton FLASH sequence with the following parameters: TE/TR, 1.17/2.33 ms; matrix size, 64 x 64; FOV, 60 x 60 mm; slice thickness, 2.5 mm; excitation flip angle, 15°. An ECG-gated shim was used to reduce the proton linewidth below 150 Hz and 250 Hz respectively for the mouse and the rat.

One millilitre (for a rat) and 200 μl (for a mouse) of hyperpolarized [1$-^{13}$C] or [2$-^{13}$C]pyruvate was injected over 10s via tail vein cannula. ^{13}C MR pulse-acquire cardiac spectra were acquired over 60 s immediately following the injection with the following parameters: TR, 1 s; excitation flip angle 15 °; sweep width 13,021 Hz; acquired points 2,048; frequency centred on the C_1 pyruvate resonance. 60 single spectra were acquired.

All cardiac spectra were analysed using the AMARES algorithm with JMRUI [263] for metabolic assessment of the heart. Spectra were corrected for a constant direct current offset by baseline subtraction based on the last 512 data points. The peak amplitude of *in vivo* [1-^{13}C]pyruvate, [1-^{13}C]lactate, [1-^{13}C]alanine, $^{13}CO_2$ and [^{13}C]bicarbonate and [1-^{13}C]pyruvate hydrate for [1-^{13}]pyruvate injection, and the peak amplitude corresponding to *in vivo* [2-^{13}C]pyruvate, [1-^{13}C]acetylcarnitine, [1-^{13}C]citrate, [5-^{13}C]glutamate, [1-^{13}C]pyruvate, [1-^{13}C]pyruvate hydrate, [2-^{13}C]lactate, and [2-^{13}C]alanine for [2-^{13}C]pyruvate were quantified. At the first appearance of [1-^{13}C]pyruvate for C_1 or the first appearance of [2-^{13}C]pyruvate hydrate for C_2 the spectra were summed over 30 seconds to increase the signal to noise ratios (Fig. 2.4).

Each of the metabolites was quantified as the ratio of the metabolite to either [1 $-^{13}$ C]pyruvate or [2 $-^{13}$ C]pyruvate.

All metabolites obtained from [2 $-^{13}C$]pyruvate were subsequently normalized to average pyruvate dehydrogenase (PDH) flux, as measured from the [1 $-^{13}C$]pyruvate experiment, in order to obtain any changes within the TCA cycle that was independent of PDH-flux.

All rats were imaged between 6 am, and 1 pm and all mice were imaged between 7 am and 11 am ensuring a fed metabolic state.

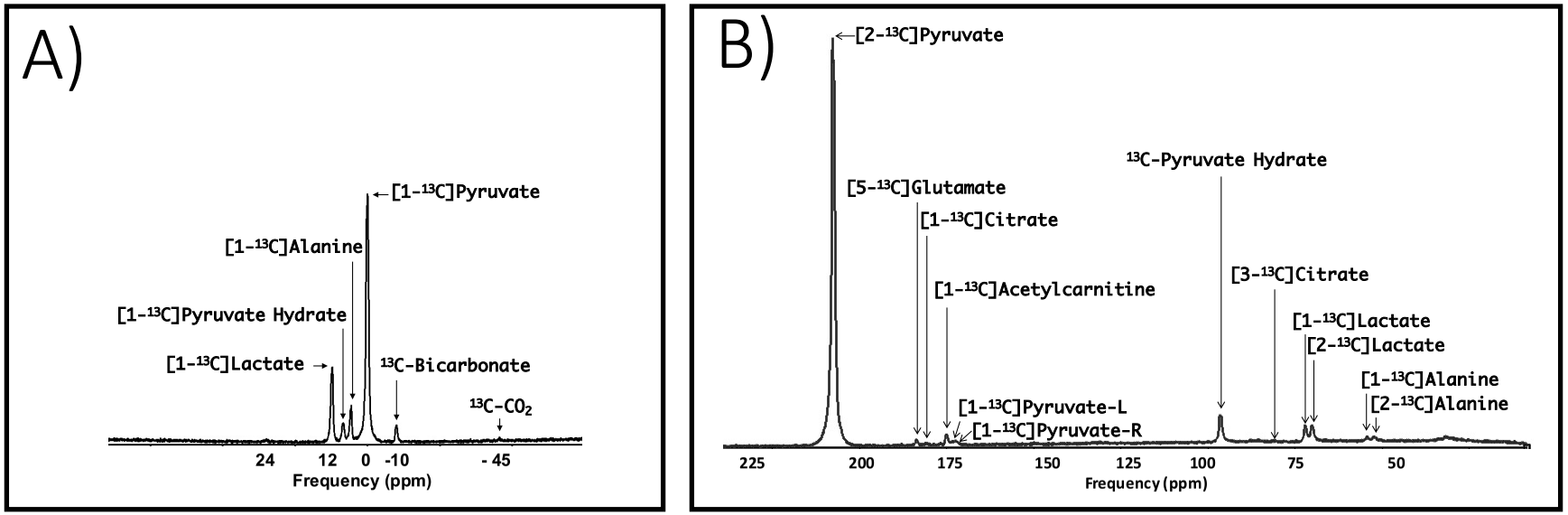

Figure 2.4: Summed spectra are showing the frequency (ppm) of each metabolite. A) Spectra acquired *in vivo* of a rat by infusion of hyperpolarised [1-^{13}C]pyruvate. B) Spectra acquired *in vivo* of a rat by infusion of hyperpolarised [2-^{13}C]pyruvate.

2.4.4 Echocardiography for Assessment of Cardiac Function

To determine any early diastolic dysfunction of the cardiac muscle a Vivid I echocardiography system (GE Healthcare, Chicago, USA) was used with an 11.5 MHz phased array 10S-RS pediatric echo probe. Imaging of the mitral valve and left ventricle were conducted. The mitral valve function was assessed from an apical four-chamber view for assessment of diastolic function. Pulsed wave Doppler was used acquiring the mitral valve early (E) and late (A) inflow velocities. Tissue Doppler was used for the acquisition of early (E') and late (A') mitral valve annulus velocities in the inter-ventricular septum and the lateral wall (LW). The parasternal short axis of the left ventricle was imaged at mid LV, where the papillary muscles and mitral valves were visible for assessment of systolic function in the form of ejection fraction (EF) and fractional shortening (FS).

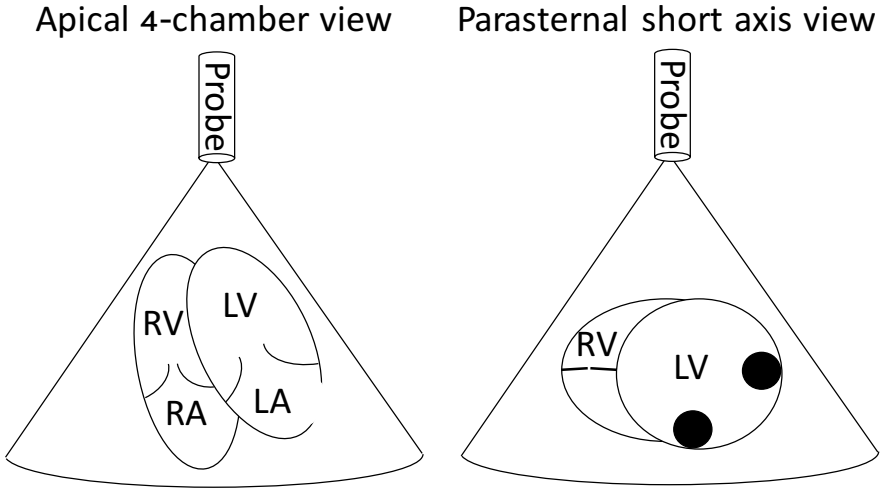

Figure 2.5: Left) Apical 4-chamber view, with the left atrium (LA), left ventricle (LV), right atrium (RA) and the right ventricle (RV) visible. **Right)** Parasternal short axis view with left and right ventricle visible, and the two papillary muscle visible in the LV.

2.5 Langendorff Perfusions

2.5.1 Krebs-Henseleit and Albumin Buffer Preparation

Two 12 litres bottles were rinsed with hot double distilled water (ddH_2O). One bottle was filled with ddH_2O (10 L) and was gassed with 5 % CO_2 and 95 % O_2.

Chemical formular	Name	Concentration [mM]
NaCl	Sodium chloride	118
KCl	Potassium chloride	4.7
$MgSO_47H_2O$	Magnesium sulfate heptahydrate	12
$CaCl_22H_2O$	Calcium chloride dihydrate	1.3
Na_2EDTA	Disodium ethylenediaminetetraacetate dihydrate (EDTA)	0.5
$C_6H_{12}O_6$	Glucose	11
$NaHCO_3$	Sodium bicarbonate	25
KH_2PO_4	Monopotassium phosphate	1.2

Table 2.1: Krebs-Henseleit buffer preparations added to 12 L of purified water in the order shown above.

Compounds were added into the bottle in the order as stated in Table 2.1. A ten minute period was left between the calcium chloride dihydrate and the disodium EDTA. The buffer was made up to the total volume of 12 L with ddH_2O before being filtered (filter 1: 0.8 μm, filter 2: 0.45 μm).

The day before perfusions an albumin KH buffer was prepared. Krebs-Henseleit (KH) buffer (250 ml) was used for each heart. To the KH-buffer 1.5 % (w/v) of bovine serum albumin (BSA; 1.5 %; Lampire, USA) was added and allowed to dissolve fully. This prepared albumin KH buffer was first filtered as before, and then to allow for chelation of free calcium by albumin, it was placed in dialysis tubing, which was semi-permeable, and inserted in the 12 litres bottle containing albumin-free KH buffer, and left overnight.

Albumin KH buffer was prepared freshly every two days of perfusions to avoid calcium dissociation.

2.5.2 Palmitate Stock Preparation

Palmitate stock was prepared with a concentration of 100 mM. Palmitic acid (2.56 g) (MW 256, PO500) was inserted in a glass bottle, and ethanol (2 ml) was added. The bottle was put in a 70 $^{\circ}C$ water bath to help the palmitate to dissolve. Potassium carbonate (1.38 g) was dissolved in the minimum amount of ddH_2O. With a pastette, it was slowly transferred to the palmitate solution. The water bath was heated for approximately five hours until the solution was dry. The solution was made

up to 100 ml in fresh saline (0.9 g NaCl in 100 ml ddH_2O). The palmitate stock was stored in a refrigerator until needed.

2.5.3 Radioactive ^{3}H Palmitate Albumin Krebs-Henseleit Buffer Preparation

A non-radioactive palmitate stock (100mM) was heated to liquid form at 70 $°C$. Albumin KH buffer was heated slowly to 30 °C, and 0.4 mM of palmitate was added with a heated pipette tip. The albumin KH buffer was spiked with 0.2 μCi/ml of $[9,10-^3\text{H}]$palmitate for assessment of fatty acid oxidation rates. The solution was stirred until everything was fully dissolved. The ^{3}H palmitate albumin KH buffer will subsequently be referred to as the albumin buffer.

2.5.4 Langendorff Ischemia Reperfusion Protocol

Fed animals were euthanized using an overdose of anaesthesia with 5 % isoflurane vol:vol in 2 litres/min O_2. The weight of the animal was taken, and once both the pedal and corneal reflexes ceased, the chest cavity was opened, and the heart was excised and put immediately in ice cold KH buffer. The heart was weighed, trimmed and the aorta exposed and hung on a retrograde Langendorff perfusion apparatus (Fig. 2.6).

Excess tissue was removed from the heart and weighed. A water-filled PVC balloon, which was connected via a polythene tube to a calibrated pressure transducer, a bridge amplifier, and a PowerLab data acquisition system (AD Instruments, Oxfordshire, UK), was inserted into the left ventricle. The balloon was inflated to an end diastolic pressure of 4-8 mmHg. The recirculating buffer was oxygenated during perfusions, and any bubbles were cleared from the recirculating albumin buffer (200 ml). The beating heart was inserted into the recirculation chamber, and the KH buffer was switched to the recirculating albumin buffer [92] The temperature was kept constant at 37 $°C$ (Fig. 2.7).

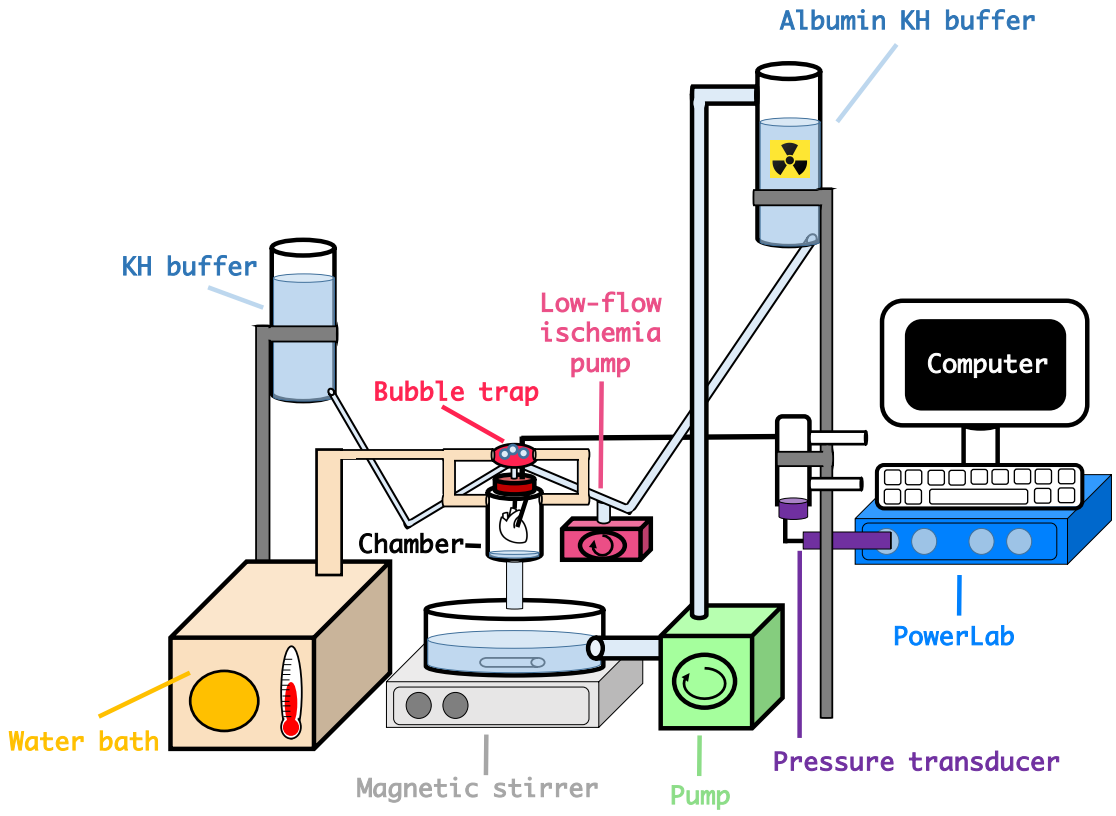

Figure 2.6: A schematic overview of a Langendorff perfusion apparatus. A water bath (yellow) keeps the KH buffers (blue) warm. A bubble trap (red), traps the bubbles if any get formed in the buffers, prior to reaching the heart. The chamber (black) keeps the heart beating in a warm environment. A PVC balloon placed in the left ventricle of the heart is connected to a pressure transducer (purple), which is connected to a PowerLab (dark blue) and a computer (white). A pump (green) recirculates the buffer, that is stirred on a magnetic stirrer (grey), and a low-flow ischemia pump (pink) diverges the flow during low-flow ischemia.

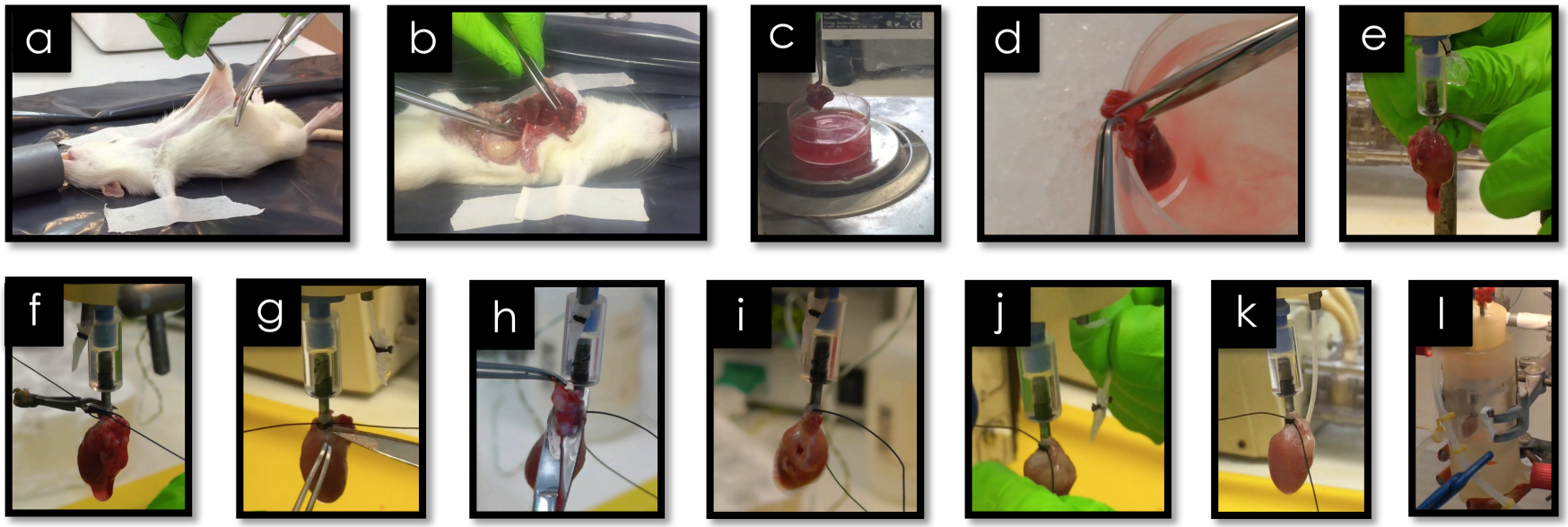

Figure 2.7: Langendorff perfusion protocol. **a)** The rat's chest cavity was opened. **b)** The heart was excised while beating. **c)** The wet weight of the heart was taken. **d)** Excess tissue was removed, and the aorta was exposed. **e)** The aortic cannula was attached to the aortic tubing. **f)** The aorta was secured with a clip and was secured with a suture. **g)** The clip was removed, and the pulmonary artery was snipped. **h)** Excess tissue was removed. **i)** The left atrium/pulmonary vein was exposed. **j)** A PVC balloon was inserted into the left ventricle. **k)** The balloon was inflated and secured with a suture. **l)** The cannulated heart was secured in a chamber that was temperature controlled.

The hearts were hung initially on warm KH buffer in the Langendorff perfusion mode at a constant pressure of 100 mmHg and subsequently switched to 200 ml of recirculating albumin buffer. Hearts were left to adjust to the albumin buffer for ten minutes before initiating the protocol. At the start of the protocol ($t = 0$ min), two aliquots (0.6 ml each) were sampled. Throughout the entire protocol aliquots of 1.2 ml of the recirculating buffer were collected every 4 minutes. Low-flow ischemia was applied at ($t = 21$ min) with the flow reduced to 0.4 ml/min/gww for 30 minutes, and the heart was reperfused at ($t = 51$ min) for another 30 minutes before it was freeze-clamped whilst still beating on the perfusion apparatus at ($t = 80$), Figure 2.8 shows the breakdown of the timeline.

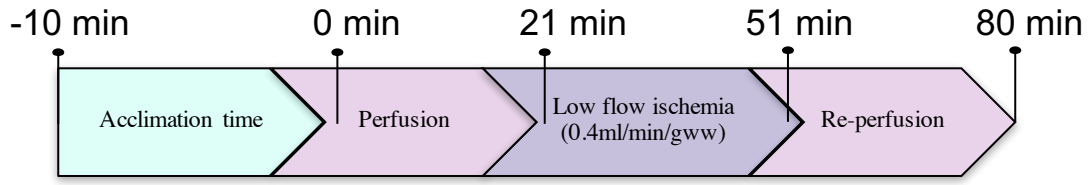

Figure 2.8: Timeline for Langendorff perfusion protocol. Before the start of the protocol, there is a ten minute acclimation time with the albumin buffer. Following the acclimation time, the protocol is started with retrograde perfusion of the aorta for 20 minutes before the flow is reduced to 0.4 ml/min/gram wet weight (gww) for 30 minutes. Finally, the heart is reperfused with full flow through the aorta for 30 minutes before it is clamped and submerged in liquid nitrogen.

2.5.5 Assessment of Cardiac Function

Cardiac function was assessed with a pressure transducer catheter connected to the PVC balloon that was inserted into the LV. A waveform of the left ventricular pressure was recorded (Fig. 2.9) from which the heart rate (HR), End Systolic Pressure (ESP), and End Diastolic Pressure (EDP) was measured, and the Left Ventricular Developed Pressure (LVDP) and Rate Pressure Product (RPP) were calculated (eq. 2.8).

$$LVDP = ESP - EDP \tag{2.7}$$

$$RPP = LVDP \times HR \tag{2.8}$$

where:

$$LVDP = \text{Left Ventricular Developed Pressure [mmHg]}$$

$$ESP = \text{ End Systolic Pressure [mmHg]}$$

$$EDP = \text{End Diastolic Pressure [mmHg]}$$

$$HR = \text{Heart Rate [bpm]}$$

$$RPP = \text{Rate Pressure Product [mmHg]}$$

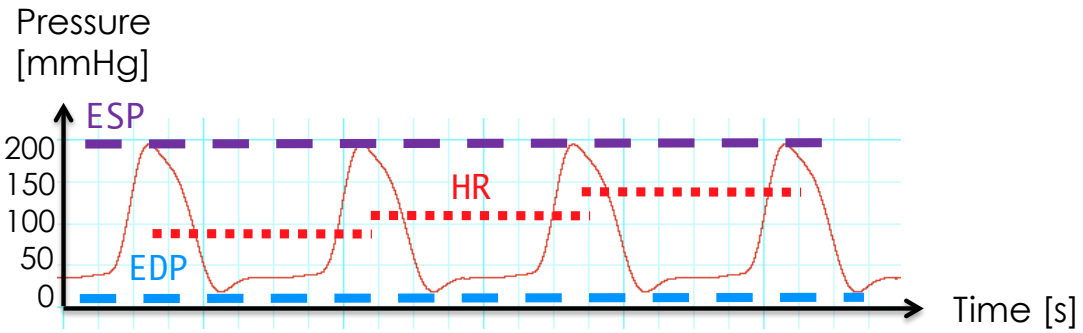

Figure 2.9: A functional trace of a Langendorf perfused heart pre-ischemia. The trace shows the pressure from the left ventricle (LV) from which heart rate (HR), End Systolic Pressure (ESP), End Diastolic Pressure (EDP) were calculated.

2.5.6 Measurement of Myocardial Palmitate Oxidation

The rate of fatty acid (palmitate) oxidation was calculated from the production of ^3H_2O in the perfusate buffer as described by Lopaschuk *et al.* [144] by separating ^3H_2O from ^3H palmitate in the aliquoted samples (Fig. 2.10).

This separation was done using a chloroform: methanol Folch extraction [92]. For all 22 aliquots, two falcon tubes were labelled, and the extraction was done in two steps followed by a final step counting the radiation:

Step 1. The first set of falcon tubes each contained 1.88 ml of chloroform: methanol

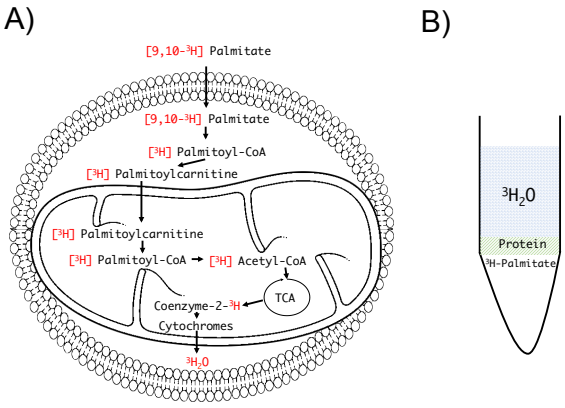

Figure 2.10: Palmitate transport into cardiomyocyte. **A)** ^{3}H labelled palmitate and its transport into the cardiomyocyte [144]. **B)** The separation phases using Folch extraction. The top layer is ^3H_2O, middle layer consist of protein and the bottom layer is the organic ^3Hpalmitate [92].

(1:2), 0.625 ml of chloroform, and 0.625 ml of 2 M potassium chloride (KCl) in 0.4 M of hydrochloric acid (HCl) solution (KCl-HCl). Perfusate buffer (0.5 ml) was added, and the falcon tubes were rotated at slow speed for ten minutes (Stuart Laboratory Rotor SB3) and left to stand for 30 minutes allowing for separation of the organic layer and the aqueous layer.

Step 2. The upper aqueous layer was removed from the previous tubes and placed in a second set of falcon tubes that each were filled with 1 ml of chloroform, 1 ml of methanol and 0.9 ml of KCl-HCl (0.4 M) solution. The solutions were rotated at slow speed for ten minutes (Stuart Laboratory Rotor SB3) and left to stand for another 30 minutes before the aqueous layer was separated from the organic layer and inserted into empty falcon tubes.

Step 3. The upper aqueous layer (0.5 ml), from each of the previous tubes, was added to 10 ml of Ecolite liquid scintillation cocktail (BP Medical, USA) and was subjected to scintillation counting (PerkinElmer, USA). For the specific activity (t = 0 min) 0.5 ml of the original perfusate buffer was mixed with 10 ml of scintillation liquid. The cumulative fatty acid oxidation (palmitate) for each sample was given by the following formula

$$\frac{(S_{t=x} - S_{t=0}) \times 8.26 \times 2 \times RB}{(SA - S_{t=0}) \times (\frac{2}{palm})} \tag{2.9}$$

where:

$$S = \text{Sample [cpm]}$$
$$RB = \text{ Recirculating Buffer [ml]}$$
$$SA = \text{Specific Activity [cpm]}$$
$$palm = \text{Palmitate [mM]} = 0.4 \text{ mM}$$
$$8.26 = \text{Dilution factor}$$

The cumulative fatty acid oxidation for each sample was plotted as a function of time to obtain fatty acid oxidation rates (μmol/min), which then were normalized to heart wet weight (gww). Finally, all fatty acid oxidation rates were normalized to work (rate pressure product) to obtain the oxidation rate per work undertaken.

2.6 Tissue Collection

All animals were euthanized in the fed state with 5 % isoflurane vol:vol in 2 litres/min O_2, followed by removal of the heart. For some experiments, the hearts were excised for Langendorff perfusion where they were submerged in cold KH buffer, and for other experiments, the hearts were immediately freeze-clamped in liquid nitrogen for biochemical analysis. Blood samples, taken from the chest cavity, were centrifuged (1,202 g, 10 min, 4 °C) and submerged in liquid nitrogen before being stored at -80 $°C$ for later biochemical analysis. The weight of kidneys was acquired. The epidydimal fat pads were weighed, and the right tibia length was measured.

2.7 Extractions for Metabolomics

Heart tissue (30-50 mg) was crushed under liquid nitrogen and put in tubes. Chloroform: methanol (2:1) was added (1 ml) to each tube. The tissues were homogenised with a Precellys 24 (Bertin, Montigny-le-Bretonneux, France) spun at 3,700 g for 2 x 30 seconds. Subsequently, ddH_2O (400 μl) was added to each tube. All samples were placed in a 30 °C water bath with a sonicator for 10 minutes to mix the solvent and disrupt the membranes. The samples were then

centrifuged for 5 minutes at 1,202 g, and the aqueous, lipid and protein layers were transferred to separate Eppendorf tubes. The aqueous layers were placed in a speed-vacuum (Savant, Thermo Fisher Scientific, USA) to evaporate. The lipid layers were placed open in a fume hood to evaporate. The dried products were frozen and sent to Department of Biochemistry at the University of Cambridge for metabolomics analysis. Metabolomics performed on plasma samples were sent to the Department of Chemistry at the University of Oxford.

2.8 Blood Analysis

Terminal fed blood was collected at the time of culling from the chest cavity. Fasted blood was collected in an anaesthetised state following an overnight fast two days prior to the time of culling. Capillary tubes (Microvette, Kent Scientific, USA) with a push cap containing heparin were used for fasted blood collection from the saphenous vein under anaesthesia. Terminal blood or fasted blood were centrifuged (Eppendorf Centrifuge 5415R, Eppendorf, Hamburg, Germany) at 1,202 g for 10 minutes at 4 °C and subsequently frozen in liquid nitrogen and stored at -80 °C. Plasma samples were analysed for glucose, lactate, triacylglycerides, cholesterol, low-density lipoprotein, high-density lipoprotein and β-hydroxybutyrate using an ABX Pentra 400 (Horiba ABX Diagnostics, Irvine, CA, USA). Plasma samples were analysed for pH, carbon dioxide partial pressure (pCO_2), oxygen partial pressure (pO_2), ctHB, potassium (K^+), sodium (N^+), calcium (Ca^{2+}) and chloride (Cl^-) using a blood gas analyzer (ABL, Radiometer, Denmark). NEFA and insulin levels were measured as described in Sections 2.9.1 and 2.9.2 respectively.

2.9 Biochemical Analysis

2.9.1 Non-Esterified Fatty Acid Assay

Non-Esterified Fatty Acids (NEFA) were measured with an FA115 assay kit (RANDOX Laboratories, Crumlin, UK). Regents were reconstituted as set out in the manufacturer's protocols. The calibration curve contained a blank, low

standard, medium standard and a high standard. R1 (80 μl) was added to wells of a 96 well plate, 4 μl of blood plasma was added, it was incubated at 37 $^{\circ}C$ for ten minutes. Finally, R2 (160 μl) was added to the wells, again the plate was incubated at 37 $^{\circ}C$ for ten minutes and read on a plate reader (FLUOstarOmega, BMG Labtech, Offenberg, Germany) at 550 nm.

2.9.2 Insulin ELISAs

An insulin Enzyme-Linked Immunosorbent Assay, ELISA (Mercodia, Sweden) was used to measure plasma insulin levels. Plasma (10 μl) was pipetted in duplicate into wells containing anti-insulin antibodies. After that, 100 μl of enzyme-conjugate was added followed by an incubation of 2 hours at room temperature. Following the incubation, the wells were washed to unbind enzyme labelled antibodies. 200 μl 3,3',5,5'- tetramethylbenzidine (substrate TMB) was added to detect the bound conjugate, and the reaction was stopped by adding sulfuric acid to give a colourimetric endpoint that was read on a plate reader (FLUOstarOmega, BMG Labtech, Offenberg, Germany) at 450 nm. Results were analysed using a standard curve of known insulin concentrations.

2.9.3 L-Carnitine ELISAs

Free L-carnitine levels were measured in plasma and tissue (approximately 25 mg) using a standard L-carnitine assay kit (MAK063, Sigma Aldrich, UK, Catalog Number MAK063). Manufacturers protocols were followed unless stated otherwise. In brief, the protocol was as follows: L-carnitine standards were prepared as stated in the kit, generating a blank, 2, 4, 6, 8, and 10 nmol/well standards. Carnitine assay buffer (100 μl) was added to either 25 μl of plasma or 25 mg of tissue and was homogenised using a Precellys 24 (Bertin, Montigny-le-Bretonneux, France) spun at 3,700 gfor 2 x 30 seconds. The sample preparation was filtered with 10 kDa MWCO spin filters to remove proteins. Assay reactions were set up as instructed in the kit and the absorbance was measured at 570 nm on a plate reader (FLUOstarOmega,

BMG Labtech, Offenberg, Germany). Results were analysed using a standard curve of known L-carnitine concentrations.

2.9.4 Western Blotting

Approximately 50 mg of tissue was crushed with a pestle and mortar in liquid nitrogen, later the exact weight of the tissue was normalized. Lysis buffer (75 mM Tris HCl (pH 6.8), 121.5 mM sodium dodecyl sulphate (SDS), 4 M urea, 2.7 mM glycerol, and 1.7 ml ddH_2O) was added (100 ml), and a protein assay was run to obtain the protein concentration of every lysate. Every sample (5 μl) was diluted with 95 μl of ddH_2O. A protein kit was used (Pierce Albumin, ThermoFisher Scientific USA), and manufacturers protocols were followed. Standards and samples were analysed in duplicates.

Protein lysate (30 μg) was used to load the samples on to sodium dodecyl sulphate polyacrylamide gel electrophoresis (12.5 % SDS-PAGE) gels, which then were separated by electrophoresis at a constant voltage of 200 V [20]. The protocol was run for approximately 40 minutes.

The gel was transferred to a nitrocellulose membrane in a transfer tank, that was run at a constant current (180 mA) for 1 hour [20]. Protein loading and the transfer was confirmed with Ponceau staining (Sigma-Aldrich Ltd., Dorset, UK).

Membranes were rinsed with ddH_2O and were blocked with 5 % dried milk (dissolved in Tris-buffered saline Tween; TBS-T) for 1 hour. Incubation with a primary antibody was left overnight in a cold room.

Following a washing step with TBS-T for 30 minutes, the membranes were incubated for 2 hours with a secondary antibody (Insight Biotechnology, conjugated to horseradish peroxidase) before being washed again and finally placed on a C-Digit blot scanner (LI-COR, USA) for imaging bands using a chemiluminescent detection system, and using Image Studio Lite software (Li-COR, USA) for quantification.

Protein expression of pyruvate dehydrogenase Kinase 4(PDK4), mitochondrial uncoupling protein 3 (UCP3), medium-chain Acyl-CoA dehydrogenase (MCAD), α-ketoglutarate (αKG), glucose transporter type 4 (GLUT4), and the loading of

Cyclophilin B were assessed and was expressed standardised to a control sample (Table 2.2).

Primary Antibody	Molecular weight	Product number	Supplier
PDK4	46 kDa	AB38242	Abcam
UCP3	34 kDa	AB3477	Abcam
MCAD	45 kDa	SC49047	Santa Cruz
αKG	113 kDa	SC49591	Santa Cruz
GLUT4	54.8 kDa	Dr. Geoff Holmann	University of Bath
Cyclophilin B	21 kDa	AB16045	Abcam

Table 2.2: Table shows primary antibodies used together with their molecular weight and the supplier.

2.10 Statistical Analysis

All statistical analysis was performed on GraphPad Prism7 (La Jolla, Ca, USA). All results are expressed as $mean\pm$ standard deviation (SD) unless stated otherwise. Two-way analysis of variance (ANOVA) was undertaken with Sidak's multiple comparison test if an interaction term was detected. One-way ANOVA was performed, followed by Dunnett's multiple comparison post hoc. Unpaired Student t-test was evaluated where appropriate. Differences between groups were considered significant if $p < 0.05$.

The second, feeling his tusk
Cried, "Ho! What have we here
So very round and smooth and sharp
To me 'tis mighty clear
This wonder of an elephant
Is very like a spear."

3

Functional and Metabolic Characterisation of the Diabetic Heart

Contents

3.1 Chapter Overview 64
3.2 Background 65
3.3 Neonatal Diabetes Mellitus (NDM) 66
3.3.1 Mouse Model of NDM 68
3.4 Streptozotocin (STZ)-Induced Type 1 Diabetes 69
3.5 Progression of Diabetes and Early Metabolic Changes 70
3.6 Chapter Aims 70
3.7 Methods 71
3.7.1 Mouse Model of Neonatal Diabetes Mellitus (NDM) . . 71
3.7.2 Establishing an Appropriate Model of STZ-Induced Type 1 Diabetes 72
3.7.3 Statistical Analysis 74
3.8 Results 74
3.8.1 Cardiac Metabolism and Function in a Mouse Model of NDM 74
3.8.2 Cardiac Metabolism and Function in STZ-Induced Models of Type 1 Diabetes 80
3.8.3 Exploration of the Temporal Effects of STZ-Induced Diabetes on Cardiac Metabolism and Function using Hyperpolarized ^{13}C MRS and CINE MRI 87
3.9 Discussion 94
3.9.1 Cardiac Metabolism and Function in a Mouse Model of NDM 94
3.9.2 Cardiac Metabolism and Function in STZ-Induced Models of Type 1 Diabetes 96

3.9.3 Temporal Effects of STZ-Induced Diabetes on Cardiac Metabolism and Function 98
3.9.4 Conclusion and Future Perspective 99

3.1 Chapter Overview

This chapter established an appropriate model of diabetes with cardiac metabolic and functional impairments that were sustained over a sufficient duration to enable subsequent studies, where a treatment response of elevating and reducing L-carnitine would be investigated.

Two models of diabetes that induced hyperglycaemia was investigated. Initially, a genetic mouse model of inducible neonatal diabetes mellitus (NDM) was used, which was treated with glibenclamide to reverse diabetes. Further to this, the often used STZ-induced T1D model was explored with two different doses injected in both the fed and fasted state. The progression of cardiac dysfunction was explored in both models, in order to establish a time-point for subsequent treatment.

PDH-flux and relative aerobic to anaerobic metabolism was decreased in the NDM model, this was observed in conjunction with cardiac functional impairments. Glibenclamide treatment showed for the first time to elevate cardiac output and reverse the metabolic alteration *in vivo* as observed with hyperpolarized MRS.

The high dose (HighD) injected STZ group during fasting showed decreased stroke volume and cardiac output, this occurred in combination with a suppression in the metabolic conversion of pyruvate to bicarbonate, lactate and alanine in the *in vivo* myocardium at two weeks post diabetes induction. In contrast, the restoration of normal cardiac function at six weeks after the onset of diabetes coincided with an elevation of the flux into lactate and alanine. This may suggest that some functional benefit is obtained from the ability to redirect pyruvate into alternative metabolic pathways.

Even though the NDM mouse model gave robust changes in cardiac function and metabolism, the MRI data was noisy, tissue was scarce, and insufficient amounts

of blood could be obtained for further investigations. The HighD STZ-induced T1D model, injected in the fasted state was the most reproducible among those investigated and gave the most severe metabolic and functional decline. Moreover, hearts were larger than in the mouse model and fasted blood could be obtained weekly. Furthermore, cardiac depression and metabolic alterations were observed over the six weeks of progression of diabetes, making it suitable for applying treatments during this time-course.

Therefore the HighD STZ model injected in the fasted state was chosen as the more suitable model for investigating treatment response in the subsequent chapters.

3.2 Background

In the work described in this chapter, two different models of diabetes were explored to assess and characterise their cardiac dysfunction and to follow the progression of both cardiac metabolic and functional decline. These two different models of diabetes induce hyperglycaemia, an independent risk factor in cardiac dysfunction [103].

Although anatomy and function are different between rodents and humans, the STZ-induced diabetes model using rats is the most common model of human diabetes, because it induces similar chronic complications as in human diabetes such as cardiovascular disease, retinopathy, nephropathy and polyneuropathy [274]. Another model for diabetes is a transgenic mouse model, which exhibits a human neonatal diabetes mellitus (NDM) mutation (Kir6.2-V59M) in the β-cells. Diabetes in this model can be rapidly induced. However, unlike the STZ model, the diabetes can be reversed with the use of a sulfonylurea, like glibenclamide. Even though this is a model of human neonatal diabetes, it expresses hyperglycaemia as well as hypoinsulinemia, as is the case for T1D. This is a good model for investigating chronic hyperglycaemia and any metabolic or functional changes that occur post induction/treatment in order to understand the underlying metabolic changes in the diabetic heart better.

3.3 Neonatal Diabetes Mellitus (NDM)

Neonatal diabetes mellitus (NDM) is diagnosed within the first nine months of life. It is a rare disorder that can either be permanent (lifelong) or transient (disappears but could reappear later in life). NDM is associated in 50 % of cases with a mutation in the KCNJ11 (potassium voltage-gated channel subfamily J member 11) gene [60], or in the ABCC8 (ATP binding cassette transporter sub-family C member 8) gene. KCNJ11 encodes the ATP sensitive potassium channel (K_{ATP}) subunit Kir6.2. ABCC8 encodes the sulfonylurea receptor subunit SUR1. β-cell K_{ATP} channels consist of Kir6.2 subunits and SUR1 subunits. The state of the K_{ATP} channels is regulated by ATP/ADP levels. Intracellular ATP binds to the Kir6.2 subunit, which triggers its closure, a single ATP molecule can inhibit the K_{ATP} channel [156]. The opening of the K_{ATP} channel is triggered by binding of Mg-ADP to the SUR1 subunit (Fig. 3.1) [266].

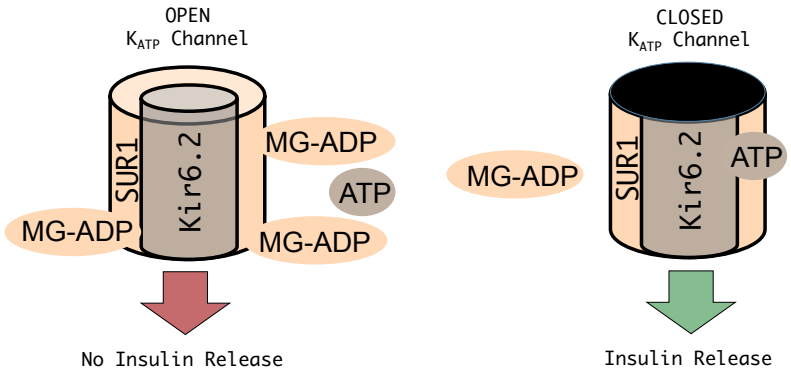

Figure 3.1: K_{ATP} channels are open when Mg-ADP are bound to the SUR1 subunit, this does not result in a release of insulin **(left)**. K_{ATP} channels are closed when intracellular ATP is bound to the Kir6.2 subunit. This results in a release of insulin **(right)**.

Glucose homeostasis is regulated by insulin secretion. β-cells detect glucose levels and secrete insulin through the signalling molecule; ATP [118]. With low plasma glucose levels, the K_{ATP} channels are open preventing insulin release. A rise in plasma glucose levels increases the ATP/ADP ratio resulting in a closure of the K_{ATP} channels. Closure of the channel initiates sodium channels to open leading to depolarization of the membrane, which results in an influx of calcium, that triggers insulin release [25] (Fig. 3.2). Any functional or structural defect of

the K_{ATP} channels can impair insulin secretion. NDM patients have an overactive K_{ATP} channel, which through increased Mg-ADP sensitivity, forces the channel to stay open preventing insulin release. However, the SUR1 subunit can be inactivated by a class of drugs called sulfonylureas, such as glibenclamide or tolbutamide [2]. The sulfonylureas bind to the K_{ATP} subunit SUR1, which closes the K_{ATP} channels allowing insulin secretion (Fig. 3.2).

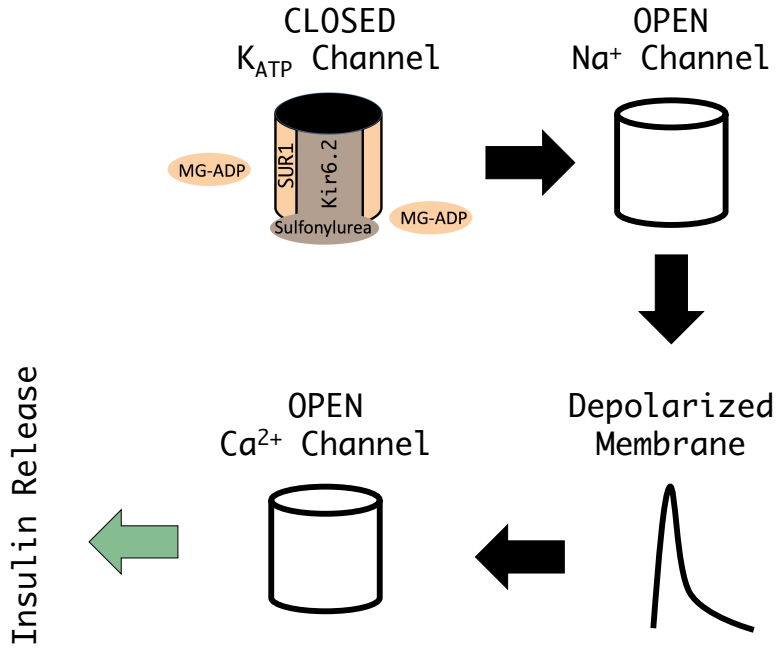

Figure 3.2: Sulfonylureas bind to K_{ATP} subunit SUR1, or ATP binds to Kir6.2, which both can trigger closure of the K_{ATP} channel. This closure initiates sodium channels to open, leading to a depolarization of the membrane, which results in an influx of calcium, that triggers insulin release [25].

Historically NDM would be treated with insulin therapy. However, a groundbreaking report written by Pearson *et al.* in 2006 validated the effectiveness of oral sulfonylurea treatment in NDM caused by mutations in KCNJ11 and ABCC8. This meant that patients could switch from lifelong injections of insulin to finite oral sulfonylurea treatments [195]. Sulfonylureas (K_{ATP} channel blockers) are today used in NDM and T2D but are for apparent reasons ineffective in T1D.

3.3.1 Mouse Model of NDM

A transgenic mouse model, which expresses a human NDM mutation (Kir6.2-V59M) in the β-cells is a good model for investigating chronic hyperglycaemia/ hypoinsulinemia without dyslipidaemia [103]. This Kir6.2-V59M mouse model expresses a mutation in the Kir6.2 subunit in the K_{ATP} channel of the β-cells, which prevents insulin release following glucose stimulation (Fig. 3.3). The mutation is a valine-to-methionine substitution at position 59 (V59M), Cre-lox technology is used to express the mutation in β-cell [76, 210]. The diabetes can be induced with tamoxifen injection and can be reversed by treating with glibenclamide, a sulfonylurea, that closes the K_{ATP} channels.

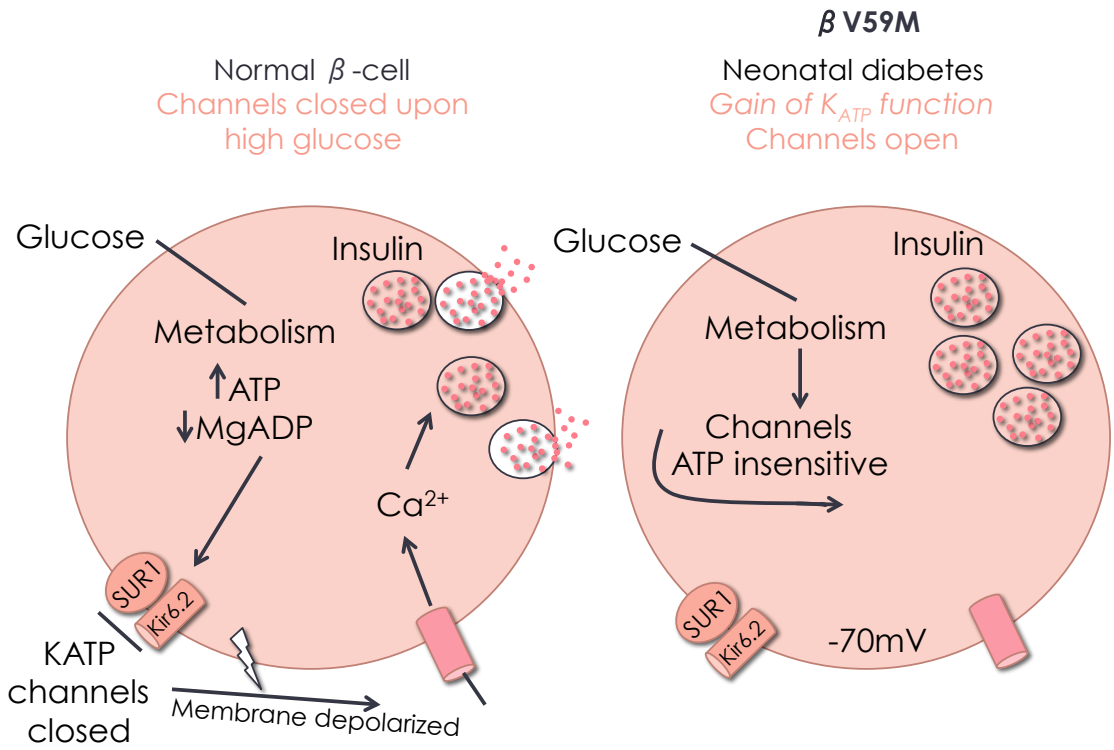

Figure 3.3: Left) With high plasma glucose levels, glucose enters the β-cell and is phosphorylated to glucose-6-phosphate (G6P). G6P is metabolised through glycolysis and oxidative phosphorylation to form ATP. ATP inhibits K_{ATP} channels and therefore promotes membrane depolarization and insulin release. **Right)** Chronic hyperglycaemia impairs oxidative metabolism leading to lower levels of ATP generation in response to glucose levels, resulting in inhibition of K_{ATP} channel closure, electrical activity and release of insulin. Adapted from Brereton *et al.* [24].

Many studies have confirmed that this mutation leads to diabetes in mice [25, 76, 119]. Some studies have shown insulin content to decline to 20 % by five weeks following tamoxifen injection, and others have shown a complete depletion. It is believed that this reduction is due to sustained hyperglycaemia [157] and that the sensitivity of K_{ATP} channels to ATP is not a fixed parameter, but also relies on both lipid levels and acyl-CoA, which have all been shown to reduce the ATP sensitivity of the K_{ATP} channel [86, 23].

3.4 Streptozotocin (STZ)-Induced Type 1 Diabetes

Streptozotocin ($2-deoxy-2-(3-methyl-3-nitrosoureido)-d-glucopyranose$), STZ, is an antibiotic agent produced by the soil bacterium *Streptomyces achromogenes*, that is used to induce diabetes in experimental animals [206]. STZ inhibits DNA synthesis destroying the β-cells. STZ is taken up through the glucose transporter 2 (GLUT2) specifically on the β-cells of the pancreas, but can also be found in renal tubular cells and hepatocytes [64]. GLUT2 is an essential factor in the sensitivity of the pancreatic β-cells to glucose, and is a low-affinity glucose transporter [184]. The α-cells as well as the extra-pancreatic parenchyma, are unaffected by STZ. STZ is approved by the FDA for metastatic β-cell cancer patients [215] and has not been shown to result in diabetes in humans [283]. Human β-cells are more resistant to STZ, this could be due to a 100-fold lower expression of GLUT2 in humans, where instead there is a higher expression of GLUT1 [51].

Many studies have shown cardiac dysfunction in STZ-induced T1D [280, 31, 281]. Shiomi *et al.* have shown that STZ-induced T1D in mice exacerbates left ventricular dysfunction [233]. Also, Cosyns *et al.* have shown that STZ-induced T1D in rats results in cardiomyopathy [45]. STZ causes remodelling of the myocytes, which leads to a decrease in cross sectional areas and a reduction in cell length [169].

3.5 Progression of Diabetes and Early Metabolic Changes

Progression is commonly studied in type 2 diabetes (T2D). If the disease is caught early, the patient can manage it through weight loss, healthy meals and exercise, all aimed to improve their glucose sensitivity. At later stages, medication is almost unavoidable. However, progression is not commonly studied in T1D. It is an autoimmune disorder, where the destruction of the β-cells leads to a lifelong dependency on insulin. Recently, however, it has been shown that even T1D progresses at an early stage, and maybe a treatment could be more effective at a specific time-point if we understood this progression. Insel *et al.* showed that individuals at risk of getting T1D progress at variable, but predictable rates, through identifiable stages. Stage 1; they identified two or more islet autoantibodies, but normal glucose levels. Stage 2; they showed the onset of dysglycaemia but yet no symptoms. Stage 3; they showed the onset of symptomatic disease [101]. So not only does T1D progress over the course of the disease but it also progresses at the onset of the disease.

3.6 Chapter Aims

The work described in this chapter aimed to establish an appropriate model of diabetes with cardiac dysfunction and to follow the progression of both cardiac metabolic and functional decline in an untreated model, in order to establish appropriate time scales to investigate treatment effects in the subsequent chapters. Initially, a genetic mouse model (Kir6.2-V59M) of neonatal diabetes was used to compare the metabolic and functional decline over time, and to investigate the *in vivo* metabolic and functional recovery when treated with glibenclamide. Subsequently, a rat model of T1D was induced with both a high and a low dose of the β-cell toxin; streptozotocin (STZ) in both a fed and a fasted state to test for model variability. The model that varied less was then scanned with hyperpolarized

[1−^{13}C]pyruvate and cardiac CINE imaging at two and six weeks post induction of diabetes to explore the temporal progression of metabolic and functional changes.

3.7 Methods

3.7.1 Mouse Model of Neonatal Diabetes Mellitus (NDM)

Mice expressing an inducible Kir6.2-V59M transgene specifically in pancreatic β-cells were generated. Transgene expression was induced by tamoxifen injection, as previously described [25]. Kir6.2-V59M mice were used before gene induction as their own controls.

Two weeks after the induction of diabetes, a subset of mice was subcutaneously implanted with two pellets each releasing 25 mg glibenclamide over 21 days (Innovative Research of America, Florida, USA), under 2 % isoflurane vol:vol anaesthesia.

Food and water were provided ad libitum. Body weight and blood glucose levels were monitored routinely. All animals were anaesthetised with isoflurane and subjected to MR imaging and hyperpolarized MR spectroscopy (MRS) as described in Sections 2.4.2 and 2.4.3 at different time points as illustrated in Figure 3.4.

The transgenic (Kir6.2-V59M) mouse model of diabetes was assessed in two groups. In Group 1 the reversibility of the diabetes was studied (n = 10) and was assessed with hyperpolarized MRS and CINE MRI at baseline, two weeks after diabetes induction with tamoxifen, and again two weeks after treatment with glibenclamide. In Group 2, the progression of NDM was studied. This group was never treated with glibenclamide (n = 8), and was assessed with hyperpolarized MRS and CINE MRI at 24 hours after induction of diabetes with tamoxifen, and then following eight weeks and six months of diabetes they were assessed again with only CINE MRI, to further explore the temporal effects of the disease progression on cardiac function.

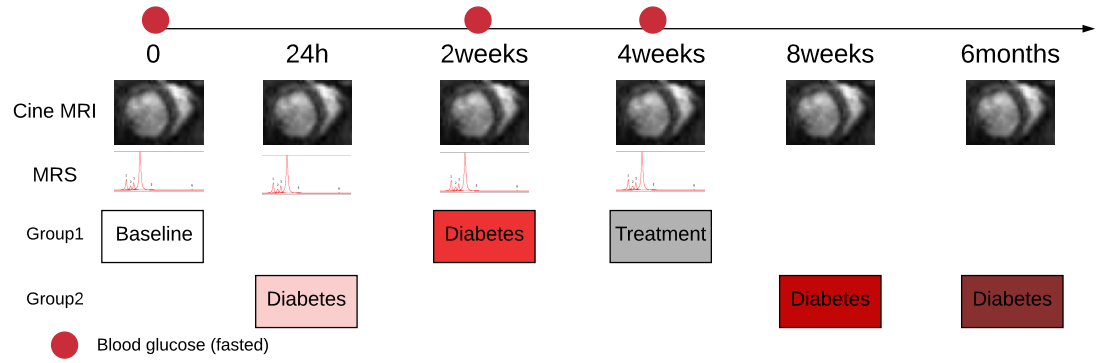

Figure 3.4: Experimental design of K_{ATP} mouse model. This figure shows a schematic overview of the imaging time-points for the different K_{ATP} mouse groups. Diabetes stands for after tamoxifen induction, where the mouse has developed neonatal diabetes mellitus (NDM). Treatment stands for after glibenclamide treatment has been given.

3.7.2 Establishing an Appropriate Model of STZ-Induced Type 1 Diabetes

Twenty eight healthy male Wistar rats (∼200 g) were randomly divided into five groups as described in Table 3.1; high dose (HighD) STZ (55 mg/kg) injected **a)** in the fasted state, or **b)** in the fed state, **c)** low dose (LowD) STZ (25 mg/kg) injected in the fasted state, or **d)** in the fed state, as well as **e)** citrate buffer injected in the fasted state to act as controls (CTR).

Injection state	Citrate buffer	Low dose of STZ (25 mg/kg)	High dose of STZ (55 mg/kg)
Fasted	CTR (n = 8)	LowD (n = 4)	HighD (n = 8)
Fed		LowD (n = 4)	HighD (n = 4)

Table 3.1: Twenty eight animals are divided into five groups including high(HighD) and low dose (LowD) injection of STZ in both the fed and fasted state. Controls were injected with citrate buffer in the fasted state to act as controls (CTR).

Food and water were provided ad libitum. Glucose sampling was obtained at

one, two, four and six weeks post STZ injection as described in Section 2.2.

Two weeks post STZ injection all animals were anaesthetised with isoflurane and subjected to MR imaging and hyperpolarized MR spectroscopy (MRS) as described in Sections 2.4.1 and 2.4.3.

Six weeks post STZ injection all high dose STZ injected animals and controls were anaesthetised again with isoflurane and subjected to MR imaging, hyperpolarized MR spectroscopy (MRS). The fasted HighD group was also subjected to echocardiography. The experimental setup is shown in Figure 3.5.

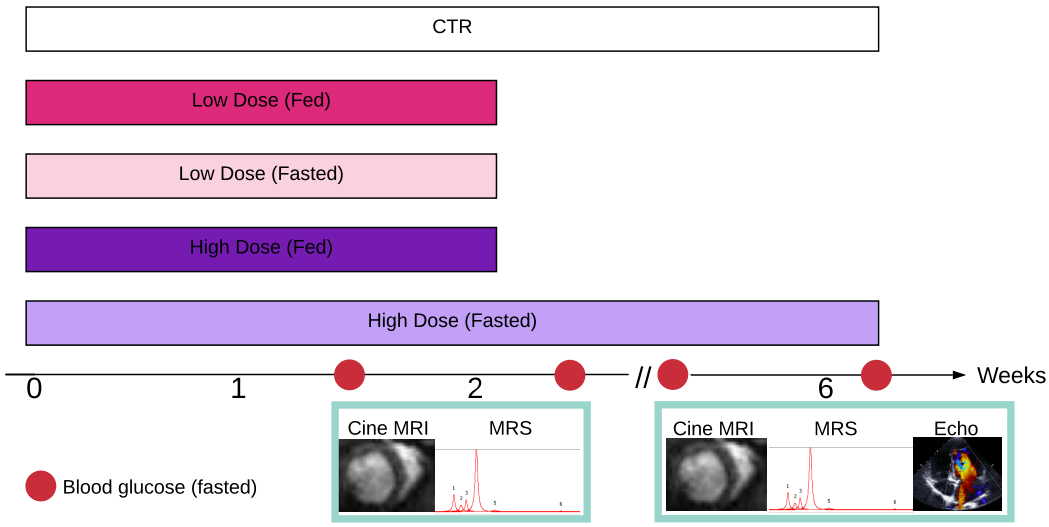

Figure 3.5: Experimental design of streptozotocin induced rats. This figure shows a schematic overview of the imaging time-points for the different streptozotocin rat models (controls; CTR, low dose; LowD, high dose; HighD), and when glucose levels were measured.

3.7.3 Statistical Analysis

All results are expressed as mean ± standard deviation (SD). Significance was established between two groups with an unpaired t-test. If multiple groups were present an ordinary one-way ANOVA analysis with Dunnett's multiple comparison test post hoc was used. If progression was evaluated a two-way ANOVA analysis was used with Sidak's multiple comparison test post hoc. Regression was established with Goodness of fit using an F-test analysis. Values were considered to be significant if $p < 0.05$.

3.8 Results

3.8.1 Cardiac Metabolism and Function in a Mouse Model of NDM

3.8.1.1 Group 1: Reversibility of NDM with Glibenclamide

Weight and Blood Profile

Blood glucose levels were significantly increased in the Kir6.2-V59M model when the transgene was inducted with tamoxifen (25.5 ± 6 mmol/L) at two weeks post injection ($p < 0.0001$) compared to baseline (7.1 ± 1 mmol/L). The blood glucose levels were restored to baseline 7.9 ± 2 mmol/L following two weeks of treatment with glibenclamide ($p < 0.0001$, Fig. 3.6A).

Body weight decreased from 30 g ± 3 g at baseline to 27 g ± 3 g at two weeks post induction of diabetes, although not significantly. Animals gained 15 % in weight following treatment with glibenclamide compared to after two weeks of diabetes ($p = 0.008$, Fig. 3.6B).

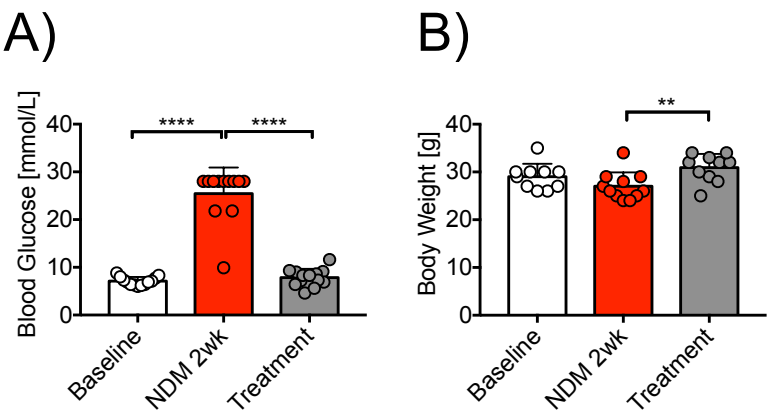

Figure 3.6: **A)** Blood glucose at baseline (white), diabetes at two weeks (red), and glibenclamide treatment (2 x 25 mg/21 day release) (grey). **B)** Body weight in grams at baseline, diabetes at two weeks (red), and glibenclamide treatment (grey). Data presented as mean ± SD. One-way ANOVA analysis with Sidak's multiple comparisons test, where $^{**}p < 0.01$, $^{***}p < 0.001$.

Cardiac *In Vivo* Function

Cardiac function decreased with the development of diabetes (two weeks post induction). Stroke volume (SV) was decreased by 25 % compared to baseline (p = 0.05) and cardiac output (CO) was decreased by 23 % compared to baseline (p = 0.03) with diabetes. Cardiac output was also significantly reduced at two weeks of diabetes when normalized to body weight, cardiac index (p = 0.026). With treatment, CO increased 30 % compared to at two weeks of diabetes (p = 0.03). No differences were observed in stroke volume or cardiac output between baseline and treatment (Fig. 3.7).

Two weeks of diabetes reduced end diastolic lumen (EDL) by 18% and end systolic lumen (ESL) by 11 % compared to at baseline. Glibenclamide treatment increased myocardial mass by 13 % (p = 0.05) and heart rate by 7 % compared to diabetes at two weeks (Table 3.2).

Cardiac *In Vivo* Metabolism

With the development of diabetes, flux through pyruvate dehydrogenase (PDH) was significantly decreased by 51 % two weeks post tamoxifen induction (p = 0.038,

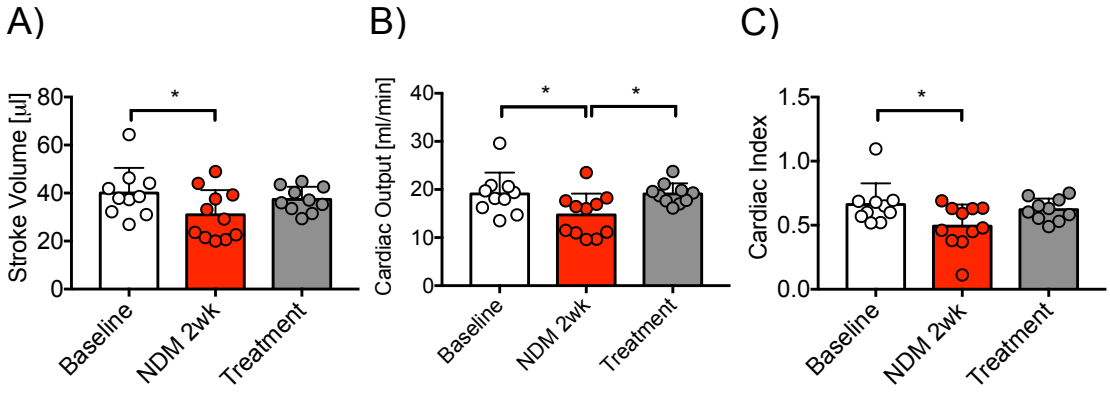

Figure 3.7: *In vivo* CINE MRI obtained at baseline (before tamoxifen induction), then following two weeks of diabetes, and finally after two weeks reversal of diabetes with glibenclamide therapy. Where possible, the same mouse was studied in all three conditions. **A)** Stroke volume (SV). **B)** Cardiac Output (CO). **C)** Cardiac Index, that is cardiac output normalized to body weight. Data presented as mean ± SD. One-way ANOVA analysis with Sidak's multiple comparisons test, where $^{*}p < 0.05$

Parameter	Baseline	Diabetes 2wk	Treatment 2wk
Body weight (g)	29.0 ± 2.7	27 ± 2.9	30.9 ± 2.9^{++}
Blood glucose, fed (mM)	7.1 ± 0.8	25.5 ± 5.5 ***	7.8 ± 1.8^{+++}
Average heart Mass (mg)	86.8±20.9	84.8±13.2	96.1±11.3^{+}
Cardiac Index (CO/BW)	0.66±0.17	0.49±0.17***	0.62±0.09^{+}
Ejection Fraction (%)	67.9±6.9	64.7±5.7	67.1±6.5
Heart Rate (bpm)	483±35	479±51	515±31
End Diastolic Lumen (µl)	59.7±16.2	48.6±17.9	56.0±8.7
End Systolic Lumen (µl)	19.6±8.2	17.7±8.3	18.6±5.6

Table 3.2: Characteristics of Kir6.2-V59M mice before tamoxifen injection (baseline), two weeks after injection of tamoxifen (diabetes, DB), and after two weeks implantation of glibenclamide (GLB) pellets (2 x 25 mg/21 day release pellets). Data presented as mean ± SD, $n = 10$, one-way ANOVA where $^{***}p < 0.001$ compared to baseline, $^{+++}p < 0.001$ compared to diabetes

unpaired t-test), as indicated by reduced conversion of hyperpolarized pyruvate into bicarbonate. Bicarbonate signal was not different after two weeks of treatment with glibenclamide compared to at baseline (p = 0.764, unpaired t-test, Fig. 3.8A). Incorporation of ^{13}C label from pyruvate into lactate and alanine were unchanged at all time points (Fig. 3.8BC), however the bicarbonate over lactate ratio, a measure

of the ratio of aerobic to anaerobic flux, was reduced by 63 % at two weeks of diabetes compared to at baseline (p =0.0005), and increased again after treatment by 123 % compared to at two weeks of diabetes (p = 0.012, Fig. 3.8D).

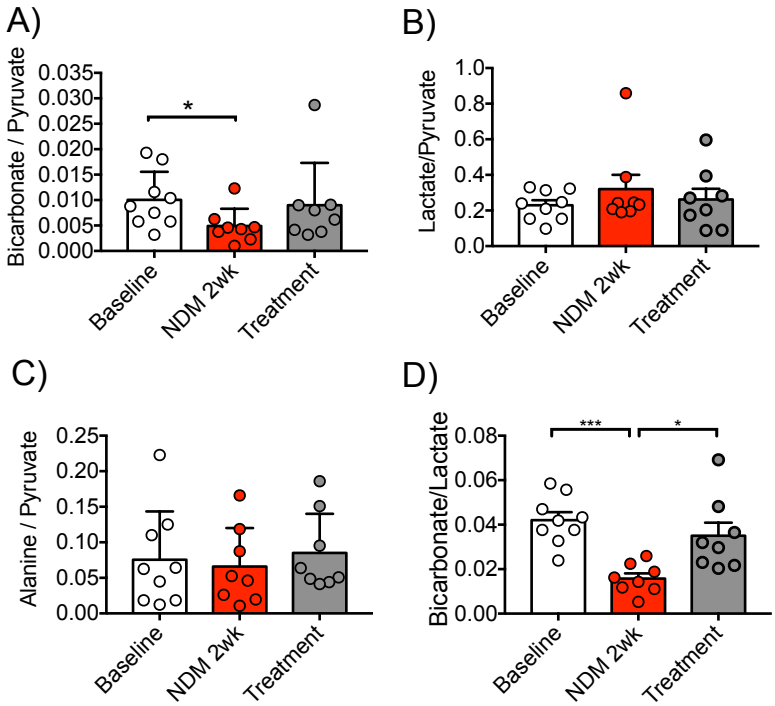

Figure 3.8: *In vivo* effects of infusion of hyperpolarized [1 $-^{13}$ C]pyruvate. Spectra summed over 30 s, beginning at the first appearance of the pyruvate peak. **A)** Bicarbonate/pyruvate ratio. **B** Lactate/pyruvate ratio. **C)** Alanine/pyruvate ratio. **D)** Bicarbonate/lactate ratio. Data presented as mean ± SD. One-way ANOVA, where $^{*}p < 0.05$, $^{***}p < 0.001$.

3.8.1.2 Group 2: Progression of NDM

Weight and Blood Profile

Body weight decreased 18 % at eight weeks compared to at 24 hours (p = 0.002) and was significantly reduced six months post diabetes induction compared to at 24 hours (p = 0.0006, Fig. 3.9).

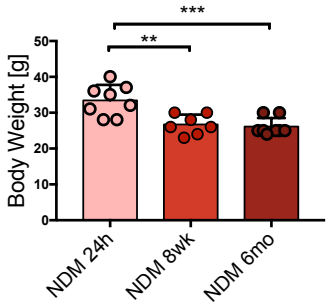

Figure 3.9: Body weight at 24 hour post diabetes induction with tamoxifen, at eight weeks, post diabetes induction, and at six months post diabetes induction. Data presented as mean ± SD. One-way ANOVA analysis with Sidak's multiple comparisons test, where $^{**}p < 0.01$, $^{***}p < 0.001$.

Cardiac *In Vivo* Function

Cardiac function decreased with an increased duration of diabetes. Stroke volume (p < 0.0001), stroke index (p = 0.013), cardiac output (p < 0.0001), and cardiac index (p = 0.013) were all significantly decreased at eight weeks of diabetes compared to at 24 h of diabetes. Stroke volume and cardiac output were also significantly depressed at six months compared to 24 h of diabetes (p < 0.0001), however when normalized to body weight the differences in stroke index and cardiac index could not be observed at six months of diabetes (Fig. 3.10 BCDE). Average myocardial mass was significantly decreased at both eight weeks (p < 0.0001) and six months of diabetes (p = 0.0004) compared to at 24 hours of diabetes. End diastolic lumen was also reduced significantly at eight weeks of diabetes (p = 0.02) and six months of diabetes (p = 0.04) compared to at 24 h of diabetes, but end systolic lumen was unchanged across the groups (Fig. 3.10 FGH). There was no change in heart rate or heart rate over body weight ratio (Fig. 3.10IJ).

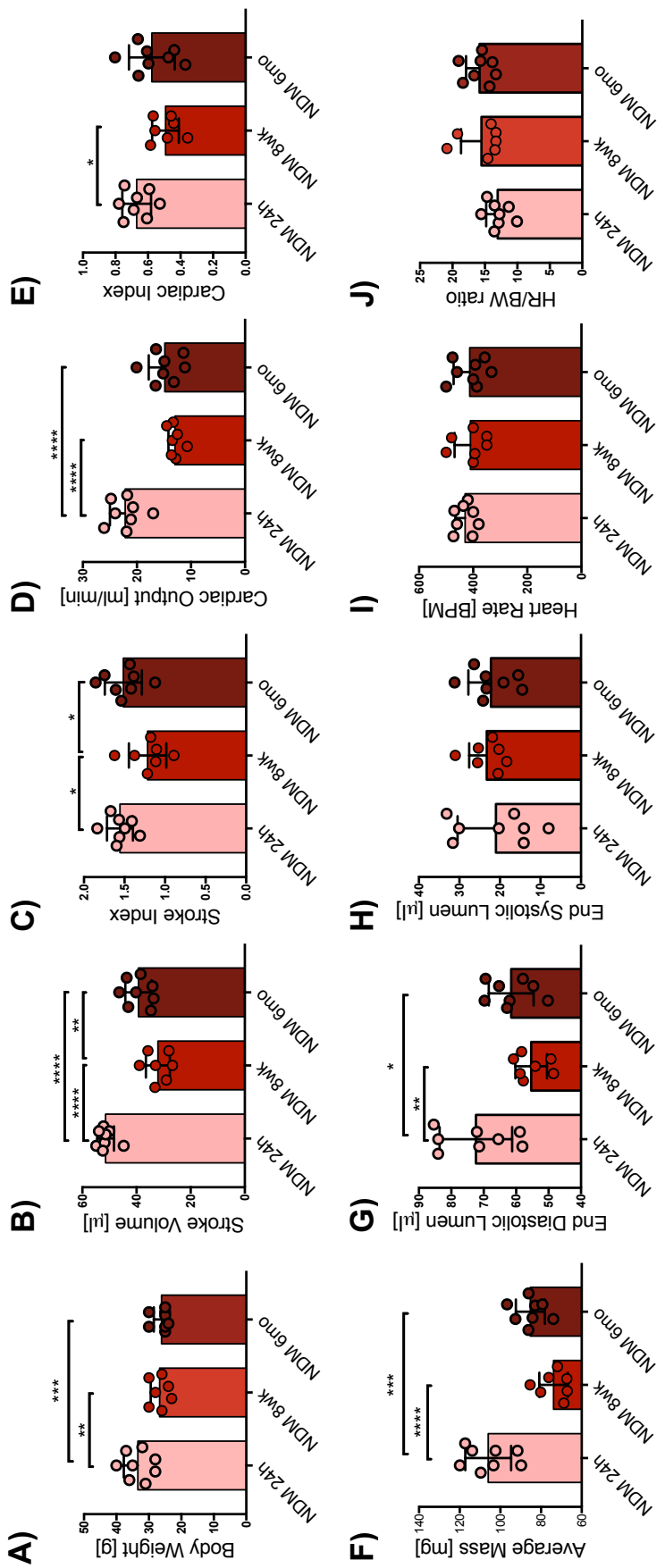

Figure 3.10: CINE MRI obtained at 24 hours post tamoxifen induction, then following eight weeks of diabetes, and six months of diabetes. Where possible, the same mouse was studied at all three stages. **A)** Body weight, BW [g]. **B)** Stroke Volume, SV [μl]. **C)** Stroke Index (SI). **D)** Cardiac Output, CO [ml/min]. **E)** Cardiac Index, CI. **F)** Average Mass [mg]. **G)** End Diastolic Lumen, EDL [μl]. **H)** End Systolic Lumen, ESL [μl]. **I)** Heart Rate, HR [bpm]. **J)** Heart Rate normalized to Body Weight, HR/BW. Data presented as mean $\pm$ SD. One-way ANOVA analysis with Sidak's multiple comparisons test, where $^{*}p < 0.05$, $^{**}p < 0.01$ $^{***}p < 0.001$, $^{****}p < 0.0001$.

3.8.2 Cardiac Metabolism and Function in STZ-Induced Models of Type 1 Diabetes

3.8.2.1 Weight and Blood Profile

There was no significant difference in body weight between control animals injected with citrate buffer (CTR) and animals injected with a low dose of STZ (LowD, 25 mg/kg) irrespective of whether injected during the fed or fasted state. The fed HighD group had 26 % lower body weight than controls 43 days post STZ injection ($p = 0.0001$), and the fasted HighD group had 28 % lower body weight than controls 43 days post STZ injection ($p = 0.0001$). The fed and fasted HighD groups were not significantly different from each other. HighD animals injected in the fasted state had smaller standard deviations than HighD animals injected in the fed state (Fig. 3.11).

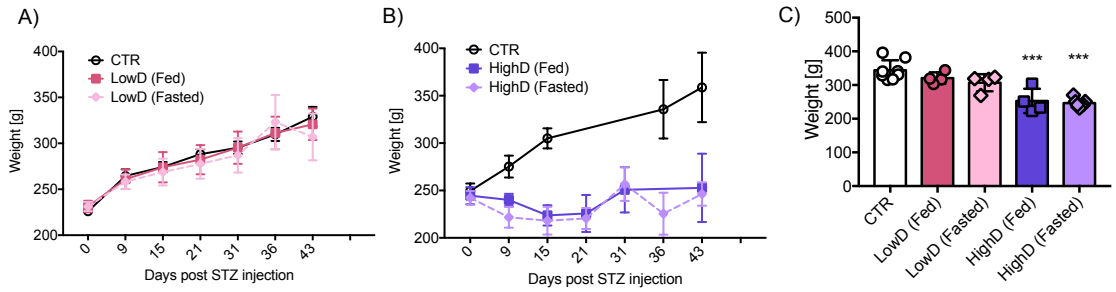

Figure 3.11: Weight shown from 0 to 43 days post streptozotocin (STZ) injection in low dose of STZ (LowD) and high dose of STZ (HighD) as well as controls (CTR). **A)** Weights of control and diabetic animals injected at fed and fasting with low dose STZ (25 mg/kg). **B)** Weight of control and diabetic animals injected at fed and fasting with high dose STZ (55 mg/kg). **C)** Weight of all groups at 43 days post STZ injection. Data presented as mean ± SD. One-way ANOVA compared to CTR with Dunnett's multiple comparison test. $^{***}p < 0.001$

If the low dose STZ group was fed when injected, no significant difference in blood glucose levels was observed at either 10 or 45 days post STZ injection. Even when the animals were fasted, the low dose animals did not show a significant change in blood glucose levels compared to controls until 45 days post STZ injection. At this stage, the blood glucose levels were only elevated slightly (7.8 ± 0.6 mmol/L $p = 0.05$) compared to the controls (Fig. 3.12).

A higher dose of STZ induced higher glucose levels and at an earlier time point post STZ injection (ten days). Animals in both the fed and fasted state

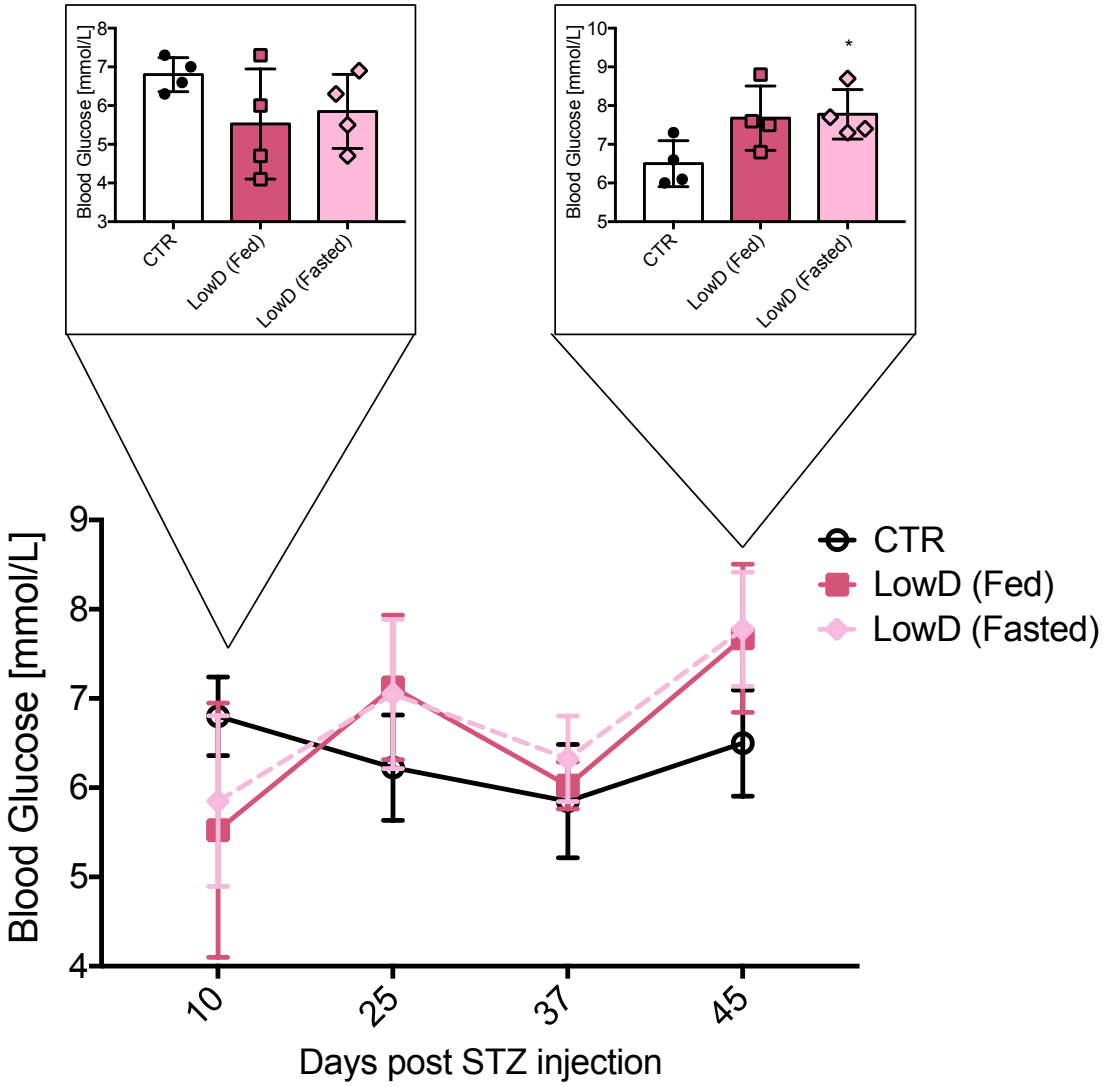

Figure 3.12: Blood glucose measurements after 12h fasting throughout the study. Blood glucose of control (CTR) and diabetic animals injected post fed and fasting with a low dose (LowD) of STZ (25 mg/kg) Mean ± SD. One-way ANOVA where $^*p < 0.05$.

prior to STZ injection in the HighD groups demonstrated significant elevations in blood glucose levels. However, the fasted group demonstrated a more sustained elevation in blood glucose levels over time compared to controls (21.0 ± 2 mmol/L, p = 0.0001, Fig. 3.13).

Water intake was 577 % higher in the high dose injected fasted animals than in the control animals 43 days post STZ injection (Fig. 3.14A). Food intake was 83 % higher in the high dose injected fasted animals than in the controls 43 days post STZ injection (Fig. 3.14B). Even though water and food intake was not measured

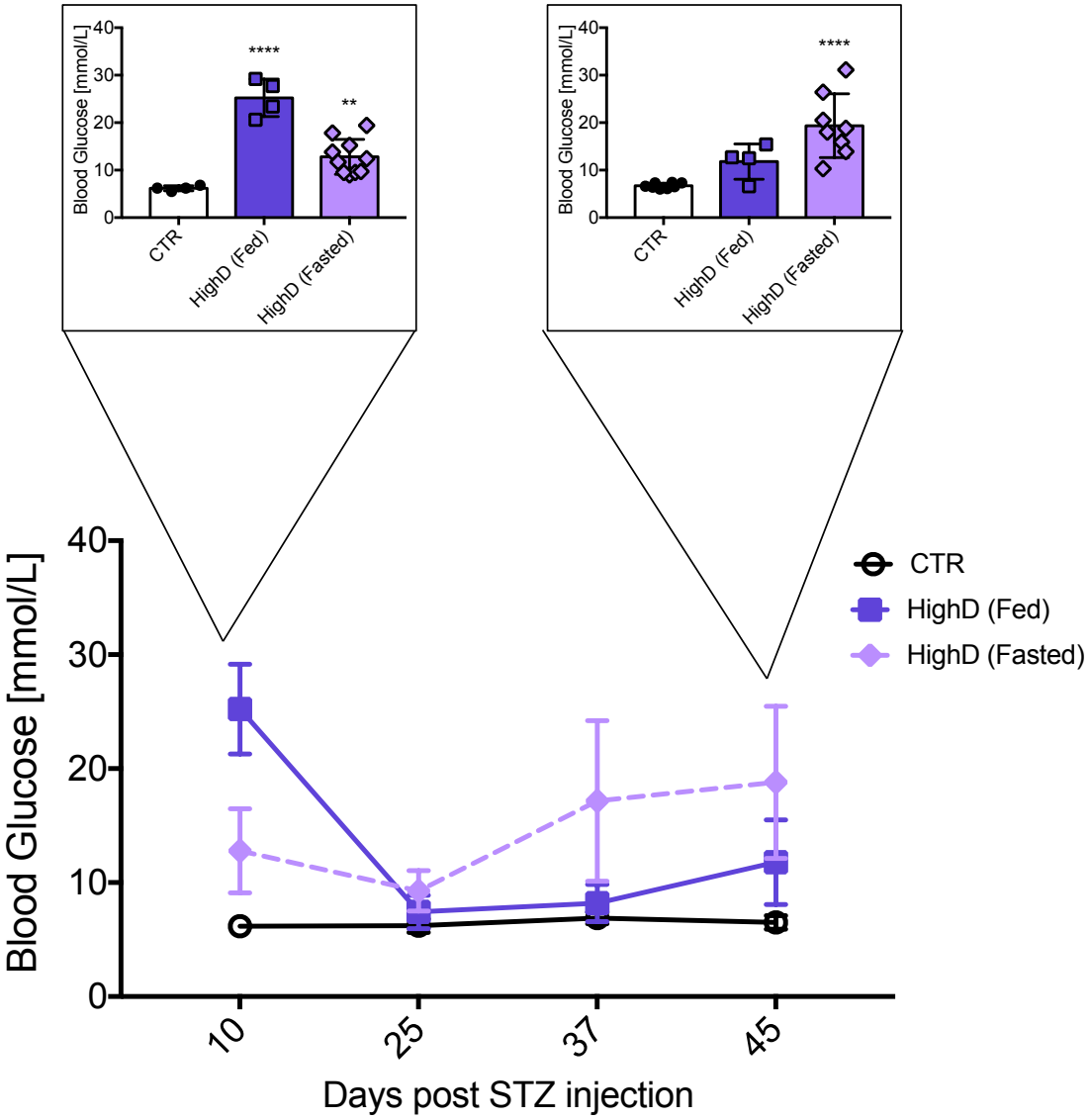

Figure 3.13: Blood glucose measurements after 12h fasting throughout the study. Blood glucose of control (CTR) and diabetic animals injected post fed and fasting with a high dose (HighD) of STZ (55 mg/kg). Data presented as mean ± SD. One-way ANOVA where $^{**}p < 0.01$,$^{****}p < 0.0001$.

in the fed HighD STZ group nor the low dose injected STZ groups (LowD), it was evident for all STZ groups, that water bottles needed more frequent refilling and that the cages needed to be changed more frequently than for the control groups due to higher volumes of urine.

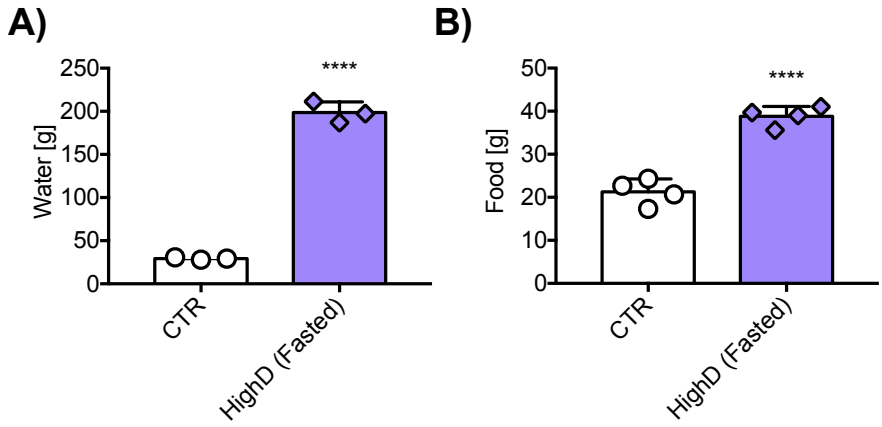

Figure 3.14: Intake of food/water per day per rat in control (CTR) and high dose (HighD) injected STZ animals **A)** Water intake in grams. **B)** Food intake in grams. Data presented as mean ± SD. Unpaired t-test, where $^{****}p < 0.0001$

3.8.2.2 Cardiac *In Vivo* Function

Heart rate was unaltered between all STZ groups and controls at two weeks (CTR: 420 ± 60 bpm, LowD (Fed): 460 ± 90 bpm, LowD (Fasted): 410 ± 30 bpm, HighD (Fed): 410 ± 30 bpm, HighD (Fasted): 350 ± 50 bpm). Cardiac output (CO) was significantly depressed by 28 % (p = 0.025) in the fasted high dose STZ injected animals compared to controls at two weeks (Fig. 3.15B), but no differences were seen in the other groups.

Average mass and stroke volume (SV) was unchanged across all groups, but the stroke index (SI) elevated in the fed HighD group by 28 % (p = 0.023) and 27 % (p = 0.042) in the fasted LowD group at two weeks post STZ injection compared to controls (Fig. 3.15ABC). End systolic lumen decreased by 42 % in the LowD fed group (p = 0.05) and decreased by 58 % in the HighD fed group compared to the controls (p = 0.01). End diastolic lumen decreased by 21 % in the HighD fed (p = 0.05) compared to controls, although the HighD fasted group decreased by 12 % it failed to reach statistical significance with a two-way ANOVA analysis (p = 0.037, unpaired t-test). Ejection fraction was increased by 10 % in the fed LowD groups (p = 0.043) and increased in the fed HighD by 18 % (p = 0.013) compared to controls. The HighD fasted group stayed unchanged (Fig. 3.15DEF).

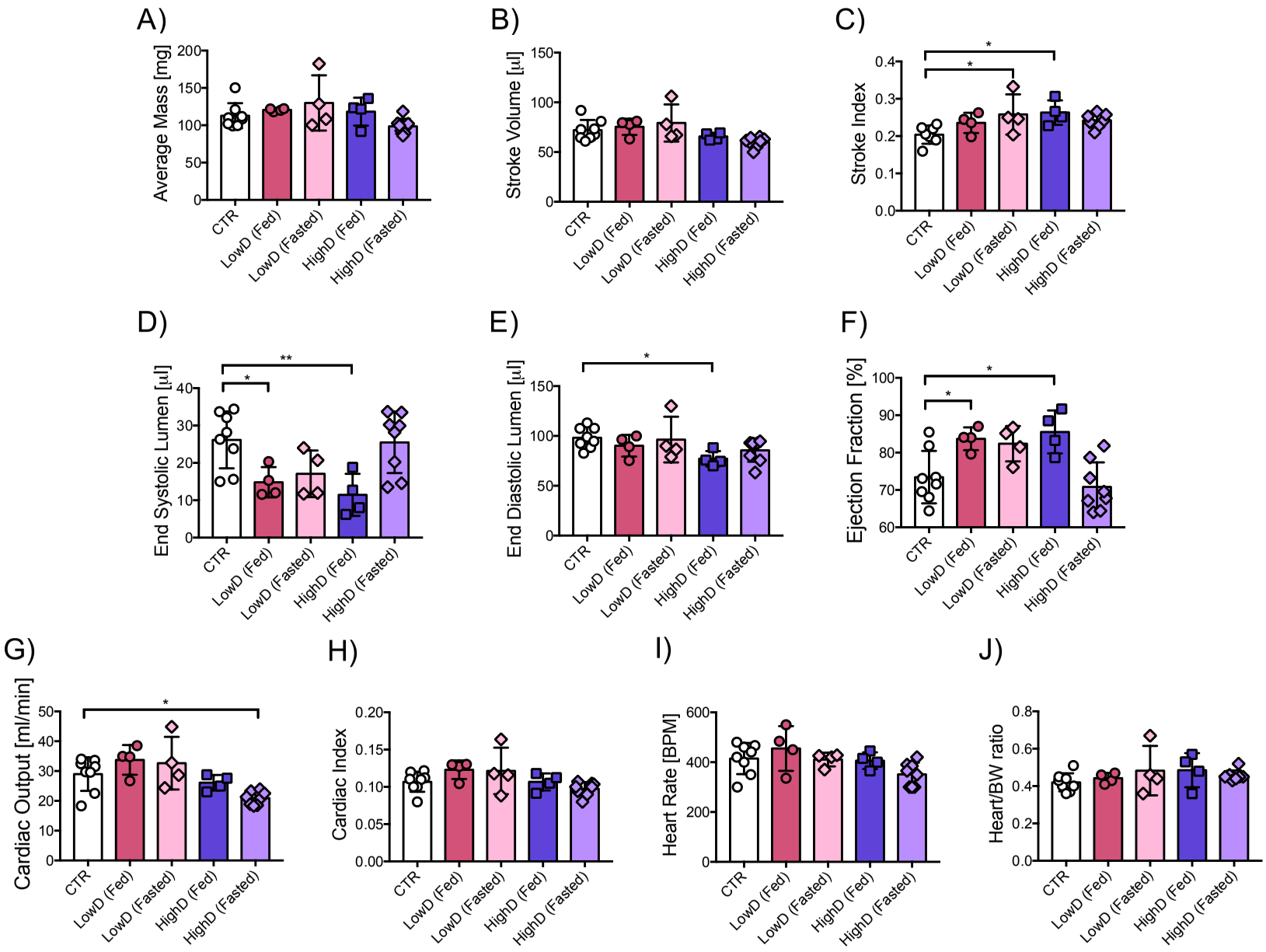

Figure 3.15: CINE MRI of cardiac function acquired two weeks post STZ/citrate buffer injection in control (CTR), low dose (LowD) and high dose (HighD) injected animals in fed and dasted state. **A)** Average myocardial wall mass of the left ventricle obtained from end diastolic and end systolic mass. **B)** Stroke volume (SV) obtained from the difference of end diastolic lumen and end systolic lumen. **C)** Stroke index (SI), SV normalized to body weight. **D)** End systolic lumen (ESL). **E)** End systolic lumen (EDL). **F)** Ejection fraction (EF). **G)** Cardiac output (CO). **H)** Cardiac index (CI), CO normalized to body weight. **I)** Heart rate (HR). **J)** HR normalized to body weight (HR/BW). Data presented as mean ± SD. Two-way ANOVA analysis with Sidak's multiple comparison test $^{*}p < 0.05, ^{**}p < 0.01$.

3.8.2.3 Cardiac *In Vivo* Metabolism

The cardiac bicarbonate to pyruvate ratio, a measure for PDH-flux, was decreased by 64 % ($p = 0.04$) and the alanine to pyruvate ratio was depleted by 61 % ($p = 0.02$) in the fasted HighD group compared to the controls at two weeks. Incorporation of ^{13}C into alanine was 78 % lower in the fed group compared to the fasted HighD group, although the bicarbonate to pyruvate ratio was not significantly reduced in the fed HighD group. The lactate to pyruvate ratio was unchanged in all groups at two weeks. LowD injected animals had unchanged bicarbonate and lactate levels. Even though alanine did not reach statistical significance, it was reduced by 23 % in the fasted LowD group compared to the controls (Fig. 3.16).

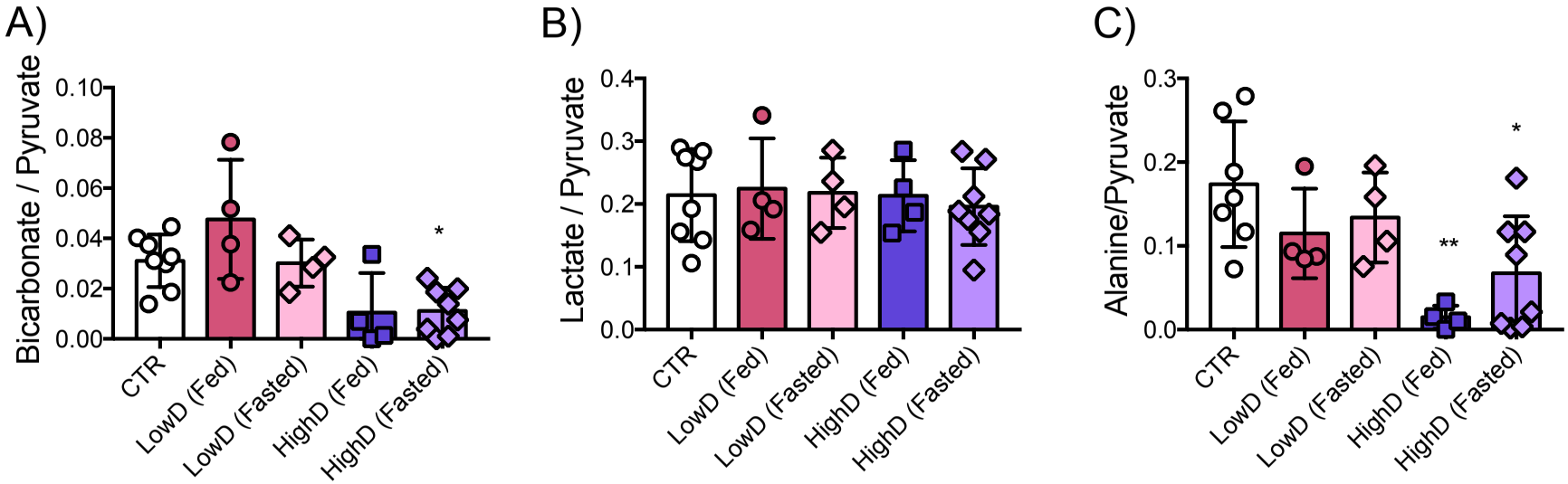

Figure 3.16: *In vivo* effects on cardiac metabolism through infusion of hyperpolarized [1-^{13}C]pyruvate two weeks post STZ injection. Pyruvate's metabolic products (bicarbonate, lactate and alanine) were summed over 30 seconds and normalized to the pyruvate peak. Citrate buffer injection in control rats (CTR,white), high dose (HighD) STZ injection in the fasted rats and fed rats (purple), as well as low dose (LowD) STZ injection in the fasted and fed rats (magenta). **A)** Bicarbonate/pyruvate ratio. **B)** Lactate/pyruvate ratio. **C)** Alanine/pyruvate ratio. Data presented as mean ± SD. One-way ANOVA adjusted for multiple comparisons. Comparing to controls (CTR). $^{*}p < 0.05$,$^{**}p < 0.01$.

3.8.3 Exploration of the Temporal Effects of STZ-Induced Diabetes on Cardiac Metabolism and Function using Hyperpolarized ^{13}C MRS and CINE MRI

When HighD is stated in this section, it is referred to the fasted high dose injected STZ model, unless otherwise stated.

3.8.3.1 Blood Profile

In line with the development of T1D, blood glucose was significantly elevated compared to controls at both two and six weeks. Blood glucose levels progressively increased from 16 ± 3 mmol/L at two weeks to 19 ± 7 mmol/L at six weeks post high dose STZ injection (p = 0.036, Fig. 3.17).

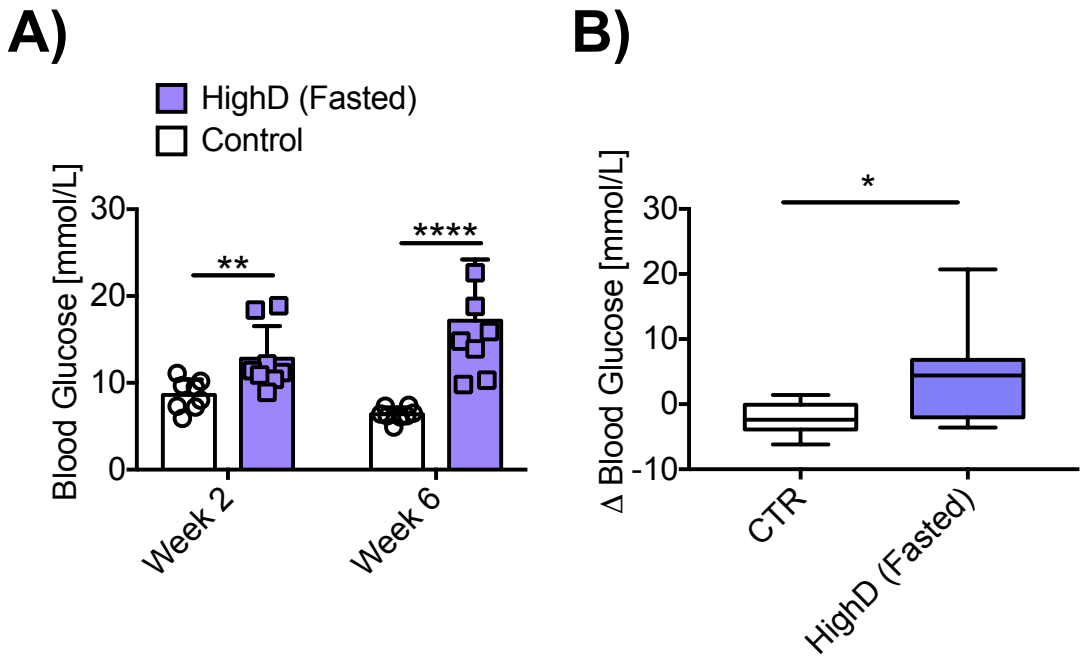

Figure 3.17: **A)** Blood glucose levels obtained in fasted state at two and six weeks. Two-way ANOVA with Sidak's multiple comparison, where $^{**}p < 0.01$, $^{***}p < 0.001$. **B)** A box-and-whisker plot showing median from minimum to maximum of differences between blood glucose levels at six weeks and two weeks. High dose STZ injections in fasted state (purple) and controls injected with citrate buffer in fasted state (white). Data presented as mean ± SD. Unpaired two-tailed t-test, where $^{*}p < 0.05$.

3.8.3.2 Cardiac *In Vivo* Function

Systolic and diastolic function was assessed with echocardiography at six weeks post STZ injection. Ejection fraction was similar across groups, although the HighD group had higher variations. Fractional shortening was 21 % lower in the HighD group compared to controls at six weeks ($p = 0.05$, unpaired t-test). E/E' measured in the lateral wall was 20 % higher in the HighD group compared to the control, although it failed to reach statistical significance ($p = 0.08$, unpaired t-test), and E/E' ratio in the septum was 24 % lower in the HighD group, although it also failed to reach statistical significance ($p = 0.08$, unpaired t-test, Fig. 3.18).

Ejection fraction as observed on CINE MRI was unaltered across both groups and at both time-points (Fig. 3.19A). Stroke volume was reduced in the HighD group compared to controls at both two and six weeks ($p = 0.049$, Fig. 3.19B), and when stroke volume was normalized to body weight, there was a significant increase in the HighD group compared to the controls at both two and six weeks ($p = 0.006$, Fig. 3.19C). Heart rate over body weight was elevated in the HighD group compared to the control group at both time-points ($p = 0.032$). Cardiac output was significantly reduced in the HighD group compared to controls at both time-points ($p = 0.0003$), but this was mostly driven by the reduced body weight in the HighD group compared to controls at both time-points ($p < 0.0001$), which resulted in no differences observed in cardiac index (Fig. 3.19DEF).

Average mass was significantly decreased in the HighD groups compared to controls at both time points ($p = 0.008$, Fig. 3.19G) and body weight was lower in the HighD compared to the controls at both time-points ($p < 0.0001$). Although both body weight and myocardial mass significantly increased in controls at six weeks compared to at two weeks ($p = 0.03$ Fig. 3.19H).

Cardiac output decreased by 28 % in the fasted HighD group compared to the control group ($p = 0.02$), but cardiac index was unchanged across all groups. Heart rate and heart rate normalized to body weight were all unchanged across all groups (Fig. 3.15GHIJ).

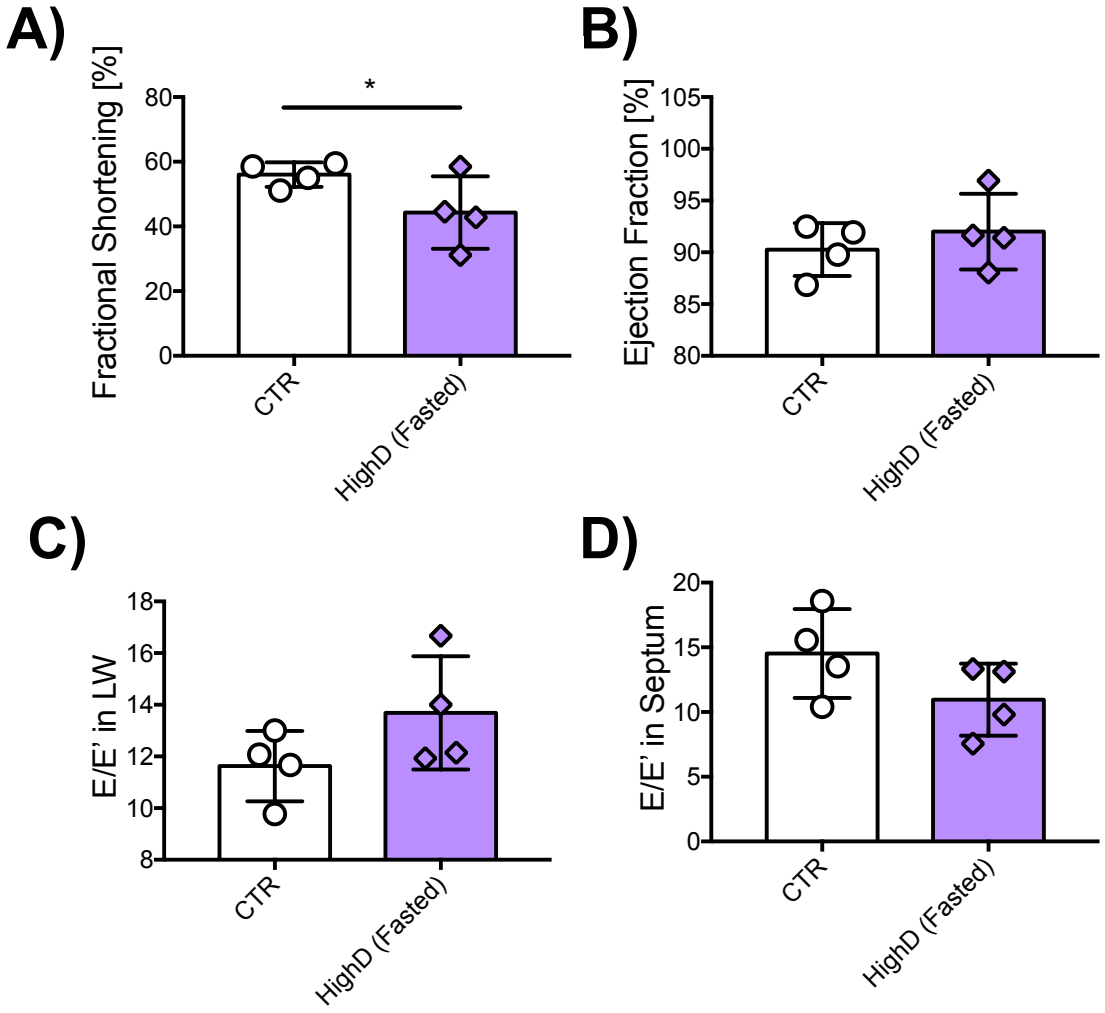

Figure 3.18: Echocardiography obtained at six weeks post STZ/citrate buffer injection. **A)** Fractional Shortening, FS [%], assumes symmetrical contraction. **B)** Ejection Fraction, EF [%] calculated based on Simpson's model and does not assume symmetrical contraction. **C)** E/E' ratio which is mitral valve blood inflow over mitral annulus velocities in the lateral wall. **D)** E/E' ratio which is mitral valve blood inflow over mitral annulus velocities in the septum. Data presented as mean ± SD. Unpaired t-test, where $^{*}p < 0.05$.

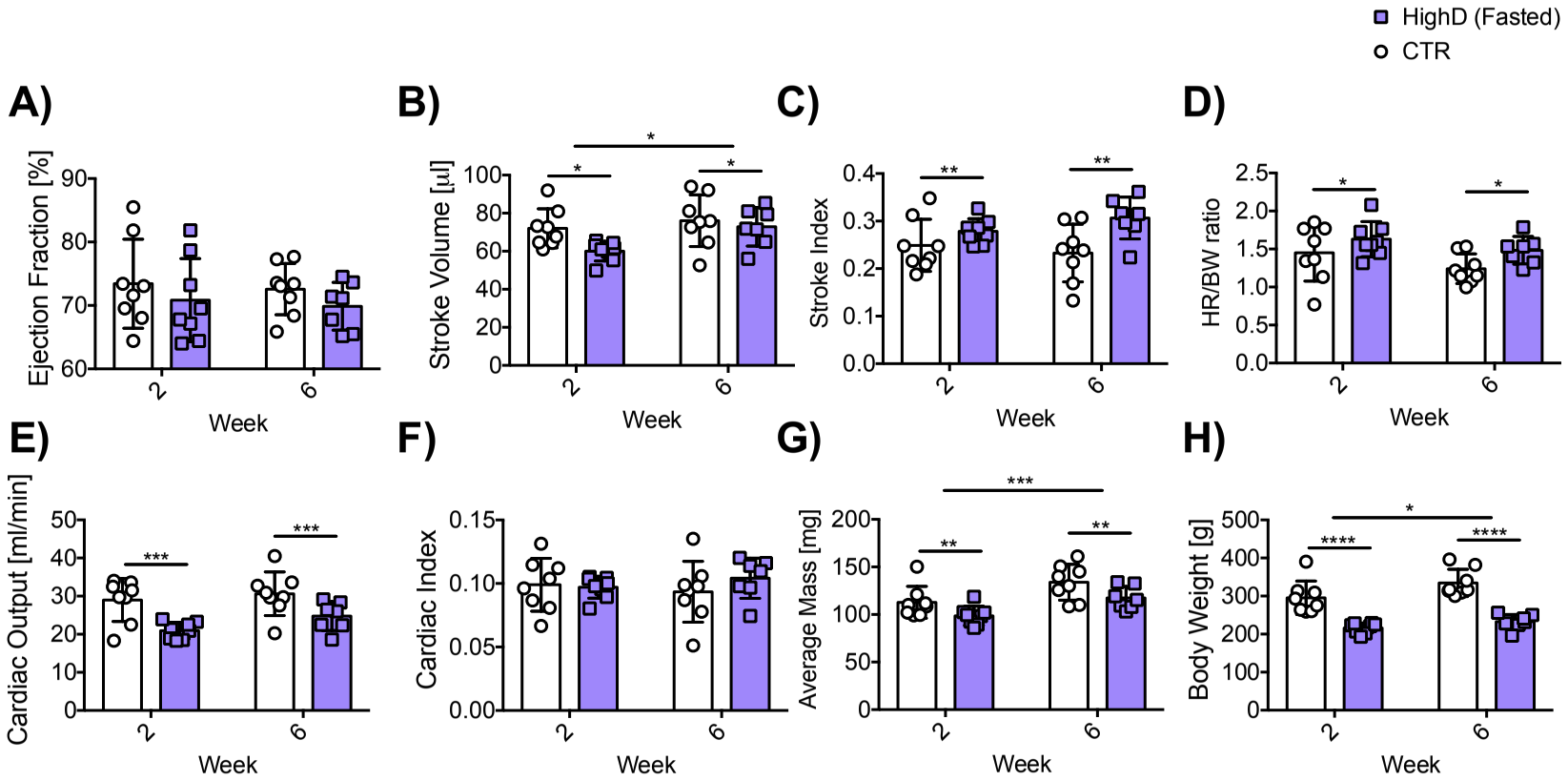

Figure 3.19: CINE MRI of the cardiac function acquired at two and six weeks post STZ/citrate buffer injection. **A)** Ejection fraction, EF [%]. **B)** Stroke volume, SV [μ] obtained from the end diastolic and systolic lumen. **C)** Cardiac output, CO [ml/min]. **D** Heart rate over body weight ratio, HR/BW. **E)** Body weight, BW [g]. **F)** Stroke index, SV/BW. **G)** Cardiac Index, CO/BW. **H)** Average myocardial mass [mg]. Citrate buffer injection in control rats (white) and high dose STZ injection in fasted rats (purple). Data presented as mean $\pm$ SD. Two way ANOVA with Sidak's multiple comparison, where $^{*}p < 0.05$, $^{**}p < 0.01$,$^{***}p < 0.001$, $^{****}p < 0.0001$.

3.8.3.3 Cardiac *In Vivo* Metabolism

With the development of diabetes, flux through pyruvate dehydrogenase (PDH) as indicated by reduced incorporation of ^{13}C into bicarbonate was significantly decreased at both time-points studied. PDH-flux was reduced by 80 % in HighD compared to controls at six weeks ($p < 0.0001$). PDH-flux was unaltered between the two time-points for the HighD group. However, it increased by 59 % in the CTR group over the two time-points (p = 0.002, Fig 3.20A). The incorporation of ^{13}C label from pyruvate into lactate was significantly elevated in the HighD group compared to controls at six weeks. A multiple comparison test showed a 165 % elevation in lactate at six weeks in the HighD group compared to the controls (p = 0.0046), and an elevation of 140 % in lactate at six weeks in the HighD group compared to at two weeks in the HighD group (p = 0.0078, Fig 3.20B). The incorporation of ^{13}C label from pyruvate into alanine showed a 57 % reduction in the HighD group compared to controls at two weeks (p = 0.05). Alanine elevated over time for the HighD group by 168 % at six weeks compared to at two weeks (p = 0.016, Fig 3.20C). Finally, the bicarbonate over lactate ratio was significantly reduced in the HighD group compared to controls at both two and six weeks ($p < 0.0001$), and the ratio increased in controls by 83 % at week six compared to week two (p = 0.0047, Fig 3.20D).

There was a significant negative correlation between bicarbonate and blood glucose levels at both two and six weeks post STZ injection ($R^2 = 0.3$, p = 0.04, Fig. 3.21A). Lactate levels for all time-points were positively correlated with glucose levels ($R^2 = 0.4$, p = 0.006, Fig. 3.21B), mostly driven by the later time point. Interestingly alanine had a biphasic correlation, where it was strongly negatively correlated with blood glucose levels at two weeks ($R^2 = 0.8$, p = 0.004), but then reversed to a positive correlation at six weeks ($R^2 = 0.6$, p = 0.02, Fig. 3.21C). Furthermore, there was a correlation between stroke volume and alanine levels at all time points ($R^2 = 0.3$, p = 0.03, Fig. 3.21F).

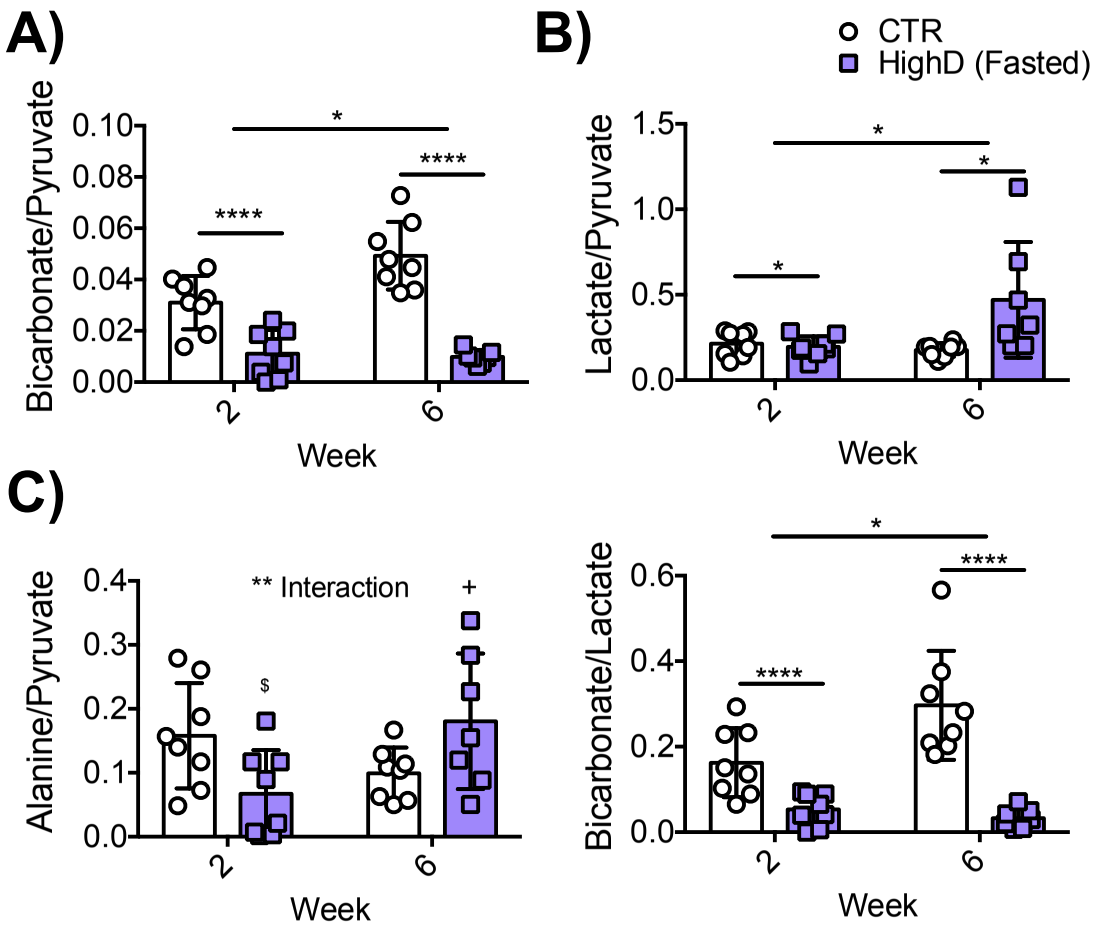

Figure 3.20: *In vivo* effects of infusion of hyperpolarized [1-^{13}C]pyruvate at two and six weeks post STZ injection. The acquired spectra are summed over 30 seconds, and pyruvate's metabolic products; bicarbonate, lactate, and alanine are normalized to the pyruvate peak. **A)** Bicarbonate over pyruvate ratio. **B)** Lactate over pyruvate ratio. **C)** Alanine over pyruvate ratio. **D)** bicarbonate/pyruvate over lactate/pyruvate ratio measure for aerobic/anaerobic flux. Citrate buffer injection in control rats (white) and high dose STZ injection in fasted rats (purple). Data presented as mean ± SD. Two way ANOVA with Sidak's multiple comparison, where $^{*}p < 0.05$, $^{**}p < 0.01$, $^{****}p < 0.0001$ and $^{+}p < 0.05$ compared to HighD at two weeks, $^{\$}p < 0.05$ compared to control at two weeks.

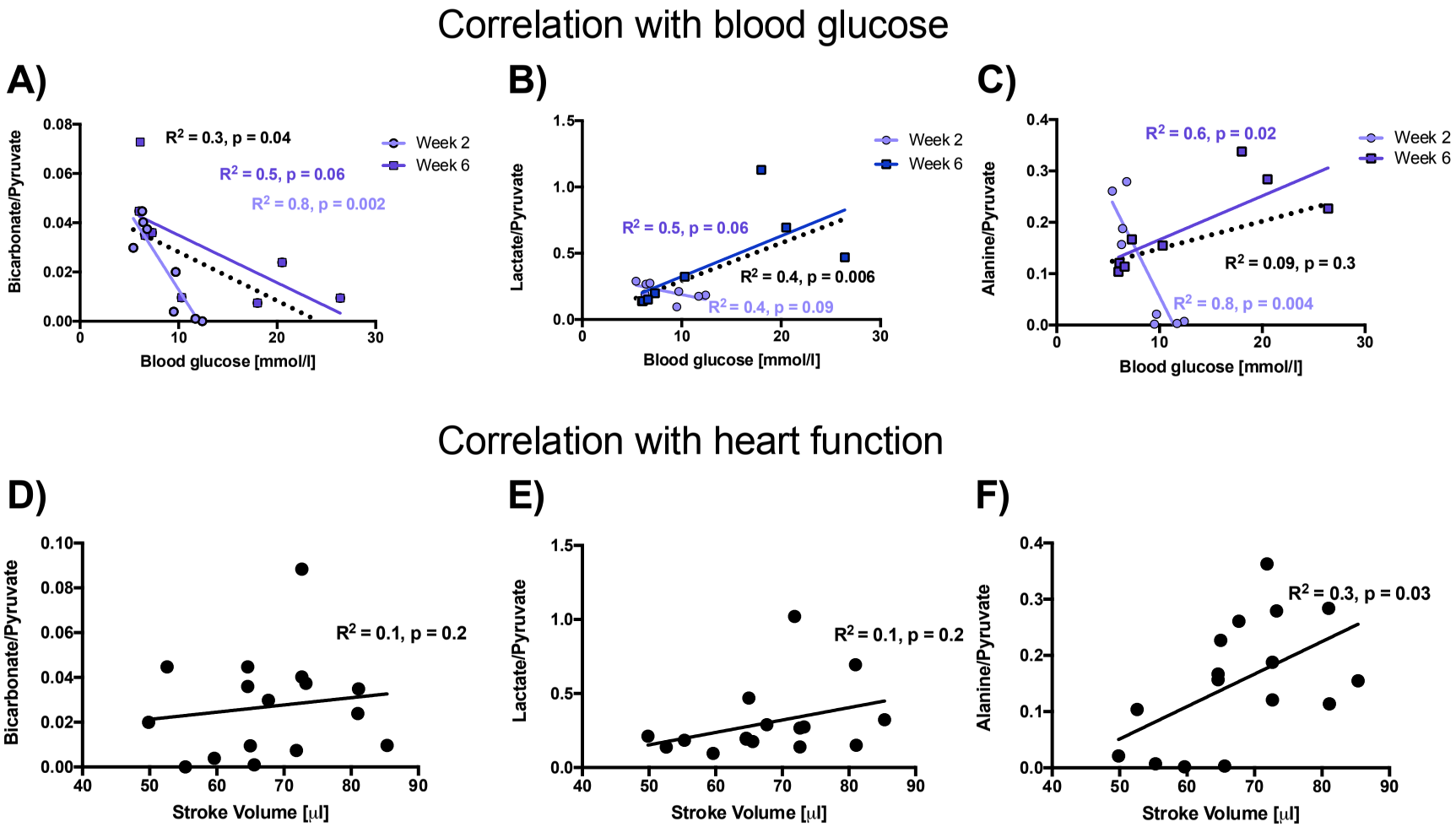

Figure 3.21: Correlation between cardiac metabolism and blood glucose levels **(A-C)**. The correlations with blood glucose levels are illustrated separately for two weeks (light purple) and six weeks (purple) post STZ/citrate buffer injections, as well as both weeks together (black dotted line). Correlation between cardiac metabolism and heart function at both two and six weeks post STZ/citrate buffer injections **(D-F)**. Linear regression with Goodness of Fit analysis, F-test analysis if the slope is significantly different from non-zero.

3.9 Discussion

Mortality rates used to be high in the pre-treatment era of T1D, but with improved glycaemic control, mortality rates have decreased [122]. Diabetes still increases the incidence of cardiac failure. More literature states, that cardiac failure is linked with changes in cardiac metabolism, Herrmann and Dechard described the failing heart in 1939 to be "an engine without fuel" [94]. Understanding the metabolic changes that occur in the diabetic heart may be vital to understanding the pathophysiology of the cardiac effects of diabetes. By improving this understanding, a treatment can more easily be applied to remodel metabolism and function in the diabetic heart.

In this work, two different models of diabetes were assessed together with their cardiac function and metabolism. Hyperpolarized MRS was shown to be an excellent method to assess *in vivo* metabolic changes, and cardiac function was assessed *in vivo* with both MRI and echocardiography. These findings can help elucidate the metabolic and functional remodelling observed in response to treatments.

3.9.1 Cardiac Metabolism and Function in a Mouse Model of NDM

Studies have shown that there is a relationship between substrate oxidation and cardiac function in diabetes [38]. In this model of neonatal diabetes, weight loss was induced as well as increased blood glucose levels were observed, which were both normalized with glibenclamide treatment. This is not surprising since this model of neonatal diabetes, when injected with tamoxifen, inhibits ATP to close the K_{ATP} channel, thereby preventing insulin release. The closing of the K_{ATP} channel can occur again with glibenclamide treatment, and thereby secretion of insulin occurs [8].

PDH-flux was reduced with diabetes in the *in vivo* mouse heart. This metabolic change occurred together with functional changes in the heart. The increased glucose levels resulted in inhibition of PDH-flux which lowers entry of glucose derived pyruvate into the TCA cycle. Hyperglycemia has been shown to impair cardiac function and metabolism previously without any changes in lipids [214]. Both the functional and metabolic changes were reversed with glibenclamide treatment.

Neither lactate nor alanine was changed in the heart at any of the time points studied. The lack of metabolic alterations in alanine and lactate could have been due to an elevated noise in the signal obtained from the mouse model. The rat model reached 800 % higher amplitudes than the mouse model reached, and there was a higher noise acquired from the mouse model (Fig. 3.22).

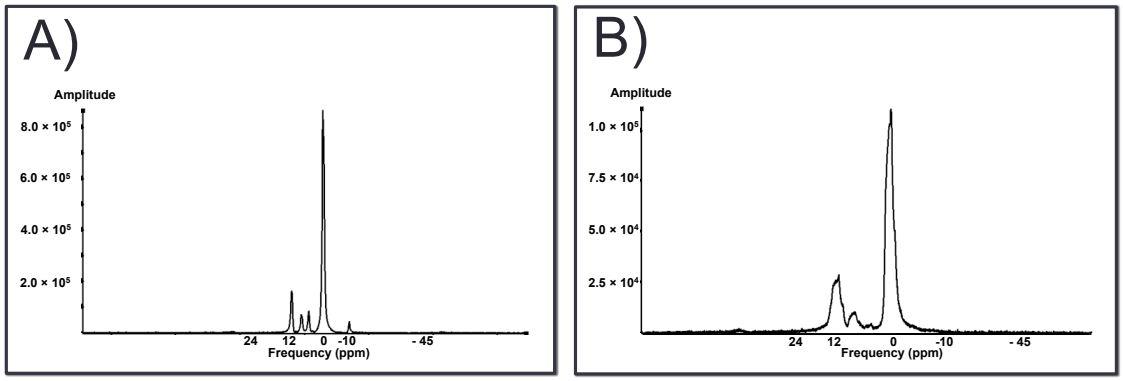

Figure 3.22: Signal to noise comparison between a mouse and a rat model. *In vivo* effects of infusion of hyperpolarized $[1-^{13}C]$pyruvate. Spectra summed over 30 seconds, beginning at the first appearance of the pyruvate peak. **A)** Spectra showed for the STZ induced rat model after two weeks of diabetes. **B)** Spectra showed for neonatal mouse model after two weeks of diabetes.

Cardiac progression of this model of neonatal diabetes was followed until six months post tamoxifen injection. Cardiac output, cardiac index and stroke volume were decreased at eight weeks of diabetes. However, stroke index elevated at six month post diabetes induction compared to both at two weeks and eight weeks of diabetes. This could suggest a later functional adaptation to the metabolic changes in this model of diabetes. However, *in vivo* metabolism was not measured at these time-points and would have been interesting to validate if there was a redirection of pyruvate conversion into lactate and alanine at the later stages as subsequently seen in the STZ model.

This study has shown the potential for hyperpolarized MRS and CINE MRI to study the changes in cardiac metabolism and function that occur alongside the development of a reversible model of T1D and how the reversible action with glibenclamide can affect metabolism and function.

However, due to the low sensitivity of the metabolic findings, other models were also investigated, in order to find a suitable model for investigating treatment response in the subsequent chapters.

3.9.2 Cardiac Metabolism and Function in STZ-Induced Models of Type 1 Diabetes

This study confirms what previous literature reports of the streptozotocin model have shown; all streptozotocin models exhibited polydipsia (excess drinking), polyuria (excess urine production), glucosuria (excess glucose in the urine), which was tested 1-2 days post STZ injection, polyphagia (excess eating) and hyperglycaemia [173, 90, 97]. Hyperglycaemia was not observed in the fed low dose injected group.

3.9.2.1 Weight and Blood Profile

The streptozotocin-induced diabetic animals that were given a low dose of 25 mg/kg of STZ, had a steady weight gain throughout the study similar to the control animals. The streptozotocin-induced diabetic animals that were given a high dose of 55 mg/kg did not have any weight gain throughout the study and were significantly smaller at 43 days post STZ injection than the controls. Previous studies have shown decreased food-uptake immediately post STZ injection and then, as animals lose weight, the food intake increases [97], which is confirmed in this study with the HighD fasted model at 43 days post STZ injection. This could be explained by an inability to metabolise carbohydrate, due to the lack of insulin. A lack of insulin shifts the energy balance to be more reliant on fatty acids resulting in increased mobilisation of fat stores, and therefore a weight loss is seen in these animals.

All low dose and high dose injected STZ animals exhibited glucosuria one and two days post STZ injection, and none were excluded from the study. Even though glucosuria was observed two days post STZ injection, the animals that were fed prior to the STZ injection did not have significantly higher blood glucose levels 43 days post STZ injection regardless of the dose given. Fed HighD animals already expressed higher glucose levels at ten days post STZ injection, however the glucose levels dissipated and were no longer significantly higher than controls at 43 days post

STZ injection. Fasting prior to STZ injection gave more reliable diabetic animals that sustained the high glucose levels over time, unlike in the fed animals. This is further confirmed in the low dose injected animals, which only increased their glucose levels to be significant at 43 days post injection. If the animals were not fasted prior to STZ injection glucose and STZ could be in competition for uptake in the postprandial state, since GLUT2 has a low-affinity for glucose, and STZ is taken up by GLUT2, it could explain why the fasted animals show more reproducible results [64]. This study shows that the higher dose of STZ (55 mg/kg) and fasting prior to injection results in more severe hyperglycaemia than the lower dose of STZ (25 mg/kg) and feeding prior to STZ injection. It is expected that a higher dose of STZ will damage more β-cells and therefore produce higher blood glucose levels [43, 154].

3.9.2.2 Cardiac *In Vivo* Metabolism and Function

Studies have previously shown that blood glucose levels are correlated with PDH-flux [139]. PDH activity regulates the balance between fat and carbohydrate metabolism, and if it is impaired, the heart is forced to rely on more fatty acids, that are not as oxygen efficient. The heart expressed lower PDH activity with the higher dose of STZ, utilizing less glucose for ATP production. Of all the STZ models investigated, only the high dose animals injected in the fasted state exhibited significantly lower PDH-flux in the heart. Due to the lower severity of diabetes found in the animals, that were fed prior to STZ injection and in the animals given a low dose, but in the fasted state, sufficient pyruvate could still enter the mitochondria and maintain flexibility in substrate selection. However, there might be a delicate balance, likely at a later time-point, at which point PDH-flux would have been impaired even in the fed STZ animals, and the fasted low dose injected animals.

It was not just PDH-flux that was altered, even though ^{13}C incorporation into lactate in the heart was unchanged at two weeks, the ^{13}C incorporation into alanine, a measure of alanine aminotransferase (ALT), was depressed in both the fed and in the fasted high dose STZ injected animals at two weeks. Also, the low dose injected animals in the fed state had depleted alanine levels at two weeks. This suggests that

the diabetic hearts either had a smaller pool of free alanine or lower activity of ALT. The ALT alterations could possibly precede the PDH-flux changes and therefore may represent an impairment of cardiac function, since the fed high dose injected STZ model seemed to be the second most severe model of diabetes, and could with more time have shown PDH-flux as well functional alterations. Alanine, a gluconeogenic pre-cursor, is still inhibited by two weeks of diabetes, but then is activated six weeks after diabetes. It has been previously shown that ALT alters with type 2 diabetes in the heart, and alanine changes have been commonly observed in diabetes [126, 127].

Despite metabolic changes, the low dose animals did not show a reduction in cardiac function. However, the high dose animals showed depression of cardiac output and stroke volume already at two weeks, and the functional changes were more severe in the fasted group than in the fed group. These changes could mean that metabolic remodelling happens prior to functional remodelling.

Furthermore, these results could also point toward alanine being an important biomarker for early metabolic and functional alterations in diabetes. However, further investigations are needed.

3.9.3 Temporal Effects of STZ-Induced Diabetes on Cardiac Metabolism and Function

The temporal effects of the most severe STZ model; fasted high dose injected STZ (HighD) were investigated. This study suggests a progressive change in cardiac metabolism and function following the onset of T1D.

STZ is the compound of choice for a reproducible induction of diabetes [129] and as expected the blood glucose levels increased over six weeks of diabetes and stayed significantly higher than the blood glucose levels in the control animals. These diabetic hearts were oxidizing significantly less glucose to sustain their ATP demand and were switching to more fatty acid metabolism [93, 126]. The more severe diabetes and the higher blood glucose levels, observed in the high dose fasted animals, results in a switch to fatty acid oxidation and most likely to ketone utilisation [253, 139], impairs pyruvate oxidation and therefore lowers PDH-flux [139].

In control animals, PDH activity increased over time, this is expected due to the gain of weight and gain of myocardial mass that were observed at six weeks compared to at two weeks. PDH activity was significantly lower in the high dose fasted diabetic group at both time-points, even though, myocardial mass increased at six weeks compared to at two weeks, but body weight was unaltered. The relationship between glucose levels and PDH-flux is stronger in the early time points post STZ injection. This is not due to a lowering of blood glucose levels, but in contrast due to even higher glucose levels, while PDH-flux remains low and does not lower further.

This study has shown the potential for hyperpolarized MRS and CINE MRI to study the progressive changes in cardiac metabolism and function that occur alongside the development of T1D diabetes. Such studies will allow for a better understanding of the interactions between metabolism and function in the diabetic heart and may provide new insight into novel therapeutics as discussed in later chapters.

3.9.4 Conclusion and Future Perspective

This chapter explores two different hypoinsulinemia untreated non-obese diabetic models, which both show cardiac metabolic and functional changes.

Alterations of metabolism and functional progression of diabetes are shown for the first time *in vivo* in a genetic mouse model of neonatal diabetes. The first *in vivo* metabolic and functional response is observed post glibenclamide in the mouse model, and how it reverses the diabetic phenotype. Furthermore, *in vivo* metabolism and functional progression is for the first time explored in the streptozotocin-induced T1D rat model, using MRI and hyperpolarized MRS. A fasted high dose injected STZ model showed the most reproducible and severe metabolic and functional changes *in vivo*. It is evident that the hearts in both models are adaptive to their metabolic pathways accommodating the functional changes. Both the severity of diabetes and the progression of the disease support these stepwise changes. However even though the alterations were similar between the mouse and the rat models, more metabolic changes were observed with the streptozotocin-induced fasted rat model. The signal to noise ratio was higher in the rat model compared to the mouse

model, and therefore the HighD STZ model injected in the fasted state was a more suitable model for investigating treatment response in the subsequent chapters.

Such studies allow for a better understanding of the interactions between metabolism and function in the diabetic heart. Hyperglycaemia is a critical factor for cardiac alterations, and therefore tight glucose control might be essential in keeping diabetic hearts from impairments. Studies like this may provide new insight into novel therapeutics for heart disease in diabetic subjects.

The third approached the animal
And happening to take
The squirming trunk within his hands,
Then boldly up and spake;
"I see", quoth he, "The elephant
Is very like an snake."

4

Feasibility Studies: Establishing Therapeutic Effects on Metabolism and Function in Healthy Hearts

Contents

4.1 Chapter Overview 102
4.2 Background 102
4.3 Chapter Aims 105
4.4 Methods 106
4.4.1 Langendorff Perfused Healthy Hearts 106
4.4.2 Daily L-Carnitine and Mildronate Treatment in the Healthy Heart 106
4.5 Results 108
4.5.1 Langendorff Perfused Healthy Hearts 108
4.5.2 Daily L-Carnitine Treatment in the Healthy Heart . . . 117
4.5.3 Daily Mildronate Treatment in the Healthy Heart . . . 120
4.6 Discussion 122
4.6.1 Langendorff Perfused Healthy Hearts 122
4.6.2 Daily L-Carnitine Treatment in the Healthy Heart . . . 123
4.6.3 Daily Mildronate Treatment in the Healthy Heart . . . 124
4.6.4 Conclusion and Future Perspective 124

4.1 Chapter Overview

This chapter combined several feasibility studies that were necessary for the rest of this thesis. Langendorff perfusions were used to determine the effects of treatment on ischemia reperfusion in diabetic hearts, but initially, in this chapter, an appropriate low-flow ischemic rate was established. Subsequently it was investigated whether the acute addition of L-carnitine to the perfusate buffer could modulate the detrimental effects of ischemia in healthy hearts, and finally, feasibility studies were investigated to reduce or elevate L-carnitine levels in plasma and heart tissue by daily i.p. injections of either L-carnitine or Mildronate.

This chapter established a less restrictive low-flow rate of 0.4 ml/min/gram wet weight (gww) to be the optimal flow rate to use during ischemia, as a flow rate of 0.33 ml/min/gww led to very poor recovery post-ischemia of the healthy hearts.

Furthermore, the effects of L-carnitine added acutely to the perfusate buffer in healthy hearts seemed to either unalter or potentially even reduce functional recovery post-ischemia. However, despite a potentially detrimental effect in healthy hearts, a beneficial effect on diabetic hearts was still hypothesized, since the diabetic heart naturally has elevated fatty acids. In contrast to the addition of L-carnitine in the perfusate buffer, a different administration route was explored (i.p. injections). Oral L-carnitine treatment was not administered due to the lack of effects observed in diabetic animals in the literature. L-carnitine treatment was given daily through i.p. injections in healthy animals and this chapter confirmed an elevation of free L-carnitine in plasma already after two weeks of treatment. Also *in vivo* elevation of acetylcarnitine was observed in the heart. Finally, this chapter showed a decrease of free L-carnitine in heart tissue and an absence of L-carnitine in plasma of healthy animals treated with only two weeks of daily i.p. injections of Mildronate.

4.2 Background

As described in Section 1.5, L-carnitine is both taken up through food sources (mostly meat) and is also synthesised by the body [108]. With age, myocardial L-carnitine

levels diminish and so does the rate limiting enzyme (CPT1) for fatty acyl-CoA uptake into the mitochondria [44, 81]. The organ most affected by this decline is the heart because fatty acids are the preferred energy source (Section 1.3). A decrease in L-carnitine levels, therefore, leads to an alteration in myocardial substrate metabolism. There are mixed studies that show if oral treatments are beneficial or detrimental. The human body can take up L-carnitine through food or supplements, even though the body can biosynthesise it as well, and vegetarians have been shown to have reduced circulatory levels of L-carnitine [181]. L-carnitine is critical for maintaining myocardial energy metabolism and a sufficient cardiac function. As Richard Kunin said: "The path to nutritional health is paved with carnitine " [46].

L-carnitine has been recognized as a nutritional supplement in cardiovascular disease. Its mechanisms of action are unclear, in some cases, it has shown to enhance carbohydrate metabolism and in other cases, it has been shown to elevate fatty acid oxidation. L-carnitine has been shown to be effective in conditions, where there is elevated oxidative stress such as ischemic heart disease [32, 124]. Cardiac efficiency has been postulated to improve through inhibition of fatty acid oxidation and thereby increasing glucose oxidation [104]. Although many other studies have shown that it elevates fatty acid oxidation, the mechanisms of L-carnitine are therefore not entirely understood and need further investigation. Several studies have demonstrated beneficial effects in the *ex vivo* heart post-ischemia [148, 26, 106, 67, 175]. During ischemia in the Langendorff perfused heart, L-carnitine levels decrease to about 30 % in heart tissue [148]. L-carnitine treatment (10 mM) has shown in the isolated perfused heart to reduce fatty acid inhibition of glucose oxidation and promote glucose oxidation rates in the presence of high levels of fatty acids (1.2 mM of palmitate). These perfused hearts were given 10 mM of L-carnitine in the perfusate buffer for 60 minutes prior to ischemia, protecting them against ischemic injury and improving functional recovery [28]. Without the presence of L-carnitine, glucose oxidation is reduced post-ischemia with the presence of 1.2 mM of palmitate in the buffer and a poor recovery is observed post-ischemia [146].

Although high rates of fatty acid oxidation impair glucose oxidation and therefore functional recovery in ischemia reperfused hearts [140], another study has shown that higher levels of palmitate concentrations (1.2 mM compared to 0.4 mM) improve functional recovery with L-carnitine added to the buffer, but with low glucose concentrations (1.2 mM), in the isolated perfused heart. Despite the low concentration of glucose, and in their absence, functional recovery was shown to be the worst post-ischemia. Adding L-carnitine (5 mM) to the perfusate buffer improved recovery post-ischemia significantly with both high and low concentration of palmitate compared to not adding L-carnitine. Recovery was also shown to improve when adding L-carnitine, if high concentrations of palmitate were used, compared to not adding L-carnitine [149]. It is suggested that an accumulation of acyl-CoA post-ischemia results in myocardial dysfunction and that L-carnitine is associated with an ability to lower acyl-CoA accumulation post-ischemia through elevation of acylcarnitines [252, 98].

In contrast, Diaz *et al.* have shown that recovery post-ischemia in the isolated perfused heart treated with L-carnitine worsens and does not stimulate glucose oxidation. This was in part because very low levels of L-carnitine had been used (1 mM) but could be in part due to the unknown palmitate concentration used, if any [56].

L-carnitine might, therefore, have both a positive (at high doses) and a negative effect (at low doses) on functional recovery post-ischemia, and on glucose oxidation, so it might be critically bound to the L-carnitine dose given, but most certainly also on the experimental conditions used and other substrates that are available.

It is not just the concentration of L-carnitine that is critical for the outcome post-ischemia, but also the administration route of L-carnitine has proven to be important. In the previous studies discussed in this section, L-carnitine effects were shown in the isolated perfused heart, when added directly to the perfusate buffer, but what happens when the treatment is given *in vivo*, while also a correct balance of hormonal, regulatory and functional responses can occur.

Beneficial effects have not always been observed if L-carnitine is given orally [22, 15, 212]. Bazotte *et al.* failed to show any modification of fatty acid oxidation in healthy hearts after four weeks of oral treatment, even though free L-carnitine was elevated in the plasma and heart [15]. This lack of modification could have been due to normal levels of fatty acids in the healthy heart, and therefore no requirement for a change of metabolic substrate utilisation. Rodrigues *et al.* also failed to show any benefits in healthy animals after six weeks of oral L-carnitine treatment on both total L-carnitine pool, plasma lipids, and on cardiac function [212].

L-carnitine is not fully absorbed orally, since before reaching the systemic system it has to pass the gut and the liver first. The intestinal mucosa appears to be saturated at higher doses [91]. The rate of biosynthesis of L-carnitine in healthy humans does not appear to be affected by the amount of L-carnitine intake through the diet nor through the renal re-absorption of L-carnitine [209]. Even some detrimental effects have been shown with oral treatments with L-carnitine. Koet *et al.* have demonstrated that dietary L-carnitine intake promotes atherosclerosis in mice through the production of trimethyl-N-oxide (TMAO) by intestinal microbiota [115].

In contrast, many studies have shown beneficial effects when L-carnitine treatment has been given in diseases such as diabetes through daily i.p injection compared to when given orally. L-carnitine showed a beneficial effect on cardiac function in the ischemic reperfused heart [213]. L-carnitine treatment in diabetes will be discussed further in the next chapter.

Mildronate has also been shown to improve recovery post-ischemia in disease but has not shown any detrimental effects in control hearts, so it has been proven safe [137]. Mildronate treatment in diabetes will be discussed further in Chapter 6.

4.3 Chapter Aims

In order to investigate what effect L-carnitine has on *in vivo* and *ex vivo* metabolism and function, several feasibility studies were necessary to establish optimal protocols for subsequent Chapters. The purpose of the work described in this chapter was to establish an optimal ischemic low-flow rate in Langendorff perfused healthy hearts

and to explore the effects of L-carnitine addition in the buffer on healthy hearts. With an optimal low-flow established for ischemia, this protocol would allow for investigation of metabolic and functional recovery post-ischemia for later examination of both L-carnitine and Mildronate in diabetic hearts (Chapters 5 and 6).

Furthermore, the aim was to investigate through two feasibility studies, whether L-carnitine levels could be increased with two weeks of daily L-carnitine treatment (i.p.), and whether L-carnitine could be decreased with two weeks of daily Mildronate treatment (i.p.). Given these results, the treatments would be continued and used in diabetes in the subsequent chapters (Chapters 5 and 6).

4.4 Methods

4.4.1 Langendorff Perfused Healthy Hearts

Initially, 20 healthy male Wistar rats (∼200 g) were kept on standard chow for five weeks before the hearts were excised and perfused in a Langendorff perfusion method. Two different low-flow rates and the addition of L-carnitine in the buffer were investigated.

Hearts were excised and perfused as described in Chapter 2. L-carnitine (10 mM) was added to the buffer at the onset of the Langendorff protocol in ten hearts. The other ten hearts were perfused with normal perfusate buffer. The hearts were acclimatized to the albumin buffer for ten minutes prior to the onset of the protocol. Hearts were subjected to 20 minutes of normal flow, followed by 30 minutes of either 0.33 ml/min (n = 10) or 0.4 ml/min (n = 10) for 30 minutes before hearts again were perfused with normal flow for another 30 minutes (Fig. 4.1)

4.4.2 Daily L-Carnitine and Mildronate Treatment in the Healthy Heart

Subsequently, a feasibility study was carried out with 12 healthy male Wistar rats with an average weight of 233 ± 7 g at the start of daily i.p. treatment with either saline, L-carnitine or Mildronate for two weeks. The experimental design is shown in Figure 4.2. The metabolic effects of L-carnitine treatment were investigated with

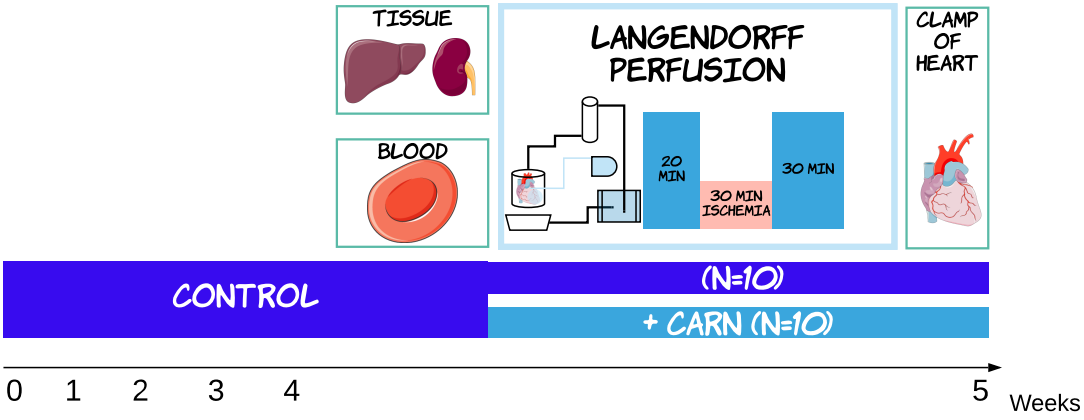

Figure 4.1: Experimental design. The figure shows a schematic of the tissue/blood collection (week 4) and timing of the Langendorff ischemia reperfusion protocol followed by freeze clamping the heart.

[1−^{13}C]pyruvate to obtain PDH-flux and with [2−^{13}C]pyruvate to examine TCA cycle intermediates as well as *in vivo* acetylcarnitine levels as described in Section 2.4.3. All control, L-carnitine or Mildronate treated animals were anaesthetized with isoflurane and subjected to CINE MRI as described in Section 2.4.1, and animals were also subjected to echocardiography as described in Section 2.4.4. At the end of the treatment, all animals were anaesthetized with isoflurane and euthanized to obtain tissues. The experimental design is shown in Figure 4.2. L-carnitine levels were measured in the plasma and in the heart tissue of only the control and Mildronate treated group as described in Section 2.9.3.

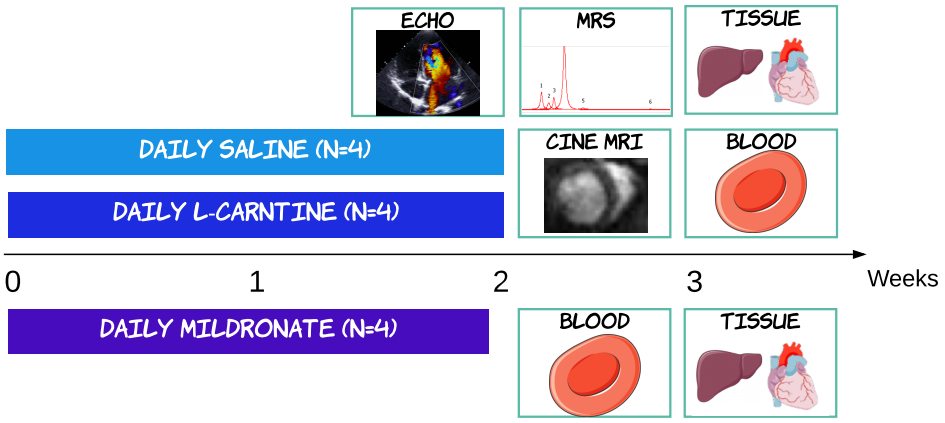

Figure 4.2: Experimental design. The figure shows a schematic of the treatment period (week 1 and 2), echocardiography (week 2), MRI and MRS (week 3), blood collection (Week 3 and 4), and tissue collection (week 4). The imaging time-points were only undertaken in control and L-carnitine treated groups.

4.5 Results

4.5.1 Langendorff Perfused Healthy Hearts

20 male Wistar healthy hearts were perfused with and without L-carnitine. No difference was observed in the body weight at the time of euthanasia (CTR: 340 ± 30 g, Carn: 330 ± 20 g), and there was no change in the wet heart weight, kidney weight, fat pad weights, nor in the tibia length (Fig.4.3).

4.5.1.1 Establishing a Low-flow Ischemic Rate for Langendorff Perfused Hearts

The hearts (all L-carnitine treated and untreated hearts included) that were subjected to a low-flow rate of 0.4 ml/min/gww recovered 52 ± 20 % of their initial rate pressure product (RPP) at reperfusion, whereas the hearts that were subjected to a low-flow rate of 0.33 ml/min/gww recovered on average 28 ± 20% of their initial rate pressure product (RPP) at post-ischemia. RPP post-ischemia was

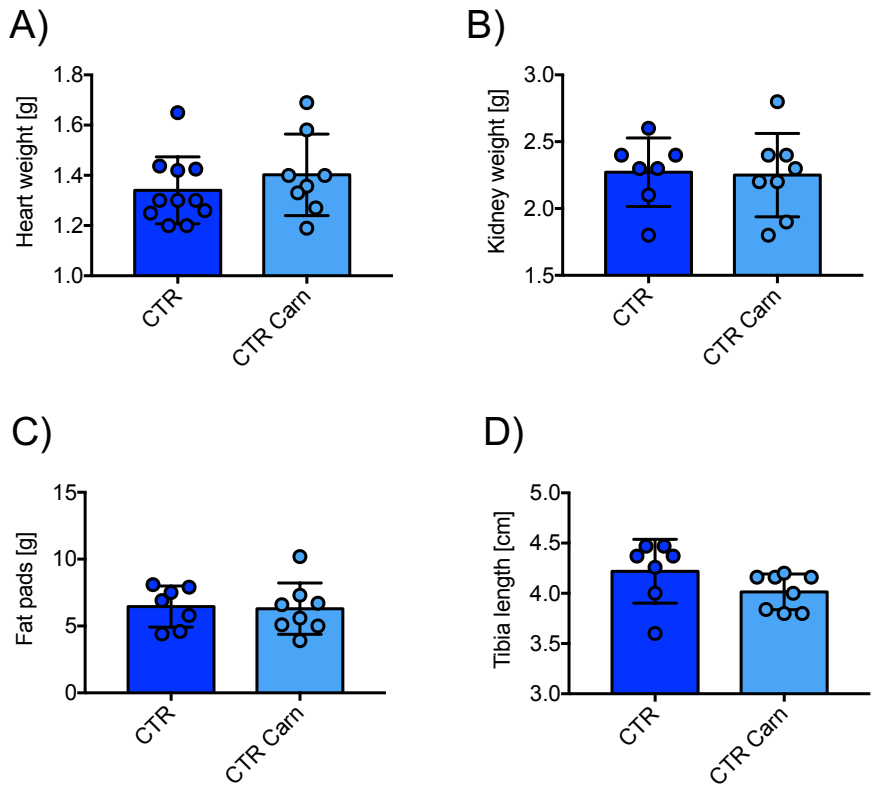

Figure 4.3: Tissues taken at the time of euthanasia. **A)** Weight of the heart. **B)** Weight of both kidneys. **C)** Weight of fat pads. **D)** Length of the right tibia.

99 % higher for the low-flow rate of 0.4 ml/min/gww compared to 0.33 ml/min/gww ($p = 0.047$). The percent RPP recovery between post- and pre-ischemia for the low-flow rate of 0.33 ml/min/gww ranged between 12 % to 77 %, where all, except one heart, recovered below 31 % of pre-ischemic RPP. The range for the low-flow rate of 0.4 ml/min/gww was between 26 % to 93 % of RPP recovery, where 77 % of the hearts recovered more than 50 % of their pre-ischemic RPP (Fig. 4.4).

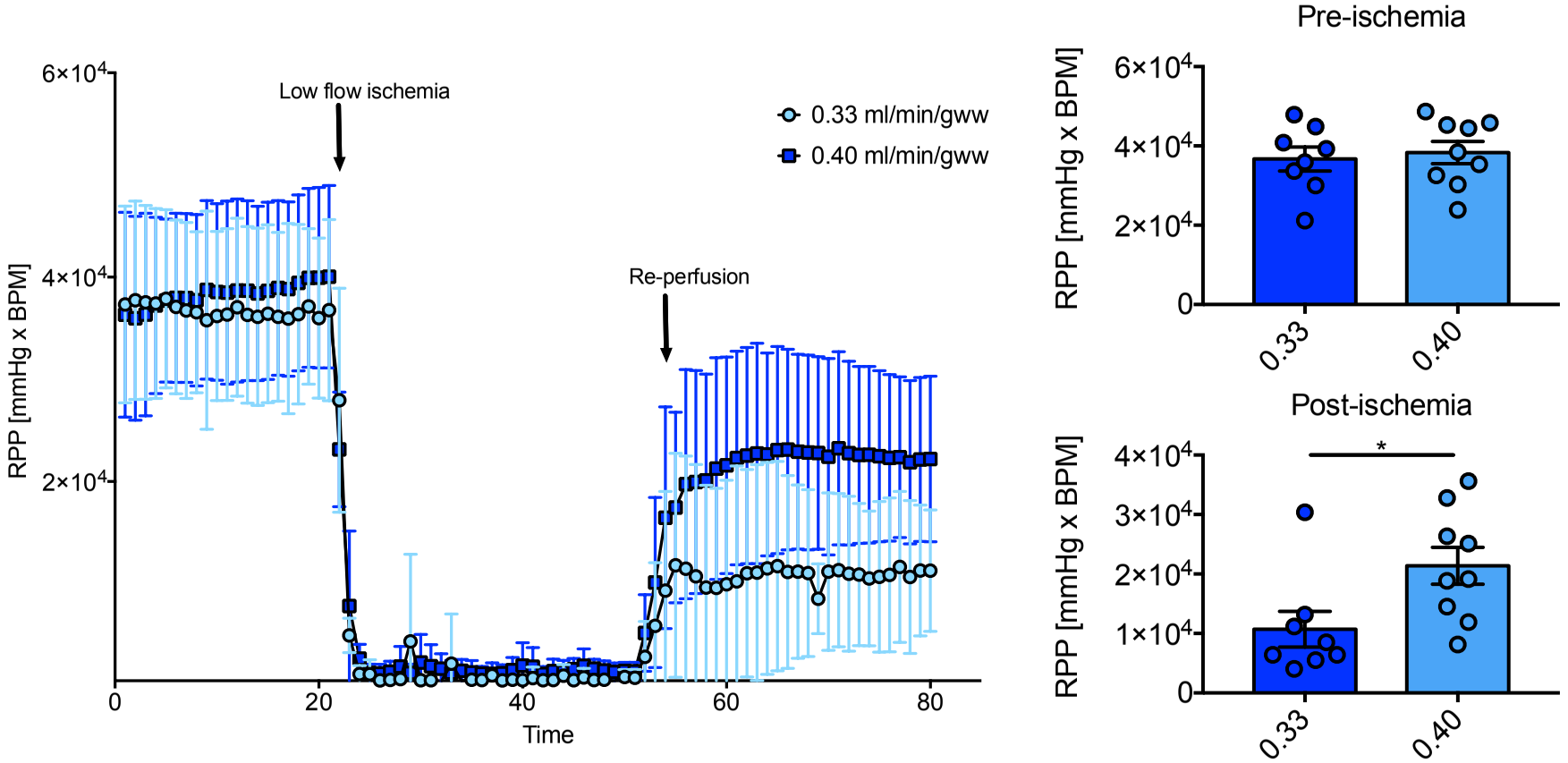

Figure 4.4: Rate pressure product (RPP) shown from Langendorff ischemia reperfusion, where pre-ischemia is t = 1:20 min, ischemia is t = 21:50 min, and reperfusion/post-ischemia is t = 52:80 min. Includes all controls and all L-carnitine perfusions. Two different low-flow rates are displayed, 0.33 and 0.4 ml/min/gww. Unpaired t-test, where $^*p < 0.05$

.

4.5.1.2 The Effects of L-Carnitine on Langendorff Perfused Control Hearts

The hearts that were subjected to a low-flow rate of 0.4 ml/min/gww were either given L-carnitine in the buffer or not. The control hearts recovered their rate pressure product (RPP) faster with a steeper slope (2394 ± 500 mmHg) compared to the L-carnitine treated group (1888 ± 300 mmHg). When all time-points post-ischemia were taken into consideration, RPP failed to reach statistical significance over the time-course of reperfusion compared to the saline treated control group (Fig. 4.5A). Diastolic pressure, DiaP (Fig. 4.5B), developed pressure, DevP (Fig. 4.5C), and systolic pressure, SysP (Fig. 4.5D) failed to reach statistical significance over the time-course of reperfusion, although all three parameters appeared reduced with L-carnitine treatment compared to controls.

Subsequently, it was investigated if an average of the last ten minutes pre-ischemia and an average of the last ten minutes post-ischemia would show any significant differences between the two groups. The functional parameter traces are also shown over the full 80 minute protocol. RPP (Fig. 4.6), HR (Fig. 4.7), DevP (Fig. 4.8), SysP (Fig. 4.9), and DiaP (Fig. 4.10) showed no significant differences detected over the last ten minutes of pre-ischemia between the groups. And no significant differences were observed in the last ten minutes post-ischemia in any functional parameters when comparing the two groups.

Fatty acid oxidation rates, before ischemia was induced, were 0.164 ± 0.008 μmol/min/gww for controls, and 0.14 ± 0.08 μmol/min/gww for L-carnitine (Fig. 4.11A). Post-ischemia, fatty acid oxidation rates were 0.16 ± 0.3 μmol/min/gww for controls and 0.11 ± 0.09 μmol/min/gww for the L-carnitine group (Fig. 4.11A). No significant differences were observed between the control and L-carnitine group, not even when fatty acid oxidation rates were normalized to rate pressure product (Fig. 4.11B).

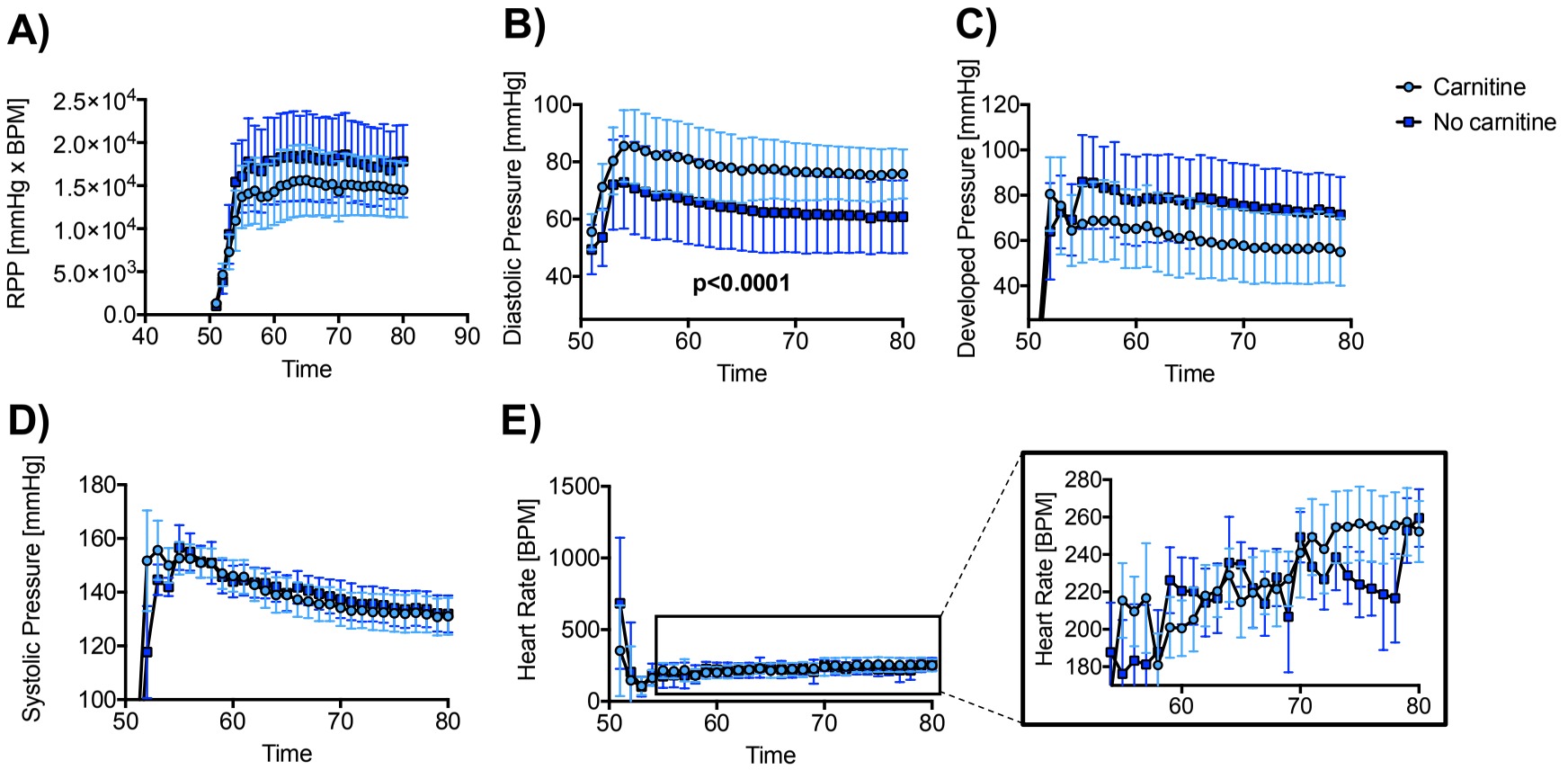

Figure 4.5: Langendorff perfusion for the low-flow rates 0.4 ml/min/gww traces displayed post-ischemia. **A)** Rate pressure product, RPP [mmHg]. **B)** Diastolic pressure, DiaP [mmHg]. **C)** Developed pressure, DevP [mmHg]. **D)** Systolic pressure, SysP [mmHg]. **E)** Heart rate, HR [bpm]. All time points displayed as mean ± SD. The significance of the differences is determined by a two-way ANOVA.

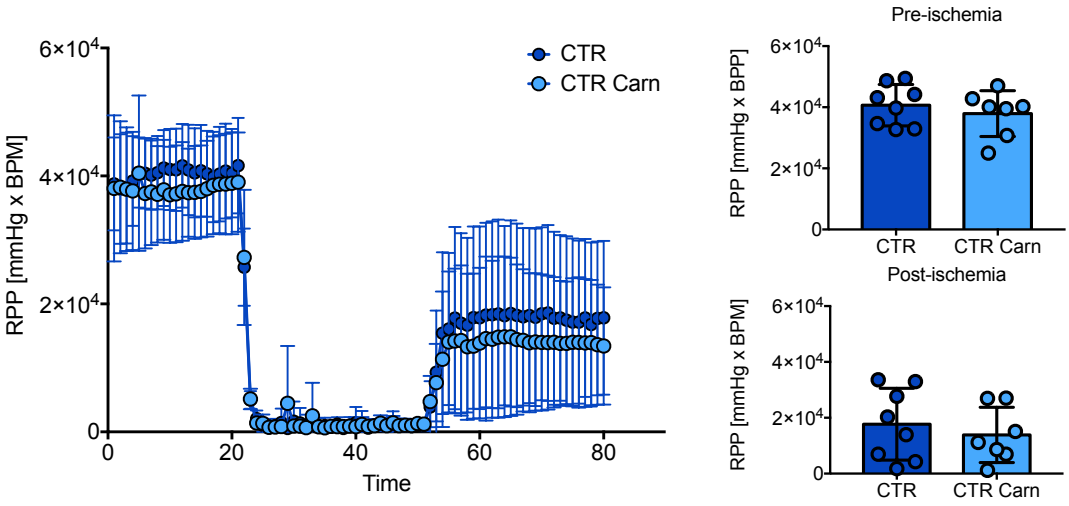

Figure 4.6: Rate pressure product (RPP) for t = 0:80 min for the low-flow rates of 0.40 ml/min/gww. L-carnitine added to perfusate buffer at t = -10 min (light blue), no added L-carnitine (dark blue). Average RPP for last 10 min at pre-ischemia, and average RPP for last 10 min at post-ischemia. All data point displayed as mean ± SD. Unpaired t-test, where $^*p < 0.05$.

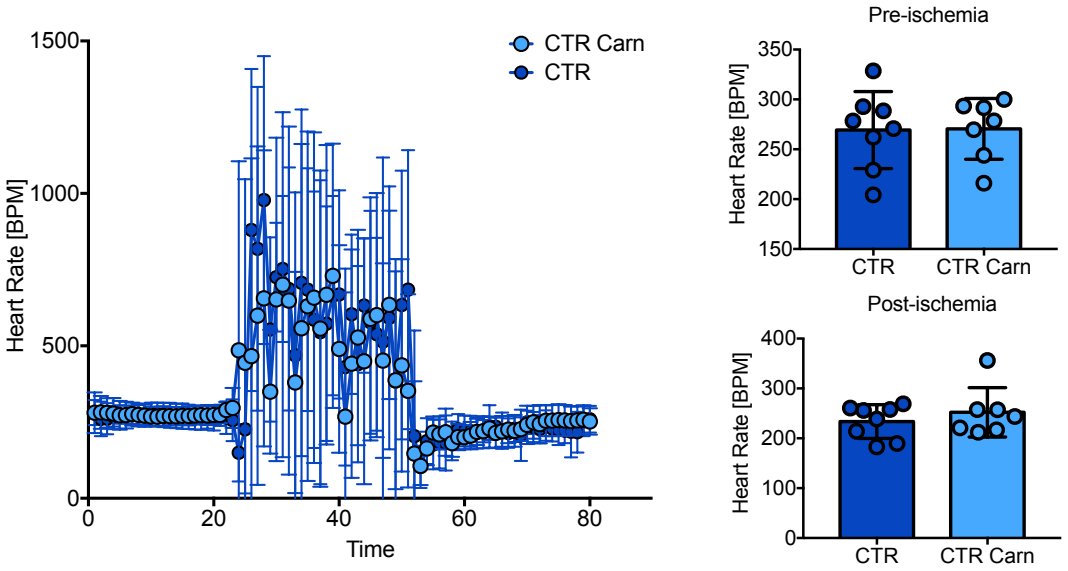

Figure 4.7: Heart rate (HR) for t = 0:80 min for the low-flow rates of 0.40 ml/min/gww. L-carnitine added to perfusate buffer at t = -10 min (light blue), no added L-carnitine (dark blue). Average HR for last 10 min at pre-ischemia, and average HR for last 10 min at post-ischemia. All data point displayed as mean ± SD. Unpaired t-test, where $^*p < 0.05$.

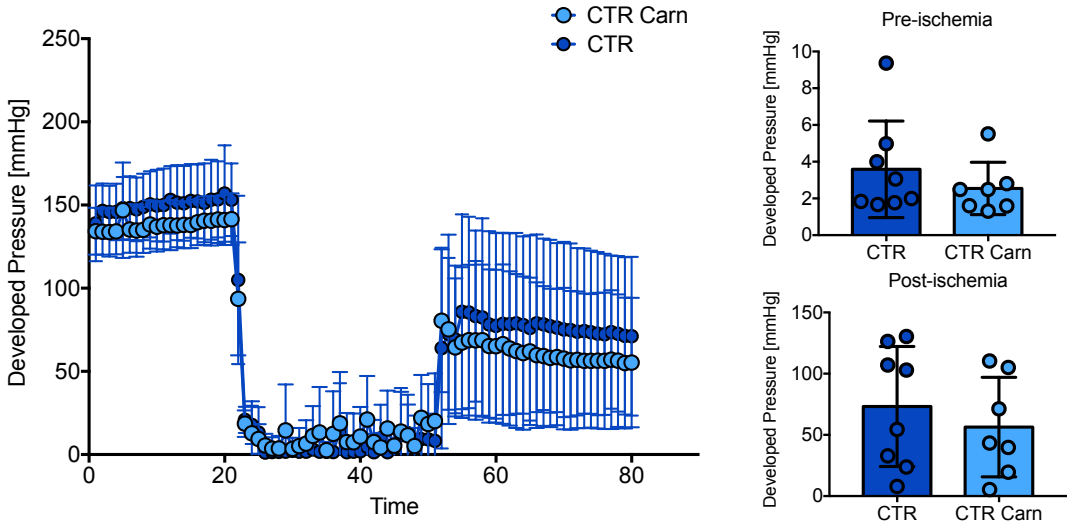

Figure 4.8: Developed pressure (DevP) for t = 0:80 min for the low-flow rates of 0.40 ml/min/gww. L-carnitine added to perfusate buffer at t = -10 min (light blue), no added L-carnitine (dark blue). Average DevP for last 10 min at pre-ischemia, and average DevP for last 10 min at post-ischemia. All data point displayed as mean ± SD. Unpaired t-test, where $^*p < 0.05$.

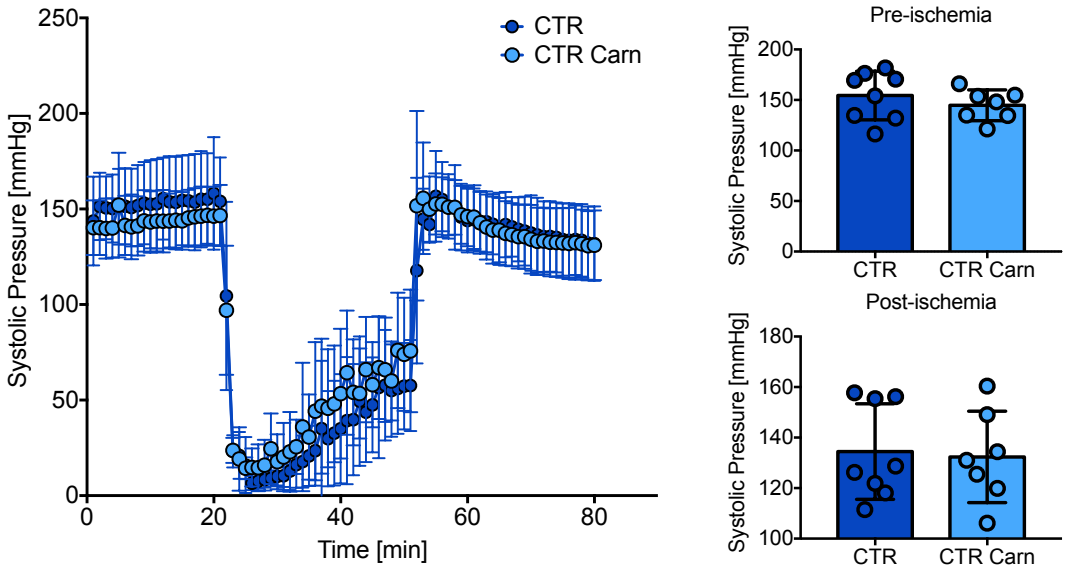

Figure 4.9: Systolic pressure (SysP) for t = 0:80 min for the low-flow rates of 0.40 ml/min/gww. L-carnitine added to perfusate buffer at t = -10 min (light blue), no added L-carnitine (dark blue). Average SysP for last 10 min at pre-ischemia, and average SysP for last 10 min at post-ischemia. All data point displayed as mean ± SD. Unpaired t-test, where $^*p < 0.05$.

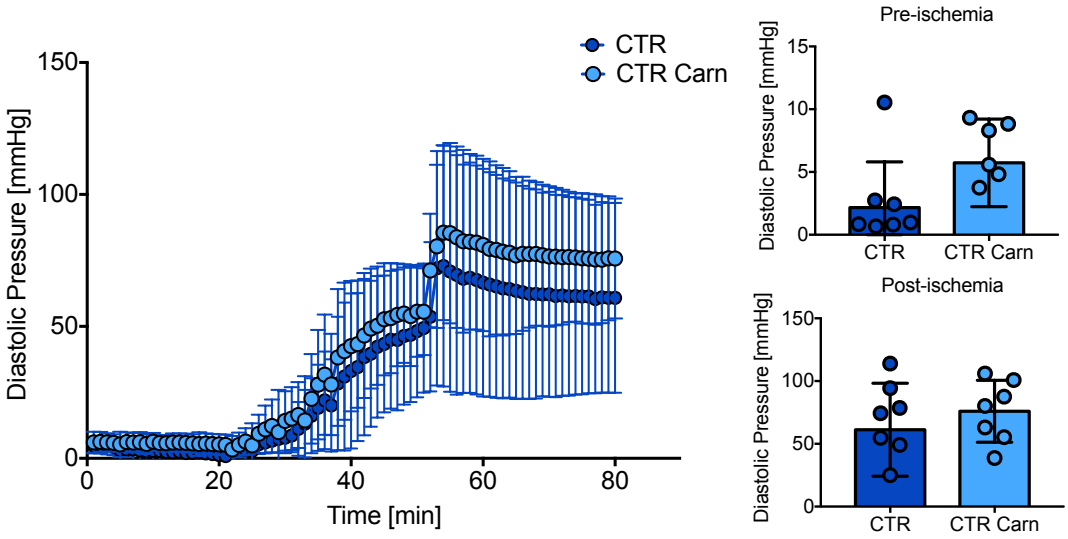

Figure 4.10: Diastolic pressure (DiaP) for t = 0:80 min for the low-flow rates of 0.40 ml/min/gww. L-carnitine added to perfusate buffer at t = -10 min (light blue), no added L-carnitine (dark blue). Average DiaP for last 10 min at pre-ischemia, and average DiaP for last 10 min at post-ischemia. All data point displayed as mean ± SD. Unpaired t-test, where $^{*}p < 0.05$.

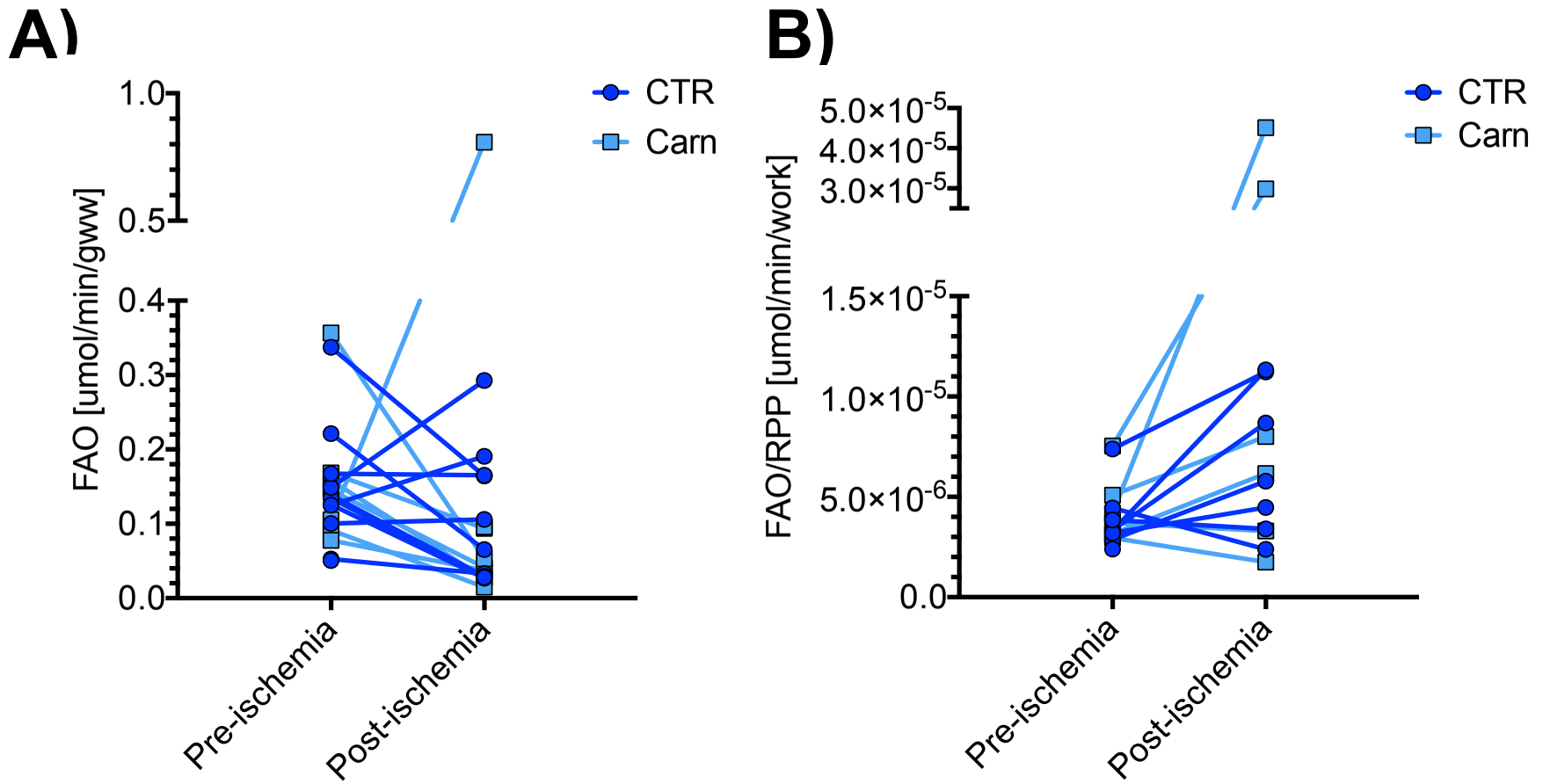

Figure 4.11: Langendorff perfusion fatty acid oxidation rates in healthy hearts with and without L-carnitine. **A)** Fatty acid oxidation (FAO) at pre-ischemia (basal) and post-ischemia. **B)** Fatty acid oxidation (FAO) normalized to work (RPP) at pre-ischemia (basal) and post-ischemia.

4.5.2 Daily L-Carnitine Treatment in the Healthy Heart

L-carnitine treated controls gained less body weight (BW: 11 ± 9 g) and had smaller fat pads (FP: 2 ± 0.04 g) compared to the saline treated controls (BW: 37 ± 5 g, FP: 4.6 ± 0.5 g). Body weight at the end of treatment was 267 ± 11 g for controls, and 253 ± 6 g for the L-carnitine treated group (Fig. 4.12) .

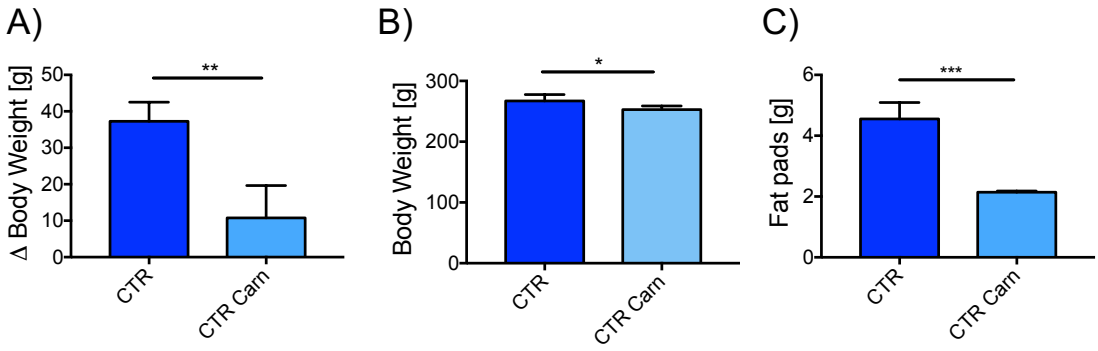

Figure 4.12: Daily saline treated rats (blue), daily L-carnitine treated rats (light blue). **A)** Body weight changes between the start of treatment and two weeks post treatment. **B)** Body weight at the end of two weeks of treatment. **C)** Fat pads obtained at the time of euthanasia two weeks post treatments. All data represented as mean ± SD. Unpaired t-test $^{*}p < 0.05.$,$^{**}p < 0.01$,$^{***}p < 0.001$.

Cardiac output was 20 % higher in the L-carnitine group compared to the saline group, although this failed to reach statistical significance (p = 0.09). Cardiac index (CI) was 25 % higher for L-carnitine treated animals ($p = 0.04$), and diastolic function analysis by echocardiography showed that the E/E' ratio was 54 % higher in the L-carnitine treated group compared to the saline group ($p = 0.05$), indicating diastolic dysfunction (Fig. 4.13).

Hyperpolarized [2−^{13}C] pyruvate MRS demonstrated elevated acetylcarnitine levels in the myocardium of L-carnitine treated animals by 142 % although it failed to reach statistical significance ($p = 0.09$). Blood plasma analysis showed significantly increased levels of free L-carnitine in the treated group after two weeks of daily L-carnitine treatment by 45 % ($p = 0.011$, Fig. 4.14).

With hyperpolarized [1−^{13}C]pyruvate MRI no significant differences were observed in the metabolites. Furthermore, no other cardiac functional parameters showed any alteration (Table 4.1).

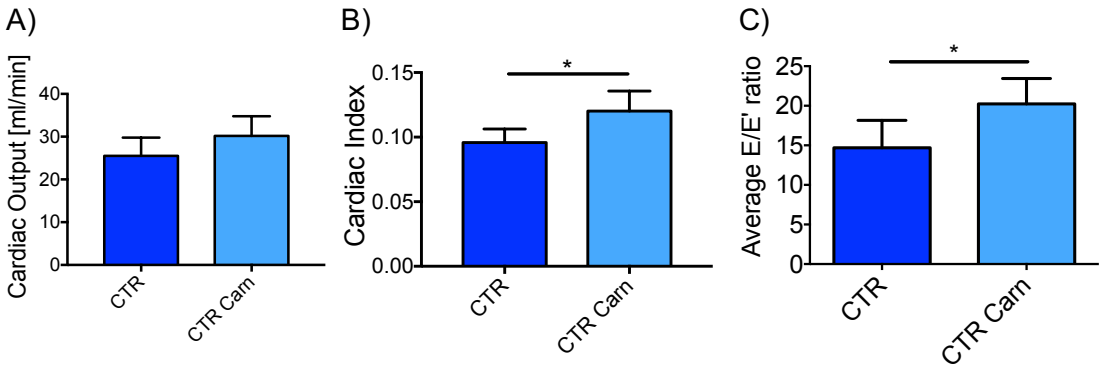

Figure 4.13: Daily saline treated rats (blue), daily L-carnitine treated rats (light blue). **A)** Cardiac output (CO) acquired with CINE MRI two weeks post treatment. **B)** Cardiac Index, that is CO normalized to body weight. **C)** Mitral blood inflow normalized to mitral annulus velocities averaged over the velocities in the lateral wall and the septum, E/E' ratio. Unpaired t-test $^{*}p < 0.05$.

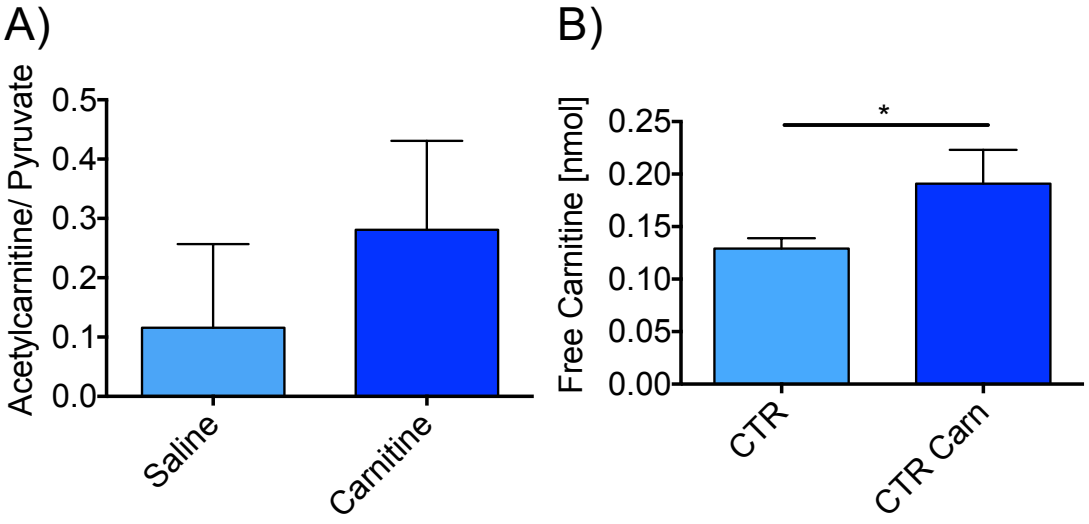

Figure 4.14: A) *In vivo* hyperpolarized [2−^{13}C] pyruvate MRI. Spectra summed over 30 seconds and acetylcarnitine levels normalized to the maximum pyruvate peak. **B)** L-carnitine measured from terminal blood plasma. Saline treated animals (light blue), and L-carnitine treated animals (blue), $^{*}p < 0.05$.

Mean ± SD	Control (n = 4) + saline	Control (n = 4) + L-carnitine	p-value (Unpaired t-test)
Bicarbonate +CO_2/Pyruvate	0.061 ± 0.03	0.070 ± 0.01	0.95
Lactate/Pyruvate	0.136 ± 0.01	0.149 ± 0.05	0.62
Alanine/Pyruvate	0.060 ± 0.005	0.086 ± 0.04	0.21
Bicarbonate/Lactate	0.369 ± 0.3	0.332 ± 0.03	0.82
Glutamate/2-Pyruvate	0.189 ± 0.2	0.054 ± 0.08	0.21
Cardiac Output [µl]	26 ± 4	30 ± 5	0.19
Average Mass [mg]	117 ± 10	121 ± 20	0.72
Ejection Fraction [µl]	74 ± 9	75 ± 4	0.92
Heart Rate [BPM]	400 ± 50	434 ± 40	0.29
Stroke Volume [µl]	65 ± 10	70 ± 10	0.54
Stroke Index [µl/g]	0.25 ± 0.03	0.28 ± 0.03	0.15

Table 4.1: Two week daily L-carnitine effects on metabolism and function. Table shows mean ± SD for the metabolites from hyperpolarised [1−^{13}C]pyruvate and [2−^{13}C]pyruvate MRS, and for cardiac function assessed with CINE MRI. The groups were treated with either two weeks of saline or L-carnitine (i.p.).

4.5.3 Daily Mildronate Treatment in the Healthy Heart

Mildronate treated controls had 20 % higher body weight compared to the saline treated controls ($p = 0.0035$) at the time of euthanasia. However, the body weight difference over the two weeks of treatment was unchanged between the two groups (CTR: 37 ± 5, CTR Mil: 45 ± 17). Fat pads were similar in both groups (CTR: 4.6 ± 0.5 g, CTR Mil: 4.8 ± 0.6 g, p < 0.5, Fig. 4.15).

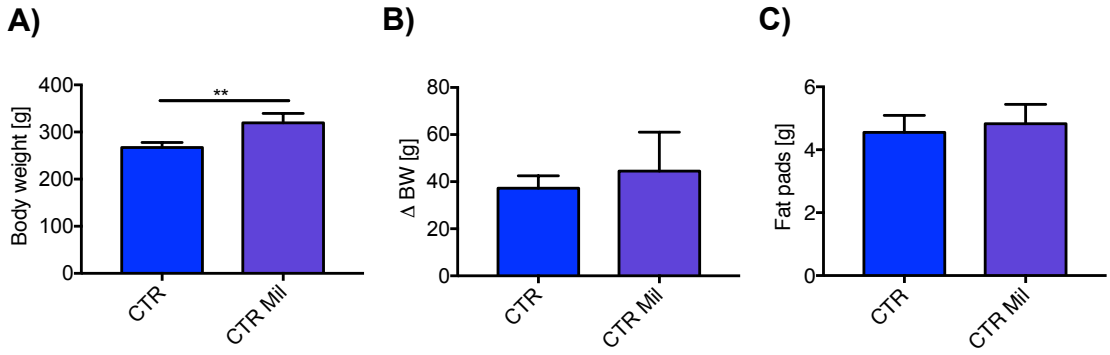

Figure 4.15: Daily saline treated control, CTR (blue), daily mildronate treated control, CTR Mil (purple). **A)** Body weight following two weeks of treatment. **B)** Difference in body weight between 14 days and start of treatment. **C)** Fat pads measured 14 days post treatment. Unpaired t-test $^{*}p < 0.05$,$^{**}p < 0.01$.

Free L-carnitine failed to be detected in the blood plasma and was determined as no free L-carnitine present in the blood. (Fig. 4.16)

However, L-carnitine was measured in the heart tissue (Fig. 4.17). L-carnitine levels were significantly reduced by 14 % in the Mildronate treated group compared to the controls (p = 0.01, unpaired t-test, Fig. 4.17).

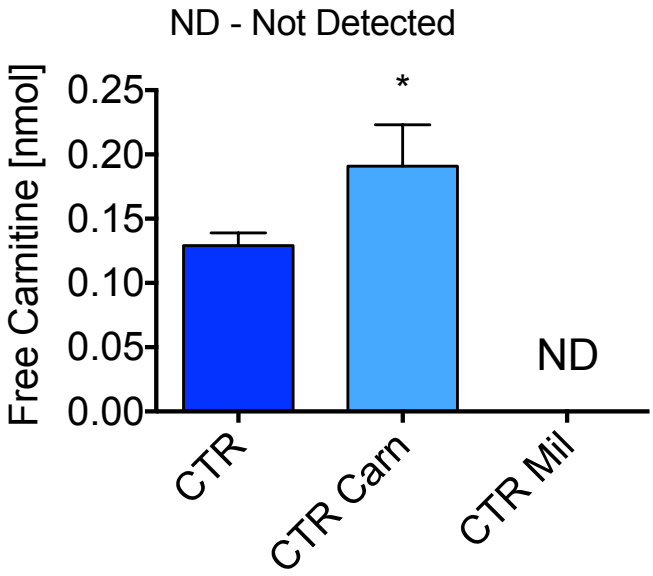

Figure 4.16: Free L-carnitine measured in plasma. Daily saline treated control, CTR (blue), Daily L-carnitine treated control (light blue) daily mildronate treated control (ND - Not Detected). Data presented as mean ± SD. Unpaired t-test $^{*}p < 0.05$ compared to CTR.

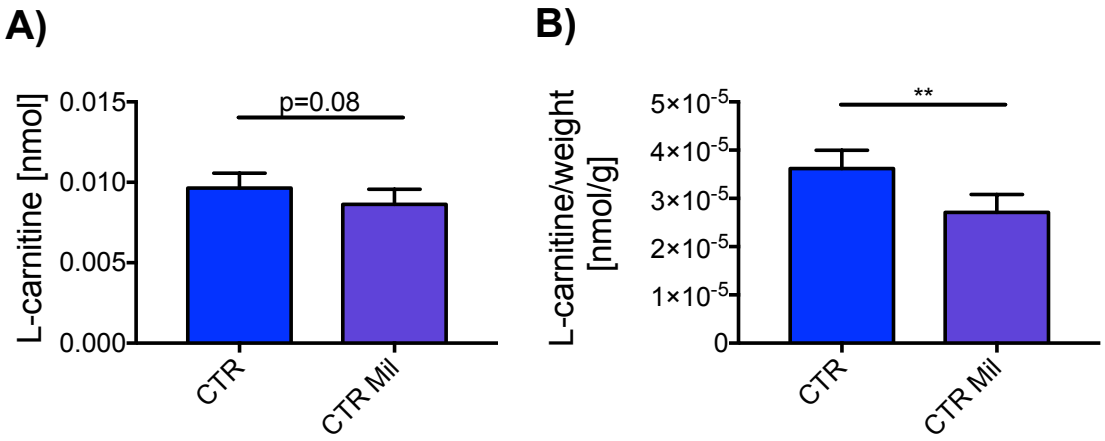

Figure 4.17: Daily saline treated control, (CTR, blue), daily Mildronate treated control, (CTR Mil, purple). **A)** L-carnitine levels measured in heart tissue following two weeks of treatment. **B)** L-carnitine levels normalized to body weight at two weeks following treatment. Data presented as mean ± SD. Unpaired t-test, where $^{**}p < 0.01$.

4.6 Discussion

4.6.1 Langendorff Perfused Healthy Hearts

4.6.1.1 Establishing a Low-flow Ischemic Rate for Langendorff Perfused Hearts

It is of no surprise that a more restrictive low-flow rate leads to a lower functional recovery post-ischemia. Even so, it is crucial that the low-flow ischemic rate does not result in 100 % recovery so that treatment effects can be observed. Rate pressure product (RPP) post-ischemia recovered on average 50 % of the pre-ischemic RPP with a low-flow rate of 0.4 ml/min/gww. Since there was one heart that reached 93 % RPP recovery, this low-flow rate achieved the maximum recovery post-ischemia allowed and was therefore not increased further.

Given these results, the low-flow ischemic rate of 0.4 ml/min/gww was chosen as the low-flow rate used in all subsequent Langendorff perfusions in this thesis.

4.6.1.2 L-Carnitine Effects on Langendorff Perfused Control Hearts

L-carnitine was added "acutely" just to the perfusate buffer prior to the start of the Langendorff protocol in healthy hearts. RPP for the L-carnitine group stayed consistently below the RPP of the control group post-ischemia. This difference was mostly driven by an elevated diastolic pressure post-ischemia, and therefore a reduced developed pressure was observed in the L-carnitine group while maintaining the same heart rate and systolic pressure between the two groups. This experiment was most likely underpowered, and it did not reach statistical significance. Averaging the functional parameters over the last ten minutes of pre-ischemia, and over the last ten minutes post-ischemia, showed no difference between the groups.

L-carnitine has previously been shown not to protect healthy hearts from ischemia when added to the perfusate buffer [235, 56, 191, 106]. The mechanisms differ from other derivatives of L-carnitine, like propionyl-L-carnitine and acetyl-L-carnitine, that have shown a protective effect in healthy perfused isolated rat heart [235].

The decreased functional recovery in the L-carnitine group was not accompanied by any significant changes in fatty acid oxidation rates even though 33 % of the

cases had elevated FAO rates post-ischemia when treated with L-carnitine. Due to a subtle change in functional decline, there might also be a subtle elevation of FAO that does not reach significance. The worsened functional recovery might, therefore, be accompanied by a reduction in glucose oxidation induced by the ischemia, which has previously been suggested [56] but also induced by low fatty acid concentration used in the buffer together with L-carnitine. In the absence of fatty acids, L-carnitine has failed to affect glucose oxidation, due to a relief of the inhibitory effect of acetyl-CoA/CoASH, and thereby recovery post-ischemia is worsened [29].

Besides, a decrease in FAO rates have been shown in the presence of L-carnitine, but with higher concentrations of palmitate used (1.2 mM) than in this study (0.4 mM) [29]. This might suggest that due to the low concentration of fatty acids used in this study, recovery post-ischemia worsens in the healthy hearts. However in pathological cases, L-carnitine is in contrast known to improve cardiac function post-ischemia [148, 22, 258, 213], therefore depending on the condition and experimental setup, L-carnitine treatment can lead to opposite effects on myocardial function and metabolism [56].

4.6.2 Daily L-Carnitine Treatment in the Healthy Heart

A pilot study was carried out to validate that L-carnitine could be elevated in healthy control animals following daily i.p. treatment of L-carnitine for two weeks.

L-carnitine treatment in healthy animals led to less weight gain ($p = 0.002$), and lower fat pad weights ($p = 0.0007$). This is likely because L-carnitine is transporting more fatty acids to be oxidized and therefore promoting utilization of adipose tissue. L-carnitine has shown to promote weight loss in rats, cats and even in humans, where L-carnitine has been shown to ameliorate hunger [262, 35, 202].

Together with weight loss, L-carnitine increases cardiac index (CI), even though cardiac output (CO) was unchanged, therefore weight loss might be remodelling the heart function, and most specifically the diastolic function, which shows an elevation in tissue Doppler E/E' ratio. E/E' has previously been shown to be a

predictor for cardiac events [231] and a longer follow-up on these animals would be critical to validate this prognosis.

However, unlike the unaltered PDH-flux, lactate and alanine, these L-carnitine treated animals had a 142 % elevation of acetylcarnitine in the myocardium as shown by *in vivo* hyperpolarized MRS, although it failed to reach statistical significance ($p = 0.09$). This elevation might be from the transportation of long-chain fatty acids into the mitochondria as supported by the weight loss. Elevation of L-carnitine was supported by a significant increase of free L-carnitine in blood plasma.

Given these results the treatment was undertaken in a larger cohort of animals after two weeks of diabetes, to mirror the disease progression in diabetes. These studies are described in Chapter 5.

4.6.3 Daily Mildronate Treatment in the Healthy Heart

Subsequently, a pilot study was carried out to validate if L-carnitine could indeed be reduced in healthy animals following daily i.p. treatment with Mildronate.

Mildronate treatment in healthy animals lead to higher body weight ($p = 0.004$) compared to the saline treated controls, but no change in fat pad weights was observed.

L-carnitine was reduced by 25 % in heart tissue, when normalized to body weight ($p = 0.007$), and was not present in the blood plasma. Mildronate was, therefore, inhibiting fatty acids entering into the mitochondria.

So in contrast to L-carnitine treatment, Mildronate treatment reduces L-carnitine levels in plasma and heart, and the metabolic and functional effects of this treatment can now be studied in a diabetic heart as described in Chapter 6.

4.6.4 Conclusion and Future Perspective

This chapter established a low-flow rate for ischemia in Langendorff perfused healthy hearts, and it explored the effect of acute addition of L-carnitine in the perfusate buffer. Acute L-carnitine added to perfusate buffer show potential detrimental effects to cardiac function *ex vivo* explored with Langendorff perfusions, although it failed

to reach statistical significance. Addition of L-carnitine to the buffer, is however in this chapter only examined in healthy hearts, and due to altered substrate utilisation in pathology, the addition of L-carnitine might have beneficial effects in the diabetic heart. Although the addition of acute L-carnitine in the buffer is not explored in the diabetic heart in this thesis. A treatment effect of daily i.p. injections of L-carnitine will be explored in both diabetic and healthy hearts in Chapter 5.

However, prior to these studies, this chapter also explored if L-carnitine could be elevated with L-carnitine treatment and reduced with Mildronate treatment in healthy hearts through two weeks of daily i.p. injections. Both treatments were shown to successfully elevate and reduce L-carnitine respectively, and will, therefore, be used in two other cohorts of animals after two weeks of diabetes. These studies are described in Chapters 5 and 6.

The fourth stretched out his eager hand
And felt about the knee;
"What most this mighty beast is like
Is mighty plain," quoth he;
"Tis clear enough the elephant
Is very like a tree."

5

Effects of L-Carnitine Supplementation on the Diabetic Heart

Contents

5.1 Chapter Overview 128
5.2 Background 129
5.3 Chapter Aims 133
5.4 Methods 133
5.5 Results 138
5.5.1 Weight and Blood Profile 138
5.5.2 Cardiac *In Vivo* Function 145
5.5.3 Cardiac *In Vivo* Metabolism 148
5.5.4 Tissue Analysis 152
5.5.5 Cardiac *Ex Vivo* Function 157
5.5.6 Cardiac *Ex Vivo* Fatty Acid Metabolism 163
5.6 Discussion 167
5.6.1 Summary of Key Findings 167
5.6.2 Daily L-Carnitine Treatment in the *In Vivo* Type 1 Diabetic Heart 168
5.6.3 Effects of L-Carnitine on Functional and Metabolic Recovery Post-Ischemia 172
5.6.4 Daily L-Carnitine Treatment in the *In Vivo* Healthy Heart 174
5.6.5 Conclusion and Future Perspective 176

5.1 Chapter Overview

The type 1 diabetic (T1D) population have reduced L-carnitine levels in their plasma when compared to the healthy population [155, 153, 155, 256]. Children that develop T1D early in life have been shown to have reduced levels of L-carnitine at birth [155], and the leading cause of death in T1D is cardiovascular disease, that is also associated with reduced L-carnitine levels [247, 128]. Improving our understanding of the metabolic changes that occur in the diabetic heart may be vital in understanding the pathophysiology of the cardiac effects of diabetes. L-carnitine might be able to prevent some of the complications of diabetes and heart disease. This chapter shows the metabolic and functional effects of daily L-carnitine supplementation on the streptozotocin (STZ)-induced diabetic rodent heart.

Diabetic rats showed elevated blood glucose at two weeks post STZ injection, but there was no further increase in blood glucose over the duration of the L-carnitine treatment. In contrast blood glucose levels in the saline treated diabetic group showed a significant and progressive increase in hyperglycaemia over the three weeks of treatment. Whilst average left ventricular mass, stroke volume, ejection fraction, end diastolic lumen size, heart rate and cardiac output were all depressed in the two diabetic groups, L-carnitine showed an improvement in end diastolic lumen in the diabetic group. Metabolic alterations accompanied the functional changes, both alanine and lactate were significantly increased in the diabetic groups, whilst L-carnitine treatment increased alanine even further. Flux through pyruvate dehydrogenase was reduced in both diabetic groups compared to the control groups. L-carnitine treatment, however, increased acetylcarnitine levels and decreased triacylglycerides in the diabetic group. Furthermore, L-carnitine treatment normalized β-hydroxybutyrate in the diabetic animals to the levels of the controls. The L-carnitine diabetic hearts recovered significantly better post-ischemia, compared to the saline treated diabetic group. The percentage FAO recovery, normalized to cardiac work, was reduced with L-carnitine treatment in both control and diabetic groups, showing a shift in metabolism away from fatty acids post-ischemia.

This chapter showed beneficial effects of L-carnitine supplementation in diabetic hearts. Despite demonstrating small differences in cardiac function, L-carnitine treatment slowed the progression of hyperglycaemia and normalized fatty acid oxidation recovery as well as functional recovery post-ischemia. This study showed a potential improvement in diastolic relaxation both in the *in vivo* and *ex vivo* heart. It is possible that systolic function may be improved over an even more extended treatment duration [213].

L-carnitine supplementation leads to alterations in metabolism in the *in vivo* heart and can improve oxidation rates and function after ischemia. It has shown multiple beneficial effects in the diabetic heart affirming that the balance of energy sources the heart is using is of critical importance. The use of L-carnitine supplementation in the diabetic heart appears beneficial but needs further investigation.

5.2 Background

The heart is reliant mostly on fatty acids for energy production, and fatty acids require L-carnitine to be taken up into the mitochondria. Transportation of fatty acids into the mitochondria is undertaken by L-carnitine, that also acts as a buffer of excess acetyl-CoA via acetylcarnitine in the mitochondria (Section 1.5). Ever since primary L-carnitine deficiency (PCD) was discovered in 1973, and was shown to lead to cardiomyopathy, that could be reversed through L-carnitine treatment [109], an extensive amount of studies have been undertaken to investigate L-carnitine's role in disease.

It is not just primary L-carnitine deficiency that leads to heart disease, several other diseases have shown secondary L-carnitine deficiency, such as type 1 diabetes (T1D) [203, 153], and type 2 diabetes (T2D) [36], as well as cardiomyopathy that is not caused by PCD [95], ischemia and myocardial infarction [54], end stage renal disease that requires hemodialysis [47, 112, 17], Alzheimer's disease [170] and even HIV infections [99], all show reduced levels of L-carnitine in tissues as well as in plasma compared to healthy controls.

In 1964 Wittels and Bressler found out that the cardiac muscle is in need of L-carnitine to function. By depleting myocardial L-carnitine in the guinea pig, they found that it lead to cardiomyopathy [278]. L-carnitine facilitates fatty acid oxidation, can enhance glucose oxidation, and improves total energy expenditure [68], through these mechanisms L-carnitine supplementation protects cardiac function in disease and has also been shown to improve outcomes for diabetic patients [213, 131, 212].

T1D patients have lower free and total L-carnitine levels in the plasma compared to the healthy population, and it worsens with the duration of disease leading to long-term complications [155, 153, 212, 264]. T2D patients, particularly insulin-dependent patients, are also at a higher risk of L-carnitine deficiency than the healthy population [160, 68]. L-carnitine reduction in diabetic patients is either caused by diabetes itself, perhaps due to high glucose levels, or on the other hand, that L-carnitine deficiency itself leads to diabetes and cardiac diseases. However, the underlying mechanisms, of why cardiac diseases and diabetes lead to secondary L-carnitine deficiency, are unknown. Some studies have shown L-carnitine depletion prior to the development of T1D, suggesting L-carnitine deficiency could be a contributing factor in T1D disease development [155]. Mamoulakis *et al.* have shown that L-carnitine concentrations in T1D also reduce with time, and could be associated with the long-term complications of diabetes [153]. But it could also be that the further reduction in L-carnitine is due to age, since L-carnitine levels diminish with age even in the healthy population [44, 81]. As seen by these studies, L-carnitine and its function are very complex, it has shown multiple effects on the balance of energy sources used in the diabetic heart [58], and by understanding the underlying mechanism of L-carnitine, it might be possible to improve the prognosis for diabetic patients.

It has been shown that insulin sensitivity can be improved with a 2 hour constant infusion of L-carnitine, and plasma free L-carnitine levels can be elevated with insulin treatment. Insulin is known to stimulate acetyl-CoA carboxylase, producing malonyl-CoA, which inhibits mitochondrial fatty acid uptake, increasing free L-carnitine, due

to less binding to acyl-CoA for transportation into mitochondria. Plasma lactate levels have also been shown to be reduced, and glucose oxidation increased following a two hour infusion of L-carnitine. Interestingly insulin sensitivity was only shown to improve in diabetic patients, and not in healthy controls [168, 249]. L-carnitine might therefore also act by up-regulating PDH activity by buffering excess acetyl-CoA, if there is already an elevation in fatty acids, suggesting that beneficial effects are only observed if there is already an abnormal shift in substrate utilisation.

Despite the above findings several studies have failed to find any changes in insulin levels, when treating with L-carnitine [82, 212], even though many have found both reduced glucose levels, TAG, FFAs and ketone levels [213, 194], without insulin changes. One explanation could be that a more extended and maybe a higher dose of L-carnitine is necessary, after all, no studies report treatments with long term L-carnitine clamps. A two hour 10 mg/kg/h infusion might be more effective than the standard 3 g/kg/day for 2-6 weeks, and therefore it can be challenging to compare constant infusion with other administration routes since both the administration route as well as the dose is essential.

Streptozotocin rats are known to have elevated food and water consumption [4], and therefore the glucose effects seen with L-carnitine treatment could be due to a lower intake of food or even a removal of intermediate lipids that would lower glucose levels [213]. L-carnitine has nevertheless shown to be beneficial in both cardiac diseases, diabetes and diabetic hearts [213, 199, 194].

In diabetes that is poorly controlled, the demand of L-carnitine increases due to elevated levels of fatty acid oxidation but also due to increased acyl-CoA, requiring L-carnitine for the clearance by formation of acylcarnitine [277]. The diabetic heart is known to have poor functional recovery post-ischemia, because of a low ability to utilise glucose, which is a more oxygen efficient fuel. L-carnitine treatment in the diabetic *ex vivo* heart has shown improved functional recovery post-ischemia using a working heart mode and showed an increased ability to oxidise pyruvate during ischemia [26]. Jian *et al.* have demonstrated that the cardioprotective effects in the isolated Langendorff perfused heart stem from a reduction of the

ratio of acetyl-CoA/CoA [106]. Long-chain fatty acyl-CoA is increased in the diabetic perfused heart, and it is suggested to be due to a decrease of free L-carnitine advancing a reduction in ATP production through inhibition of adenine nucleotide translocase (ANT) in the mitochondria [41, 193, 198]. Other studies have shown that long-chain fatty acyl-CoA levels decline after L-carnitine treatment [199, 198], as these reductions alleviate the diabetic heart from a metabolic burden. Rodrigues *et al.* also showed that L-carnitine significantly improved functional recovery in the streptozotocin-induced diabetic heart using working heart perfusion, and found lipid levels to be reduced.

Normal lipid metabolism is therefore crucial for maintaining cardiac function. However the underlying mechanisms of L-carnitine's beneficial effects are still unknown, and it might be due to many different mechanisms depending on the condition and substrate state of the heart. A recent study showed that L-carnitine possibly acts by activating the PI3K/mTOR/AKT pathway that is significant in proliferation, and promotion of growth in the cells. This study found, when PI3K inhibitors were given prior to L-carnitine treatment, the cardioprotective effects were no longer observed post-ischemia in the perfused heart [282].

Myocardial infarction patients have also been shown to benefit from L-carnitine treatment. In a randomized, double-blind, placebo-controlled trial patients were treated with daily L-carnitine for four weeks if there was suspected myocardial infarction based from electrocardiogram (ECG) examinations. And it was found that patients given L-carnitine had reduced angina pectoris, and reduced arrhythmias due to improved energetics and demonstrating smaller left ventricular enlargements, manifesting the cardioprotective effects of L-carnitine [239]. Another study investigating coronary artery disease found that L-carnitine resulted in an overall improved cardiac performance [239]. And this has also been supported by a multi-centre, randomized, double-blind, placebo control trial (the CEDIM trial) investigating 472 patients, to establish the effects of L-carnitine in patients with myocardial infarction [100]. They have shown that a significant improvement in relaxation of the left ventricle, both end diastolic and end systolic lumen have been decreased, without

any changes in ejection fraction, furthermore the number of deaths in the placebo group was 70 % greater than in the L-carnitine group [100, 67].

5.3 Chapter Aims

This study aimed to investigate the effects of L-carnitine supplementation on cardiac metabolism and function in the diabetic rat heart. Two groups of diabetics and two groups of healthy matched controls were studied. Daily L-carnitine or daily saline treatment was initiated two weeks post induction of diabetes. Following two weeks of treatment, all animals were scanned with hyperpolarized [1$-^{13}$C]pyruvate and [2$-^{13}$C]pyruvate to investigate TCA cycle intermediates as well as acetylcarnitine levels. Cardiac function was assessed *in vivo* with both echocardiography and CINE MRI. Ischemia reperfusion Langendorff perfusions were undertaken in a subgroup of animals to establish recovery and fatty acid oxidation rates post-ischemia. Subsequently, blood profile and metabolomics in the heart were assessed to validate the *in vivo* findings.

5.4 Methods

Seventy-two healthy male Wistar rats (∼200g) were randomly divided into four groups as listed below. All animals were either injected with STZ (55 mg/kg) or citrate buffer at the onset of the protocol as described in Section 2.2.

Two weeks after STZ/citrate buffer injection, all animals were initiated on daily morning i.p. treatments with either saline or L-carnitine, which was continued until tissue collection.

The dose of L-carnitine treatment was 3 g/kg/day. And the saline treatment was matched to the volume of the L-carnitine treated animals. Treatments were given while animals were conscious but restrained. Weight and well-being were monitored daily, and some animals were excluded from the study if they reached a humane end point (Fig. 5.1). The four groups were as follows:

① T1D group treated with daily i.p. injections of saline (STZ).

② T1D group treated with daily i.p. injections of L-carnitine (STZ Carn).

③ Control group treated with daily i.p. injections of saline (CTR).

④ Control group treated with daily i.p. injections of L-carnitine (CTR Carn).

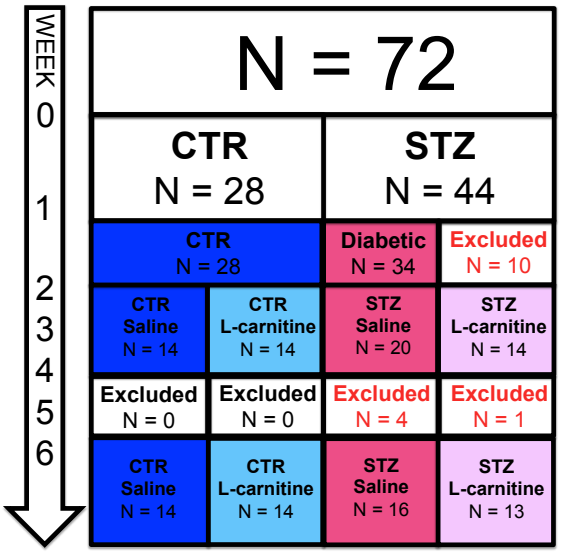

Figure 5.1: Animal numbers used. Ten animals were excluded initially at week one if they did not have diabetes, or they had too high blood glucose levels. Animals were also excluded if they reached a humane end point (N = 5).

Four weeks after the onset of the protocol, all animals were anaesthetized with isoflurane and subjected to MR imaging, hyperpolarized MR spectroscopy (MRS) as well as echocardiography as described in Sections 2.4.1, 2.4.3, and 2.4.4, before animals were euthanized and tissues were obtained five weeks post STZ injection as described in Section 2.6 (Fig. 5.2).

Fasted ketone levels were measured one, two, four and five weeks after STZ/citrate buffer injection as described in Section 2.2. Fasted blood samples were obtained at one, two, four and five weeks post STZ injection, and fed blood samples were obtained at the time of tissue collection as described in Section 2.8.

Thirty of the animals were continued on the protocol for one additional week, where hearts were extracted for Langendorff ischemia reperfusion five weeks post

onset of the protocol as described in Section 2.5.4. Three heart perfusions were undertaken daily.

The hearts were acclimatised to the albumin buffer for ten minutes prior to the onset of the protocol. Hearts were subjected to 20 minutes of normal flow, followed by 30 minutes of a low-flow rate of 0.4 ml/min before hearts were reperfused with normal flow for another 30 minutes (Section 2.5, Fig. 2.8). Fatty acid oxidation rates were measured as described in Section 2.5.6.

The subset of animals that were not perfused had the hearts extracted as described in Section 2.7 and low molecular weight metabolites were assessed with metabolomics in the hearts. Liquid chromatography and mass spectrometry were undertaken by Professor Jules Griffin and Dr. James West the Department of Biochemistry at the University of Cambridge. Short, medium and long-chain acyl-carnitines were measured. All short chain acyl-carnitines were averaged below 10 carbon, all medium chain acyl-carnitines were averaged between 12 and 16 carbons, and all long-chain acyl-carnitines were averaged above 16 carbons.

Insulin and NEFA levels were measured in the fed and fasted blood five weeks post STZ/citrate buffer injection, as described in Sections 2.9.2 and 2.9.1.

All fed blood samples were analysed for LDL, HDL, cholesterol, lactic acid, glucose and 3-OHB using an ABX Pentra 400 (Horiba ABX Diagnostics, California, USA) as described in Section 2.8. Blood gas measurements were collected from fed blood samples five weeks post STZ/citrate buffer injection using a blood gas analyser, as described in Section 2.8.

Heart tissue was crushed, and free L-carnitine was measured as described in Section 2.9.3 and protein expression was measured as described in Section 2.9.4.

All data are presented as mean ± SD unless otherwise stated. Two-way ANOVA was used for assessment of significance examining the effect of STZ injection and the effect of L-carnitine. When an interaction term was shown as significant Sidak's multiple comparisons was used post hoc. Student t-test was employed between two groups, where stated, although this significance is not illustrated on the figures. This was done when a trend was observed but failed to reach statistical significance with ANOVA analysis.

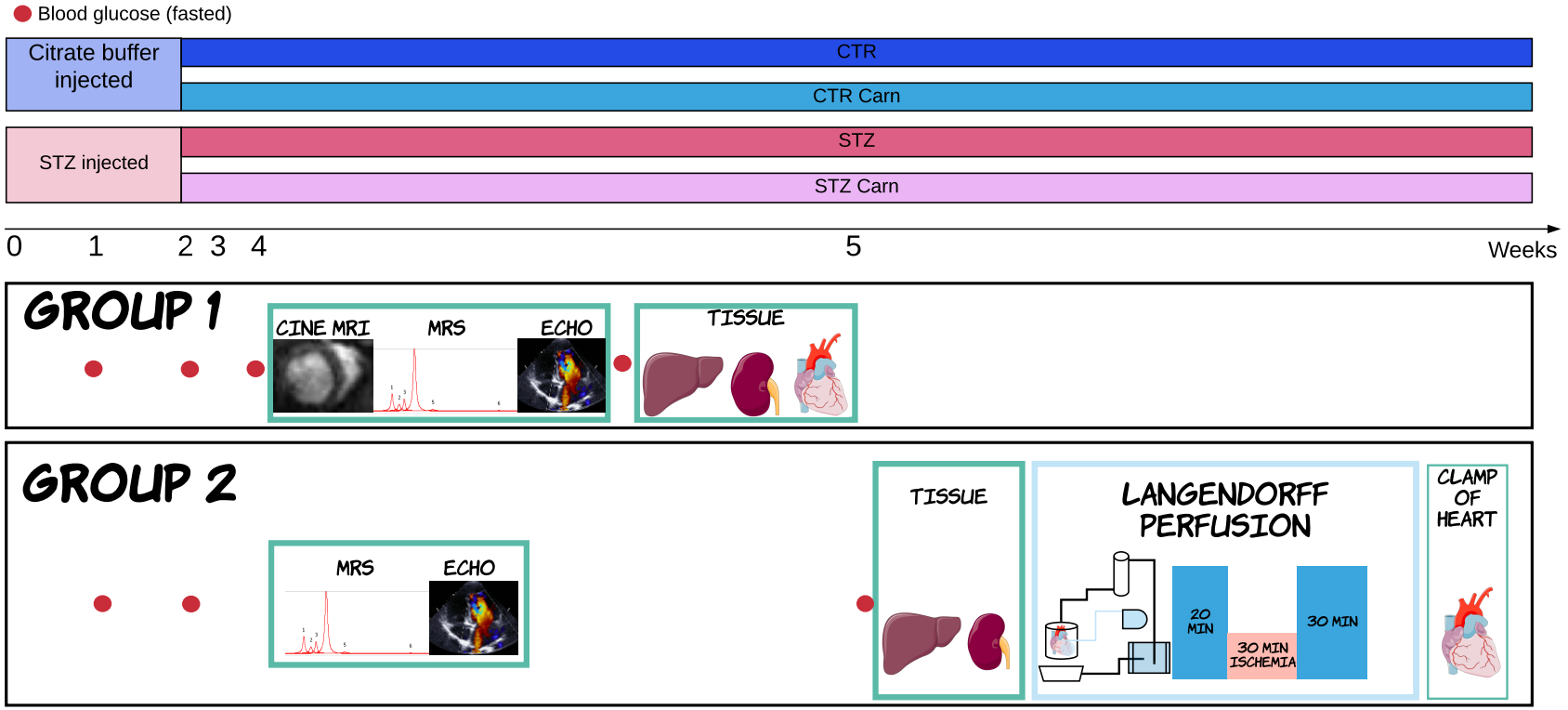

Figure 5.2: Experimental design. This figure shows a schematic of the imaging time-points and blood sampling for the four different groups (CTR, CTR Carn, STZ, STZ Carn). Some animals were continued to Langendorff perfusion (Group 2).

5.5 Results

Diabetic animals were established through a single STZ injection, with a success rate of 72 % (Fig. 5.1). Diabetes was induced two weeks before the start of daily treatment with either saline or L-carnitine. 80 % of the saline treated diabetic group proceeded to the end of the protocol, and 93 % of the L-carnitine treated diabetic group proceeded to the end of the protocol.

5.5.1 Weight and Blood Profile

All animals gained weight over the treatment duration. The control groups gained 9 % of their initial body weight over the course of the treatment, and the diabetic groups gained 3 % of their body weight over the treatment course. Diabetes resulted in a reduction in body weight of 25 % compared to the controls ($p < 0.0001$), and L-carnitine reduced body weight by 7 % compared to the saline treated groups (Fig. 5.3).

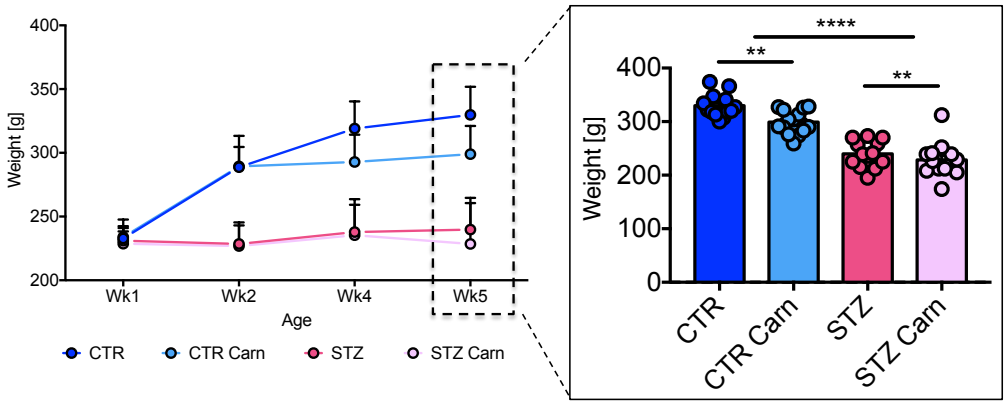

Figure 5.3: Body weight measured from control rats (CTR) and diabetic rats (STZ). **Left)** Body weight from the day of STZ/citrate buffer injection. **Right)** Body weight five weeks post STZ injection. Data presented as mean ± SD. Two-way ANOVA $^{**}p < 0.01$,$^{****}p < 0.0001$.).

Fat pads were 76 % smaller in the diabetic groups compared to the control groups ($p < 0.001$), and whilst L-carnitine as a factor in the two-way ANOVA had no effect on the fat pad weights, an unpaired t-test showed that L-carnitine reduced fat pads in the control group significantly ($p = 0.02$, unpaired t-test). The length of the tibia was 5 % shorter in the diabetic groups compared to the control groups ($p < 0.05$),

and whilst L-carnitine treated animals in both diabetic and control groups had shorter tibia, it failed to reach statistical significance (p = 0.06). The weight of the two kidneys was 13 % elevated with diabetes compared to the controls (p = 0.003), however, with L-carnitine treatment the weight reduced 11 % (p = 0.009) in both control and diabetic groups. The hypertrophy index (calculated as the kidney weight normalized to body weight) showed an elevation of 30 % with diabetes compared to controls (p < 0.0001). L-carnitine reduced the hypertrophy index by 9 % in the diabetic group compared to the saline treated diabetic group (p = 0.047, Fig. 5.4).

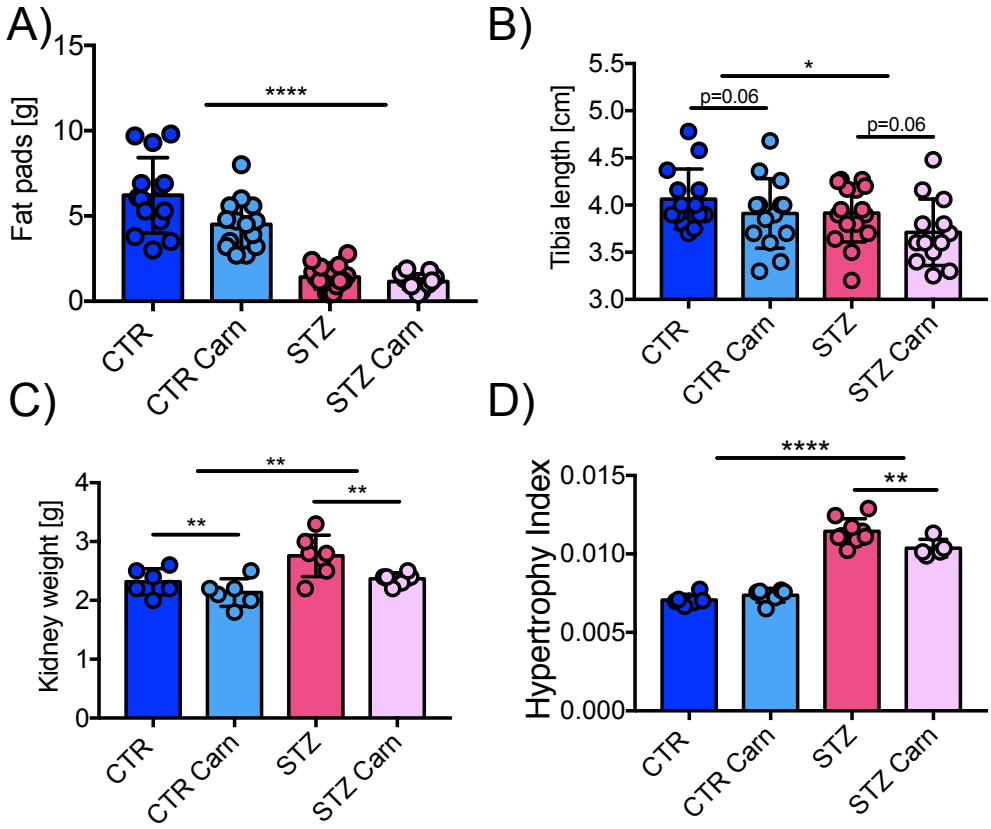

Figure 5.4: Tissue collection five weeks post STZ/citrate injection. **A)** Fat pads taken at the time of tissue collection. **B)** Right tibia length measured at the time of tissue collection. **C)** Total sum of the left and right kidney weights. **D)** Kidney hypertrophy index (kidney weight/body weight) at the time of tissue collection. Data presented as mean ± SD. Two-way ANOVA comparing all groups adjusted for multiple comparisons $^{*}p < 0.05, ^{**}p < 0.01, ^{****}p < 0.0001$.

Blood glucose levels were elevated in both the diabetic groups at two and five weeks post STZ/citrate buffer injection (Fig. 5.5A). The saline treated diabetic group showed a significant and progressive increase in hyperglycaemia over the three weeks of treatment. However, whilst the L-carnitine treated diabetic group showed elevated blood glucose at two weeks, there was no further increase over the duration of treatment, with some animals even showing a decrease in blood glucose levels (Fig. 5.5B).

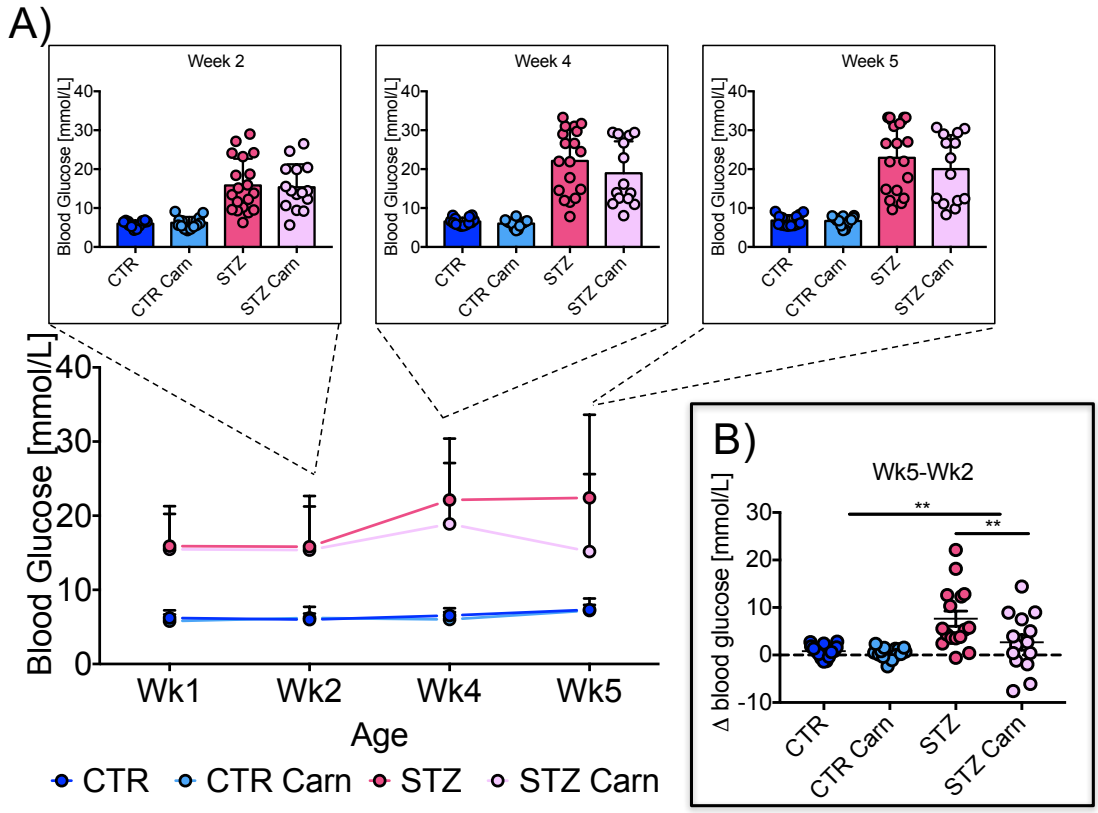

Figure 5.5: Blood glucose concentration measured in the fasted state from control animals (CTR) and diabetic animals (STZ). **A)** Fasted blood glucose levels measured two weeks after STZ injection. **B)** Fasted blood glucose levels measured five weeks after STZ injection. **C)** Difference in blood glucose concentrations during the treatment with saline and L-carnitine daily, between week five and week two. Data presented as mean ± SD. Two-way ANOVA with Sidak's multiple comparisons $^{**}p < 0.01$.

Insulin levels were significantly reduced in the diabetic groups in both the fed state ($p < 0.001$) and the fasted state ($p = 0.013$), compared to the controls. L-carnitine decreased insulin levels in the fed state, which was mostly driven by a 46 % reduction in insulin levels in the control group ($p = 0.002$, Fig. 5.6).

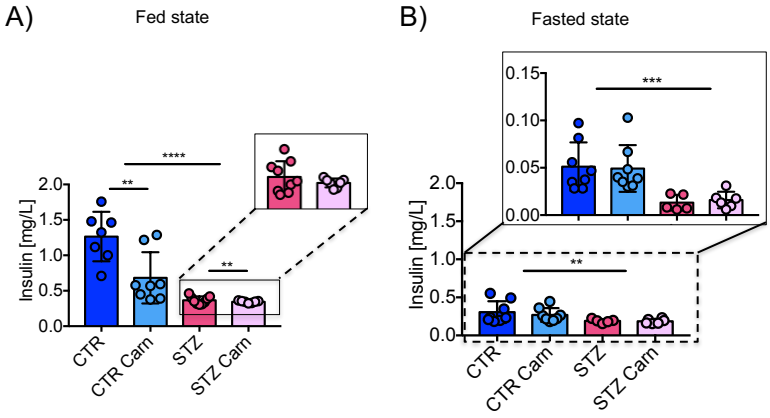

Figure 5.6: Insulin measured in fed and fasted state. **A)** Insulin in the fed state, terminal bloods. **B)** Insulin in the fasted state five weeks post STZ/citrate buffer injection. Data presented as mean ± SD. Two-way ANOVA $^{**}p < 0.01$,$^{***}p < 0.001$,$^{****}p < 0.0001$.

Fasted insulin levels were used for a homeostatic model assessment (HOMA) to assess insulin resistance (IR), which was elevated by 83 % in the diabetic groups compared to the control groups ($p = 0.02$), there was no significant effect with L-carnitine treatment (Fig. 5.7).

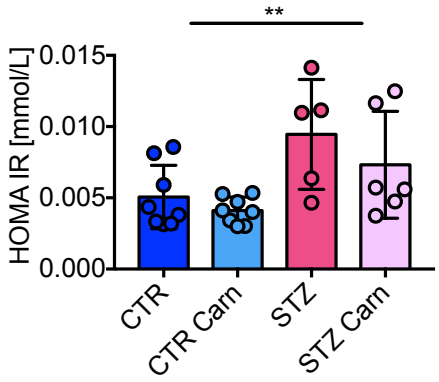

Figure 5.7: Insulin sensitivity. Insulin resistance; HOMA IR [mmol/L]. Data presented as mean ± SD. Two-way ANOVA $^{**}p < 0.01$.

Ketone bodies were measured at the same time as blood glucose levels after an overnight fast. Five weeks post STZ induction there was a 31 % decrease in the levels of fasted ketone bodies in the diabetics compared to the control groups, and no effect was observed with L-carnitine treatment (Fig. 5.8).

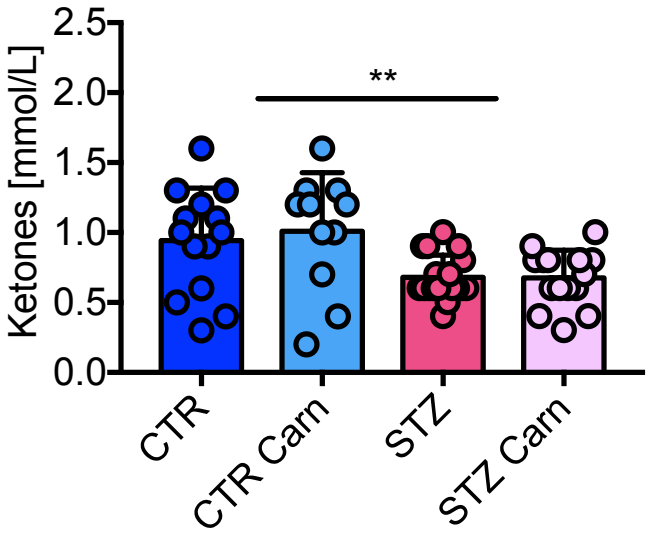

Figure 5.8: Fasted ketone levels five weeks post STZ/citrate buffer injection. Saline treated control rats (CTR), L-carnitine treated control rats (CTR Carn), saline treated diabetic rats (STZ), and L-carnitine treated diabetic rats (STZ Carn). Data presented as mean ± SD. Two-way ANOVA analysis $^{**}p< 0.01$.

Glucose levels measured in the fed state at five weeks post STZ/citrate buffer injection were 288 % higher in the diabetic groups compared to the control groups ($p < 0.0001$). Lactic acid was unchanged across all groups in the fed blood plasma, and β-hydroxybutyrate (3-OHB) was 230 % elevated in the diabetic groups compared to the control groups ($p < 0.0001$). L-carnitine reduced levels of 3-OHB mainly in the diabetic group by 51 % ($p = 0.005$, Fig. 5.9).

Furthermore, low density lipoproteins (LDL) were unchanged across all groups, high density lipoproteins (HDL) were elevated by 48 % in the diabetic groups compared to the control groups ($p = 0.0001$), and L-carnitine reduced HDL in both control and diabetics by 14 % ($p = 0.005$).

Cholesterol was elevated 28 % in the diabetic groups compared to the control groups ($p = 0.0045$), L-carnitine reduced cholesterol by 14 % in both diabetic and control groups, but it failed to reach statistical significance ($p = 0.08$).

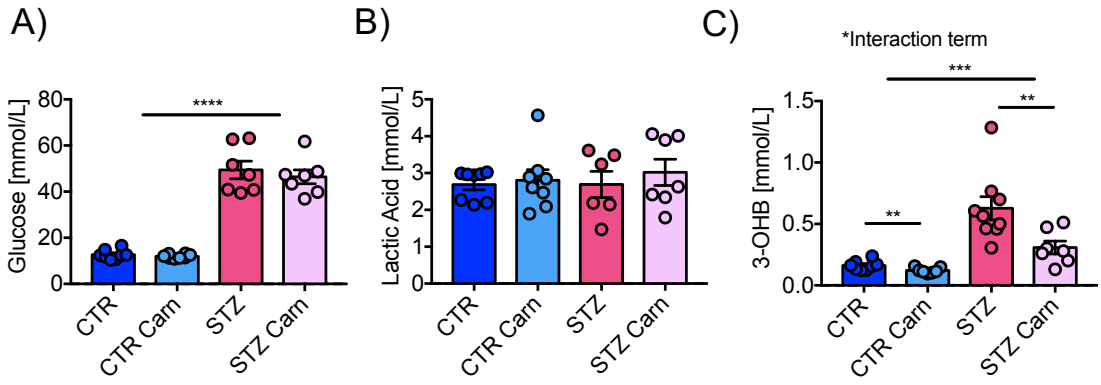

Figure 5.9: ABX Pentra 400 measurements taken from fed state serum five weeks post STZ/citrate buffer injection. **A)** Glucose levels [mmol/L]. **B)** Lactic acid concentrations [mmol/L]. **C)** β-hydroxybutyrate [mmol/L]. Data presented as mean ± SD. Two-way ANOVA with Sidaks multiple comparison test post hoc, where $^{**}p < 0.01$, $^{***}p < 0.001$, $^{****}p < 0.0001$.

Triglycerides (TAG) were lowered by 46 % with L-carnitine treatment in both the diabetic and the control group ($p = 0.0005$, Table. 5.1).

Blood gas measurements were obtained from the fed plasma five weeks post STZ/citrate buffer injection. Saline treated diabetic animals had a pH level of 7.6 ± 0.1 and the saline treated control animals had a similar pH level of 7.6 ± 0.03. L-carnitine elevated pH by 1.3 % in both the control (7.7 ± 0.1) and the diabetic group (7.7 ± 0.1, $p = 0.012$). L-carnitine reduced pCO_2 by 17 % in both the control and the diabetic groups ($p = 0.014$) Calcium was significantly increased by 9 % in the diabetic group ($p = 0.03$, Table. 5.1), and no effect was observed with L-carnitine treatment.

Blood Profile	Control (CTR)		Diabetes (STZ)		2-way ANOVA
Mean ± SD	Saline	L-carnitine	Saline	L-carnitine	p-value Treatment/Group (interaction)
LDL [mmol/L]	0.2 ± 0.1	0.2 ± 0.1	0.2 ± 0.1	0.2 ± 0.1	0.4900/0.4900
HDL [mmol/L]	0.70 ± 0.07	0.65 ± 0.09	1.1 ± 0.2	0.9 ± 0.1	0.0050/0.0001
Cholesterol [mmol/L]	2.1 ± 0.6	1.9 ± 0.4	2.8 ± 0.7	2.3 ± 0.2	0.0840/0.0045
TAG [mmol/L]	2.6 ± 0.9	1.1 ± 0.5	2.4 ± 1	1.6 ± 0.7	0.0005/0.7000
Fasted NEFA [mmol/L]	0.08 ± 0.03	0.08 ± 0.04*	0.3 ± 0.2	0.1 ± 0.1*	0.13/0.005 (0.046)
Fed NEFA [mmol/L]	0.2 ± 0.1	0.3 ± 0.1	0.2 ± 0.2	0.5 ± 0.2	0.0130/0.0980
pH	7.6 ± 0.03	7.7 ± 0.1	7.6 ± 0.1	7.7 ± 0.08	0.012/0.726
pCO_2 [kPa]	4.7 ± 0.4	3.6 ± 1	4.1 ± 0.6	3.7 ± 0.8	0.014/0.517
pO_2 [kPa]	33 ± 2	32 ± 2	29 ± 6	33 ± 1	0.459/0.315
cBase [mmol/L]	8.0 ± 0.8	10 ± 3	10 ± 3	11 ± 3	0.079/0.191
cK^+ [mmol/L]	5.7 ± 0.5	6.2 ± 0.8	6.7 ± 1.7	6.2 ± 0.9	0.932/0.233
cNa^+ [mmol/L]	138 ± 3	136 ± 2	136 ± 6	133 ± 2	0.091/0.145
cCa^{2+} [mmol/L]	1.27 ± 0.07	1.2 ± 0.1	1.3 ± 0.2	1.4 ± 0.3	0.701/0.027
cCl^- [mmol/L]	99 ± 3	99 ± 3	100 ± 6	97 ± 5	0.433/0.880

Table 5.1: ABX Pentra 400 and blood gas measurements taken from fed state serum five weeks post STZ/citrate buffer injection. Results presented as mean ± SD. Two-way ANOVA with multiple comparisons if the interaction term was significant.

5.5.2 Cardiac *In Vivo* Function

Echocardiography measurements were noisy. Fractional shortening showed no differences across any groups. Ejection fraction was decreased by 10 % in the diabetic groups compared to the controls ($p = 0.035$). An example can be seen between a control heart treated with saline and a diabetic heart treated with saline (Fig. 5.10)

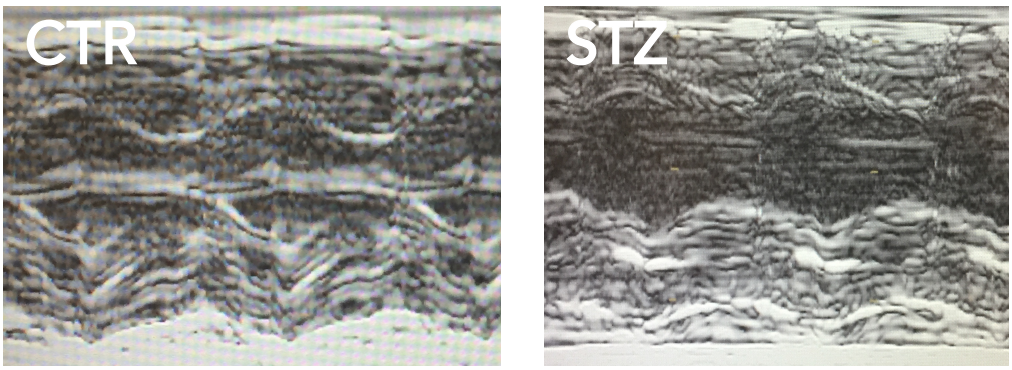

Figure 5.10: Echocardiography five weeks post STZ/Citrate buffer injection. Examples of three cardiac cycles imaged with echocardiography with M-mode imaging with the papillary muscles visible. Left is an example of a saline treated control, and right is an example of a saline treated diabetic.

Diastolic early to late filling ratio (E/A ratio) through the mitral valve was decreased by 8 % with L-carnitine treatment in the diabetic group ($p = 0.05$, Table 5.2).

Echocardiography	Control (CTR)		Diabetes (STZ)		2-way ANOVA
Mean ± SD	Saline	L-carnitine	Saline	L-carnitine	p-value Treatment/Group (interaction)
Fractional Shortening (FS) [%]	47 ± 6	46 ± 5	40 ± 12	39 ± 9	0.65/0.07
Ejection Fraction (EF) [%]	83 ± 5	82 ± 4	75 ± 12	74 ± 10	0.85/0.035
Early filling (E) [m/s]	0.57 ± 0.18	0.61 ± 0.22	0.70 ± 0.24	0.63 ± 0.19	0.23/0.27
Late filling (A) [m/s]	0.57 ± 0.10	0.51 ± 0.08	0.46 ± 0.12	0.60 ± 0.16	0.60/0.85
E/A ratio	0.96 ± 0.26	0.99 ± 0.24	1.02 ± 0.16	0.84 ± 0.17	0.05/0.17
Septum E/E' ratio	12.6 ± 4.5	12.1 ± 5.1	11.9 ± 4.3	16.4 ± 6.9	0.17/0.08
Lateral wall E/E' ratio	13.2 ± 4.6	14.2 ± 6.5	14.9 ± 4.4	16.7 ± 6.9	0.59/0.35

Table 5.2: Echocardiography five weeks post STZ/Citrate buffer injection. Cardiac diastolic function obtained from four-chamber view measuring the pulse wave velocity through the mitral valve and tissue doppler as well systolic function obtained through M mode imaging from the two-chamber view. Results presented as mean ± SD. Two-way ANOVA adjusted for multiple comparisons.

Average myocardial mass was reduced by 19 % in the diabetic groups compared to control groups ($p = 0.0001$) with no effect of L-carnitine in either control or in diabetes (Fig. 5.11A).

Stroke volume (SV) was reduced by 21 % in the diabetic groups compared to the control groups ($p < 0.0001$), with an interaction term showing significance. L-carnitine decreased SV in the control group by 15 % ($p = 0.02$), and it failed to alter SV in diabetics. Stroke index (SI) as calculated as SV normalized to body weight, was elevated by 5 % in the diabetic groups compared to the control groups ($p = 0.001$), with an interaction term showing significance, however even with Sidak's post hoc test, L-carnitine showed no effect on SI in controls or in diabetics (Fig. 5.11BC).

L-carnitine elevated ESL by 39 % ($p = 0.0005$). EDL was reduced by 13 % in the diabetic groups compared to the control groups ($p = 0.0004$), with an interaction term showing significance, that showed L-carnitine elevated EDL by 16 % in the diabetic group ($p = 0.015$, Fig. 5.11DE).

Ejection fraction (EF) was reduced by 9 % in the diabetic groups compared to the control groups ($p = 0.006$). L-carnitine decreased EF by 11 % in both the control group and the diabetic group ($p = 0.002$, Fig. 5.11F).

Cardiac output (CO) was 33 % lower in the diabetic groups compared to the control groups ($p < 0.0001$), with a significant interaction term showing that L-carnitine reduced CO by 15 % in the control group ($p = 0.045$), but no effect of L-carnitine was observed in diabetes. Cardiac index (CO normalized to body weight) showed no significant effects across any groups.

HR was significantly reduced by 15 % in the diabetic groups compared to the control groups ($p < 0.0001$), there were no effects of L-carnitine in either group. When HR was normalized to body weight, it was elevated by 24 % in the diabetic groups compared to the control groups. Again there was no effect observed with L-carnitine treatment (Fig. 5.11IJ).

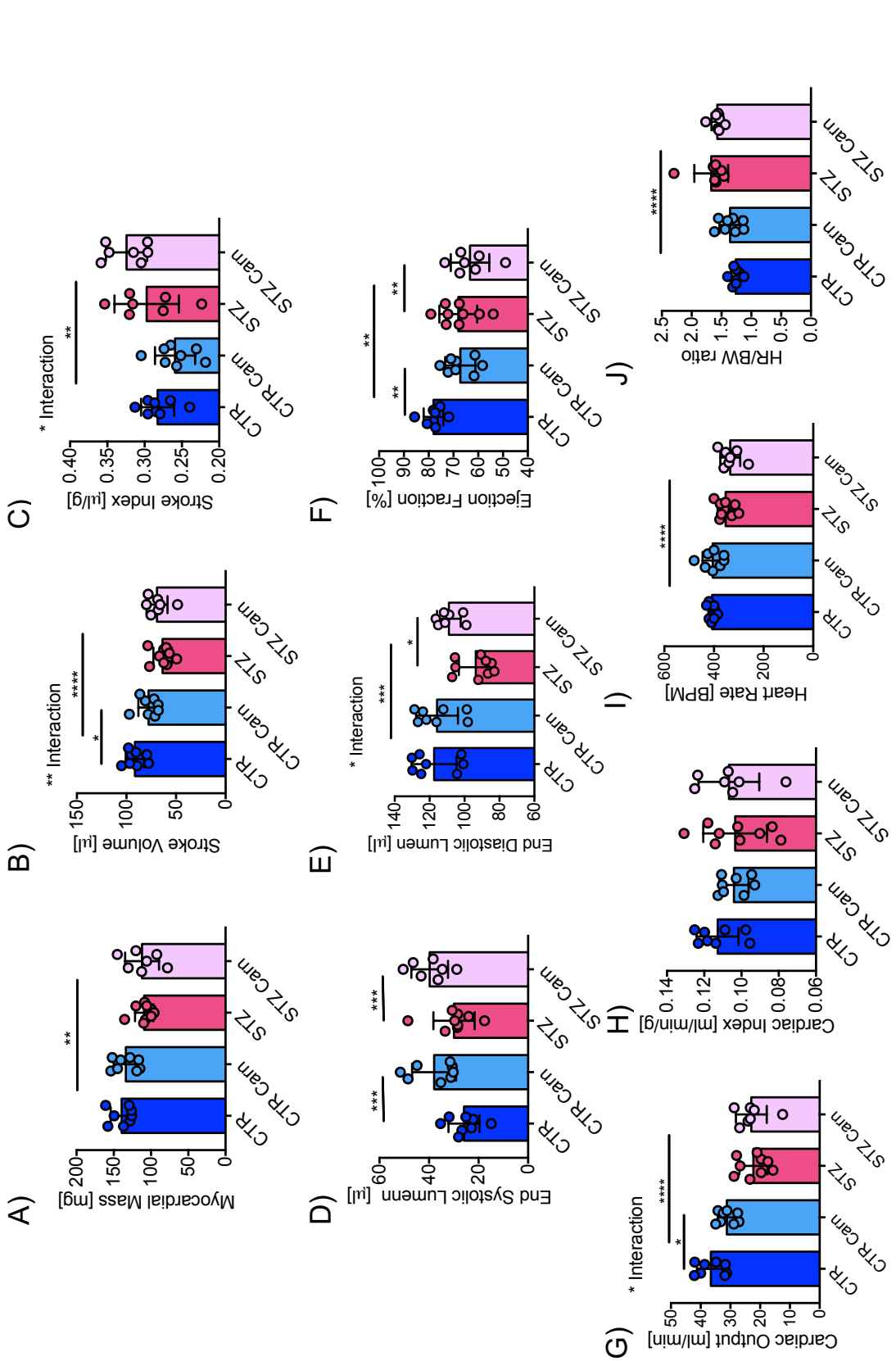

Figure 5.11: Cardiac function acquired with CINE MRI. **A)** Average myocardial wall mass of the left ventricle obtained from end diastolic and end systolic mass. **B)** Stroke volume (SV) obtained from the difference of the end diastolic lumen and end systolic lumen. **C)** Stroke index (SI), SV normalized to body weight. **D)** End systolic lumen (ESL). **E)** End systolic lumen (EDL). **F)** Ejection fraction (EF). **G)** Cardiac output (CO). **H)** Cardiac index (CI), CO normalized to body weight. **I)** Heart rate (HR). **J)** HR normalized to body weight (HR/BW). Data presented as mean ± SD. Two-way ANOVA analysis with Sidak's multiple comparison test $^{*}p < 0.05$, $^{**}p < 0.01$, $^{***}p < 0.001$, $^{****}p < 0.0001$.

5.5.3 Cardiac *In Vivo* Metabolism

Flux through pyruvate dehydrogenase (PDH), as indicated by the bicarbonate to pyruvate ratio, was significantly reduced by 66 % in the diabetic groups compared to the controls ($p < 0.0001$), with an interaction term showing significance ($p = 0.005$). L-carnitine reduced PDH-flux by 40 % in the control group ($p = 0.019$). L-carnitine elevated PDH-flux by 51 % ($p = 0.044$, unpaired t-test) in the diabetic group compared to the saline treated diabetic group (Fig. 5.12A).

Incorporation of the ^{13}C label from pyruvate into lactate, also a measure of the lactate dehydrogenase (LDH) flux, was elevated by 40 % in the diabetic groups compared to control groups ($p = 0.004$). There was no significant effect of L-carnitine treatment in any of the groups, although L-carnitine elevated lactate levels by 33 % in the diabetic group compared to the saline treated diabetic group ($p = 0.07$, Fig. 5.12B).

Incorporation of the ^{13}C label from pyruvate into alanine was increased by 40 % in the diabetic groups compared to the control groups ($p = 0.027$). L-carnitine elevated alanine by 29 % in both control and diabetic groups ($p = 0.029$, Fig. 5.12C).

Hyperpolarized $[2-^{13}C]$pyruvate demonstrated ^{13}C label incorporation into glutamate, citrate and acetylcarnitine. Citrate was reduced by 63 % in the diabetic groups compared to the control groups ($p < 0.0001$) with an interaction term showing significance ($p = 0.049$). Even though L-carnitine elevated citrate by 156 % in the diabetic group compared to the saline treated diabetic group, it failed to show statistical significance ($p = 0.2$, unpaired t-test). When citrate was normalized to PDH-flux, there were no differences observed across any groups (Fig. 5.13AD).

Glutamate was reduced by 55 % in the diabetic groups compared to the control groups ($p = 0.0002$), and there was a significant interaction term ($p = 0.0002$), showing that L-carnitine reduced glutamate levels in the control group by 40 % ($p = 0.012$). When glutamate was normalized to PDH-flux, the diabetic groups had elevated glutamate by 166 % compared to the control groups ($p = 0.04$, Fig. 5.13BE).

Incorporation of the ^{13}C label into acetylcarnitine (AC) was 76 % lower in the diabetic groups compared to the control groups ($p < 0.001$). L-carnitine had no

effect on AC in the control group, but AC was elevated by 219 % in the L-carnitine treated diabetic group compared to the saline treated diabetic group ($p = 0.024$, unpaired t-test). When AC was normalized to PDH-flux, L-carnitine elevated AC by 77 % in both the diabetic and the control groups ($p = 0.05$, Fig. 5.13 CF).

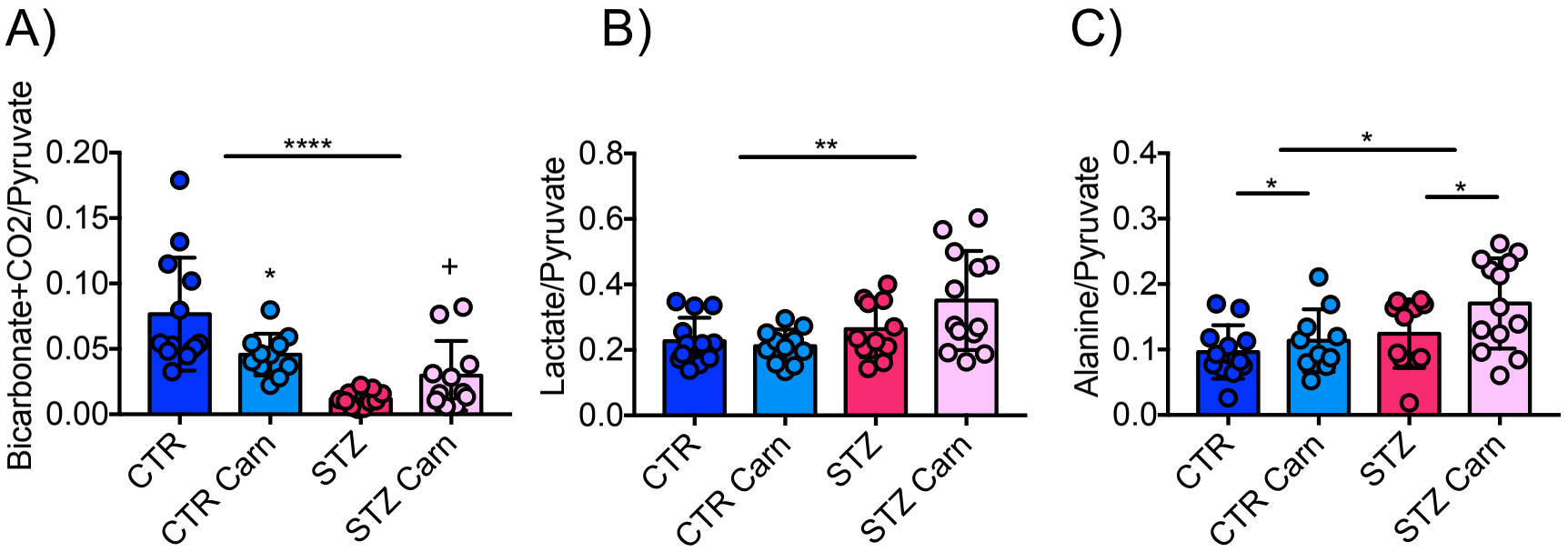

Figure 5.12: *In vivo* effects on cardiac metabolism by infusion of hyperpolarized [1−^{13}C] pyruvate. **A)** Bicarbonate/pyruvate ratio, interaction term was present (p = 0.005). $^{+}$ compared to STZ with an unpaired t-test (p = 0.044). **B)** Lactate/pyruvate ratio. **C)** Alanine/pyruvate ratio. Data presented as mean ± SD. Two-way ANOVA analysis with Sidak'smultiple comparison test post hoc. $^{*}p < 0.05$,$^{**}p < 0.01$,$^{****}p < 0.0001$.

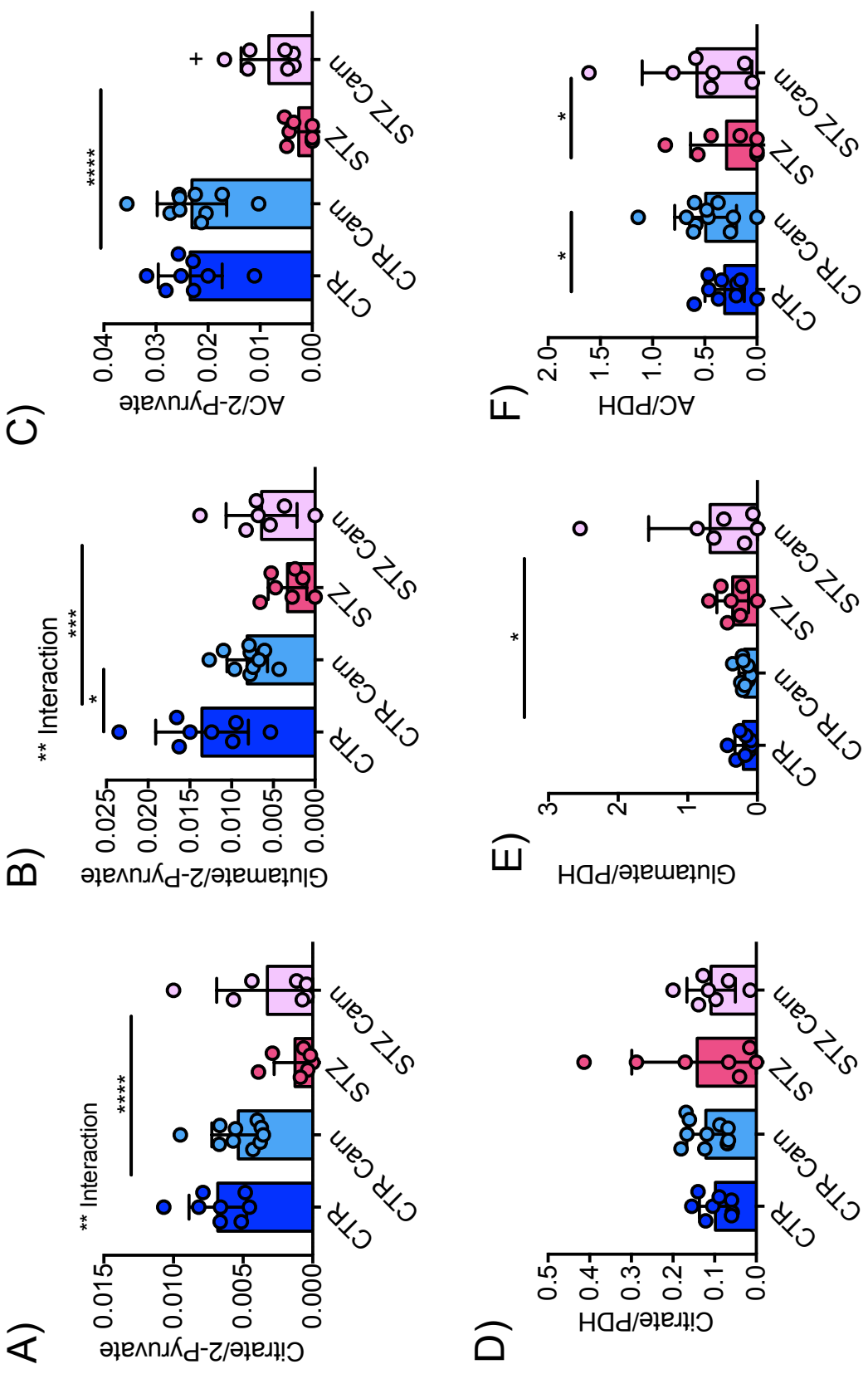

Figure 5.13: *In vivo* effects on cardiac metabolism investigated using hyperpolarized [2−^{13}C] pyruvate MRI. **A)** Citrate/2-pyruvate ratio. **B)** Glutamate/2-pyruvate ratio. **C)** Acetylcarnitine (AC)/2-pyruvate ratio, unpaired t-test ($^{+}$p = 0.024, compared to STZ). **D)** Citrate/2-pyruvate ratio normalized to PDH-flux (Bicarbonate + CO_2/pryvate). **E)** Glutamate/2-pyruvate ratio normalized to PDH-flux (Bicarbonate + CO_2/pryvate). **F)** Acetylcarnitine (AC)/2-pyruvate ratio normalized to PDH-flux (Bicarbonate + CO_2/pyruvate). Results presented as mean ± SD. Two-way ANOVA analysis with Sidak's multiple comparisons $^{*}p < 0.05$,$^{***}p < 0.001$,$^{****}p < 0.0001$.

5.5.4 Tissue Analysis

GLUT4 was down regulated in diabetes by 22 % compared to the control groups ($p = 0.05$), even though GLUT4 expression levels were reduced by 40 % in the L-carnitine treated diabetic group compared to the saline treated diabetic group, it failed to reach statistical significance with a two-way ANOVA ($p = 0.036$, unpaired t-test, Fig 5.14A).

Protein expression levels of α-ketoglutarate were unchanged across all the groups.

Even though PDK4 failed to reach statistical significance across all groups with a two-way ANOVA, PDK4 expression was elevated by 864 % in the saline treated diabetic group compared to the saline treated control group ($p = 0.02$, unpaired t-test, Fig 5.14C).

L-carnitine reduced the expression of CD36 by 45 % in both the control and diabetic groups (p 0.039, Fig 5.14D).

MCAD expression showed a two-way ANOVA significant interaction term ($p < 0.05$), however, failed to reach statistical significance between groups. Despite this, L-carnitine elevated MCAD expression by 110 % in the diabetic group compared to the saline treated diabetic group ($p = 0.05$, unpaired t-test, Fig 5.14E).

No significant differences were observed in UCP3 expression across any groups (Fig. 5.14F).

L-carnitine was measured in heart tissue after three weeks of treatment. Even though the assay failed to show a significant reduction in the diabetic hearts compared to the control hearts, there was a significant interaction term and L-carnitine treatment elevated free L-carnitine in the heart tissue by 179 % in the control group ($p = 0.01$, Fig. 5.15).

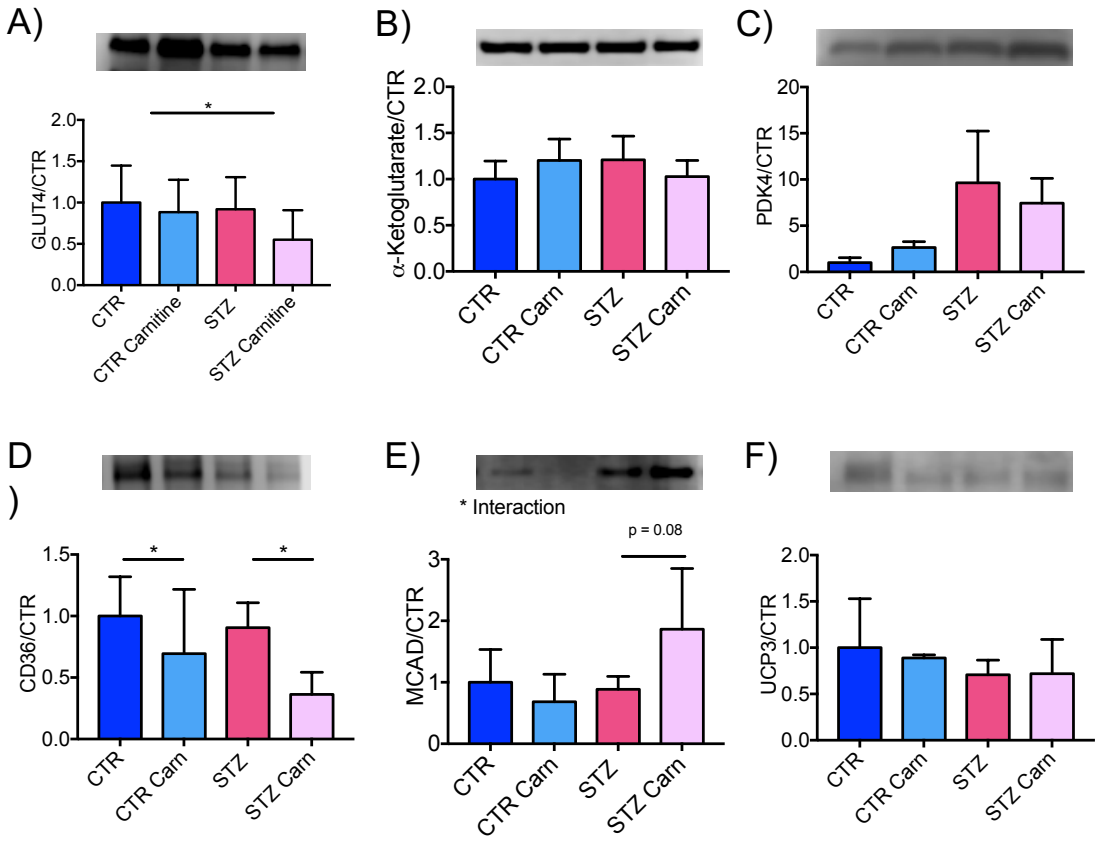

Figure 5.14: Protein expression levels were obtained from Western Blots, all values are normalized to control values. Housekeeper antibody showed no differences (cyclophilin B). **A)** GLUT4. **B)** α-ketoglutarate. **C)** PDK4. **D)** CD36/FAT. **E)** MCAD. **F)** UCP3. All data represented as mean ± SD. Two-way ANOVA with Sidak's multiple comparison test $^{*}p < 0.05$.

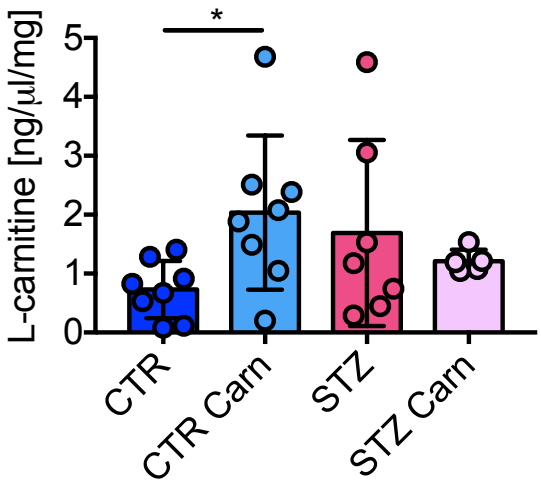

Figure 5.15: Free L-carnitine levels in heart tissue measured with an L-carnitine assay. All data represented as mean ± SD. Two-way ANOVA with Sidak's multiple comparison test $^{*}p < 0.05$.

Metabolomics

Free L-carnitine as measured with metabolomics agreed with the L-carnitine assay used for measuring free L-carnitine in the heart tissue in the control animals. There was no differences observed in free L-carnitine in the heart between the diabetic groups and the control groups. L-carnitine elevated free L-carnitine in heart tissue by 89 % in both the control and diabetic groups ($p = 0.007$, Fig. 5.16A).

Short-chain acyl-carnitines showed no differences in heart tissue with diabetes. L-carnitine elevated short-chain acyl-carnitines significantly by 61 % in both the control and diabetic groups ($p = 0.038$, Fig. 5.16B).

Medium-chain acyl-carnitines showed elevation in the diabetic groups by 88 % compared to the control groups ($p = 0.016$, unpaired t-test). L-carnitine elevated medium chain acyl-carnitines by 78 % in the control group although it failed to reach statistical significance ($p = 0.08$, Fig. 5.16C).

Long-chain acyl-carnitines showed a significant elevation in the diabetic groups by 152 % compared to the control groups ($p = 0.031$). L-carnitine elevated long-chain acyl-carnitines by 122 % in both the control and in the diabetic groups, although it failed to reach statistical significance ($p = 0.06$, Fig. 5.16D).

Most TCA cycle intermediates in the heart failed to reach statistical significance as seen in Figure 5.17. Malate was significantly elevated by 170 % with diabetes ($p = 0.03$, unpaired t-test), and with L-carnitine treatment, malate reduced by 50 % although it failed to reach statistical significance ($p = 0.1$, unpaired t-test). Aspartate was reduced by 47 % with diabetes ($p = 0.0006$, Fig. 5.17).

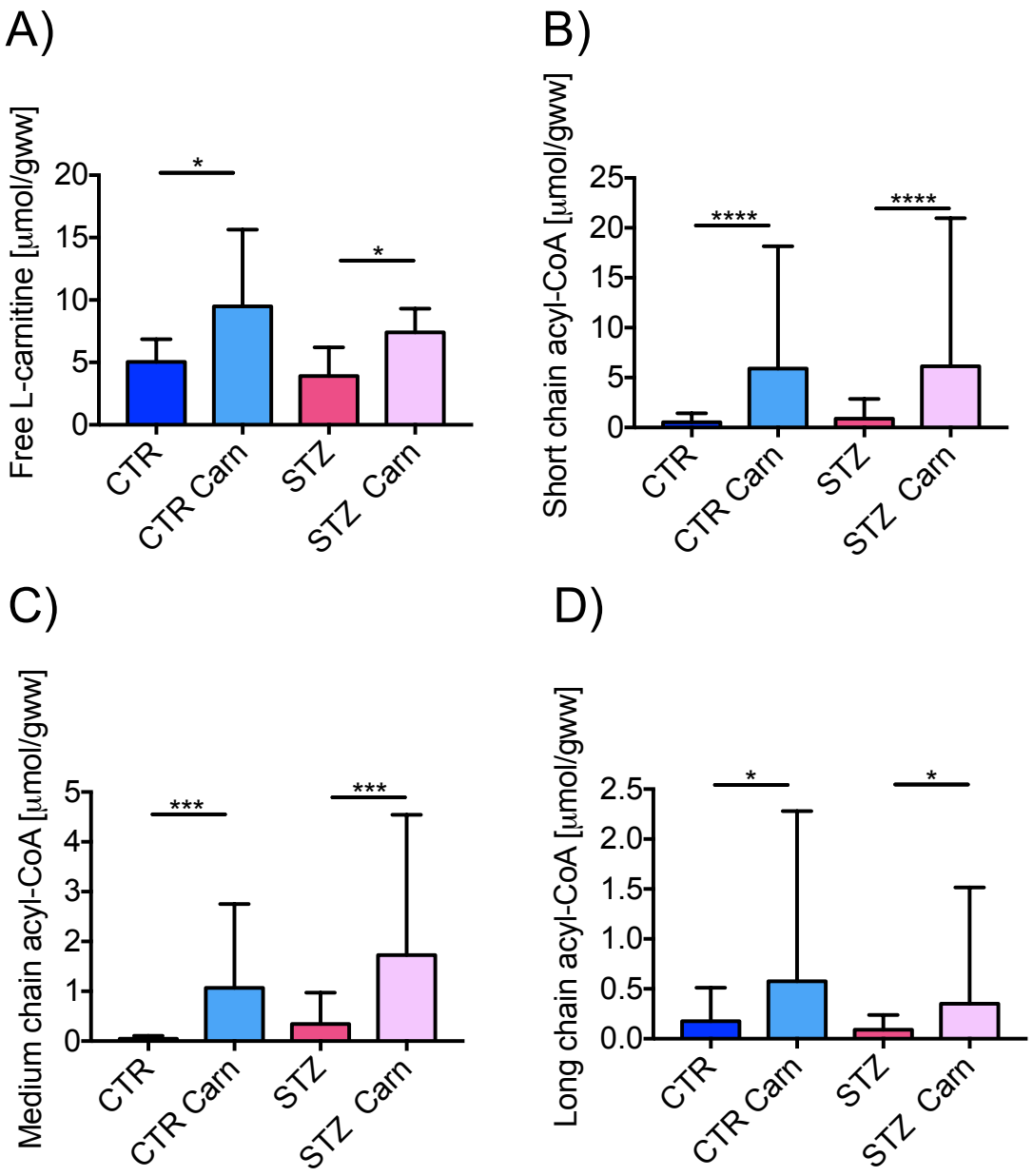

Figure 5.16: Metabolomic measures of acyl-carnitines. Short-chain, medium-chain and long-chain acyl-carnitines in heart tissue. **A)** Free L-carnitine (C0). **B)** All short-chain acyl-carnitines averaged (C2-C10). **C)** All medium-chain acyl-carnitines averaged (C12-C15). **D)** All long-chain acyl-carnitines averaged (C2-C10). Data are represented as mean ± SD. Two-way ANOVA where $^{*}p < 0.05$.

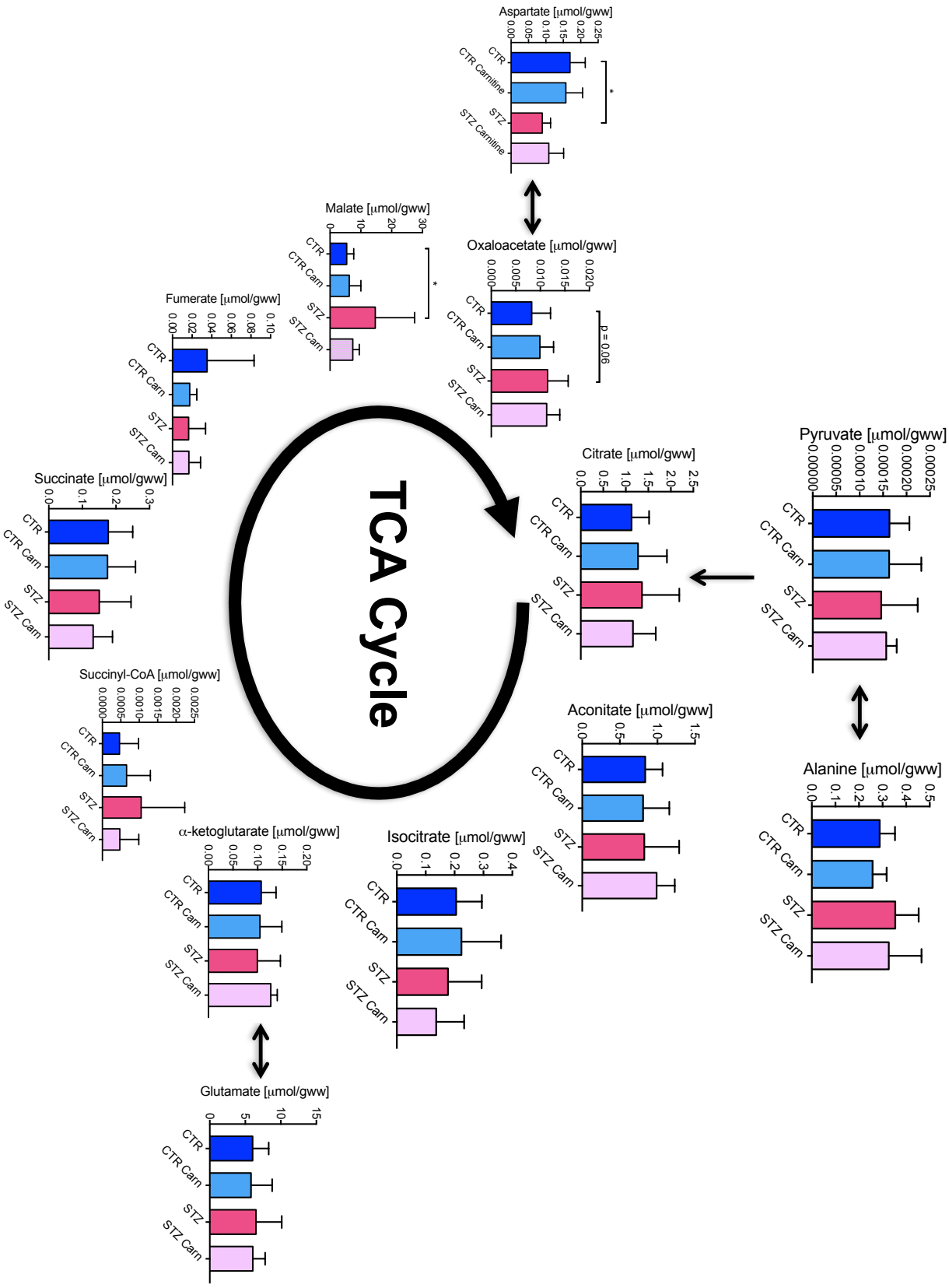

Figure 5.17: Metabolomic measures of TCA cycle intermediates. Data are represented as mean ± SD. Unpaired t-test where $^*p < 0.05$.

5.5.5 Cardiac *Ex Vivo* Function

Rate pressure product (RPP) was 37 % lower in the diabetic groups compared to the control groups post-ischemia ($p = 0.034$), even though RPP was similar pre-ischemia across all groups. There was a significant interaction term ($p = 0.007$). L-carnitine elevated RPP by 270 % in the diabetic group ($p = 0.009$, Fig. 5.18).

There was a reduction of 35 % in the developed pressure (DevP) post-ischemia in the diabetic groups compared the controls ($p = 0.028$). There was a significant interaction term ($p = 0.029$), and similarly like in RPP, L-carnitine elevated the DevP by 181 % in the diabetic group ($p = 0.015$, Fig. 5.19).

Diastolic pressure (DiaP) was elevated by 51 % in the diabetic groups compared to the control groups ($p = 0.049$, unpaired t-test) post-ischemia. L-carnitine failed to alter DiaP significantly (Fig. 5.20).

Systolic pressure (SysP) was also unchanged pre-ischemia across all groups. However, post-ischemia SysP decreased by 21 % in the diabetic groups compared to the control groups ($p = 0.0078$). Even though the two-way ANOVA showed no other differences across groups at pre- or at post-ischemia, L-carnitine elevated SysP by 22 % in the diabetic group compared to the saline treated diabetic group ($p = 0.05$, unpaired t-test, Fig. 5.21).

Heart rate (HR) was significantly reduced pre-ischemia in the diabetic groups by 20 % compared to the controls ($p = 0.01$). Furthermore, L-carnitine reduced HR pre-ischemia in both control and diabetic groups by 17 % ($p = 0.021$, Fig. 5.22). HR was unchanged post-ischemia across all groups.

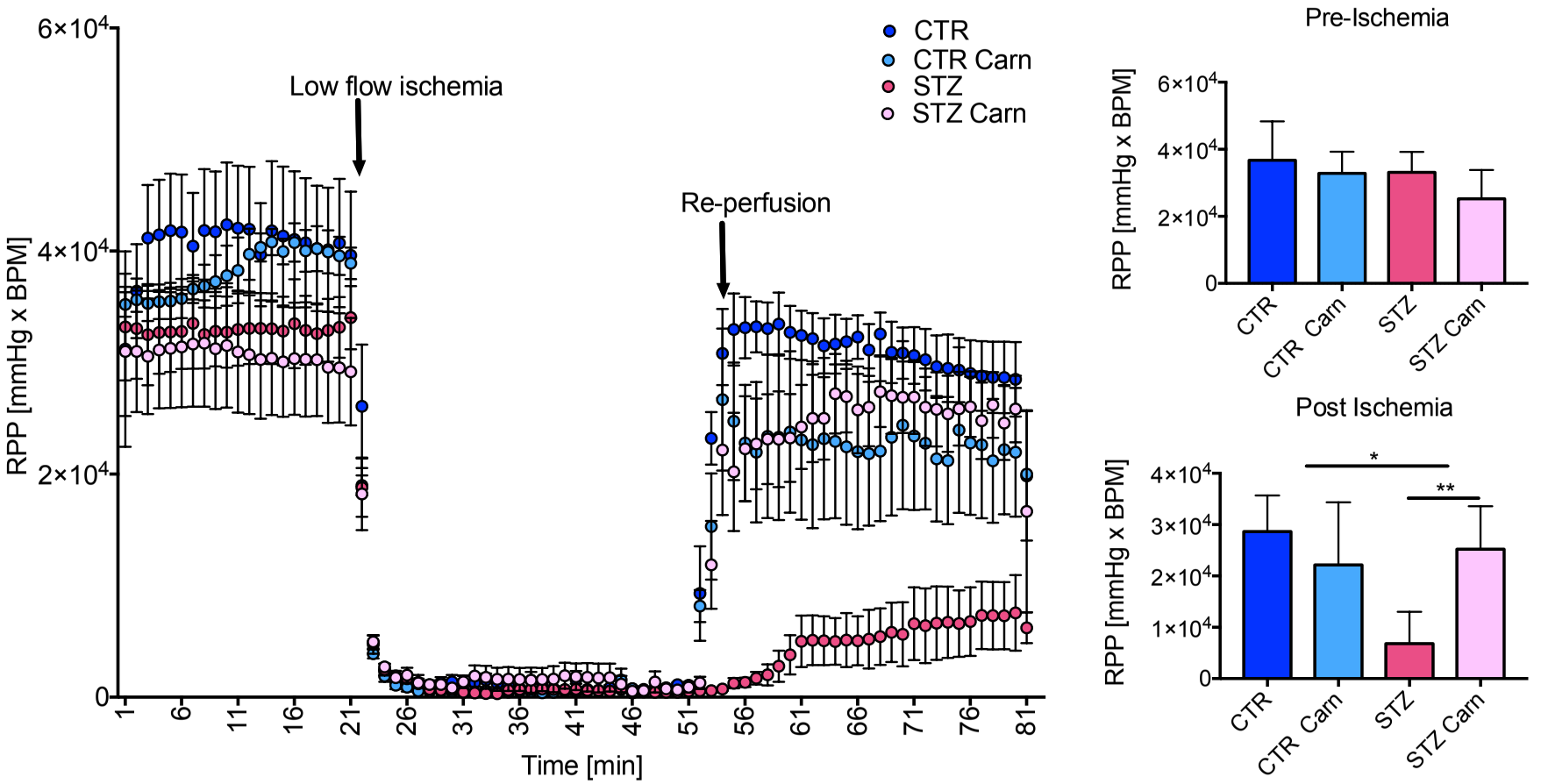

Figure 5.18: Rate pressure product (RPP) shown from Langendorff perfusions, where pre-ischemia (t = 1:20 min), ischemia (t = 21:50 min), and post-ischemia (t = 52:80 min). The low-flow rate of 0.4 ml/min/gww was used. Saline treated control (CTR, dark blue), L-carnitine treated control (CTR Carn, light blue), saline treated diabetics (STZ, magenta), L-carnitine treated diabetics (STZ Carn, light pink). Data presented as mean ± SD. Two-way ANOVA with Sidak's multiple comparisons, where $^{*}p < 0.05$, $^{**}p < 0.01$.

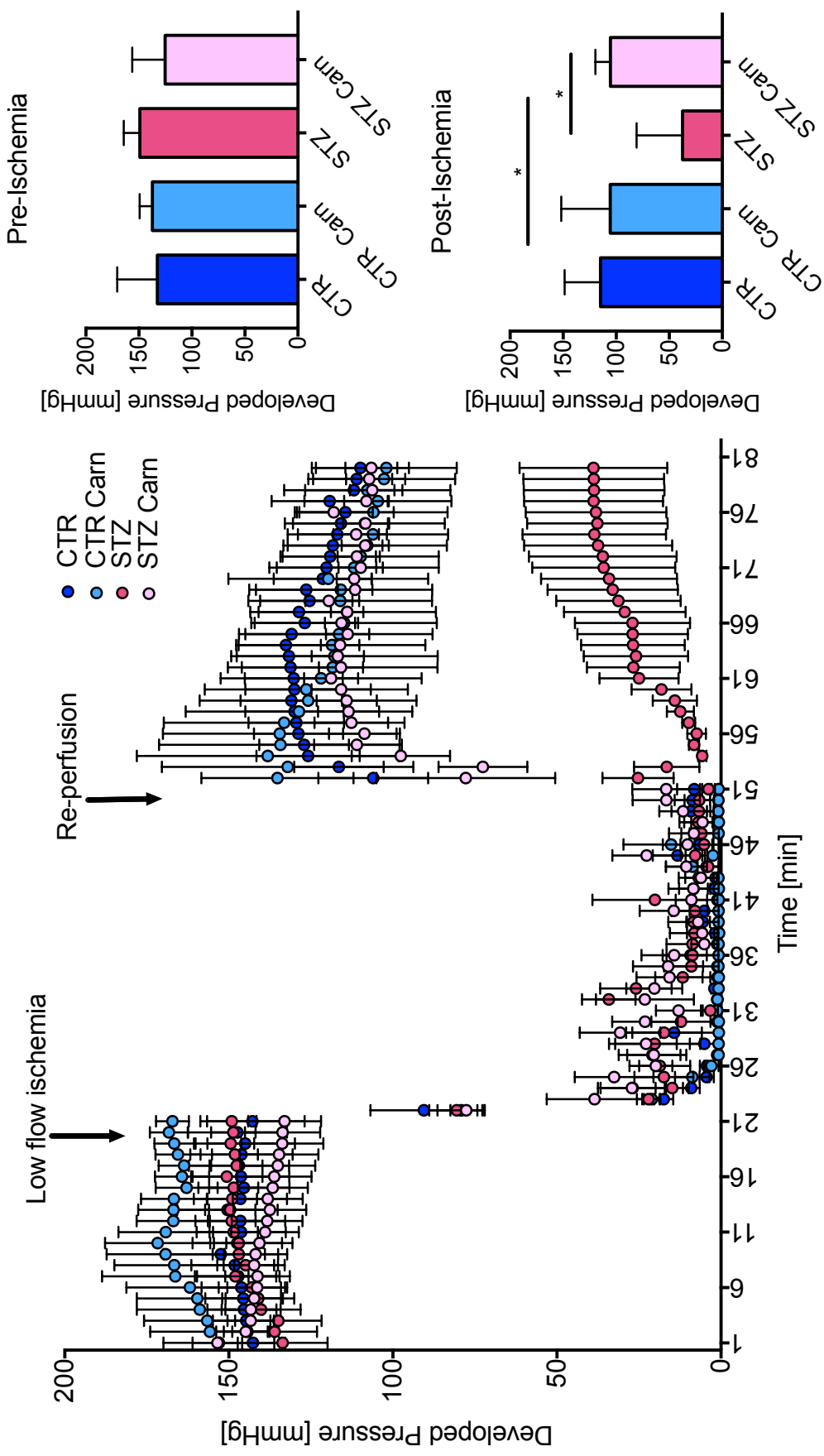

Figure 5.19: Developed pressure (DevP) shown from Langendorff perfusions, where pre-ischemia (t = 1:20 min), ischemia (t = 21:50 min), and post-ischemia (t = 52:80 min). The low-flow rate of 0.4 ml/min/gww was used. Saline treated control (CTR, dark blue), L-carnitine treated control (CTR Carn, light blue), saline treated diabetics (STZ, magenta), L-carnitine treated diabetics (STZ Carn, light pink). Data presented as mean ± SD. Two-way ANOVA with Sidak's multiple comparisons, where $^{*}p < 0.05$.

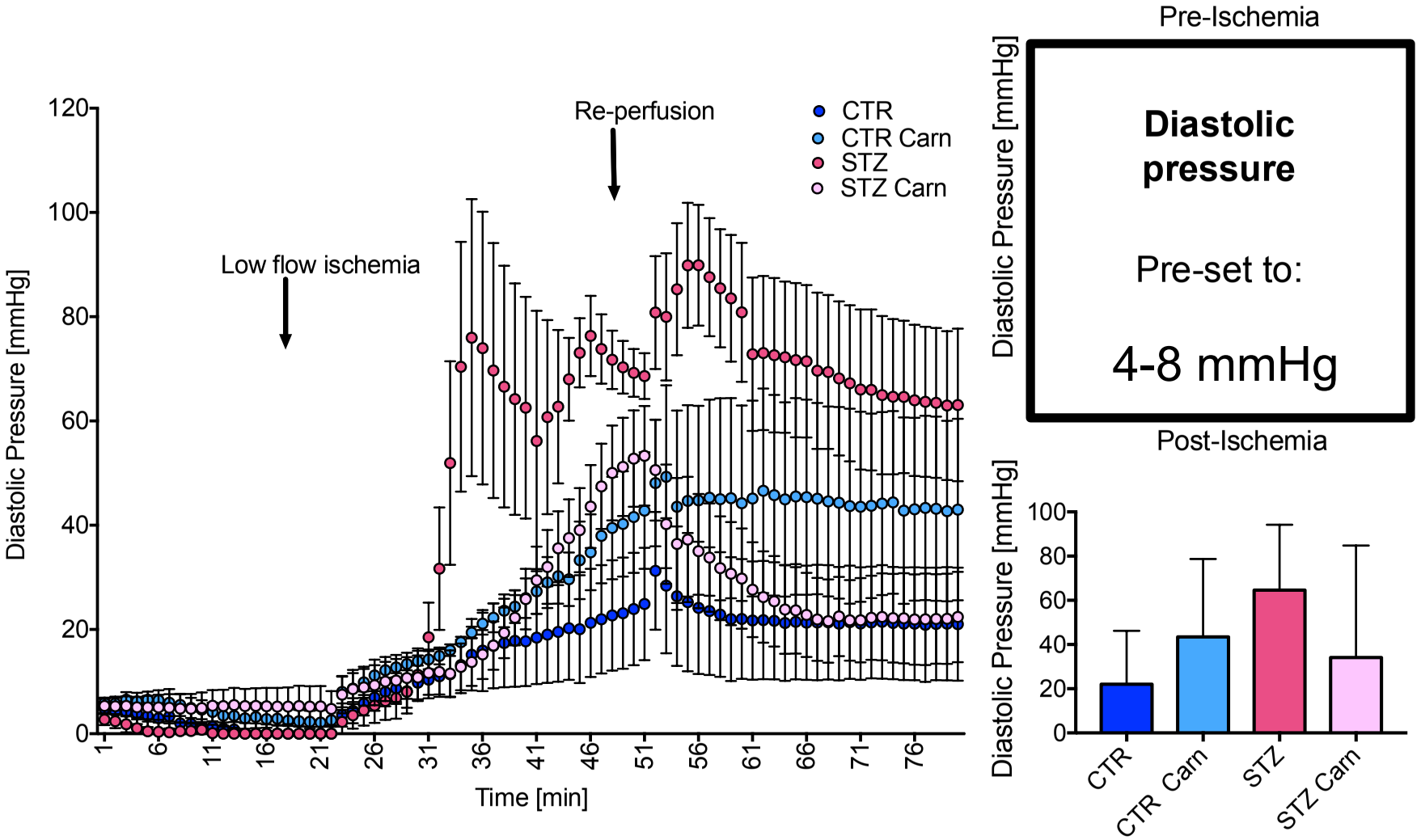

Figure 5.20: Diastolic pressure (DiaP) shown from Langendorff perfusions, where pre-ischemia (t = 1:20 min), ischemia (t = 21:50 min), and post-ischemia (t=52:80min). The low-flow rate of 0.4 ml/min/gww was used. Saline treated control (CTR, dark blue), L-carnitine treated control (CTR Carn, light blue), saline treated diabetics (STZ, magenta), L-carnitine treated diabetics (STZ Carn, light pink). Data presented as mean ± SD. Two-way ANOVA.

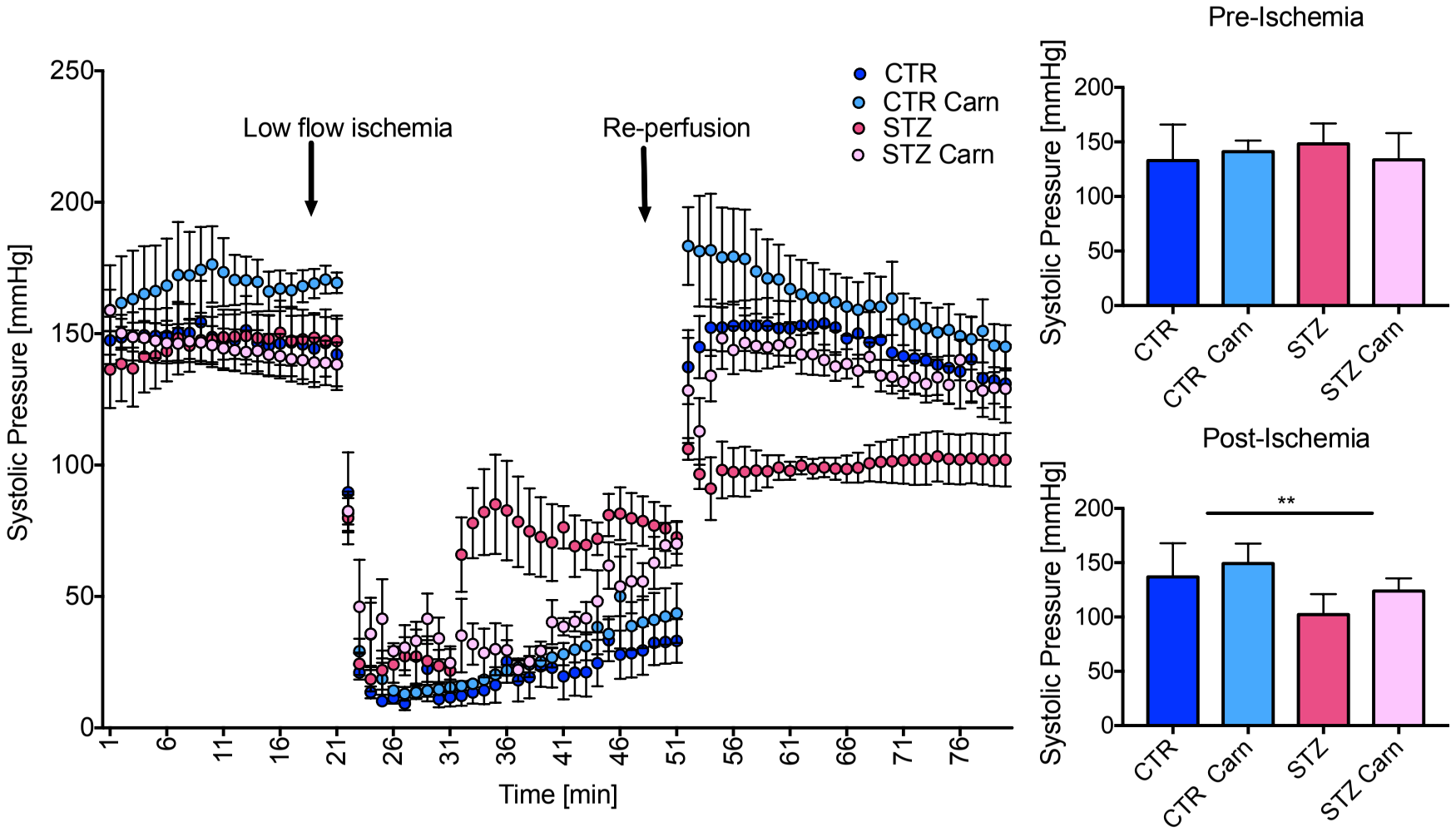

Figure 5.21: Systolic pressure (SysP) shown from Langendorff perfusions, where pre-ischemia (t = 1:20 min), ischemia (t = 21:50 min), and post-ischemia (t = 52:80 min). The low-flow rate of 0.4 ml/min/gww was used. Saline treated control (CTR, dark blue), L-carnitine treated control (CTR Carn, light blue), saline treated diabetics (STZ, magenta), L-carnitine treated diabetics (STZ Carn, light pink). Data presented as mean ± SD. Two-way ANOVA with Sidak's multiple comparisons, where $^{**}p < 0.01$.

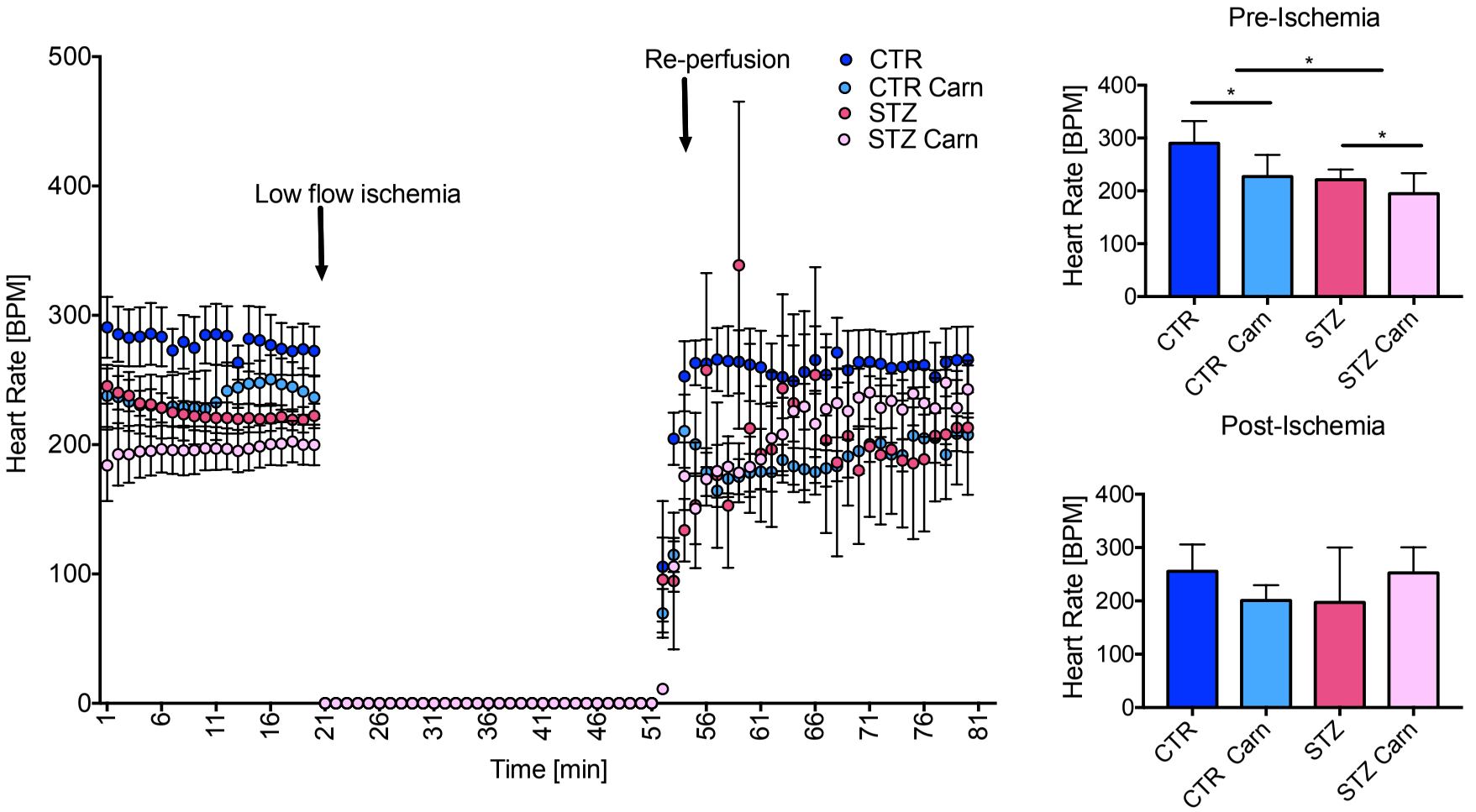

Figure 5.22: Heart rate (HR) shown from Langendorff perfusions, where pre-ischemia (t = 1:20 min), ischemia (t = 21:50 min), and post-ischemia (t = 52:80 min). The low-flow rate of 0.4 ml/min/gww was used. Saline treated control (CTR, dark blue), L-carnitine treated control (CTR Carn, light blue), saline treated diabetics (STZ, magenta), L-carnitine treated diabetics (STZ Carn, light pink). Data presented as mean ± SD. Two-way ANOVA with Sidak's multiple comparisons, where $^{*}p < 0.05$.

The percentage recovery between pre- and post-ischemia is demonstrated within the groups (Figure 5.23). The diabetic hearts failed to show significant differences with a two-way ANOVA compared to the control groups, although percentage recovery of RPP was 66 % reduced in the saline treated diabetic group compared to the control group treated with saline ($p = 0.002$, unpaired t-test). There was a significant interaction term ($p = 0.007$) that showed L-carnitine elevated RPP recovery by 43 % in the diabetic group ($p = 0.003$, Fig. 5.23A).

L-carnitine significantly elevated HR recovery by 24 % in both the control and diabetic groups ($p = 0.05$, Fig. 5.23B).

L-carnitine did not affect systolic pressure recovery, but it was decreased by 18 % in the diabetic groups compared to the control groups ($p = 0.02$, Fig. 5.23C).

The difference between pre- and post-ischemia diastolic pressure (DiaP) showed a significant interaction term ($p = 0.013$), which showed that L-carnitine reduced the difference in diastolic pressure by 78 % in the diabetic group compared to the saline treated diabetic group ($p = 0.032$, Fig. 5.23D).

Developed pressure recovery also showed a significant interaction term ($p = 0.016$), that showed L-carnitine increased the developed presure recovery by 130 % in the diabetic group compared to the saline treated diabetic group ($p = 0.022$, Fig. 5.23E).

5.5.6 Cardiac *Ex Vivo* Fatty Acid Metabolism

Fatty acid oxidation (FAO) rates were significantly reduced by 70 % in the diabetic groups compared to the control groups at pre-ischemia. No differences were observed post-ischemia across any of the groups (Fig. 5.24AB). There was a significant interaction term for FAO recovery ($p = 0.01$), that showed FAO recovery reduced by 48 % in the L-carnitine treated control group ($p = 0.04$, Fig. 5.24C). FAO rates were maintained in the saline treated control group and in the L-carnitine treated diabetic group, while FAO rates were reduced post-ischemia compared to pre-ischemia in the L-carnitine treated control group and saline treated diabetic group (Fig. 5.24D).

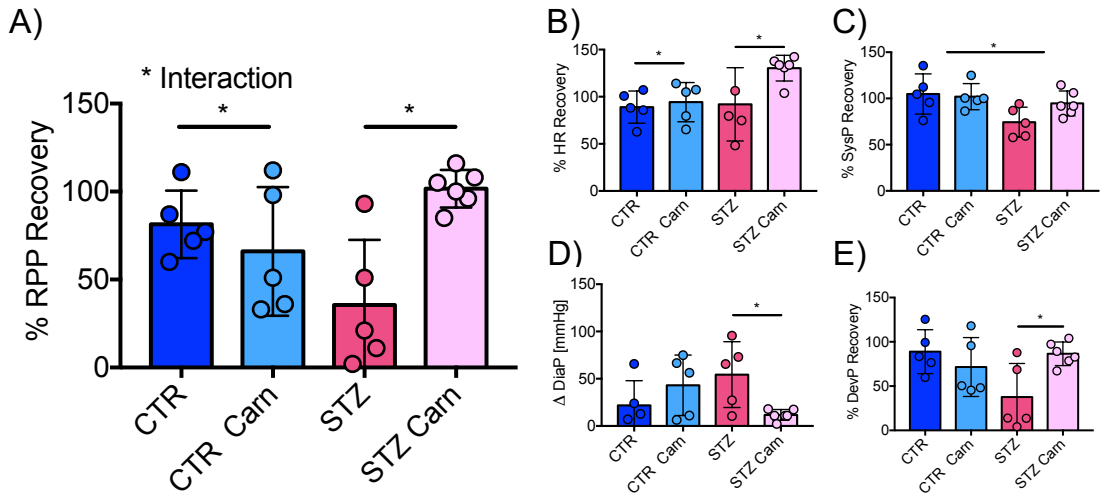

Figure 5.23: Percentage recovery between late post-ischemia (t = 70:80 min) and late pre-ischemia (t = 10:20 min). Langendorff perfusion of control and diabetic hearts, treated with saline or L-carnitine. The low-flow ischemia rate of 0.4 ml/min/gww. **A)** Rate pressure product (RPP) recovery. **B)** Heart rate recovery (HR). **C)** Systolic pressure (SysP) recovery. **D)** Difference between post-ischemia and pre-ischemia of diastolic pressure (△DiaP). **E)** Developed pressure (DevP) recovery. Data presented as mean ± SD. Two-way ANOVA adjusted for Sidak's multiple comparisons, where $^*p < 0.05$.

FAO normalized to cardiac work was not different between groups pre-ischemia. L-carnitine reduced FAO, normalized to cardiac work, post-ischemia by 36 % in both the control group and in the diabetic group, but it failed to reach statistical significance (p = 0.06, Fig. 5.25AB). L-carnitine reduced the percentage recovery of FAO normalized to cardiac work significantly in both the control group and in the diabetic groups (p = 0.039, Fig. 5.25C).

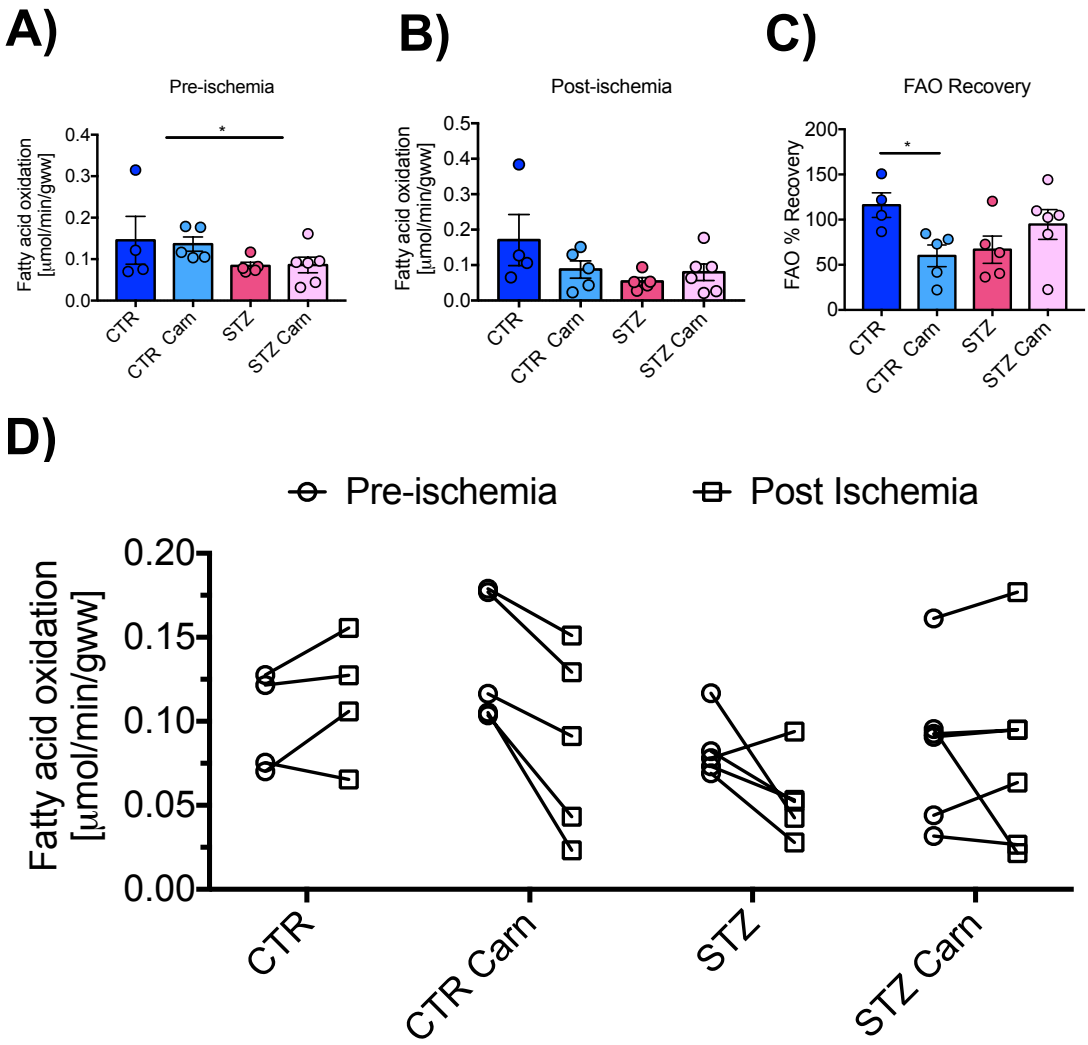

Figure 5.24: Fatty acid oxidation rates (FAO) [μmol/min/gww]. **A)** Fatty acid oxidation rates pre-ischemia. Two-way ANOVA, where $^*p < 0.05$. **B)** FAO rates post-ischemia. **C)** Fatty acid oxidation recovery [%] between post-ischemia and pre-ischemia. All data presented as mean $\pm$ SD. Unpaired two-tailed Student's t-test, where $^*p < 0.05$.

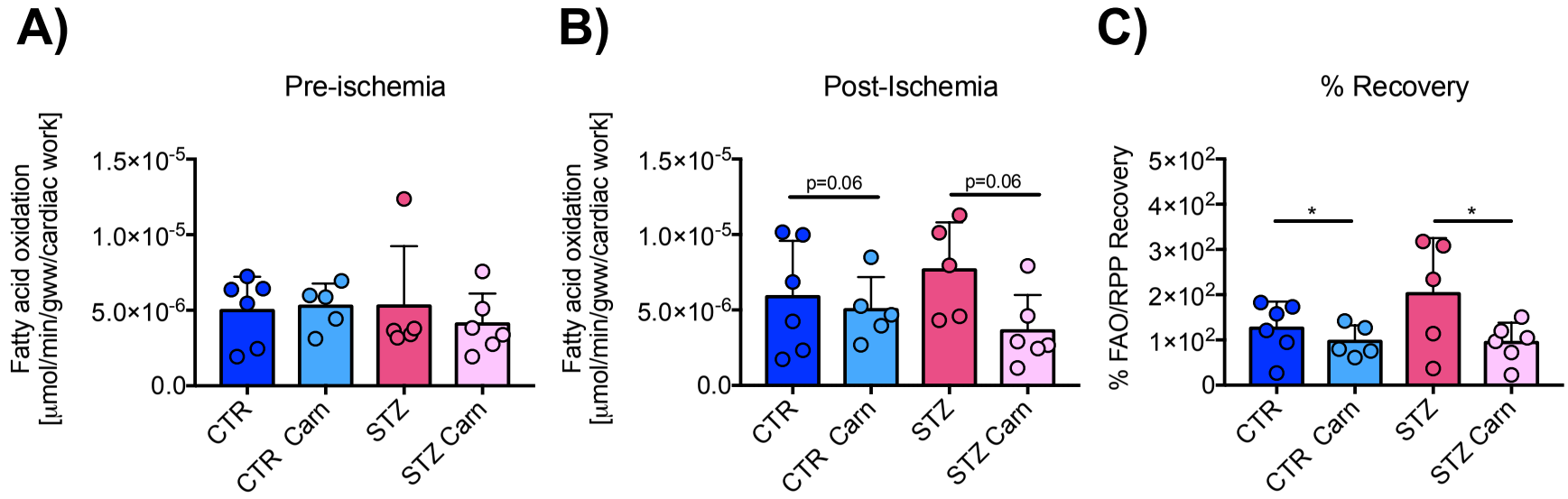

Figure 5.25: Fatty acid oxidation rates [μmol/min/gww] over cardiac work in rate pressure product [mmHg x BPM]. **A)** Fatty acid oxidation over cardiac work pre-ischemia. **B)** Fatty acid oxidation over cardiac work post-ischemia. **C)** Percentage recovery between post-ischemia and pre-ischemia. All data presented as mean ± SD. Two-way ANOVA, where $^{*}p < 0.05$.

5.6 Discussion

5.6.1 Summary of Key Findings

Summary of Key Findings in Controls

L-carnitine reduced body weight in the control animals, but it also reduced stroke volume and cardiac output, which was mainly driven by the reduction in body weight. However, L-carnitine increased end systolic lumen in the *in vivo* healthy controls, which was accompanied by a decrease in PDH-flux and glutamate in the *in vivo* heart. Acetylcarnitine levels stayed unchanged, although normalized to PDH-flux, they elevated. Free L-carnitine and short-chain acyl-carnitines increased in the heart. In the *ex vivo* healthy heart, the percentage recovery in RPP was reduced, indicating a possible detrimental effect of L-carnitine treatment in the healthy heart post-ischemia.

Summary of Key Findings in Diabetics

Blood glucose levels were significantly elevated in both diabetic groups. However, L-carnitine inhibited any further progression of blood glucose levels over the course of the treatment, despite no changes of insulin levels in the plasma. L-carnitine treatment reduced β-hydroxybutyrate significantly by 51 % , and TAG levels by 33 %. Although both diabetic groups had reduced ejection fraction, stroke volume, and cardiac output, L-carnitine improved the diastolic function both as measured with echocardiography through E/A ratio, and as measured *in vivo* with EDL, which was elevated by 16 %. The functional changes were manifested in *in vivo* metabolism, where L-carnitine elevated PDH-flux by 51 % in the diabetic group, and acetylcarnitine increased by 219 %. Free L-carnitine and short-chain acyl-carnitine were elevated in the heart. Finally, the percentage recovery of RPP post-ischemia was significantly improved by 186 % with L-carnitine treatment.

5.6.2 Daily L-Carnitine Treatment in the *In Vivo* Type 1 Diabetic Heart

The beneficial effects of L-carnitine on both cardiovascular diseases and diabetes are extensive [26, 194, 213, 106, 199, 198, 240]. This chapter showed that following two weeks of treatment more of the saline treated diabetic animals needed to be excluded from the study than L-carnitine treated diabetic animals, due to reaching the humane end point of the study. Other studies have shown high mortality rates in untreated insulin streptozotocin-induced rats [273]. This high mortality could be due to malnutrition, infection, toxicity of STZ or inadvertent injection into the urinary bladder or cecum. Even though the higher exclusion rate was not explored further in this thesis, it would suggest an early indication of the benefits L-carnitine has to offer.

Weight was reduced in the diabetic groups compared to the control groups. Not only was the weight lower, but tibia length was also smaller in the diabetic groups, proposing reduced bone growth or even bone loss. Diabetic patients, as well as streptozotocin-induced rats, are known to exhibit bone loss and alteration in tibia length [173, 63].

L-carnitine treatment slowed the progression of hyperglycaemia in the diabetic animals. L-carnitine offers potentially a method to improve control of blood glucose levels, despite no changes observed in fasted insulin levels. This would need to be explored further in insulin treated diabetic animals supplemented with L-carnitine. Wall *et al.* show insulin changes in patients treated with daily oral L-carnitine after 24 weeks of treatment [272]. Similarily a study found that L-carnitine elevates insulin levels in a streptozotocin-induced rat model [229]. However L-carnitine treatment being initiated already 72 hours post STZ injection, which could have influenced the outcomes differently compared to this study. This thesis showed much higher blood glucose levels than that demonstrated by Shahouzi *et al.*, and could be one of the reasons insulin could not be stimulated, simply because STZ destroyed most of the β-cells, while Shahouzehi *et al.* showed lower glucose levels

indicating that fewer β-cells were destroyed [229]. Many studies have, however, explored how L-carnitine improves insulin sensitivity [168, 249]. Two weeks of treatments with L-carnitine has been shown to elevate insulin levels in response to an oral glucose tolerance test (OGTT) [73], and other studies have found similar results [167]. This could suggest that even though insulin levels were not altered in the plasma in this study, insulin response to OGTT might have made the differences between the two diabetic groups more apparent.

When the body has insufficient insulin, it cannot take up glucose and will start to use fatty acids. Ketone bodies are produced from fatty acids in the liver [5] and are the only alternative fuel source for the brain. This study found a decrease in fasted ketone levels in the diabetic groups compared to the controls and showed no effect of L-carnitine treatment. One explanation for the lower fasted ketone levels in diabetes could be that the diabetic animals were using more of the ketone bodies, while the control animals still could use glucose as an energy source. Another study showed that fasted ketone levels elevate by only 10 % after a 12 hour fast, where an increase above 50 % first occurs after a 48-60 hour fast. This could have elucidated the differences between the fasted ketone levels but was not feasible to do in this study [151, 162]. However, fed ketone levels demonstrated the expected ketone response to diabetes. The ketone body β-hydroxybutyrate was elevated in the diabetic groups since the diabetic group cannot take up glucose, more fatty acids are broken down, and ketone bodies are produced [145]. A study with a two hour constant infusion of L-carnitine showed reduction in β-hydroxybutyrate, and improved insulin levels [237]. This chapter also demonstrated a reduction in β-hydroxybutyrate with chronic L-carnitine treatment in the diabetic group together with a reduction in fasted NEFA levels, which might suggest a reduction in FAO. Cholesterol was increased in the saline treated diabetic groups, as has previously been shown in the streptozotocin-induced rat model, due to a higher net production in the intestine [284]. Lipids, if accumulated in the cytoplasm, can be cytotoxic, the mitochondria cannot take up the excess of free fatty acids, and an energy deficit

occurs that leads to myocardial dysfunction. Other studies have shown an elevation of lipid levels in the plasma that were reversed with L-carnitine treatment [258].

In vivo metabolism in the L-carnitine treated diabetic group were for the first time investigated, and L-carnitine showed altered substrate utilisation in the heart. L-carnitine increased PDH-flux in the diabetic group, suggesting a slight shift away from FAO, as is also demonstrated by the inhibition of hyperglycaemia progression. Also, PDK4 showed a slight reduction, although not significant, this could validate the elevated PDH-flux observed *in vivo*. Elevation of PDH-flux could be controlled by the increased buffering mechanism of L-carnitine of excess acetyl-CoA, resulting in elevation of acetylcarnitine, as observed in this study for the first time in the *in vivo* myocardium. Even though acetylcarnitine did not replenish entirely to the control values, it indeed improved PDH-flux slightly and significantly.

L-carnitine showed few effects on TCA cycle intermediates or other metabolites. L-carnitine elevated alanine levels further in the diabetic group. The saline treated diabetic group had significantly increased malate levels, and significantly reduced aspartate levels, while this was not observed in the L-carnitine treated diabetics, suggesting that accumulation of malate is inhibited with L-carnitine. An elevation in TCA intermediates has been shown previously in the T1D heart [21]. This accumulation indicates a large availability of acetyl-CoA, which can be prevented with L-carnitine treatment, through the elevation of acetylcarnitine thereby buffering more acetyl-CoA as seen in this chapter. *In vivo* metabolism revealed reduced acetylcarnitine in the saline treated diabetic group. Although heart tissue analysis could not reveal a reduction in free L-carnitine, with L-carnitine treatment, there was a significant elevation of free L-carnitine in the heart, which validates the *in vivo* changes observed in acetylcarnitine. L-carnitine treatment elevated both short, medium and long-chain acyl-carnitine in the heart, showing the ability for lowering acyl-CoA in the heart.

These metabolic changes were manifested in the cardiac systolic function as observed *in vivo* using CINE MRI. Ejection fraction was decreased in diabetic groups compared to control groups on both CINE MRI and echocardiography. Diabetics maintained

cardiac index, although cardiac output was decreased. However, both stroke index and HR/BW elevated with diabetes, suggesting that these hearts were working more to sustain the cardiac output. Diabetics had decreased end diastolic lumen, which could potentially indicate early diastolic dysfunction, although not observed with echocardiography in this study.

Weytjens *et al.* have previously detected cardiovascular disease in streptozotocin-induced diabetic rats, although they failed to show differences in both E/A and E/E' ratios [275]. This chapter only detected a reduction in E/A ratios, when treating with L-carnitine, suggesting myocardial remodelling in response to L-carnitine. There were some limitations with the echocardiography technique used due to the sensitivity of the pediatric probe available. Streptozotocin-induced rats have previously been shown to have a calcium transient delay that can lead to cardiac diastolic dysfunction [141]. An increase of calcium and a decrease in the re-uptake of calcium both led to an overload of calcium, which affects the calcium homeostasis of the cardiomyocytes and leads to a slow relaxation of the ventricles [9]. This chapter found that calcium was elevated in the plasma in the saline treated diabetic compared to the saline treated control group, although the calcium transient was not investigated in the cardiomyocytes, it could be an additional confirmation of the diastolic dysfunction observed in the saline treated diabetic group.

L-carnitine did not only alter *in vivo* metabolism, but it also elevated end diastolic lumen, suggesting potentially an improvement in the diastolic function, which was supported by a decrease in E/A ratio using echocardiography. However, L-carnitine elevated end systolic lumen and reduced ejection fraction, suggesting that L-carnitine even though it improved diastolic function, the diabetic groups still had reduced systolic function. It is worth noting that although function was improved compared to the saline treated diabetic group, the L-carnitine treated diabetic group still had elevated plasma glucose levels, reduced PDH-flux and elevated β-hydroxybutyrate compared to the control group.

L-carnitine has shown other effects than in the circulatory and cardiovascular system, and it has been shown to improve kidney disease. Kidney disease is a

common complication of diabetes and streptozotocin is known to lead to diabetic nephropathy, which is the leading cause of end-stage renal failure [164]. Early diabetes usually presents with renal hypertrophy, which is suspected to be caused by hyperglycaemic induced alterations in metabolism and hemodynamics [230, 88]. It has been shown that it can be prevented if glucose is controlled tightly [230]. Elevated kidney weight has previously been observed in streptozotocin-induced diabetic rats, and insulin has been shown to avoid this hypertrophy [183]. The streptozotocin-induced diabetes model shows degeneration of the renal tubules, and increased glomerular space as well as basement membrane thickening [164]. In this study all the diabetic animals are uncontrolled, meaning not treated with insulin. This study found renal hypertrophy of the kidneys in the diabetic groups. And L-carnitine treatment showed a reduction in the hypertrophy index, which could also be related to the inhibition of blood glucose progression that was observed, despite no insulin treatment being initiated. Ross *et al.* demonstrated that the elevation in kidney weight was due to an increase of FAO that supplies the kidney with a source of additional energy for growth as compensatory hypertrophy in diabetes [216]. Since L-carnitine affects the balance of energy utilisation between carbohydrates and fatty acids, it might be the case that in the kidneys it is facilitating carbohydrate metabolism. Additionally, the kidneys are working harder due to the excess glucose that they need to clear. Even though the kidneys were not the focus in this study, it is indeed interesting that L-carnitine is beneficial to organs other than just the heart. Further studies are needed to elucidate the mechanism of action of L-carnitine in the kidneys.

5.6.3 Effects of L-Carnitine on Functional and Metabolic Recovery Post-Ischemia

This study explored the effect of L-carnitine on cardiac functional recovery. Instead of treating at the onset of diabetes as in the studies undertaken by Rodrigues *et al.*, treatment was employed two weeks after STZ injection, and a Langendorff method was used instead of the working heart mode. Daily L-carnitine injections

in the diabetic rats improved cardiac functional recovery post-ischemia significantly. RPP and developed pressure in the L-carnitine treated diabetic group recovered to the levels of the control groups post-ischemia. The L-carnitine treated diabetic group had reduced diastolic pressure recovery post-ischemia compared to the saline treated diabetic group, validating the *in vivo* findings.

Studies have investigated FAO in the perfused diabetic rat heart with both physiological levels of palmitate and increased levels of palmitate and have all resulted in a reduction in ATP levels as well as an elevation in long-chain acyl-CoA, but with L-carnitine treatment loss of ATP was attenuated and long-chain acyl-CoA was decreased [199, 198]. This study showed an elevation of long-chain acylcarnitines in the heart, although not significant, suggesting potential attenuation of long-chain acyl-CoA. The rate of FAO is dependent on fatty acids available. This study enforced palmitate concentrations in the diabetic hearts to match the physiological levels for controls (0.4 mM). However, palmitate concentrations should possibly have been increased in the perfusion buffer for the diabetic perfusions. This could be an explanation for why this study failed to show elevated fatty acid oxidation rates in the diabetic groups, simply due to low availability of FA. In addition, adding insulin to the buffer has previously been shown to reduce FAO rates (unpublished data from [75]), which could mean that the FAO rates for the control groups showed higher FAO levels than if insulin had been added, while the diabetic group would have been blunted from reducing FAO rates further with insulin. Therefore insulin would have decreased the FAO rates in the control group while elevating glycolytic flux and glucose oxidation rates [159], and thus FAO rates would have been elevated in the diabetic groups.

Myocardial glucose oxidation and glycolysis are reduced with the presence of elevated fatty acids [29], although glucose oxidation and glycolysis were not measured in this study, L-carnitine has previously been shown to overcome the inhibition of fatty acids on glucose oxidation, both pre- and post-ischemia [28]. This study suggests glucose oxidation stimulation pre-ischemia in the *in vivo* heart by elevating PDH-flux, enabling these hearts to improve functional recovery post-ischemia.

Nonetheless, L-carnitine decreased percentage FAO recovery, normalized to cardiac work undertaken, between pre- and post-ischemia. This contributes to the validation of the heart moving away from FAO post-ischemia if treated with L-carnitine. L-carnitine has previously been shown to up-regulate peroxisome proliferator-activated receptor (PPARα), MCAD and CPT-1 [130]. L-carnitine even reduced the expression of CD36 in this chapter, the fatty acid transporter, but it increased medium-chain acyl-carnitines although it did not reach statistical significance. Despite moving away from FAO, most of the heart's energy still relies on FAO rates, and this study suggests that medium-chain fatty acids are possibly elevated, and short-chain fatty acids decreased. Elevated levels of medium-chain fatty acids have shown to improve systolic function in diabetic patients [3], which also could have contributed to the improved functional recovery post-ischemia, observed in this study.

5.6.4 Daily L-Carnitine Treatment in the *In Vivo* Healthy Heart

Although L-carnitine stimulated glucose oxidation, and improved diastolic function *in vivo* and *ex vivo* in diabetic hearts, L-carnitine had the opposite effect on healthy control hearts.

L-carnitine induced much lower weight gain in the control group compared to the saline treated controls. Rodrigues *et al.* showed that two weeks of L-carnitine treatment led to lower uptake of food compared to normal rats [213], suggesting alleviation of perceived hunger [285]. There were no changes in the glucose levels, but there was a reduction in insulin levels during the fed state, this difference could just have been due to lower intake of food as seen previously. More importantly, no differences were observed in insulin during the fasted state, and therefore no changes in insulin resistance.

β-hydroxybutyrate was reduced with L-carnitine treatment in the control group, although only fed levels of NEFA were elevated in the L-carnitine treated control group, which again might have been due to lower intake of food, with lower insulin

levels in the fed state, it meant that carbohydrates were not stimulated, and therefore NEFAs were elevated.

However, despite very few changes in the blood profile, cardiac function was altered. L-carnitine reduced stroke volume, albeit not stroke index, although it approached significance ($p = 0.07$). L-carnitine reduced cardiac output, albeit not cardiac index, again it approached significance ($p= 0.09$). End diastolic lumen was unchanged, but L-carnitine elevated end systolic lumen and reduced ejection fraction. These changes were not detrimental to the cardiac function. However, it might be early signs that these hearts were working harder than their respective saline treated controls. A treatment lasting for longer than two weeks could have elucidated some of these differences.

These functional changes in the control heart were accompanied by remodelling in metabolism, L-carnitine treated controls had significantly reduced PDH-flux together with a reduction in glutamate, and elevation of acetylcarnitine. It is interesting that an elevation in acetylcarnitine did not lead to an elevation in PDH-flux as was seen in the diabetic group. This means that energy substrate utilisation prior to treatment might be critical for how L-carnitine is going to affect metabolism. L-carnitine reduced CD36 expression also in the control group. However, there was no change in MCAD, while there was an elevation of medium-chain acyl-carnitines, suggesting that these hearts were maybe not oxidizing more medium-chain fatty acids compared to the saline treated control group.

Function investigated *ex vivo* showed reduced heart rate in the L-carnitine treated control pre-ischemia compared to the saline treated controls. Ischemia decreased the percentage recovery in RPP. Although FAO rates were unaltered, the percentage recovery of fatty acids, normalized to cardiac work undertaken, was reduced in the L-carnitine treated controls compared to the saline treated control. This might suggest, that altering metabolism further in a well-balanced heart might be detrimental to both the cardiac function and metabolism if it should encounter ischemia. Research has shown that L-carnitine can improve functional recovery even in healthy hearts. However, palmitate concentrations had to be elevated to 1.2 mM

[28], in this study palmitate concentrations were 0.4 mM. However, where ischemia is not induced artificially, and healthy controls have normal levels of fatty acids, metabolism alterations prior to clinical ischemia will slowly adapt to the alternative substrate utilisation, and therefore L-carnitine will most likely be beneficial in these situations, but only when there are elevations of fatty acids. This study suggests that L-carnitine treatment might be detrimental for hearts that do not already have an altered substrate utilisation and therefore enforcing metabolic changes with L-carnitine might be harmful, and could worsen outcomes in case of an ischemic event.

5.6.5 Conclusion and Future Perspective

This study suggests beneficial effects of L-carnitine supplementation in streptozotocin-induced type 1 diabetes (T1D). L-carnitine may offer an alternative route for the disposal of excess glucose through increased carbohydrate oxidation, as well as via conversion to lactate and alanine. It is possible that increased buffering of acetyl-CoA units into acetylcarnitine offers relief of PDH-flux inhibition caused by excessive FAO in the diabetic heart.

However, even though L-carnitine is beneficial in diabetes, the same benefits are not observed in the control animals. These hearts do not have a need for alternative metabolic routes, to power cardiac function. In controls, L-carnitine reduced the left ventricular systolic function *in vivo* and by subjecting the hearts to ischemia *ex vivo*, L-carnitine had a detrimental effect. In contrast, L-carnitine displayed improved *in vivo* function and recovery post-ischemia, in the diabetic group.

This shows the complex mechanisms of L-carnitine that we still do not understand completely, but it confirms the beneficial effects of L-carnitine supplementation in diabetic animals. L-carnitine may offer an alternative route for the disposal of excess glucose through increased carbohydrate oxidation that possibly is beneficial in diabetes, but harmful in controls.

The fifth who chanced to touch the ear
Said, "Even the blindest man
Can tell what this resembles most;
Deny the fact who can,
This marvel of an elephant
Is very like a fan."

6

Effects of Reducing L-Carnitine in the Diabetic Heart using Mildronate

Contents

6.1 Chapter Overview 178
6.2 Background 179
6.3 Chapter Aims 181
6.4 Methods 181
6.5 Results 184
6.5.1 Weight and Blood Profile 184
6.5.2 L-Carnitine and Mildronate Levels 189
6.5.3 Cardiac *In Vivo* Function 191
6.5.4 Cardiac *In Vivo* Metabolism 193
6.5.5 Cardiac *Ex Vivo* Function 196
6.5.6 Cardiac *Ex Vivo* Fatty Acid Metabolism 203
6.5.7 Tissue Analysis 205
6.6 Discussion 206
6.6.1 Summary of Key Findings 206
6.6.2 Daily Mildronate Treatment in the *In Vivo* Type 1 Diabetic Heart 206
6.6.3 Conclusion and Future Perspective 210

6.1 Chapter Overview

One of the leading causes of mortality in type 1 diabetic patients is cardiovascular disease. Improving our understanding of the metabolic changes that occur in the diabetic heart may be vital to understanding the pathophysiology of the cardiac effects of diabetes. Studies have shown improved functional recovery post-ischemia in diabetes as well as a reduction in blood glucose levels with both L-carnitine and with Mildronate treatment, even though these two compounds have supposedly opposite mechanistic effects. L-carnitine facilitates long-chain fatty acid transport into the mitochondria while also buffering excess acetyl-CoA. One key metabolic effect observed in the diabetic heart is an increase in fatty acid oxidation. The anti-ischemic drug, Mildronate, has been shown to reduce fatty acid oxidation through inhibition of the L-carnitine transporter, OCTN2, inhibiting absorption and reabsorption of L-carnitine in tissues, while also inhibiting the biosynthesis of L-carnitine [49, 136].

In this study, the metabolic and functional effects of Mildronate treatment were investigated in the healthy and diabetic rodent heart. Hyperpolarized MRI was used to investigate *in vivo* cardiac metabolism, while CINE MRI was used for investigating *in vivo* cardiac function before all hearts were excised and perfused in the Langendorff mode to explore functional and metabolic recovery post-ischemia *ex vivo*.

This chapter showed a reduction in L-carnitine levels in the plasma with Mildronate treatment. However, this did not result in any *in vivo* functional changes in either the diabetic or the control group. Flux through pyruvate dehydrogenase was reduced in the two diabetic groups. Despite this reduction, PDH-flux was significantly elevated with Mildronate treatment in both the control and the diabetic groups together with a reduction of acetylcarnitine in the *in vivo* heart. The rate pressure product (RPP) was reduced in the two diabetic groups, and Mildronate leads to a small functional improvement post-ischemia.

Despite not seeing any *in vivo* functional differences, Mildronate treatment led to metabolic changes that elevated PDH-flux and reduced acetylcarnitine levels which resulted in improved functional recovery post-ischemia, however further studies are needed to understand the mechanism through which Mildronate increases

PDH-flux. Such studies will allow for a better understanding of the interactions between metabolism and function in the diabetic heart and may provide new insights into novel therapeutics.

6.2 Background

Coronary heart disease (CHD) is a major problem worldwide and one of the leading causes of mortality in diabetic patients [226, 185]. The T1D population continues to develop CHD and heart failure, which has been documented since the 1970s [52]. T1D patients reach a higher risk for CHD at an earlier age compared to the healthy population, and with obesity being more prevalent today even in T1D, developing insulin resistance has become more common, which increases CHD risk even further in the T1D population [185].

In CHD there is an overall impairment in the balance of the myocardial energy supply. An accumulation of long-chain fatty acids can impair insulin release and glucose oxidation [286]. CHD results in an impairment of ATP production from aerobic metabolism in the mitochondria. Even though the heart is mostly dependent on its energy supply to arise from fatty acid oxidation, glucose oxidation is preferred during ischemia, because it is more oxygen efficient, and can, therefore, improve the functional recovery of the myocardium [261].

In 1911 it was shown that chest pain could be alleviated by administering sugar to patients, and so it is not a new treatment that inhibition of fatty acid oxidation, resulting in elevation of carbohydrate metabolism, as described by Randle *et al.*, can alleviate CHD [248, 207].

Even though many studies have shown a beneficial effect of L-carnitine in diabetes and CHD [148, 26, 106, 67, 175] there have also been studies which show that reducing L-carnitine concentrations can be beneficial to the regulation of metabolism in both diabetes and CHD [132, 269, 121]. Most current therapies for CHD either try to elevate the oxygen supply to the heart or depress the heart's oxygen demand, however, therapies that can target reduction of fatty acid oxidation might be helpful in improving the prognosis of CHD [248]. There have been

several studies investigating the metabolic shift from fatty acid oxidation to glucose oxidation with drugs, such as Perhexiline, Trimetazidine and Mildronate [96].

Mildronate is a commonly used drug for CHD and is often used in diabetic patients in Eastern Europe and Asia, but has yet to receive FDA and EMA approval. The World-Anti Doping Agency (WADA) classed it as a *"metabolic modulator used by athletes to enhance performance"* in 2016 [87], and it has become infamous ever since Maria Sharapova failed a drug test for the Australian Open and was suspended by the International Tennis Federation. WADA suggest there was research that showed Mildronate improved oxygen supply to skeletal muscles, which could lead to enhanced endurance during exercise and an elevated physical capability, although evidence for this in the literature is hard to find [217, 83, 84]. More precisely the prohibition came from the athlete's "intention" to improve exercise capacity.

Even though there is no evidence yet that Mildronate improves exercise capacity, there is evidence for its cardioprotective effects. Mildronate decreases the availability of L-carnitine through inhibition of the biosynthesis of L-carnitine, inhibition of carnitine acylcarnitine translocase (CACT), and inhibition of carnitine transport type 2 protein (OCTN2) resulting in elevated clearance of L-carnitine through the urine [136]. Thereby it inhibits fatty acid metabolism and promotes carbohydrate metabolism as described in Section 1.7.

Kuka *et al.* have shown that Mildronate treatment leads to a smaller infarct size post ischemia-reperfusion in the *ex vivo* heart, and that there is reduced CPT1 dependent respiration of the mitochondria. Sesti *et al.* have confirmed these finding [227]. These changes have not been seen when treating with a combination of Mildronate and L-carnitine, suggesting that L-carnitine treatment cancels Mildronate's beneficial effects [121], but it also shows that Mildronate is not a perfect inhibitor of L-carnitine.

In contrast, Vilskersts *et al.* were able to find beneficial effects of co-treatment with Mildronate and L-carnitine in a hypertensive rat model (Dahl salt-sensitive). They have shown attenuation of endothelial dysfunction, suggesting common additive properties of these two compounds [267]. Mildronate has been shown

to reduce TMAO production from L-carnitine, which leads to a lower risk of atherosclerosis [120, 115].

Overall Mildronate increases carbohydrate metabolism in diabetes as has been shown in this thesis, and Sokolovska *et al.* has shown it to prevent diabetic neuropathy, while it lowers blood glucose levels as well as triglycerides in the circulation [245]. Despite these promising findings no high quality clinical trials treating diabetic patients with Mildronate, have been undertaken [217].

6.3 Chapter Aims

This study aimed to investigate the effects of Mildronate treatment on cardiac metabolism and function in the diabetic rodent heart. Two groups of diabetic rats and two groups of healthy matched controls were investigated. Daily Mildronate or daily saline treatment was initiated two weeks after the induction of diabetes. Following two weeks of treatment, all animals were scanned with hyperpolarized [1$-^{13}$C]pyruvate and [2$-^{13}$C]pyruvate to investigate TCA cycle intermediates and acetylcarnitine levels. Cardiac function was assessed *in vivo* with both echocardiography and CINE MRI. Functional and metabolic changes were induced in all animals by ischemia reperfusion using a Langendorff method in the isolated heart. Subsequently, blood profile and metabolomics in the plasma was assessed to validate the *in vivo* findings.

The recovery post-ischemia of hearts treated with Mildronate could help to elucidate our understanding of the mechanism of action of L-carnitine on energy metabolism in healthy and diabetic hearts.

6.4 Methods

Male Wistar rats ($\sim$250 g, n = 36) were randomly divided into four groups as listed below. All animals were either injected with STZ (55 mg/kg) or citrate buffer at the onset of the protocol as described in Section 2.2.

Two weeks after the injection of STZ/citrate buffer, all animals were initiated on daily morning intraperitoneal (i.p.) treatments with either saline or Mildronate, which was continued until tissue collection.

The dose of Mildronate treatment was 100 mg/kg/day [245]. Treatments were given while animals were conscious but restrained. Weight and well-being were monitored daily. The four groups were as follows:

(1) T1D group treated with daily i.p. injections of saline (STZ).

(2) T1D group treated with daily i.p. injections of Mildronate (STZ Mil).

(3) Control group treated with daily i.p. injections of saline (CTR).

(4) Control group treated with daily i.p. injections of Mildronate (CTR Mil).

Four weeks post STZ/citrate buffer injection all animals were anaesthetised with isoflurane and subjected to MR imaging, hyperpolarized [1−^{13}C] and [2−^{13}C]pyruvate MRI, CINE MRI, and echocardiography as described in Sections 2.4.1, 2.4.3, and 2.4.4.

Fasted blood glucose levels and weight were measured weekly. Fasted ketone levels were measured five weeks post STZ/citrate buffer injection as described in Section 2.2. Fasted blood samples were obtained at five weeks as described in Section 2.8.

Insulin and NEFA levels were measured in the fed and fasted blood five weeks post STZ/citrate buffer injection, as described in Section 2.9.2 and Section 2.9.1.

All fed blood samples were analysed for glucose, lactic acid, cholesterol, HDL, TAG and 3-OHB using an ABX Pentra 400 (Horiba ABX Diagnostics, California, USA) as described in Section 2.8.

Heart tissue was crushed and free L-carnitine was measured as described in Section 2.9.3 and protein expression of GLUT4, PDK4 and MCAD were measured as described in Section 2.9.4.

All hearts were perfused within four weeks of treatment (six weeks post STZ/citrate buffer injection). The hearts were acclimatised to the albumin buffer for ten

minutes prior to the onset of the protocol. Hearts were subjected to 20 minutes of normal flow, followed by 30 minutes of the low-flow rate of 0.4 ml/min before hearts were reperfused with normal flow for another 30 minutes as described in Section 2.5 (Fig. 6.1) to investigate metabolic and functional recovery post-ischemia. Finally, the total number of irregular heartbeat periods were counted at pre-ischemia and post-ischemia.

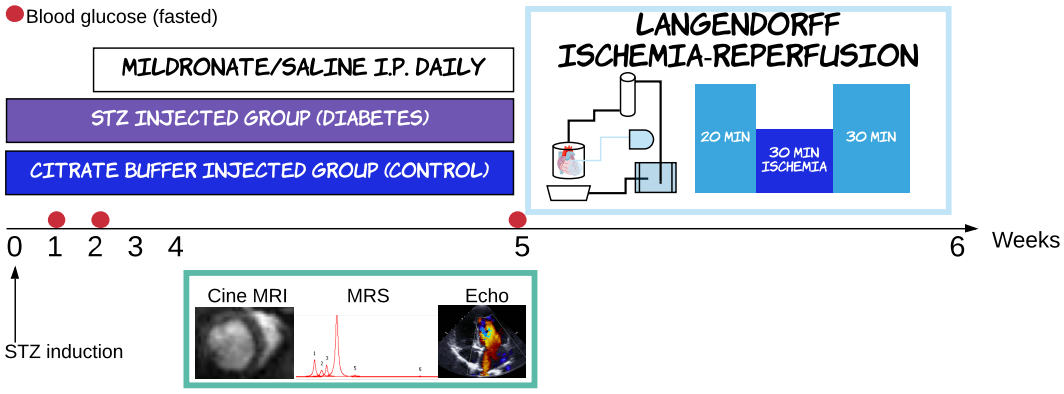

Figure 6.1: Experimental design. The figure shows a schematic design of the blood sampling, treatment initiation, imaging time-points, and the Langendorff perfusion protocol.

6.5 Results

6.5.1 Weight and Blood Profile

All animals gained weight over the duration of treatment. Controls gained significantly more weight (CTR: 360 ± 40 g, CTR Mil: 350 ± 30 g) than the diabetic animals (STZ: 260 ± 40 g, STZ Mil: 250 ± 30 g, p = 0.0002, Fig. 6.2). Kidney weight increased with diabetes (p = 0.0008). The kidney hypertrophy index increased by 73 % with diabetes (p < 0.0001), but there was no difference with Mildronate treatment. The tibia length was 6 % smaller in the diabetic groups (p = 0.01) compared to the control groups. Fat pads were significantly reduced by 74 % in the diabetic animals compared to the control animals (p < 0.001, Fig. 6.3).

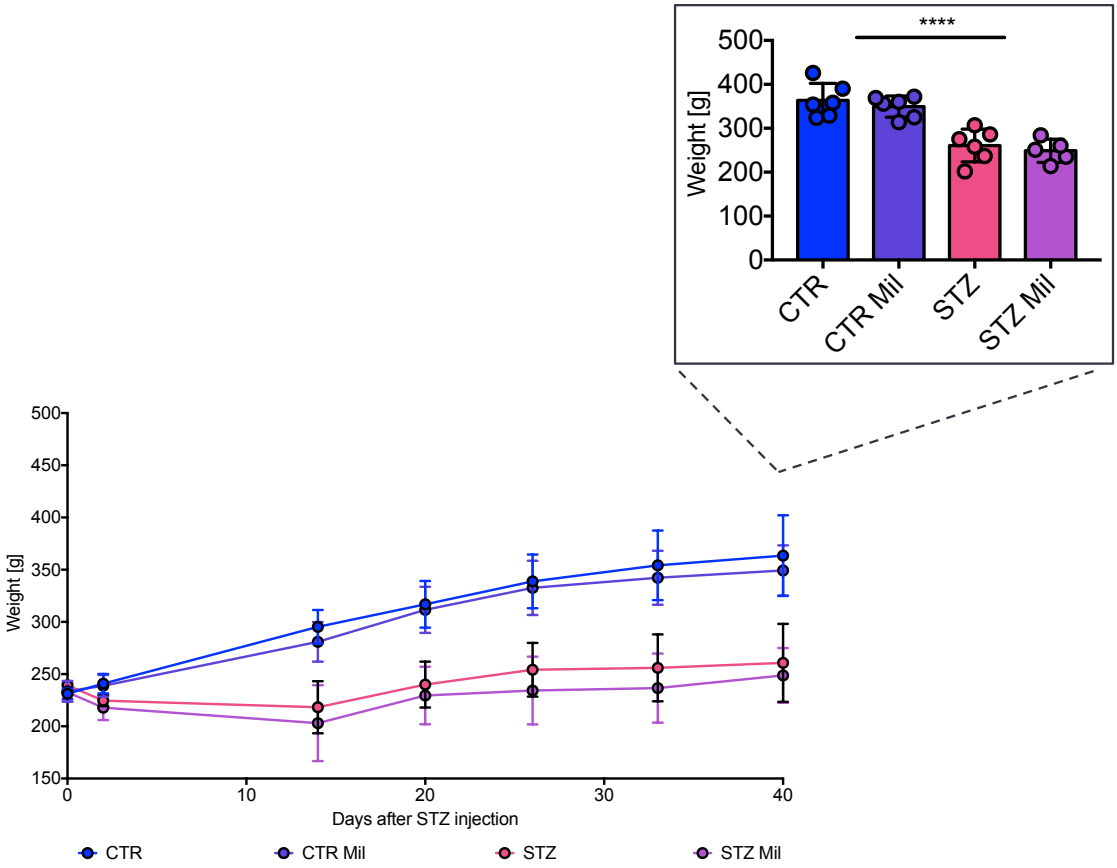

Figure 6.2: Body weight measured from control rats (CTR) and diabetic rats (STZ). Body weight from the day of STZ/citrate buffer injection to time of euthanasia. Bodyweight five weeks post STZ injection (top). All results presented as mean ± SD. Two-way ANOVA where $^{****}p < 0.0001$.

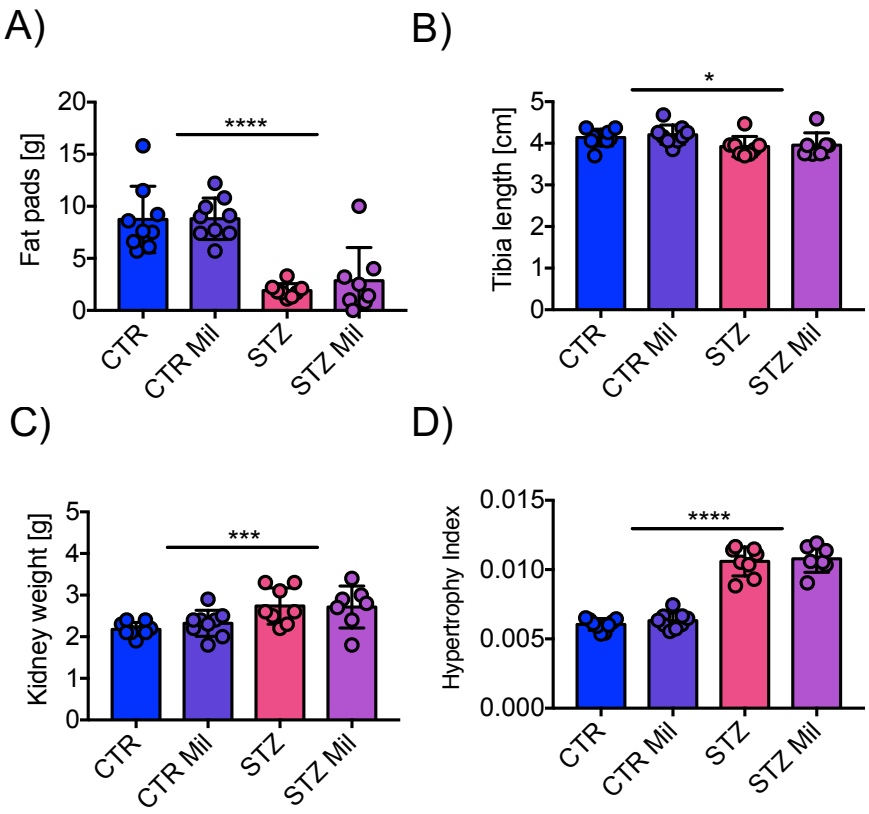

Figure 6.3: Tissue collection five weeks post STZ/citrate injection. **A)** Fat pads were taken at the time of tissue collection. **B)** Right tibia length measured at the time of tissue collection. **C)** A total sum of the left and right kidney weights. **D)** Kidney hypertrophy index (kidney weight/body weight) at the time of tissue collection. All results presented as mean ± SD. Two-way ANOVA comparing all groups adjusted for multiple comparisons, where $^{*}p < 0.05, ^{***}p < 0.001, ^{****}p < 0.0001$.

Food intake was 80 % higher in the diabetic animals compared to the control animals ($p < 0.0001$). Water intake was 586 % higher in diabetic animals than in control animals ($p < 0.0001$). Mildronate treatment lowered the food intake by 29 % ($p = 0.009$), and water intake by 59 % ($p < 0.0001$), in the diabetic group (Fig. 6.4).

Blood glucose levels were elevated in the diabetic groups at both two and five weeks post STZ injection (Fig. 6.5A) with both diabetic groups showing a significant and progressive increase in hyperglycaemia over the three weeks of treatment (Fig. 6.5B).

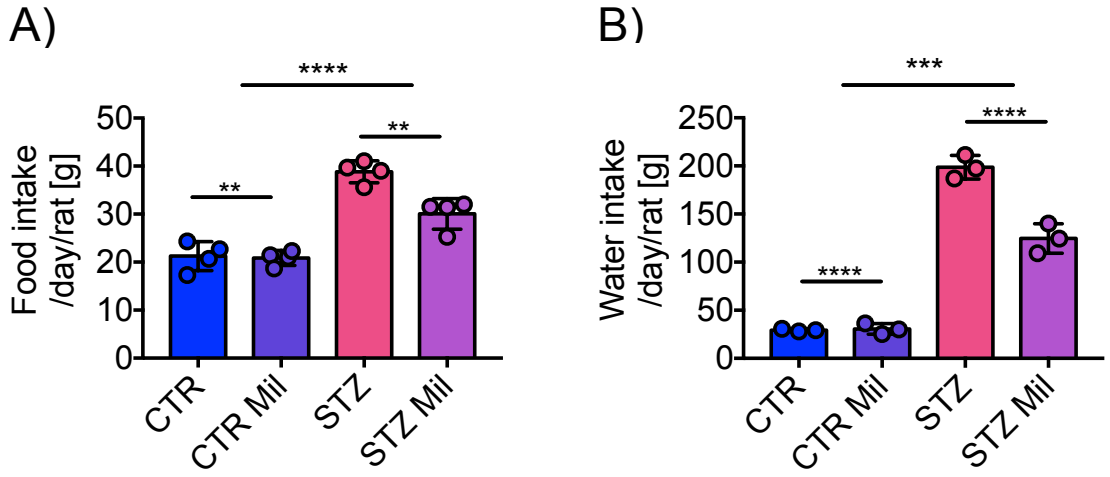

Figure 6.4: Food and water intake ad libitum. **A)** Average daily food intake per animal. **B)** Average daily water intake per animal. All results presented as mean ± SD. Two-way ANOVA comparing all groups adjusted for multiple comparisons, where $^{**}p < 0.01, ^{***}p < 0.001, ^{****}p < 0.0001$.

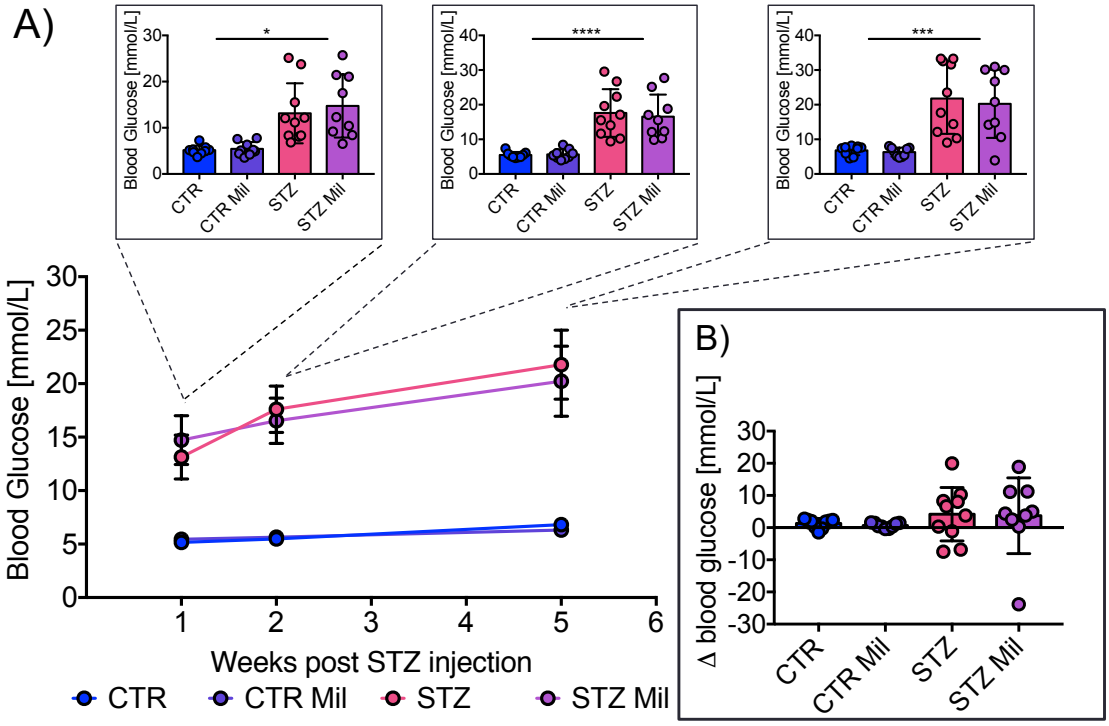

Figure 6.5: Blood glucose concentration measured in the fasted state from control animals (CTR) and diabetic animals (STZ). **A)** Fasted blood glucose levels measured at one, two and five weeks after STZ/citrate buffer injection. **B)** The difference in blood glucose concentrations during the treatment between week five and week two. All results presented as mean ± SD. Two-way ANOVA comparing all groups adjusted for multiple comparisons $^{*}p < 0.05, ^{***}p < 0.001, ^{****}p < 0.0001$.

Fed and fasted non-esterified fatty acids (NEFAs) showed no differences across any groups (Table. 6.1). Fasted insulin levels were reduced by 9 % in diabetic groups compared to the control groups ($p = 0.03$) with no effect of Mildronate treatment. The homeostatic model assessment (HOMA) quantified insulin resistance (HOMA IR) and showed that HOMA IR was 122 % higher in the diabetic groups compared to the control groups ($p < 0.001$, Table. 6.1).

Blood profile	Control (CTR)		Diabetes (STZ)		2-way ANOVA
Mean ± SD	Saline	Mildronate	Saline	Mildronate	p-value Treatment/Group (interaction)
Fed NEFA [mmol/L]	0.086 ± 0.04	0.13 ± 0.08	0.10 ± 0.04	0.12 ± 0.08	0.17/0.98
Fasted NEFA [mmol/L]	0.31 ± 0.08	0.37 ± 0.06	0.52 ± 0.59	0.38 ± 0.13	0.79/0.40
Fed insulin [mg/L]	0.52 ± 0.10	0.47 ± 0.10	0.46 ± 0.04	0.47 ± 0.04	0.59/0.27
Fasted insulin [mg/L]	0.44 ± 0.07	0.40 ± 0.06	0.39 ± 0.03	0.38 ± 0.03	0.16/0.03
HOMA IR [mmol/L]	0.009 ± 0.008	0.006 ± 0.002	0.020 ± 0.008	0.017 ± 0.006	0.17/0.0001

Table 6.1: Blood profile from fed and fasted bloods. L-carnitine concentration levels. All results presented as mean ± SD. Two-way ANOVA with the p-value calculated for either the effect of diabetes or the effect of Mildronate treatment.

Glucose levels measured in the fed state at five weeks post STZ/citrate buffer injection were 263 % higher in the diabetic groups compared to the control groups ($p < 0.0001$). Mildronate reduced fed glucose levels by 14 % in the diabetic group ($p = 0.035$). Lactic acid was unchanged across all groups in the fed blood plasma. Cholesterol was elevated by 27 % in the saline treated diabetic group compared to the saline treated control group ($p = 0.038$). HDL was increased by 48 % in the diabetic groups compared to the controls ($p < 0.0001$). There were no changes across any groups in the TAG levels. β-hydroxybutyrate (3-OHB) was 208 % elevated in the diabetic groups compared to the control groups ($p < 0.0001$), even though Mildronate reduced 3-OHB by 29 % in the diabetic group, it failed to reach statistical significance ($p = 0.10$, unpaired t-test, Fig. 6.6).

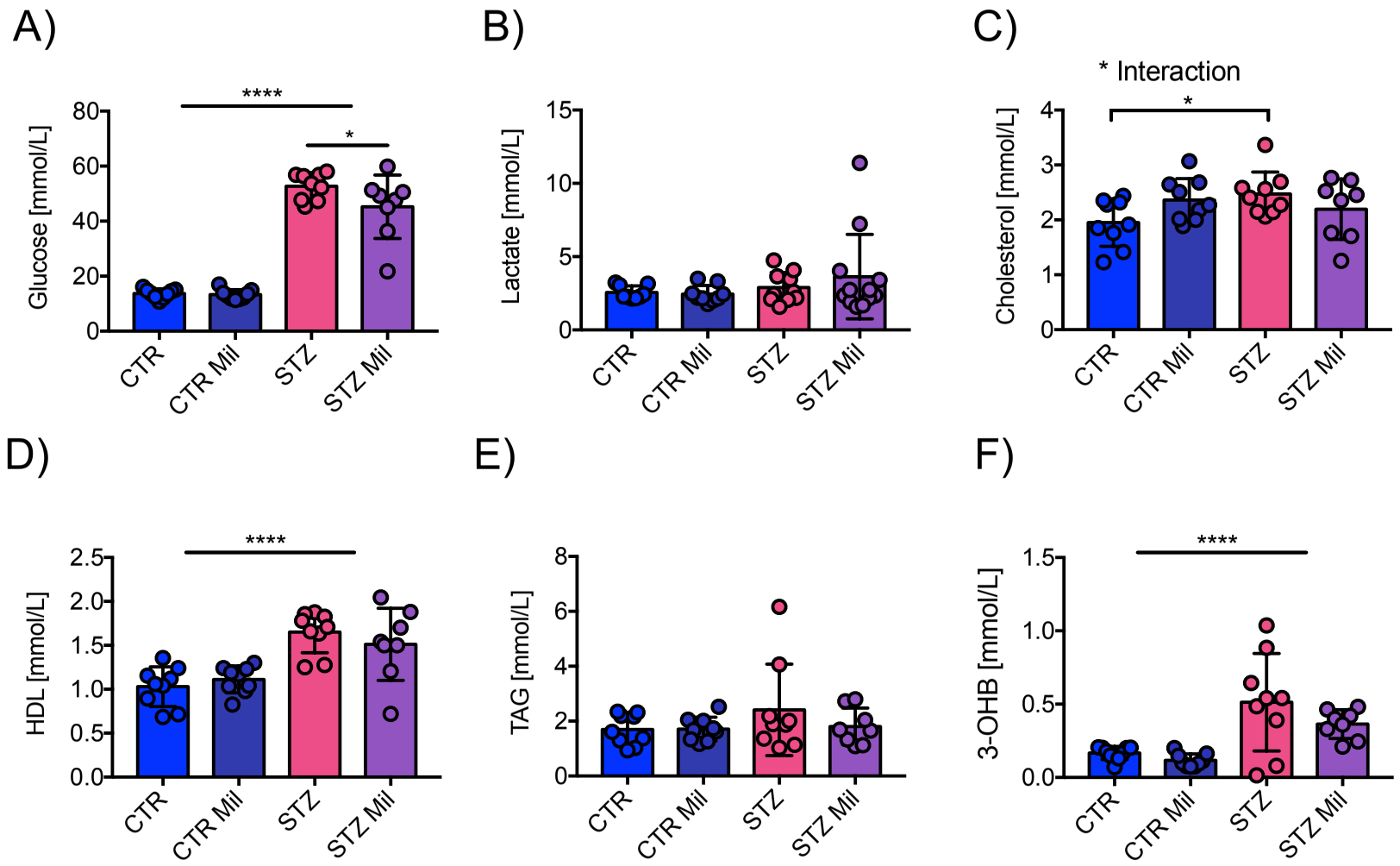

Figure 6.6: ABX Pentra 400 measurements taken from fed state serum 5 weeks post STZ/citrate buffer injection. **A)** Glucose levels. **B)** Lactic acid concentrations [mM]. **C)** Cholesterol levels [mmol/l]. **D)** High density lipoprotein (HDL) in [mmol/l]. **E)** Triglycerides (TAG) in [mmol/l]. **F)**β-hydroxybutyrate (3-OHB) in [mmol/l]. Data presented as mean ± SD. Two-way ANOVA with Sidaks multiple comparison test post hoc, where *p < 0.05, ****p < 0.0001.

6.5.2 L-Carnitine and Mildronate Levels

In the plasma, free L-carnitine was reduced in the diabetic groups by 25 % compared to the control groups ($p < 0.001$), and with Mildronate treatment free L-carnitine reduced another 43 % in both the control and the diabetic group ($p = 0.0002$, Fig. 6.7). L-carnitine was significantly reduced, as analysed with metabolomics, in the

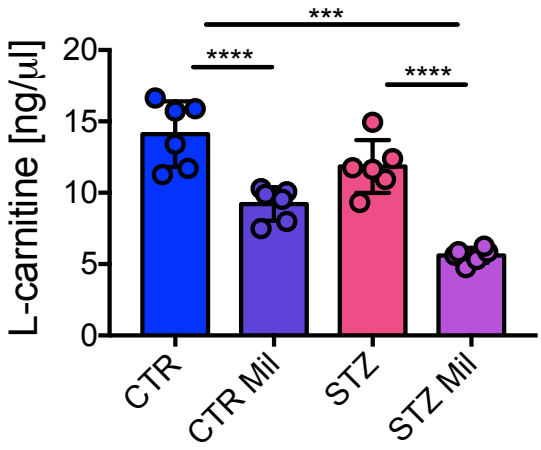

Figure 6.7: Free L-carnitine measured with an L-carnitine assay. Free L-carnitine levels in plasma [ng/μl]. All data represented as mean ± SD. Two-way ANOVA with Sidak's multiple comparison test $^{***}p < 0.001$, $^{****}p < 0.0001$.

diabetic groups compared to the control groups by 41 % ($p = 0.026$). Mildronate reduced L-carnitine levels significantly in both the control and in the diabetic groups by 56 % ($p = 0.006$, Fig. 6.8A).

Propionyl-carnitine was reduced by 38 % in the diabetic groups compared to the control groups ($p = 0.006$). Mildronate reduced propionyl-carnitine levels by 74 % in both the control and the diabetic groups ($p < 0.0001$, Fig. 6.8B).

Plasma Mildronate concentrations, as analysed with metabolomics, were undetected in the saline treated control group and the saline treated diabetic group. However, Mildronate levels were 89 % lower in the Mildronate treated diabetic group compared to the Mildronate treated control group ($p < 0.0001$, unpaired t-test, Fig. 6.9).

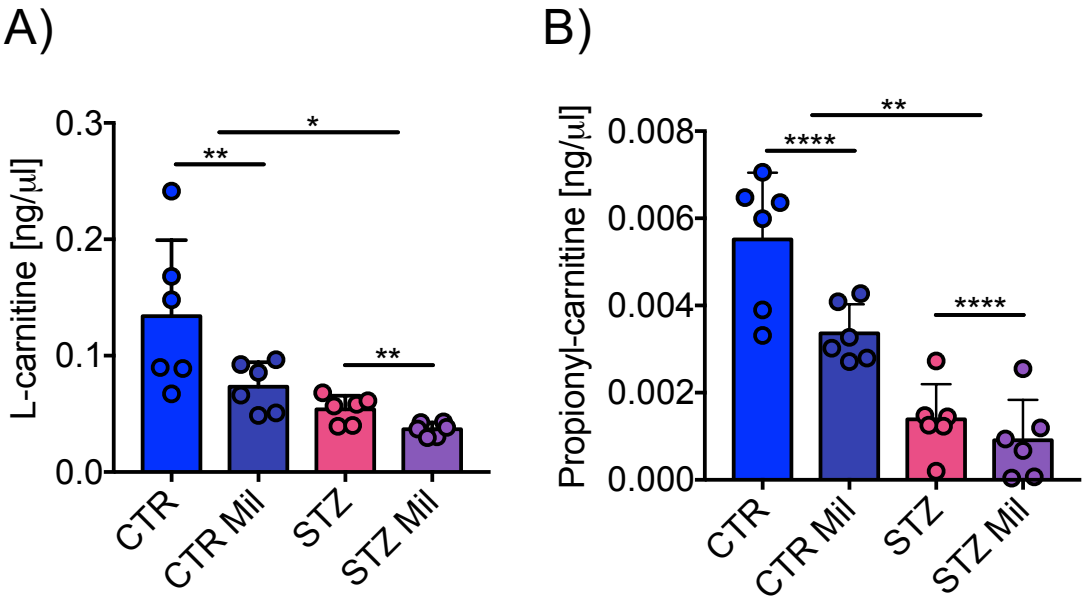

Figure 6.8: Free L-carnitine measured with metabolomics [ng/μl]. **A)** Free L-carnitine levels in plasma. **B)** propionyl-carnitine levels in plasma. All data represented as mean ± SD. Two-way ANOVA with Sidak's multiple comparison test $^{*}p < 0.05$, $^{**}p < 0.01$, $^{****}p < 0.0001$.

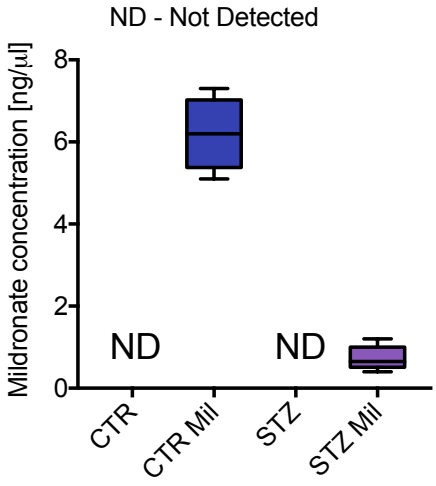

Figure 6.9: Plasma Mildronate levels as analysed with metabolomics [ng/μl]. All data represented as mean ± SD. ND is not detected.

6.5.3 Cardiac *In Vivo* Function

The variance was too large to determine any differences when assessing the systolic function with echocardiography (Table. 6.2). E/A ratio was increased by 24 % in the diabetic groups compared to the control groups ($p = 0.03$). Mildronate elevated E/E' ratio in the lateral wall by 28 % in both the control and the diabetic groups ($p = 0.05$, Table 6.2).

Echocardiography	Control (CTR)		Diabetes (STZ)		2-way ANOVA
Mean ± SD	Saline	Mildronate	Saline	Mildronate	p-value Treatment/Group (interaction)
Fractional Shortening (FS) [%]	50.3 ± 4.9	47.8 ± 5.9	46.7 ± 7.8	45.9 ± 9.6	0.50/0.25
Ejection Fraction (EF) [%]	85.3 ± 4.4	83.7 ± 4.8	82.2 ± 6.7	80.8 ± 9.1	0.49/0.17
Early filling (E) [m/s]	0.59 ± 0.16	0.69 ± 0.15	0.53 ± 0.09	0.59 ± 0.17	0.12/0.11
Late filling (A) [m/s]	0.64 ± 0.08	0.74 ± 0.115	0.69 ± 0.06	0.55± 0.08	0.53/0.28 (0.045)
E/A ratio	0.89 ± 0.25	1.07 ± 0.29	0.65 ± 0.05	0.83 ± 0.14	0.11/0.03
Septum E/E' ratio	12.7 ± 5.02	16.61 ± 8.04	14.2 ± 4.57	13.0 ± 6.18	0.28/0.99
Lateral wall E/E' ratio	13.45 ± 5.93	16.5 ± 6.68	11.58 ± 4.17	15.6 ± 2.95	0.05/0.45

Table 6.2: Echocardiography five weeks post STZ/Citrate buffer injection. The cardiac diastolic function obtained from 4-chamber view measuring the pulse wave velocity through the mitral valve and tissue doppler as well systolic function obtained through M mode imaging from the 2-chamber view. Results presented as mean ± SD. Two-way ANOVA with the p-value calculated.

When the systolic function was assessed with CINE MRI, the myocardial mass was decreased in the diabetic groups by 26 % compared to the control groups ($p < 0.0001$). Stroke volume was decreased in the diabetic groups by 17 %, but when normalized to body weight (stroke index) it was increased by 18 % in the diabetic groups compared to the control groups ($p = 0.017$). End systolic lumen was unchanged across all groups, and end diastolic lumen was decreased by 16 % in the diabetic groups compared to the control groups ($p = 0.001$). Ejection fraction, as supported by the echocardiography measurements, showed no differences across any of the groups. Even though cardiac output was decreased by 31 % in the diabetic groups compared to the control groups when cardiac output was normalized to body weight no differences were observed across any of the groups (Fig. 6.10).

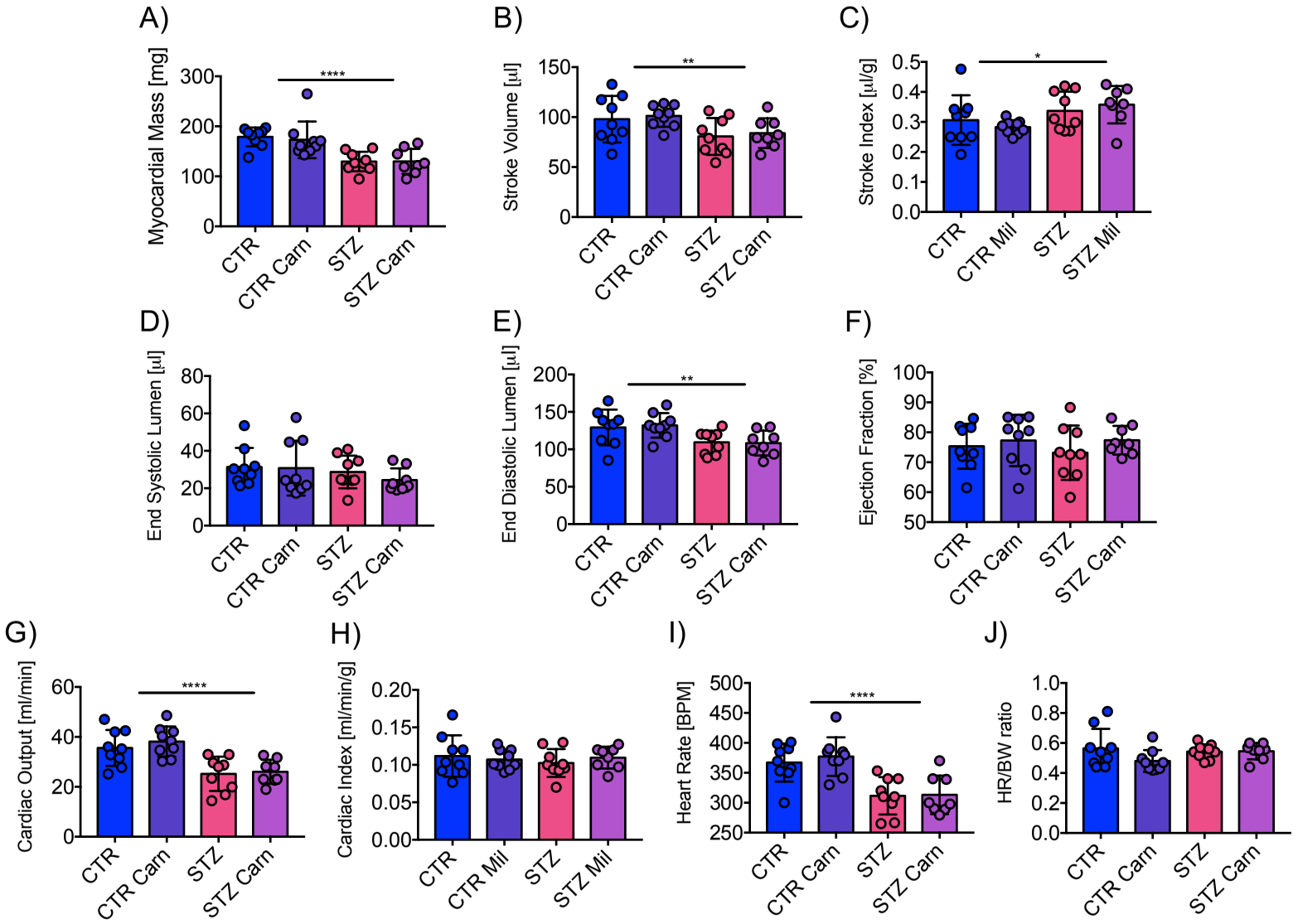

Figure 6.10: Cardiac function acquired with CINE MRI. **A)** Average myocardial wall mass of the left ventricle obtained from end diastolic and end systolic mass. **B)** Stroke volume (SV) obtained from the difference of the end diastolic lumen and end systolic lumen. **C)** Stroke index (SI), SV normalized to body weight. **D)** End systolic lumen (ESL). **E)** End systolic lumen (EDL). **F)** Ejection fraction (EF). **G)** Cardiac output (CO). **H)** Cardiac index (CI), CO normalized to body weight. **I)** Heart rate (HR). **J)** HR normalized to body weight (HR/BW). Data presented as mean ± SD. Two-way ANOVA analysis with Sidak's multiple comparison test where $^{*}p < 0.05$,$^{**}p < 0.01$,$^{****}p < 0.0001$.

6.5.4 Cardiac *In Vivo* Metabolism

Flux through pyruvate dehydrogenase (PDH), as indicated by ^{13}C label incorporation into bicarbonate and CO_2, was significantly reduced by 66 % in the diabetic groups compared to the control groups ($p < 0.0001$, Fig. 6.11A). Despite the reduction in PDH-flux for the diabetic animals, PDH-flux was elevated by 48 % with Mildronate treatment in both the control and the diabetic groups ($p = 0.035$). Incorporation of the ^{13}C label from pyruvate into lactate had a significant interaction term ($p = 0.04$) that showed Mildronate elevated lactate in the diabetic group by 55 % ($p < 0.05$). There was no change detected in alanine across any of the groups (Fig. 6.11BC).

Hyperpolarized [2$-^{13}C$]pyruvate MRI showed that neither citrate nor glutamate changed across any of the groups when analysed with a two-way ANOVA. However citrate was reduced by 63 % in the diabetic groups compared to control groups ($p = 0.07$), and Mildronate elevated citrate by 174 % in the diabetic group ($p = 0.05$, unpaired t-test). Citrate normalized to PDH-flux showed no differences across any groups (Fig. 6.12AD). Glutamate was unchanged across all groups and so was glutamate normalized to PDH-flux (Fig. 6.12BE). However, incorporation of the ^{13}C label into acetylcarnitine (AC) was significantly reduced by 75 % in the diabetic groups compared to the control groups ($p = 0.0017$). Mildronate treatment reduced AC normalized to the PDH-flux by 51 % in both the control and in the diabetic groups ($p = 0.026$, Fig. 6.11 CF).

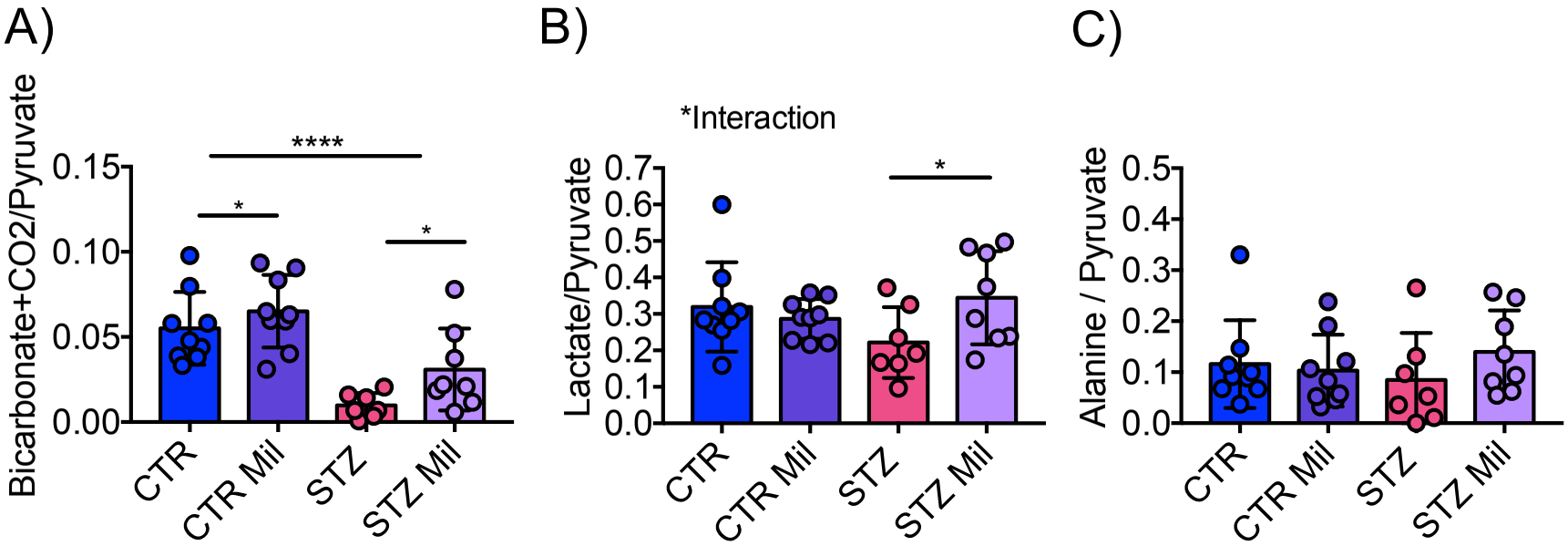

Figure 6.11: *In vivo* effects on cardiac metabolism by infusion of hyperpolarized $[1-^{13}C]$pyruvate. **A)** Bicarbonate/pyruvate ratio. **B)** Lactate/pyruvate ratio. **C)** Alanine/pyruvate ratio. Data presented as mean ± SD. Two-way ANOVA adjusted for multiple comparisons $^{*}p < 0.05, ^{****}p < 0.0001$.

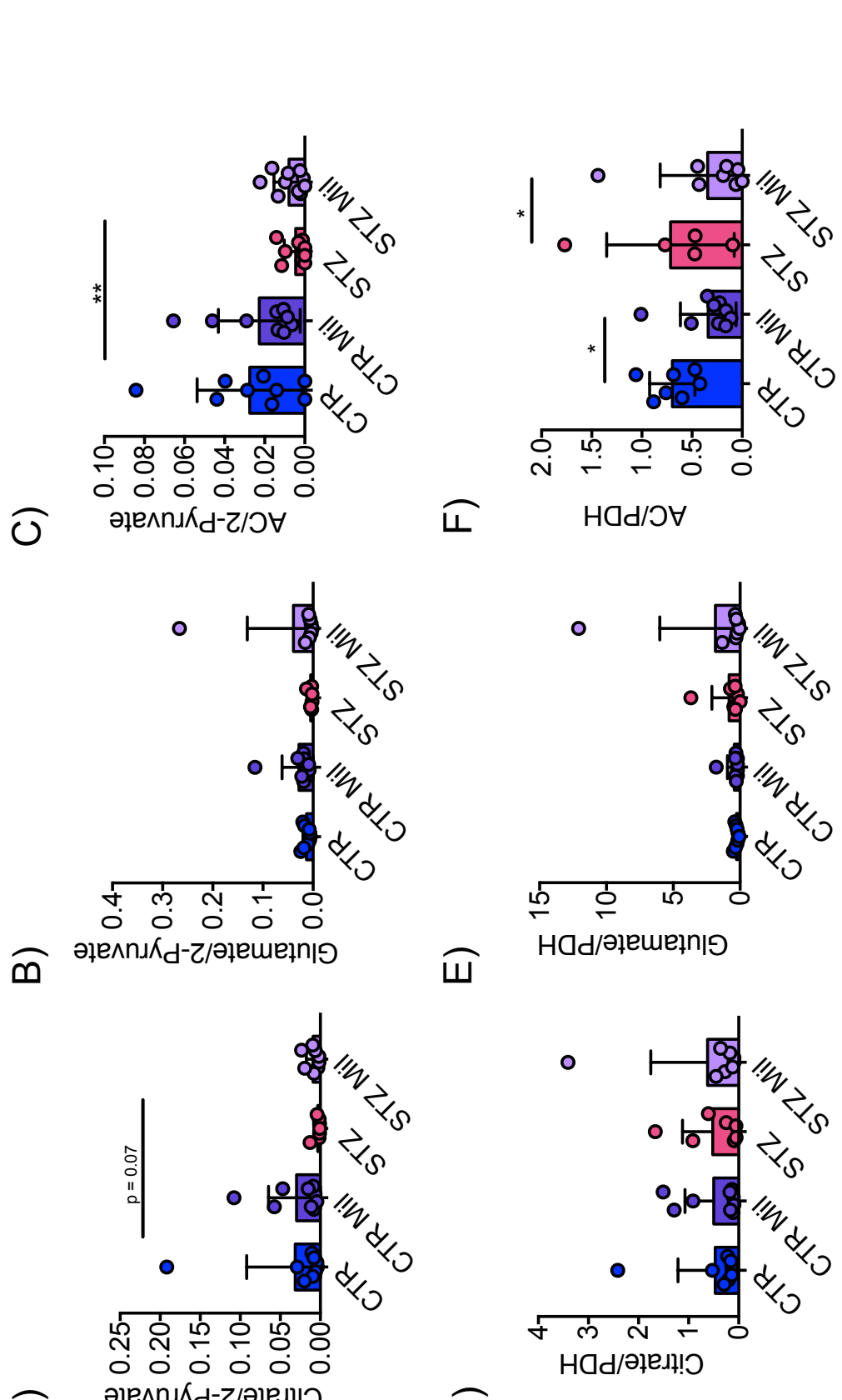

Figure 6.12: *In vivo* effects on cardiac metabolism investigated using hyperpolarized [2−^{13}C]pyruvate MRI. **A)** Citrate/2-pyruvate ratio. **B)** Glutamate/2-pyruvate ratio. **C)** Acetylcarnitine (AC)/2-pyruvate ratio, unpaired t-test ($^{+}$p = 0.024 compared to STZ). **D)** Citrate/2-pyruvate ratio normalized to PDH-flux (bicarbonate + CO_2/pryvate). **E)** Glutamate/2-pyruvate ratio normalized to PDH-flux (bicarbonate + CO_2/pryvate). **F)** Acetylcarnitine (AC)/2-pyruvate ratio normalized to PDH-flux (bicarbonate + CO_2/pryvate). Data presented as mean ± SD. Two-way ANOVA analysis with Sidak's multiple comparisons, where $^{*}p < 0.05$,$^{**}p < 0.01$.

6.5.5 Cardiac *Ex Vivo* Function

The rate pressure product (RPP) was 35 % lower in the diabetic groups compared to the control groups at pre-ischemia ($p = 0.0008$). RPP was 50 % lower in the diabetic groups compared to the control groups at post-ischemia ($p < 0.001$), Mildronate elevated RPP by 34 % in both the control and in the diabetic groups ($p = 0.04$) at post-ischemia (Fig. 6.13).

Heart rate (HR) decreased by 15 % in the diabetic groups compared to the control groups at pre-ischemia ($p = 0.003$). HR stayed reduced post-ischemia in the diabetic groups compared to the control groups ($p = 0.002$). Mildronate did not affect HR (Fig. 6.14).

Systolic pressure (SysP) was reduced by 28 % in the diabetic groups compared to the control groups ($p = 0.02$) at pre-ischemia. SysP stayed reduced post-ischemia by 26 % in the diabetic groups compared to the control groups ($p =0.02$). Mildronate elevated SysP by 27 % in both the control and in the diabetic groups ($p = 0.004$, Fig. 6.15).

Diastolic pressure (DiaP) stayed unchanged across all groups (Fig. 6.16).

Developed pressure (DevP) was reduced by 56 % in the diabetic groups compared to the control groups ($p = 0.027$) at pre-ischemia. DevP was reduced by 29 % in the diabetic groups compared to the control groups ($p = 0.017$) post-ischemia. Even though DevP stayed reduced post-ischemia, Mildronate elevated DevP by 39 % in both the control and in the diabetic groups ($p = 0.02$, Fig. 6.17).

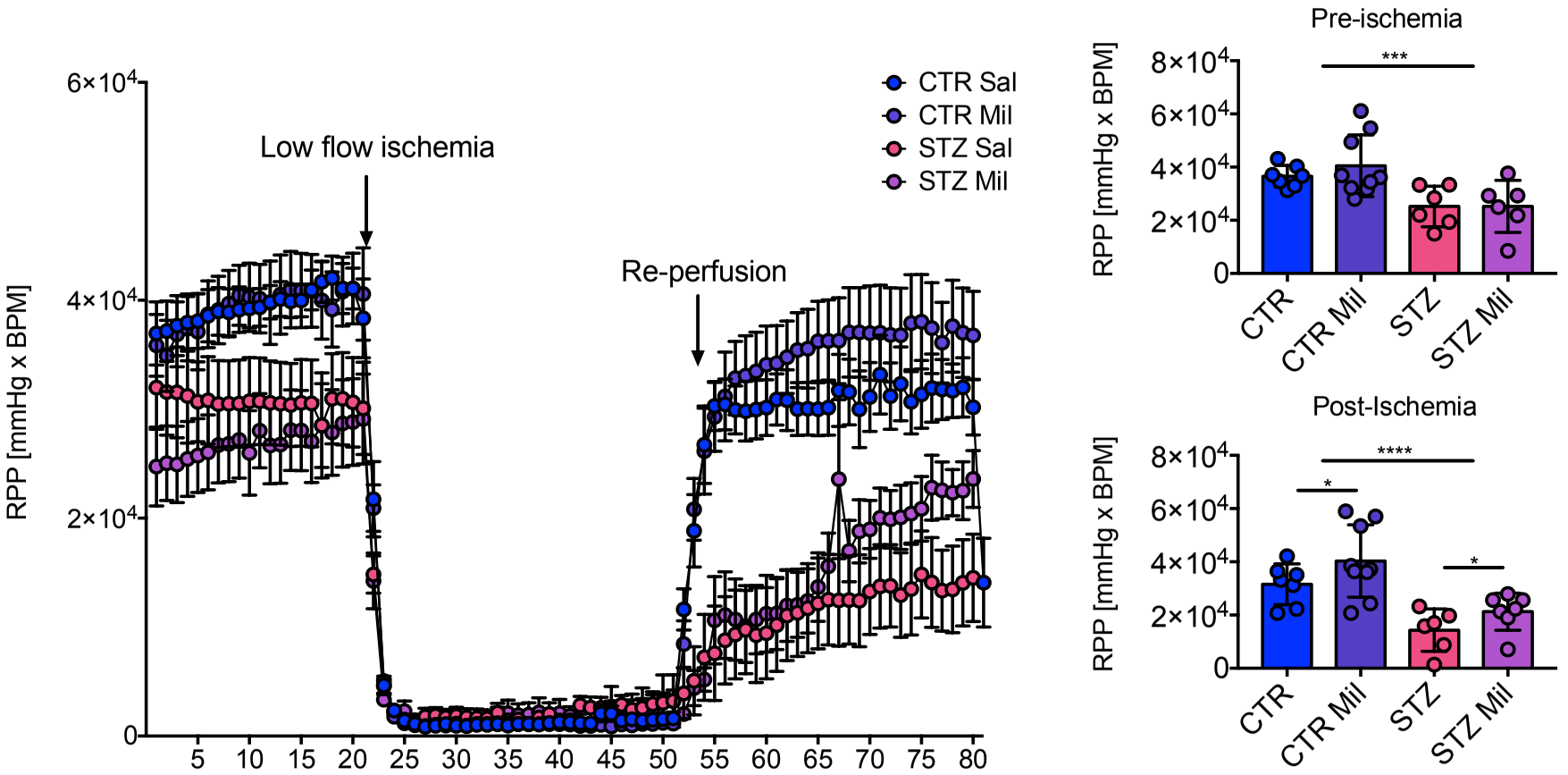

Figure 6.13: Rate pressure product (RPP) [mmHg] shown from Langendorff ischemia re-perfusion, where pre-ischemia (t = 1:20 min), ischemia (t = 21:50 min), and re-perfusion (t = 52:80 min). A flow rate of 0.4 ml/min/gww was used. Saline treated control (CTR, dark blue), Mildronate treated control (CTR Mil, purple), saline treated diabetics (STZ, magenta), Mildronate treated diabetics (STZ Mil, light purple). Average RPP for the last 10 minute of pre-ischemia and post-ischemia. Data presented as mean ± SD. Two-way ANOVA where $^{*}p < 0.05$,*** $p < 0.001$,**** $p < 0.0001$.

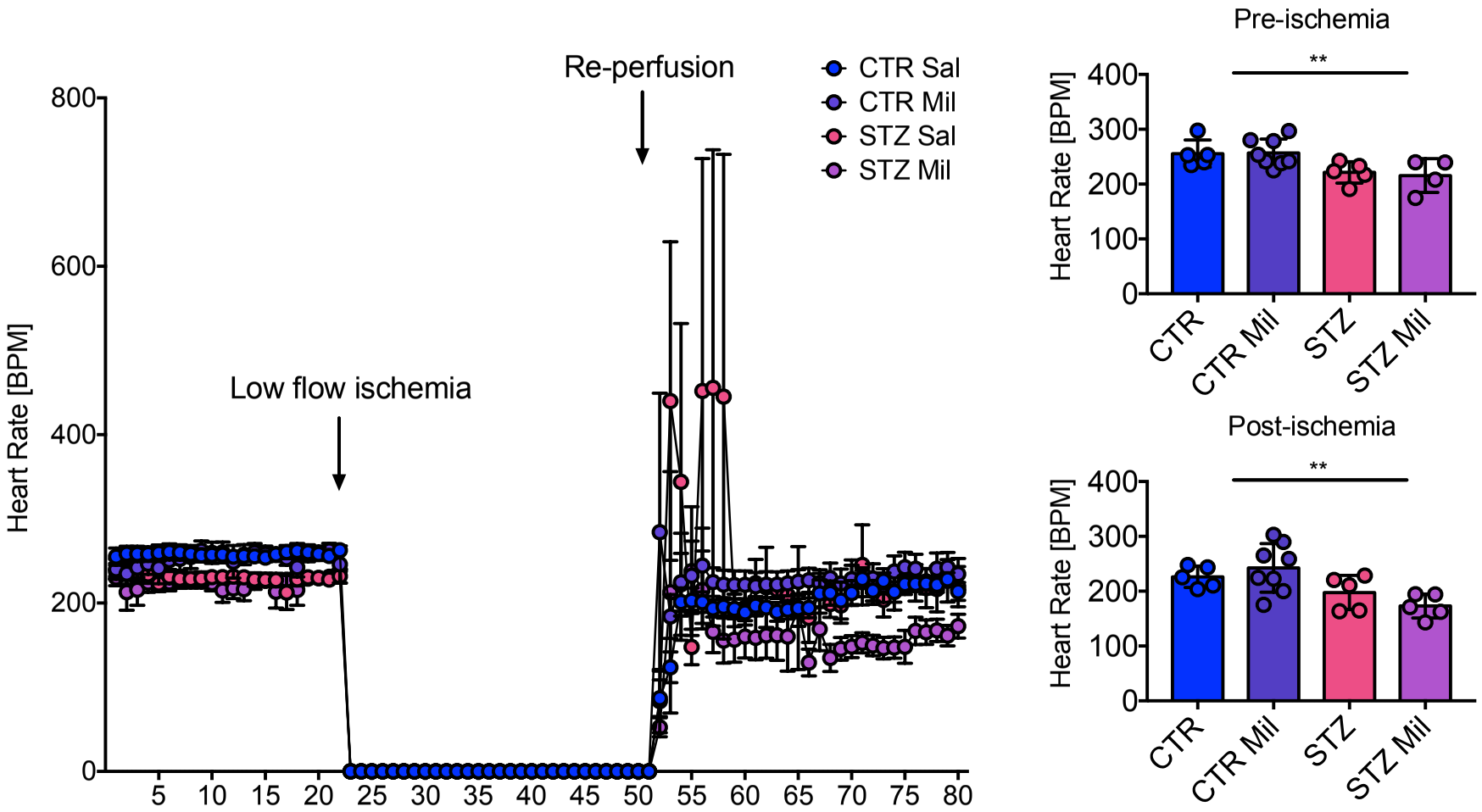

Figure 6.14: Heart rate (HR) [bpm] shown from Langendorff ischemia re-perfusion, where pre-ischemia (t = 1:20 min), ischemia (t = 21:50 min), and re-perfusion (t = 52:80 min). A flow rate of 0.4 ml/min/gww was used. Saline treated control (CTR, dark blue), Mildronate treated control (CTR Mil, purple), saline treated diabetics (STZ, magenta), Mildronate treated diabetics (STZ Mil, light purple). Average HR for the last 10 minute of pre-ischemia and post-ischemia. Data presented as mean ± SD. Two-way ANOVA, where $^{**}p < 0.01$.

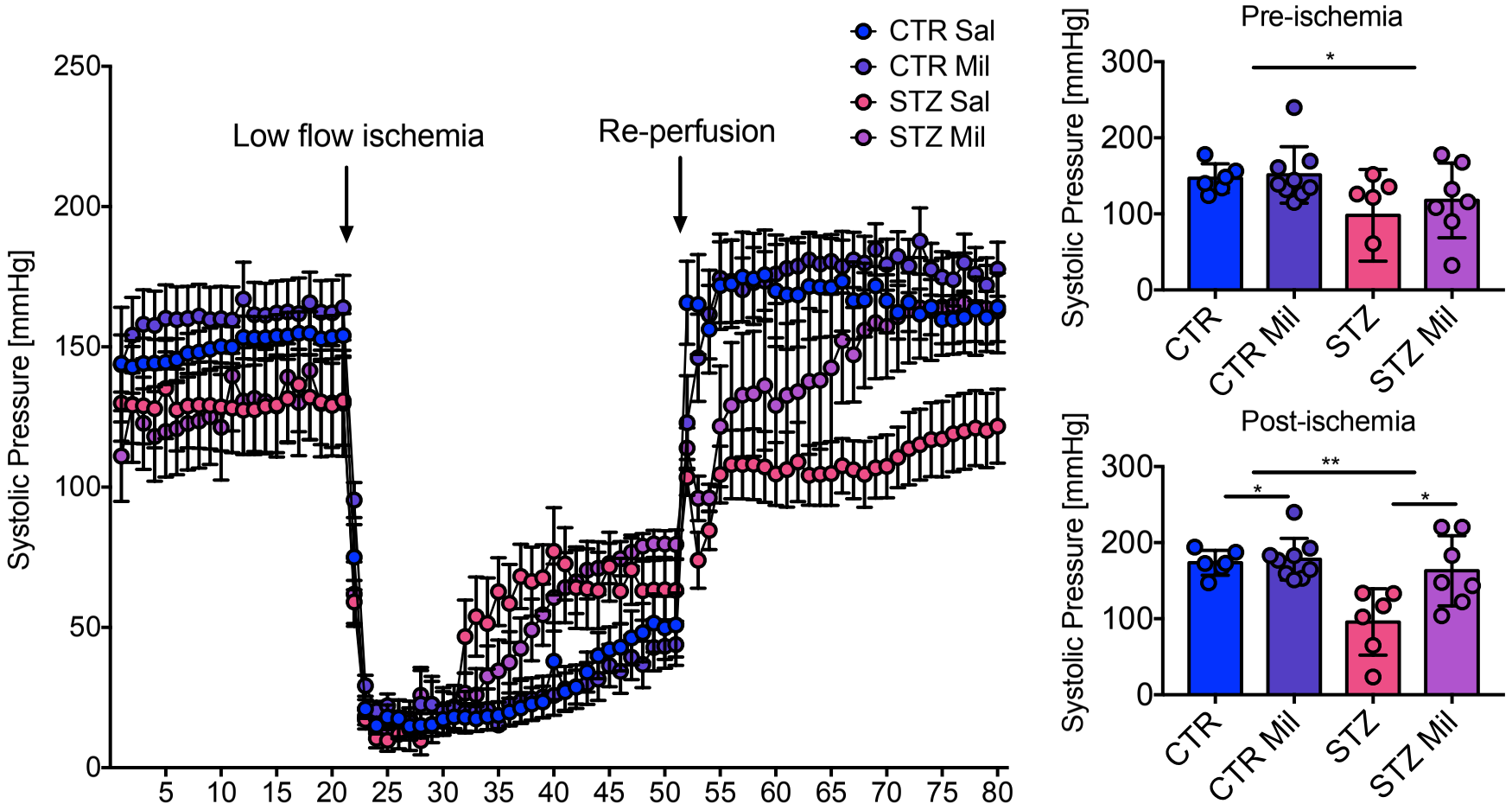

Figure 6.15: Systolic pressure (SysP) [mmHg] shown from Langendorff ischemia re-perfusion, where pre-ischemia (t = 1:20 min), ischemia (t = 21:50 min), and re-perfusion (t = 52:80 min). A flow rate of 0.4 ml/min/gww was used. Saline treated control (CTR, dark blue), Mildronate treated control (CTR Mil, purple), saline treated diabetics (STZ, magenta), Mildronate treated diabetics (STZ Mil, light purple). Average SysP for the last 10 minute of pre-ischemia and post-ischemia. Data presented as mean ± SD. Two-way ANOVA where $^{*}p < 0.05$,$^{**}p < 0.01$.

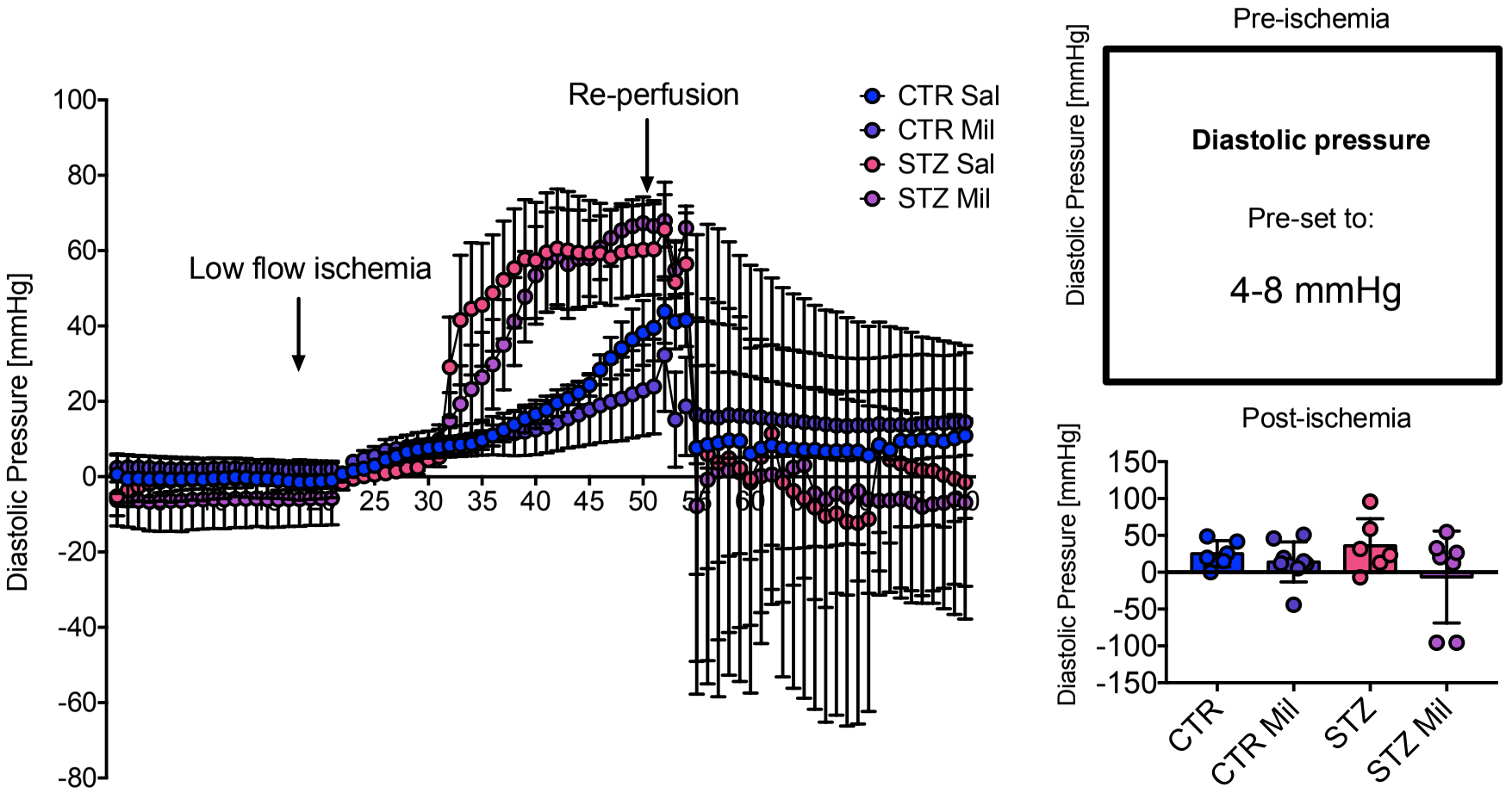

Figure 6.16: Diastolic pressure (DiaP) [mmHg] shown from Langendorff ischemia re-perfusion, where pre-ischemia (t = 1:20 min), ischemia (t = 21:50 min), and re-perfusion (t = 52:80 min). A flow rate of 0.4 ml/min/gww was used. Saline treated control (CTR, dark blue), Mildronate treated control (CTR Mil, purple), saline treated diabetics (STZ, magenta), Mildronate treated diabetics (STZ Mil, light purple). Average DiaP for the last 10 minute of pre-ischemia and post-ischemia. Data presented as mean ± SD.

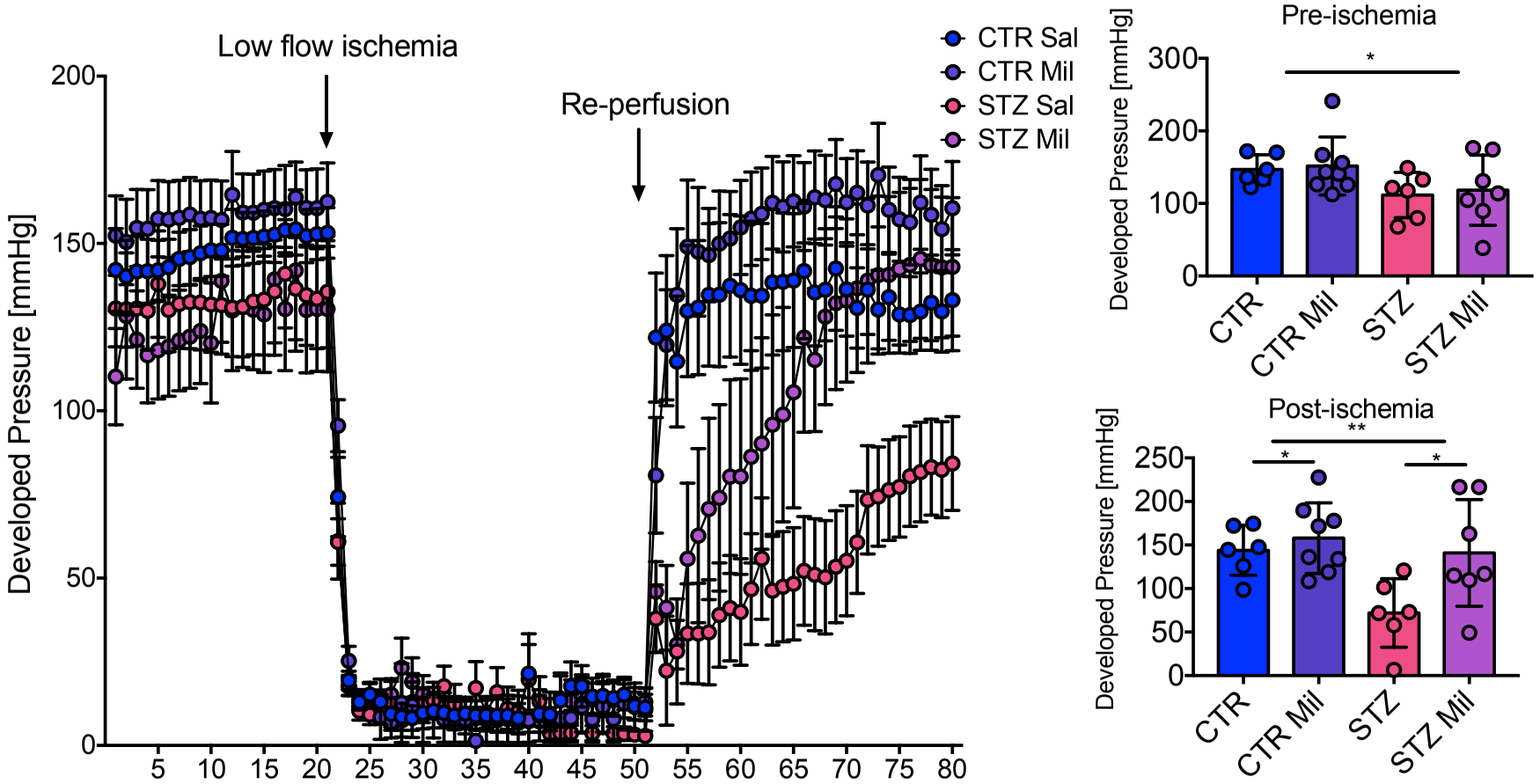

Figure 6.17: Developed pressure (DevP) [mmHg] shown from Langendorff ischemia re-perfusion, where pre-ischemia (t = 1:20 min), ischemia (t = 21:50 min), and re-perfusion (t = 52:80 min). A flow rate of 0.4 ml/min/gww was used. Saline treated control (CTR, dark blue), Mildronate treated control (CTR Mil, purple), saline treated diabetics (STZ, magenta), Mildronate treated diabetics (STZ Mil, light purple). Average DevP for the last 10 minute of pre-ischemia and post-ischemia. Data presented as mean ± SD. Two-way ANOVA where $^{*}p < 0.05$,$^{**}p < 0.01$.

The Mildronate treated control group had three times more frequent periods of irregular heartbeats than the saline treated control group. The Mildronate treated diabetic group had 13 times more frequent periods of irregular heart beats than the saline treated diabetic group (Fig. 6.18).

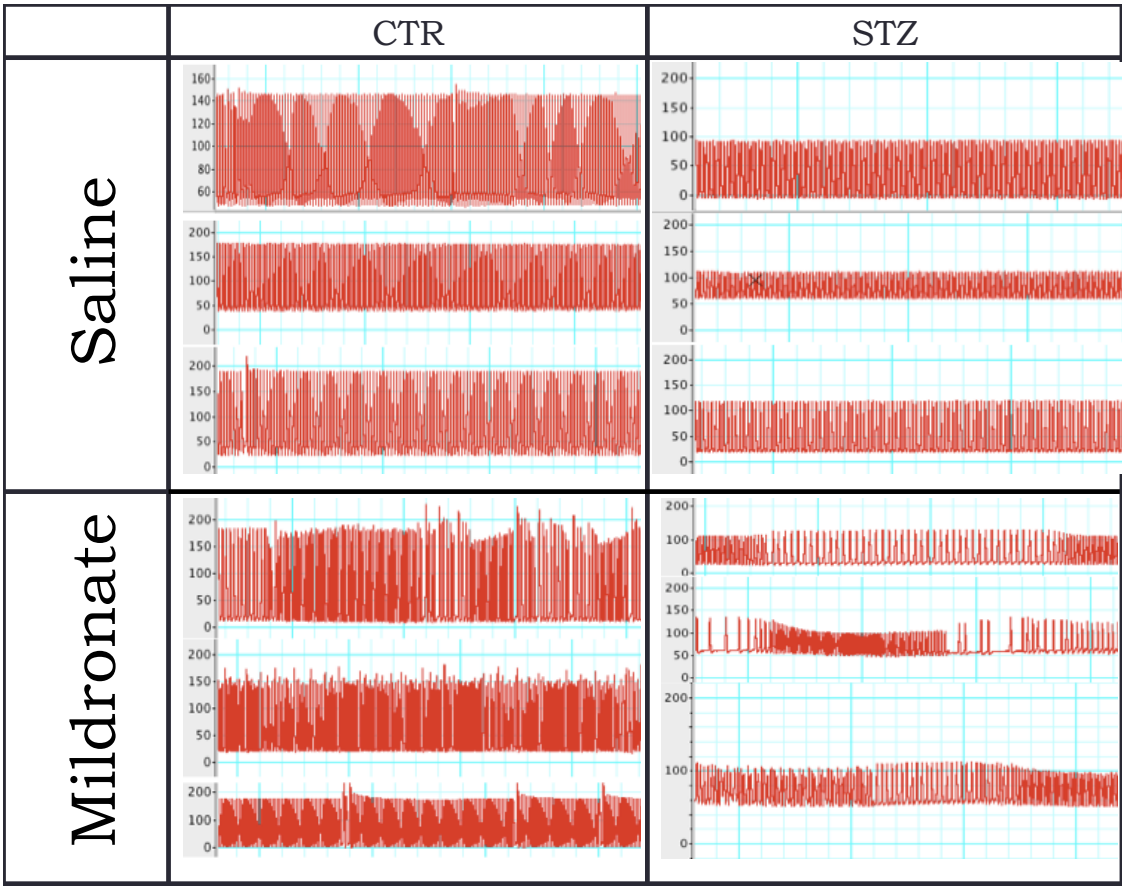

Figure 6.18: Figure shows three example traces for each group (CTR, CTR Mil, STZ, STZ Mil). The y-axis represents the pressure in the left ventricle in [mmHg]. The x-axis represents the time in seconds. Small blue squares correspond to a period two seconds, larger squares correspond to a period of ten seconds.

6.5.6 Cardiac *Ex Vivo* Fatty Acid Metabolism

The relative FAO rates normalized to cardiac work at pre-ischemia failed to show statistical significance with a two-way ANOVA. However the saline treated diabetic group had 55 % higher FAO rates than the saline treated control group at pre-ischemia ($p = 0.014$, unpaired t-test, Fig. 6.19A). Post-ischemia FAO elevated by 158 % in the diabetic groups compared to the control groups ($p = 0.004$). Mildronate did not affect FAO at post-ischemia (Fig. 6.19B). FAO percentage recovery between pre- and post-ischemia elevated by 110 % in the diabetic group compared to the control groups ($p = 0.015$, Fig. 6.19C). The absolute FAO rates failed to reach statistical significance across any groups (Fig. 6.19D).

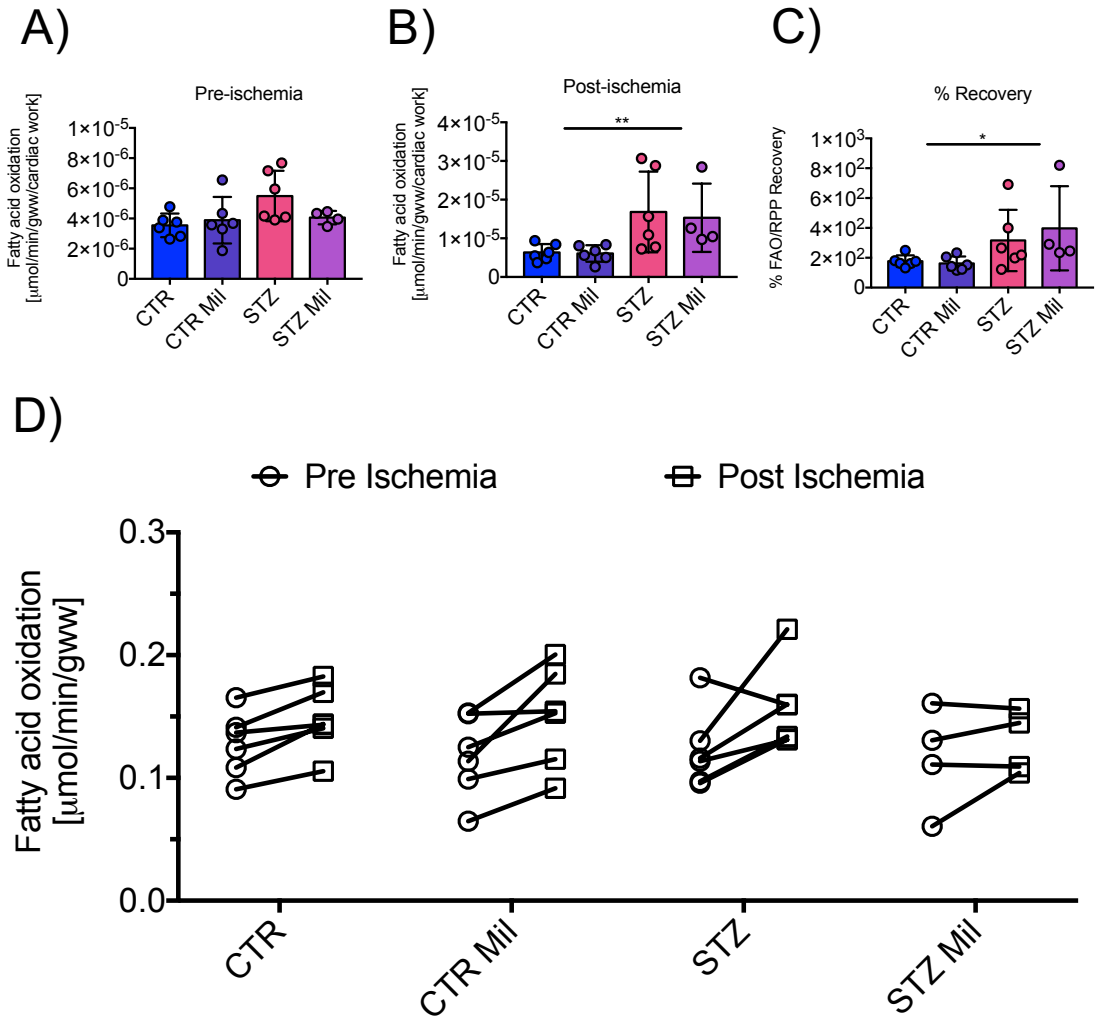

Figure 6.19: Fatty acid oxidation rates [μmoll/min/gww] over cardiac work in rate pressure product [mmHg x BPM] presented as mean ± SD. **A)** Fatty acid oxidation over cardiac work pre-ischemia. **B)** Fatty acid oxidation over cardiac work post-ischemia. **C)** Percentage recovery between post-ischemia and pre-ischemia. **D)** Fatty acid oxidation rates in [μmoll/min/gww] displayed pre-ischemia and post-ischemia. Data presented as mean ± SD. Two-way ANOVA with Sidak's multiple comparison, where *p < 0.05, **p $<$ 0.01.

6.5.7 Tissue Analysis

GLUT4 was down-regulated in the diabetic groups by 108 % compared to the control groups ($p = 0.005$), there was no change in the protein expression induced by Mildronate.

PDK4 was up-regulated by 603 % in the diabetic groups compared to the control groups ($p < 0.0001$), there was no change in the protein expression induced by Mildronate.

MCAD expression showed no changes across any of the groups.

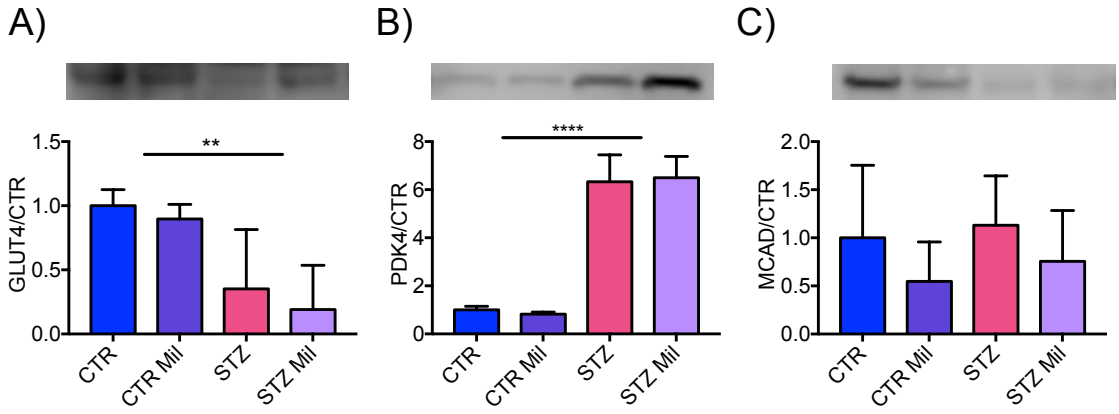

Figure 6.20: Protein expression levels obtained from Western Blots. All values normalized to control values. Housekeeper antibody, Cyclophilin B, showed no differences. **A)** GLUT4. **B)** PDK4. **C)** MCAD. All results presented as mean ± SD. Two-way ANOVA where $^{**}p < 0.01$, $^{****}p < 0.0001$.

6.6 Discussion

6.6.1 Summary of Key Findings

Mildronate reduced food and water intake in the diabetic group, although it did not affect the fasted glucose or insulin levels. Mildronate reduced fed glucose levels by 14 % in the diabetic group. These effects were seen in association with a significant reduction in L-carnitine levels in the plasma, that were reduced by 43 % with Mildronate treatment. Furthermore, even though both the control group and the diabetic group were treated with the same dose and frequency of Mildronate, there were higher concentrations of Mildronate found in the plasma in the control group than in the diabetic group. Mildronate showed no effect on *in vivo* cardiac function, but it elevated PDH-flux and lactate significantly in diabetes while reducing acetylcarnitine in the *in vivo* heart. Mildronate improved RPP *ex vivo* at post-ischemia, even though it did not reach the control levels of RPP, this was driven by an improved systolic pressure in the diabetic hearts with Mildronate treatment. Finally, despite the *ex vivo* improvements post-ischemia, Mildronate induced irregular heart beats in both the controls and the diabetics.

6.6.2 Daily Mildronate Treatment in the *In Vivo* Type 1 Diabetic Heart

There have been some studies showing the beneficial effects of Mildronate treatment on both CHD and in diabetes [132, 269, 121, 245]. This chapter showed that the diabetic groups gained less weight than the control groups. Mildronate did not affect weight gain in either group which is consistent with the literature [245]. Even though diabetic animals had higher kidney weight, smaller tibia lengths, reduced heart weight and fat pads, none of these were altered with Mildronate treatment. PPARα transcription factors like PDK4 was activated in the diabetic groups, suggesting a loss of fat stores, but no differences were observed with Mildronate treatment.

The diabetic groups had higher food and water intake per day, which is consistent with previous findings in the same model [105]. However, Mildronate decreased food

and water uptake in both diabetic and control groups, despite this no differences in body weight were observed.

Similarly, glucose levels progressed and stayed elevated throughout the study. No effects from Mildronate were detected on the fasted glucose levels. However, Mildronate reduced fed glucose levels at five weeks post STZ injection in the diabetic group, but there were no changes in plasma fatty acids or triglycerides levels. An explanation for the decreased fed glucose levels could be the reduced food intake. Fasted insulin levels were decreased in the diabetic group, but there was no effect of Mildronate treatment. Also β-hydroxybutyrate elevated in the diabetic group and although β-hydroxybutyrate did not decrease significantly in the Mildronate treated group compared to the saline treated diabetic group, there was a trend observed. All of these findings together suggest Mildronate inhibits fatty acid oxidation and can stimulate glucose oxidation, despite no changes in insulin levels. Previous studies have shown improvements in the both fed and fasted blood glucose levels and triglycerides, where no insulin changes were observed with Mildronate treatment [245].

Mildronate was only present in the groups that were treated with Mildronate as expected, although the diabetic group had lower concentrations of Mildronate in the plasma, compared to the control group, suggesting maybe a higher clearance through the urine in line with the diabetics drinking more water. Furthermore, L-carnitine was reduced in the plasma in the saline treated diabetic group compared to the saline treated control group as observed previously [155, 153, 212, 264, 155].

This thesis has for the first time investigated the effects of Mildronate on *in vivo* metabolism and function in the rodent diabetic heart and validated them against *ex vivo* findings. The diabetic groups exhibited a decreased E/A ratio as observed with echocardiography and a reduced end diastolic lumen observed with CINE MRI, suggesting a worsening of diastolic function in the saline treated diabetic group compared to the saline treated control group. Systolic changes were similar in the saline treated diabetic group as previously described by Loganathan *et al.* [142]. However, even though cardiac output was decreased in the diabetic groups

when normalized to body weight, there was no change across any groups. Stroke index, however, elevated with diabetes suggesting that the diabetic hearts were working harder. Mildronate did not affect the systolic function, and even though it elevated E/E' ratio, suggesting a worsening of diastolic function, it only showed it in the lateral wall and not in the septum, as would have been expected, this could be contributed by the low sensitivity and high dependency on the operator of the echocardiography apparatus.

Although Mildronate showed no remodelling in the *in vivo* cardiac function, myocardial substrate utilisation changed, not just in diabetes, but also in the control groups. PDH-flux was reduced in both diabetic groups compared to the control groups as would be expected because of the elevated expression of PDK4 in the diabetic groups, a target gene for PPARα, and an inhibitor of PDH-flux. Although PDK4 showed no differences in the Mildronate treated diabetic group, there was an elevation in PDH-flux with Mildronate treatment. Coinciding with an elevation in PDH-flux, there was an increase in lactate levels in the *in vivo* myocardium, suggesting a shift away from fatty acid oxidation. Acetylcarnitine levels, when normalized to PDH-flux, were also reduced in the Mildronate treated diabetic group which is following the reduced L-carnitine levels observed in the plasma. If there is not sufficient L-carnitine, it can not buffer excess acetyl-CoA, and therefore there will be less acetylcarnitine in the heart tissue. These metabolic changes might occur before any functional changes, and since early diastolic dysfunction was detected on echocardiography, it is possible that myocardial functional changes may manifest later with more extended treatments.

With some metabolic changes observed and no *in vivo* functional changes, it was explored how these hearts would recover post-ischemia. Some studies have failed to show an effect on cardiac function in the isolated perfused heart even with eight weeks of Mildronate treatment with a higher dosage (100, 200 and 400mg/kg) [133]. Even with a more potent inhibitor of L-carnitine biosynthesis and OCTN2 (4-[ethyl(dimethyl)ammonio]butanoate; Methyl-GBB) no functional benefits could be observed, although acylcarnitines were reduced, and therefore

there was a stimulation of glucose oxidation and depression of fatty acid oxidation, which lead to attenuation of the development of atherosclerosis [268].

The lack of Mildronate induced functional changes was confirmed in the *ex vivo* hearts pre-ischemia in the Langendorff perfused method. It was though evident that diabetic hearts had a worse function than the controls. RPP, HR, SysP and DevP were all reduced pre-ischemia in the diabetic groups compared to the control groups, suggesting a worse cardiac function in diabetes. Mildronate did not affect the functional parameters at pre-ischemia, validating the *in vivo* findings.

With induced low-flow ischemia, the hearts recovered differently, and the first metabolic changes that were observed *in vivo* could explain the recovery post-ischemia. Post-ischemia, the functional parameters were still reduced in diabetic groups. However, Mildronate elevated RPP, SysP and DevP in the diabetic groups, but also in the control groups. HR was sustained at post-ischemia across all groups. Mildronate elevated PDH-flux and improved recovery post-ischemia observed *in vivo*. Despite these changes, there was, however, evidence that Mildronate induced more frequent irregular beats on both the control group and on the diabetic group, that was not observed when treating with saline. It has previously been shown that L-carnitine is a calcium chelator and can limit levels of free calcium [13, 66]. L-carnitine has also been shown to treat arrhythmias [113], so maybe Mildronate treatment impairs calcium signalling and could, therefore, result in irregular beats, although these are just speculations and need to be investigated further.

FAO did not elevate in the diabetic groups compared to the control groups. The streptozotocin-induced T1D model has previously shown elevated levels of oxidation rates of both palmitate, linoleic, oleic, and arachidonic acids. This was first observed post six weeks of streptozotocin injection, although five days post STZ injection this study failed to show any changes in FAO [111], even though it used higher levels of palmitate in the perfusion buffer (0.8-1 mM) and also had added insulin to the buffer, which was in contrast to the work undertaken for this chapter. Another study has shown that STZ-induced T1D immediately increases coronary luminal lipoprotein lipase, that breaks down TAG to NEFA [205], this could mean that

while plasma TAG and NEFA stay unchanged, this elevation of luminal lipoprotein lipase is another adaptation to fatty acids in the diabetic heart. Surprisingly there was no effect observed from Mildronate treatment on fatty acid oxidation rates; however it might be due to the lack of insulin in the buffer together with the low palmitate concentration used as discussed in Chapter 5. Furthermore, a study found elevated oxidation of endogenous fat stores in the STZ-induced T1D rats [192], so even though fatty acid oxidations rate were possibly elevated, it could have been from endogenous fat stores and not exogenous fat stores as measured in this study.

6.6.3 Conclusion and Future Perspective

This study suggests beneficial effects of Mildronate supplementation in STZ-induced T1D. Although Mildronate had no *in vivo* effect on myocardial function on the STZ-induced rat. Mildronate induced an alternative metabolic substrate utilisation in the myocardium which was beneficial, if the myocardium undertook additional stress, like low-flow ischemia. Mildronate improved myocardial functional recovery post-ischemia in the *ex vivo* heart both in the diabetic and in the control groups. Future experiments would benefit from a longitudinal study, investigating the metabolic and functional changes, to verify that the metabolic alterations indeed arise before the functional benefits observed in this study. Furthermore, comparing the metabolic and functional changes *in vivo* between Mildronate and L-carnitine treatment could elucidate our understanding of how both mechanisms of actions could be beneficial in diabetes.

The six no sooner had begun
About the beast to grope
Than, seizing on the swinging tail,
That fell within his scope,
"I see," cried he, "the elephant
Is very like a rope."

7 General Discussion

Contents

7.1 Overview 211
7.2 Effects of Diabetes on the Heart 212
7.3 L-Carnitine/Mildronate Effects on the Diabetic Heart 215

7.1 Overview

The leading cause of death in type 1 diabetic (T1D) patients is from cardiovascular disease, and a reduction in L-carnitine levels has been shown to be a common factor in both diabetes and cardiovascular disease.

The work undertaken in this thesis has shown cardiac metabolic and functional modifications in response to the progression of diabetes. Both a genetic mouse model of neonatal diabetes and a streptozotocin (STZ)-induced T1D rat model were explored. The model that was continued for use in the rest of this thesis was the fasted high dose STZ-induced rat model, due to its more severe phenotype and better signal to noise ratio on MRI.

Before investigating treatment response, a low-flow ischemic rate was optimised, while also examining the effects of adding L-carnitine to the perfusate

buffer in healthy control hearts, which showed adverse effects to functional recovery post-ischemia.

L-carnitine and Mildronate were subsequently used to modulate plasma carnitine levels to investigate the metabolic and functional effects of L-carnitine on the diabetic rodent heart. While L-carnitine is known to facilitate the transport of long-chain fatty acids into the mitochondria, Mildronate inhibits uptake of L-carnitine leading to reduced L-carnitine levels [68, 245]. Interestingly this thesis showed that both L-carnitine and Mildronate provided the ability to enhance carbohydrate metabolism and increase PDH-flux. This coincided with improved recovery post-ischemia with both L-carnitine and Mildronate treatments, although only L-carnitine prevented progressive hyperglycaemia and improved diastolic function *in vivo*. Mildronate did not affect cardiac function *in vivo*.

These studies were undertaken in untreated and uncontrolled diabetes. Insulin has been shown to enhance the effects of L-carnitine [229], so treating diabetes with a combination of insulin and L-carnitine might perhaps be crucial in providing a better understanding of the underlying mechanisms in the future.

7.2 Effects of Diabetes on the Heart

More severe diabetes was induced with a high dose of STZ if animals were fasted before STZ injection, compared to a fed state. Glucose and STZ have been shown to compete with each other, as they are both taken up by the GLUT2 transporter [64]. This could explain why the fasted animals showed more severe and reproducible results i.e. because glucose levels are lower in the fasted state providing less competition for STZ uptake. The heart adapts quickly in order to sustain cardiac function. In the STZ model, the initial depression of cardiac function occurred in combination with suppression in the metabolic conversion of pyruvate to lactate, alanine and bicarbonate. This was the immediate metabolic and functional response to a sudden lack of insulin. However, stroke index was elevated six weeks post STZ injection, which was accompanied by an elevation in the conversion of hyperpolarized pyruvate into lactate and alanine, suggesting

that some functional benefit was obtained from the ability to redirect pyruvate into alternative metabolic pathways.

Similar findings were observed in the genetic mouse model of diabetes, which showed initial depression of stroke volume, cardiac output and cardiac index. However this functional depression in the heart only occurred together with a decrease in the bicarbonate signal, and no changes were found in the alanine or lactate signal. Functional improvements occurred later compared to the STZ model. No alterations could be detected in *in vivo* lactate and alanine, most likely due to the reduced signal to noise ratio in the murine spectra.

Although less metabolic changes were found in the mouse model, it was shown that both the functional and metabolic changes could be reversed with glibenclamide treatment. Perhaps a similar reversal of function and metabolism, as observed with glibenclamide, could be obtained with insulin treatment in the STZ-induced animals, as insulin has been shown to improve body weight, left ventricular developed pressure, left ventricular contractility, and relaxation of the heart [255].

Finally, in all the STZ-induced rat models alanine changes occurred even without functional or plasma alterations, which might suggest that metabolic remodelling occurs prior to any functional changes, possibly demonstrating early changes in gluconeogenesis [126]. Further investigations with longer progression are needed, to see if even the fed low dose injected animals eventually result in cardiac remodelling.

As a more detailed analysis, the control groups and the STZ-induced diabetic groups from Chapters 5 and 6 were compared. STZ-induced diabetics from both Chapters showed a depression of *in vivo* cardiac function (Fig. 7.1) together with depletion of PDH-flux and elevation of blood glucose (Fig. 7.2). This comparison confirmed that the STZ-induced T1D model was consistent and reproducible across the two studies.

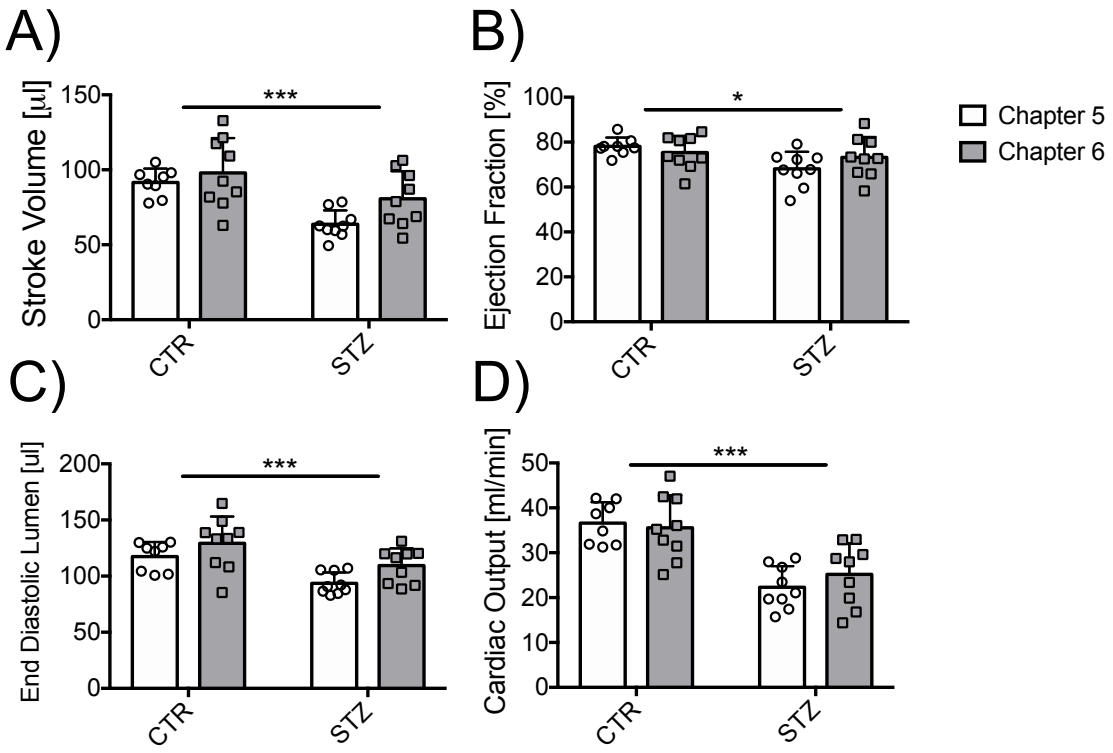

Figure 7.1: Daily saline treated control (CTR) and diabetes (STZ) post five weeks of STZ/citrate buffer injection from Chapters 5 and 6. **A)** Stroke volume (SV). **B)** Ejection fraction (EF). **C)** End diastolic lumen (EDL). **D)** Cardiac output (CO). All data represented as mean ± SD. Two-way ANOVA, where $^{*}p < 0.05$,$^{***}p < 0.001$,$^{****}p < 0.0001$.

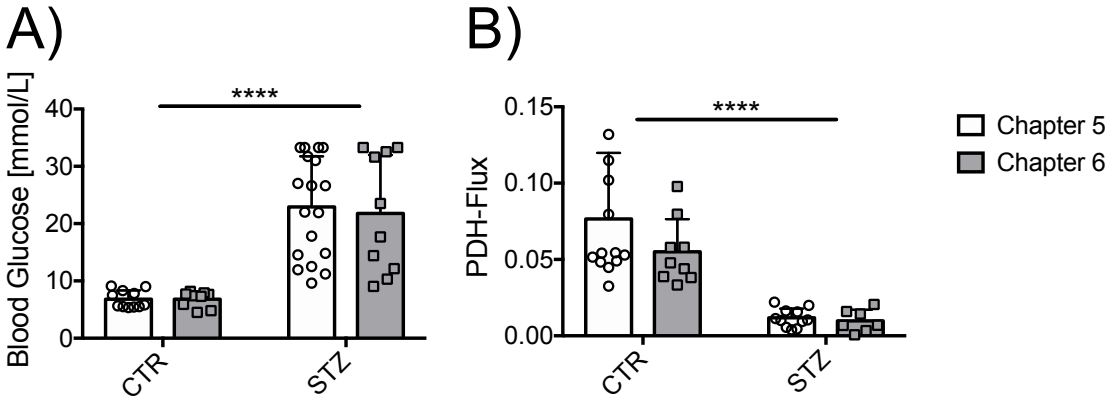

Figure 7.2: Daily saline treated control (CTR) and diabetes (STZ) post five weeks of STZ/citrate buffer injection from Chapters 5 and 6. **A)** Fasted blood glucose levels at five weeks. **B)** Bicarbonate/pyruvate ration (PDH-flux). All data represented as mean ± SD. Two-way ANOVA, where $^{****}p < 0.0001$.

7.3 L-Carnitine/Mildronate Effects on the Diabetic Heart

Most current therapies either try to elevate the oxygen supply to the heart or depress the heart's oxygen demand, however, therapies that can target the reduction of fatty acid oxidation might be helpful in improving the prognosis of CHD [248]. There have been several studies investigating the metabolic shift away from fatty acid oxidation towards glucose oxidation [96]. The work undertaken in this thesis has investigated both the effect of Mildronate and L-carnitine on the diabetic heart.

Chapter 5 showed beneficial effects of L-carnitine supplementation in diabetic hearts. Despite demonstrating only slight improvements in cardiac function, L-carnitine treatment elevated PDH-flux and slowed the progression of hyperglycaemia in the STZ-induced diabetic animals. It normalised fatty acid oxidation recovery and improved functional recovery post-ischemia. This study showed potential for recovery in diastolic relaxation both *in vivo* and *ex vivo*. Also, calcium was reduced with L-carnitine treatment in the plasma, supporting the diastolic improvements [9]. It is possible that the systolic function would have been improved with an extended treatment period, but further studies are needed to confirm this.

L-carnitine has shown multiple beneficial effects in the diabetic heart affirming that the balance of energy sources that the heart uses is of critical importance (Chapter 5). Even though L-carnitine transports fatty acids into the mitochondria, the mechanism of action in diabetes shows evidence of elevated carbohydrate metabolism through an increased buffering mechanism of excess acetyl-CoA, thereby relieving PDH-flux inhibition (e.g. PDK4 was reduced, PDH-flux elevated, hyperglycaemia did not progress further, β-hydroxybutyrate was reduced, and RPP recovery improved post-ischemia). An elevated transport of fatty acids might be more evident in the control animals, where in contrast to the diabetic group the animals showed increased weight loss, and some detrimental effects in *in vivo* and *ex vivo* function, while reducing PDH-flux, and TCA intermediates like glutamate, while acetylcarnitine levels stayed unchanged in the *in vivo* heart.

In summary this study implied that if there was an elevation of fatty acids (diabetes), L-carnitine could be beneficial potentially by offering an additional method to transport the excess supply of fatty acids but also by providing increased buffering of excess acetyl-CoA relieving its inhibition on PDH-flux. So instead of L-carnitine showing elevated fatty acid oxidation in diabetes it elevated buffering of acetyl-CoA (Fig. 7.3). However, L-carnitine did not appear to offer the same benefit in control hearts as there was not already an elevation of fatty acids or increased acetyl-CoA, and L-carnitine, therefore, was shifting the balance of energy supply towards fatty acid oxidation, decreasing PDH-flux (Fig. 7.3). Further studies are needed to understand the underlying mechanisms, but this thesis shows the importance of understanding substrate utilisation prior to L-carnitine treatment.

Chapter 6 showed a reduction in L-carnitine levels in the plasma with Mildronate treatment, although Mildronate treatment did not result in any *in vivo* functional changes in either the diabetic or control groups, in contrast to when treated with L-carnitine. Despite not observing any functional differences Mildronate treatment led to metabolic changes that were detected with hyperpolarized MRS. Elevated levels of PDH-flux were observed in both controls and diabetics. Mildronate reduced acetylcarnitine (AC) in the *in vivo* heart in both the controls and the diabetics, while L-carnitine elevated it but only in diabetics, AC stayed unchanged in controls. Mechanistically compared to L-carnitine supplementation, Mildronate had a similar effect on the diabetic group, but opposite effect on control hearts (Fig. 7.3). Mildronate, similarly to the L-carnitine treatment, showed improved functional recovery post-ischemia. However, Mildronate led to lower functional recovery post-ischemia in diabetes, compared to the L-carnitine treated diabetics. The findings imply that Mildronate induced recovery post-ischemia by modulating systolic function, while L-carnitine induced recovery post-ischemia by modulating diastolic function. Recovery post-ischemia is significantly improved in diabetic animals when treated with both L-carnitine and with Mildronate. However, L-carnitine shows superior recovery post-ischemia than Mildronate treatment does. As seen on Figure 7.3 the controls had improved RPP recovery post-ischemia with

Mildronate treatment but worse recovery with L-carnitine treatment. This was also observed with acute L-carnitine added to the buffer as described in Chapter 4.

	CONTROL		DIABETES	
	L-CARNITINE	MILDRONATE	L-CARNITINE	MILDRONATE
PLASMA				
Δ Blood glucose (fasted)	—	—	↓	—
L-carnitine	↑↑	↓	↑	↓
β-hydroxybutyrate	↓	—	↓	—
Triglycerides	↓	—	↓	—
***IN VIVO* FUNCTION**				
Stroke index	—	—	—	—
Ejection fraction	↓	—	↓	—
End diastolic lumen	—	—	↑	—
End systolic lumen	↑	—	↑	—
***IN VIVO* METABOLISM**				
PDH-flux	↓↓	↑	↑	↑↑
Lactate	—	—	↑	↑↑
Alanine	↑	—	↑	—
AC/PDH-flux	↑	↓	↑	↓
***EX VIVO* PERFUSION**				
RPP post-ischemia	—	↑	↑↑	↑
% RPP recovery	↓	—	↑	—
Δ Diastolic pressure	—	—	↓	—
% Systolic pressure recovery	—	↑	—	↑
% FAO/RPP post-ischemia	↓	—	↓	—

Figure 7.3: This figure summarises the key findings from the effect of L-carnitine and Mildronate on control and diabetes. The upward arrow represents a relative increase. The downward arrow represents a relative decrease. The straight line represents no change.

It might well be that by providing the heart with an opportunity to elevate fatty acid transport while at the same time enhancing carbohydrate metabolism, L-carnitine gives the diabetic heart the possibility of optimising its energy balance resulting in the best outcome. While giving Mildronate, even though carbohydrate metabolism is helpful post-ischemia, the heart is forced to reduce its fatty acid metabolism at all times, not allowing the freedom of the heart to chose the optimal fuel [46].

Even though L-carnitine was given, and it showed improvements, these hearts were not treated with insulin. Research suggests that insulin might improve the effects of L-carnitine, why further studies, adding both insulin and L-carnitine, are necessary to elucidate the effects on metabolism post-ischemia and to better understand the balance between metabolic and functional changes in diabetes. This could provide novel therapies in the future to reduce early cardiac death from diabetes.

And so these men of Hindostan,
Disputed loud and long,
Each with his own opinion
Exceeding stiff and strong,
Though each was partly in the right,
And each was partly wrong. — J.G. Saxe (the end)

8

Conclusion, Limitations, and Future Work

This work has highlighted a role for metabolic remodelling with the development of T1D and induced ischemia in the *ex vivo* heart. Treatments to elevate and reduce L-carnitine levels were employed, to elucidate the effects of metabolic and functional remodelling in diabetes and to ameliorate the detrimental effects of hyperglycaemia to the heart.

These studies were limited to a pre-clinical model of T1D that showed varying levels of hyperglycaemia, and therefore not as severe remodelling of heart function was observed. Furthermore, this work was limited to a 2-3 week treatment period, but a longer duration could provide further insight into the long-term beneficial effects of L-carnitine, maybe even as a co-treatment with insulin. Moreover matching substrate utilisation concentrations for the perfusion of diabetic hearts might provide more clear answers to fatty acid oxidation rates. This work has a potential for clinical translation, although, before this, the effect of insulin needs to be investigated, since today all T1D patients are treated with insulin, and L-carnitine might strengthen this control.

CINE MRI in combination with hyperpolarized MRI has highlighted that it could play a critical role in the diagnosis, prognosis and monitoring of treatment with L-carnitine and Mildronate in response to cardiovascular diseases in T1D.

9 Bibliography

[1] E.D. Dale Abel. “Glucose transport in the heart.” In: *Frontiers in Bioscience* 9.1 (2004), pp. 201–215.

[2] Lydia Aguilar-Bryan and Joseph Bryan. “Molecular biology of adenosine triphosphate-sensitive potassium channels”. In: *Endocrine Reviews* 20.2 (1999), pp. 101–135.

[3] Sophia Airhart et al. “A diet rich in medium-chain fatty acids improves systolic function and alters the lipidomic profile in patients with type 2 diabetes: A pilot study”. In: *Journal of Clinical Endocrinology and Metabolism* 101.2 (2016), pp. 504–512.

[4] A Akbarzadeh et al. “Induction of diabetes by streptozotocin in rats”. In: *Indian J Clin Biochem* 22.2 (2007), pp. 60–64.

[5] Muhammad Akram. “A focused review of the role of ketone bodies in health and disease”. In: *Journal of Medicinal Food* 16.11 (2013), pp. 965–967.

[6] Andrew JM Lewis. “Clinical translation of hyperpolarized magnetic resonance for cardiovascular and metabolic disease”. PhD thesis. University of Oxford, 2016.

[7] J. H. Ardenkjaer-Larsen et al. “Increase in signal-to-noise ratio of $>$ 10,000 times in liquid-state NMR”. In: *Proceedings of the National Academy of Sciences* 100.18 (2003), pp. 10158–10163.

[8] Frances M Ashcroft, Michael C Puljung, and Natascia Vedovato. *Neonatal diabetes and the KATP channel: From mutation to therapy*. 2017.

[9] Michelle L Asp et al. “Calcium mishandling in diastolic dysfunction: mechanisms and potential therapies.” In: *Biochimica et Biophysica Acta* 1833.4 (2013), pp. 895–900.

[10] Helen J Atherton et al. “Role of pyruvate dehydrogenase inhibition in the development of hypertrophy in the hyperthyroid rat heart: A combined magnetic resonance imaging and hyperpolarized magnetic resonance spectroscopy study”. In: *Circulation* 24.2 (2011), pp. 201–208.

[11] Daniel R Ball et al. “Hyperpolarized butyrate: a metabolic probe of short chain fatty acid metabolism in the heart.” In: *Magnetic Resonance in Medicine* 71.5 (2014), pp. 1663–9.

[12] Bing RJ Ballard F, Danforth W, Nagele S. “Myocardial metabolism of fatty acids”. In: *Journal of Clinical Investigation* 39 (1960), pp. 717–723.

[13] Saleem Ali Banihani, Mekki Bayachou, and Karem Alzoubi. “L-Carnitine is a calcium chelator: a reason for its useful and toxic effects in biological systems”. In: *Journal of Basic and Clinical Physiology and Pharmacology* 26.2 (2015), pp. 141–5.

[14] Jessica A. M. Bastiaansen, Matthew E. Merritt, and Arnaud Comment. “Measuring changes in substrate utilization in the myocardium in response to fasting using hyperpolarized [1-13C]butyrate and [1-13C]pyruvate”. In: *Scientific Reports* 6.1 (2016), p. 25573.

[15] Roberto Barbosa Bazotte et al. “Effects of oral L-carnitine and DL-carnitine supplementation on alloxan-diabetic rats”. In: *Brazilian Archives of Biology and Technology* 55.February (2012), pp. 81–88.

[16] Edwin D. Becker. “A brief history of nuclear magnetic resonance”. In: *Analytical Chemistry* 65.6 (1993).

[17] Guido Bellinghieri et al. “Carnitine and hemodialysis”. In: *American Journal of Kidney Diseases* 41.3 (2003), S116–S122.

[18] H. von Bibra and M. ST John Sutton. “Diastolic dysfunction in diabetes and the metabolic syndrome: promising potential for diagnosis and prognosis”. In: *Diabetologia* 53.6 (2010), pp. 1033–1045.

[19] F. Bloch. “Nuclear induction”. In: *Physical Review* 70.7-8 (1946), pp. 460–474.

[20] Ernest A. Boehm et al. “Increased uncoupling proteins and decreased efficiency in palmitate-perfused hyperthyroid rat heart”. In: *American Journal of Physiology-Heart and Circulatory Physiology* 280.3 (2001), H977–H983.

[21] R H Bowman. “Effects of diabetes, fatty acids, and ketone bodies on tricarboxylic acid cycle metabolism in the perfused rat heart”. In: *Journal of Biological Chemistry* 241.13 (1966), pp. 3041–8.

[22] Linda J. Brady et al. “Pharmacologic action of l-carnitine on hypertriglyceridemia in obese Zucker rats”. In: *Metabolism* 35.6 (1986), pp. 555–562.

[23] R Bränström et al. “Long chain coenzyme A esters activate the pore-forming subunit (Kir6. 2) of the ATP-regulated potassium channel.” In: *The Journal of Biological Chemistry* 273.47 (1998), pp. 31395–400.

[24] Melissa F. Brereton et al. “Hyperglycaemia induces metabolic dysfunction and glycogen accumulation in pancreatic β-cells”. In: *Nature Communications* 7 (2016), p. 13496.

[25] Melissa F. Brereton et al. “Reversible changes in pancreatic islet structure and function produced by elevated blood glucose”. In: *Nature Communications* 5.1 (2014), p. 4639.

[26] T L Broderick, D J Paulson, and M Gillis. “Effects of propionyl-carnitine on mitochondrial respiration and post-ischaemic cardiac function in the ischaemic underperfused diabetic rat heart.” In: *Drugs in RD* 5.4 (2004), pp. 191–201.

[27] T L Broderick, H A Quinney, and G D Lopaschuk. “L-carnitine increases glucose metabolism and mechanical function following ischaemia in diabetic rat heart.” In: *Cardiovascular Research* 29.3 (1995), pp. 373–8.

[28] T L Broderick et al. “Beneficial effect of carnitine on mechanical recovery of rat Hearts reperfused after a transient period of global ischemia is accompanied by a stimulation of glucose oxidation.” In: *Circulation* 87.3 (1993), pp. 972–81.

[29] Tom L. Broderick, H. Arthur Quinney, and Gary D. Lopaschuk. “Carnitine stimulation of glucose oxidation in the fatty acid perfused isolated working rat heart”. In: *Journal of Biological Chemistry* 267.6 (1992), pp. 3758–3763.

[30] Rebecca J Brown, Ninet Sinaii, and Kristina I Rother. “Too much glucagon, too little insulin: time course of pancreatic islet dysfunction in new-onset type 1 diabetes.” In: *Diabetes Care* 31.7 (2008), pp. 1403–4.

[31] Heiko Bugger and E. Dale Abel. “Molecular mechanisms of diabetic cardiomyopathy”. In: *Diabetologia* 57.4 (2014), pp. 660–671.

[32] Lorenzo A Calò et al. “Antioxidant effect of l-carnitine and its short chain esters Relevance for the protection from oxidative stress related cardiovascular damage”. In: *International Journal of Cardiology* 107 (2006), pp. 54–60.

[33] Menotti Calvani, Emilia Reda, and Edoardo Arrigoni-Martelli. “Regulation by carnitine of myocardial fatty acid and carbohydrate metabolism under normal and pathological conditions”. In: *Basic Research in Cardiology* 95.2 (2000), pp. 75–83.

[34] Matt C. Cave et al. “Obesity, inflammation, and the potential application of pharmaconutrition.” In: *Nutrition in Clinical Practice* 23.1 (2008), pp. 16–34.

[35] Sharon A. Center et al. “Influence of dietary supplementation with L-carnitine on metabolic rate, fatty acid oxidation, body condition, and weight loss in overweight cats”. In: *American Journal of Veterinary Research* 73.7 (2012), pp. 1002–1015.

[36] Youn-Soo Cha. “Effects of L-carnitine on obesity, diabetes, and as an ergogenic aid”. In: *Asia Pac J Clin Nut* 17.S1 (2008), pp. 306–308.

[37] J C Chatham and J R Forder. “A 13C-NMR study of glucose oxidation in the intact functioning rat heart following diabetes-induced cardiomyopathy”. In: *Journal of Molecular and Cellular Cardiology* 25.10 (1993), pp. 1203–1213.

[38] J C Chatham and J R Forder. “Relationship between cardiac function and substrate oxidation in hearts of diabetic rats.” In: *The American Journal of Physiology* 273.1 Pt 2 (1997), H52–8.

[39] Myriam M. Chaumeil et al. “Hyperpolarized 13 C MR imaging detects no lactate production in mutant IDH1 gliomas: Implications for diagnosis and response monitoring”. In: *NeuroImage: Clinical* 12 (2016), pp. 180–189.

[40] Albert P. Chen et al. “Using [1-13C]lactic acid for hyperpolarized 13 C MR cardiac studies.” In: *Magnetic Resonance in Medicine* 73.6 (2015), pp. 2087–2093.

[41] H. Balvin Chua and Earl Shrago. “Reversible inhibition of adenine nucleotide translocation by long chain acyl-CoA esters in bovine heart mitochondria and inverted submitochondrial particles”. In: *The Journal of Biological Chemistry* 252.19 (1977), pp. 6711–6714.

[42] A. Comment et al. “Design and performance of a DNP prepolarizer coupled to a rodent MRI scanner”. In: *Concepts in Magnetic Resonance Part B: Magnetic Resonance Engineering* 31B.4 (2007), pp. 255–269.

[43] Virginia Alice Vieira da Costa and Lucia Marques Vianna. “Biological response of spontaneously hypertensive rats to the streptozotocin administration”. In: *Brazilian Archives of Biology and Technology* 51.1 (2008), pp. 43–48.

[44] M. Costell, J.E. O’Connor, and S. Grisolía. “Age-dependent decrease of carnitine content in muscle of mice and humans”. In: *Biochemical and Biophysical Research Communications* 161.3 (1989), pp. 1135–1143.

[45] Bernard Cosyns et al. “Effect of streptozotocin-induced diabetes on left ventricular function in adult rats: an in vivo Pinhole Gated SPECT study.” In: *Cardiovascular Diabetology* 6 (2007), p. 30.

[46] Robert Crayhon. *The carnitine miracle: The supernutrient program that promotes high energy, fat burning, heart health, brain wellness, and longevity*. New York: M. Evans and Company, 2000.

[47] Botond Csiky et al. “Effect of hemodialysis session on the dynamics of carnitine ester profile changes in l-carnitine pretreated end-stage renal disease patients”. In: *International Urology and Nephrology* 45.3 (2013), pp. 847–855.

[48] Charles H. Cunningham et al. “Hyperpolarized 13C Metabolic MRI of the Human HeartNovelty and Significance”. In: *Circulation Research* 119.11 (2016), pp. 1177–1182.

[49] Maija Dambrova. “Mildronate cardioprotective action through carnitine-lowering effect”. In: *Trends in Cardiovascular Medicine* 12.6 (2002), pp. 275–279.

[50] Maija Dambrova et al. “Carnitine biosynthesis. β-hydroxylation of trimethyllysine by an α-ketoglutarate-dependent mitochondrial dioxygenase”. In: *Pharmacological Research* (2016).

[51] A De Vos et al. “Human and rat beta cells differ in glucose transporter but not in glucokinase gene expression.” In: *Journal of Clinical Investigation* 96.5 (1995), pp. 2489–2495.

[52] T. Deckert, J. E. Poulsen, and M. Larsen. “Prognosis of diabetics with diabetes onset before the age of thirtyone”. In: *Diabetologia* 14.6 (1978), pp. 371–377.

[53] C. Depre, J. L. Vanoverschelde, and H. Taegtmeyer. “Glucose for the heart.” In: *Circulation* 99.4 (1999), pp. 578–88.

[54] James J. DiNicolantonio et al. “L-carnitine in the secondary prevention of cardiovascular disease: systematic review and meta-analysis”. In: *Mayo Clinic Proceedings* 88.6 (2013), pp. 544–551.

[55] Diabetes UK. *Diabetes: FACTS and stats*. Tech. rep. 2015.

[56] R. Díaz et al. “Carnitine worsens both injury and recovery of contractile function after transient ischemia in perfused rat heart”. In: *Journal of Physiology and Biochemistry* 64.1 (2008), pp. 1–8.

[57] Michael S. Dodd et al. “In vivo mouse cardiac hyperpolarized magnetic resonance spectroscopy”. In: *Journal of Cardiovascular Magnetic Resonance* 15.1 (2013), p. 19.

[58] Torsten Doenst, Tien Dung Nguyen, and E Dale Abel. "Cardiac metabolism in heart failure: implications beyond ATP production." In: *Circulation Research* 113.6 (2013), pp. 709–24.

[59] Giovanni Donato Aquaro and Luca Menichetti. "Hyperpolarized 13C magnetic resonance spectroscopy are we ready for metabolic imaging?" In: *Circ Cardiovasc Imaging* 7 (2014), pp. 854–856.

[60] Hakan Doneray et al. "Permanent neonatal diabetes mellitus caused by a novel mutation in the KCNJ11 gene". In: *Journal of Pediatric Endocrinology and Metabolism* 27.3-4 (2014), pp. 367–71.

[61] Stephan Düwel et al. "Multiparametric human hepatocellular carcinoma characterization and therapy response evaluation by hyperpolarized 13C MRSI". In: *NMR in Biomedicine* 29.7 (2016), pp. 952–960.

[62] Dwight G Nishimura. *Principles of magnetic resonance imaging*. 1.1. Stanford University, 2010, pp. 1–224.

[63] Hassan I.H. El-Sayyad et al. "Impairment of bone growth of wistar rat fetuses of diabetic and hypercholesterolemic mothers". In: *Egyptian Journal of Basic and Applied Sciences* 2.1 (2015), pp. 1–12.

[64] Chinedum Ogbonnaya Eleazu et al. "Review of the mechanism of cell death resulting from streptozotocin challenge in experimental animals, its practical use and potential risk to humans." In: *Journal of Diabetes and Metabolic Disorders* 12.1 (2013), p. 60.

[65] Sarah D de Ferranti et al. "Type 1 diabetes mellitus and cardiovascular disease: a scientific statement from the American Heart Association and American Diabetes Association." In: *Diabetes Care* 37.10 (2014), pp. 2843–63.

[66] Anita Ferraretto et al. "L-Carnitine activates calcium signaling in human osteoblasts". In: *Journal of Functional Foods* 47 (2018), pp. 270–278.

[67] Roberto Ferrari et al. "Therapeutic effects of L-carnitine and propionyl-L-carnitine on cardiovascular diseases: A review". In: *Annals of the New York Academy of Sciences* 1033.1 (2004), pp. 79–91.

[68] JL Flanagan et al. "Role of carnitine in disease". In: *Nutrition & Metabolism* 7.1 (2010), p. 30.

[69] Alessandra Flori et al. "Real-time cardiac metabolism assessed with hyperpolarized [1-13C]acetate in a large-animal model." In: *Contrast Media & Molecular Imaging* 10.3 (2015), pp. 194–202.

[70] Daniel W. Foster. "The role of the carnitine system in human metabolism". In: *Annals of the New York academy of sciences* 1033 (2004).

[71] Keith N Frayn. *Metabolic regulation: a human perspective*. Wiley-Blackwell Pub, 2010, p. 371.

[72] Lijun Fu, Meirong Huang, and Shubao Chen. "Primary carnitine deficiency and cardiomyopathy." In: *Korean circulation journal* 43.12 (2013), pp. 785–92.

[73] Stuart D. R. Galloway, Thomas P. Craig, and Stephen J. Cleland. "Effects of oral l-carnitine supplementation on insulin sensitivity indices in response to glucose feeding in lean and overweight/obese males". In: *Amino Acids* 41.2 (2011), pp. 507–515.

[74] Pamela B. Garlick et al. “Phosphorus NMR studies on perfused heart”. In: *Biochemical and Biophysical Research Communications* 74.3 (1977), pp. 1256–1262.

[75] Giles, Lucia F. “In vivo assessment of substrate utilisation in the hypertrophied heart; The role of glycolysis and glucose oxidation in hypertrophic progression”. PhD thesis. University of Oxford, 2016.

[76] Christophe A Girard et al. “Expression of an activating mutation in the gene encoding the KATP channel subunit Kir6.2 in mouse pancreatic beta cells recapitulates neonatal diabetes.” In: *The Journal of Clinical Investigation* 119.1 (2009), pp. 80–90.

[77] Pietro Lo Giudice, Mario Bonomini, and Arduino Arduini. “A Moderate Carnitine Deficiency Exacerbates Isoproterenol-Induced Myocardial Injury in Rats”. In: *Cardiovascular Drugs and Therapy* 30.2 (2016), pp. 119–127.

[78] Klaes Golman and J. Stefan Petersson. “Metabolic imaging and other applications of hyperpolarized 13C1”. In: *Academic Radiology* 13.8 (2006), pp. 932–942.

[79] Klaes Golman, René in ’t Zandt, and Mikkel Thaning. “Real-time metabolic imaging”. In: *Proceedings of the National Academy of Sciences of the United States of America* 103.30 (2006), pp. 11270–5.

[80] Klaes Golman et al. “Molecular imaging using hyperpolarized 13C”. In: *The British Journal of Radiology* 76.2 (2003), S118–S127.

[81] Luis A. Gómez, Shi-Hua D. Heath, and Tory M. Hagen. “Acetyl-l-carnitine supplementation reverses the age-related decline in carnitine palmitoyltransferase 1 (CPT1) activity in interfibrillar mitochondria without changing the l-carnitine content in the rat heart”. In: *Mechanisms of Ageing and Development* 133.2-3 (2012), pp. 99–106.

[82] Manuel Gonzalez-Ortiz et al. “Effect of Oral L-carnitine administration on insulin sensitivity and lipid profile in type 2 diabetes mellitus patients”. In: *Annals of Nutrition and Metabolism* 52.4 (2008), pp. 335–338.

[83] Christian Görgens et al. “Mildronate (Meldonium) in professional sports - monitoring doping control urine samples using hydrophilic interaction liquid chromatography - high resolution/high accuracy mass spectrometry.” In: *Drug Testing and Analysis* 7.11-12 (2015), pp. 973–9.

[84] H. Karl Greenblatt and David J. Greenblatt. “Meldonium (Mildronate): A Performance-Enhancing Drug?” In: *Clinical Pharmacology in Drug Development* 5.3 (2016), pp. 167–169.

[85] R. Grempler et al. “Empagliflozin, a novel selective sodium glucose cotransporter-2 (SGLT-2) inhibitor: Characterisation and comparison with other SGLT-2 inhibitors”. In: *Diabetes, Obesity and Metabolism* 14.1 (2012), pp. 83–90.

[86] F M Gribble et al. “Mechanism of cloned ATP-sensitive potassium channel activation by oleoyl-CoA.” In: *The Journal of Biological Chemistry* 273.41 (1998), pp. 26383–7.

[87] WADA Laboratory Expert Group. *Minimum required performance levels for detection and identification of non-threshold substances*. Tech. rep. 2014.

[88] Jinn-Yuh Guha et al. *Epidermal Growth Factor in Renal Hypertrophy in Streptozotocin-Diabetic Rats*. Tech. rep. 1991, pp. 641–647.

[89] A Haase et al. "FLASH imaging. Rapid NMR imaging using low flip-angle pulses". In: *Journal of Magnetic Resonance* 67.2 (1986), pp. 258–266.

[90] Z S Hakim, B K Patel, and R K Goyal. "Effects of chronic ramipril treatment in streptozotocin-induced diabetic rats." In: *Indian Journal of Physiology and Pharmacology* 41.4 (1997), pp. 353–60.

[91] P. Harper, C. E. Elwin, and G. Cederblad. "Pharmacokinetics of intravenous and oral bolus doses of L-carnitine in healthy subjects". In: *European Journal of Clinical Pharmacology* 35.5 (1988), pp. 555–562.

[92] L Heather et al. "Fatty acid transporter levels and palmitate oxidation rate correlate with ejection fraction in the infarcted rat heart". In: *Cardiovascular Research* 72.3 (2006), pp. 430–437.

[93] Lisa C. Heather and Kieran Clarke. "Metabolism, hypoxia and the diabetic heart". In: *Journal of Molecular and Cellular Cardiology* 50.4 (2011), pp. 598–605.

[94] George Hermann and George M. Decherd. "The chemical nature of heart failure". In: *Annals of Internal Medicine* 12.8 (1939), p. 1233.

[95] Young Mi Hong, Hae Soon Kim, and Hye-Ran Yoon. "Serum lipid and fatty acid profiles in adriamycin-treated rats after administration of L-carnitine." In: *Pediatric Research* 51.2 (2002), pp. 249–55.

[96] John D Horowitz et al. "Modulation of myocardial metabolism: an emerging therapeutic principle". In: *Current Opinion in Cardiology* 25.4 (2010), pp. 329–334.

[97] F. C. Howarth et al. "Long-term effects of streptozotocin-induced diabetes on the electrocardiogram, physical activity and body temperature in rats". In: *Experimental Physiology* 90.6 (2005), pp. 827–835.

[98] J A Idell-Wenger, L W Grotyohann, and J R Neely. "Coenzyme A and carnitine distribution in normal and ischemic hearts." In: *The Journal of Biological Chemistry* 253.12 (1978), pp. 4310–8.

[99] I Ilias et al. "L-carnitine and acetyl-L-carnitine in the treatment of complications associated with HIV infection and antiretroviral therapy". In: *Mitochondrion* 4.2-3 (2004), pp. 163–168.

[100] Sabino Iliceto et al. "Effects of L-carnitine administration on left ventricular remodeling after acute anterior myocardial infarction: The L-carnitine Ecocardiografia Digitalizzata Infarto Miocardico (CEDIM) trial". In: *Journal of the American College of Cardiology* 26.2 (1995), pp. 380–387.

[101] Richard A Insel et al. "Staging presymptomatic type 1 diabetes: a scientific statement of JDRF, the Endocrine Society, and the American Diabetes Association." In: *Diabetes Care* 38.10 (2015), pp. 1964–74.

[102] International Diabetes Federation. *IDF Diabetes Atlas*. 2017.

[103] C Iribarren et al. "Glycemic control and heart failure among adult patients with diabetes." In: *Circulation* 103.22 (2001), pp. 2668–73.

[104] Jagdip Jaswal and John Ussher. “Myocardial fatty acid utilization as a determant of cardiac efficiency and function”. In: *Clinical Lipidology* 4.3 (2017), pp. 379–389.

[105] Guo-Jun Jiang et al. “Metformin ameliorates insulitis in STZ-induced diabetic mice”. In: *PeerJ* 5 (2017).

[106] Xie Jiang, Zeng Qiutang, and Wang Le. “The protective effect of L-carnitine on ischemia-reperfusion heart”. In: *Journal of Huazhong University of Science and Technology Med Sci]* 26.2 (2006), pp. 188–191.

[107] J.W. de Jong and R. Ferrari. *The Carnitine System - A New Therapeutical Approach to Cardiovascular Diseases*. 1995.

[108] Andrew M Kates et al. “Impact of aging on substrate metabolism by the human heart”. In: *Journal of the American College of Cardiology* 41.2 (2003), pp. 293–299.

[109] Barry S. Kendler. “Carnitine: An overview of its role in preventive medicine”. In: *Preventive Medicine* 15.4 (1986), pp. 373–390.

[110] K. R. Keshari et al. “Hyperpolarized 13C-Pyruvate Magnetic Resonance Reveals Rapid Lactate Export in Metastatic Renal Cell Carcinomas”. In: *Cancer Research* 73.2 (2013), pp. 529–538.

[111] Girish Kewalramani et al. “AMPK control of myocardial fatty acid metabolism fluctuates with the intensity of insulin-deficient diabetes”. In: *Journal of Molecular and Cellular Cardiology* 42.2 (2007), pp. 333–342.

[112] Saman Khalatbari-Soltani and Hadi Tabibi. “Inflammation and L-carnitine therapy in hemodialysis patients: a review”. In: *Clinical and Experimental Nephrology* 19.3 (2015), pp. 331–335.

[113] A Kobayashi et al. “Effects of L-carnitine on ventricular arrhythmias after coronary reperfusion.” In: *Japanese Circulation Journal* 47.5 (1983), pp. 536–42.

[114] Ulrich Koellisch et al. “Metabolic imaging of hyperpolarized [1-13C]acetate and [1-13C]acetylcarnitine - investigation of the influence of dobutamine induced stress.” In: *Magnetic Resonance in Medicine* 74.4 (2015), pp. 1011–1018.

[115] Robert A Koeth et al. “Intestinal microbiota metabolism of l-carnitine, a nutrient in red meat, promotes atherosclerosis”. In: *Nature Medicine* 19.5 (2013), pp. 576–585.

[116] V A Koivisto et al. “Cardiovascular disease and its risk factors in IDDM in Europe. EURODIAB IDDM Complications Study Group.” In: *Diabetes Care* 19.7 (1996), pp. 689–97.

[117] Stephen C. Kolwicz, Suneet Purohit, and Rong Tian. “Cardiac metabolism and its interactions with contraction, growth, and survival of cardiomyocytes”. In: *Circulation Research* 113.5 (2013), pp. 603–616.

[118] Mitsuhisa Komatsu et al. “Glucose-stimulated insulin secretion: A newer perspective.” In: *Journal of diabetes investigation* 4.6 (2013), pp. 511–6.

[119] J C Koster et al. “Targeted overactivity of beta cell K(ATP) channels induces profound neonatal diabetes.” In: *Cell* 100.6 (2000), pp. 645–54.

[120] Janis Kuka et al. “Suppression of intestinal microbiota-dependent production of pro-atherogenic trimethylamine N-oxide by shifting L-carnitine microbial degradation”. In: *Life Sciences* 117.2 (2014), pp. 84–92.

[121] Janis Kuka et al. “The Cardioprotective effect of Mildronate is diminished after co-treatment with L-carnitine”. In: *J Cardiovasc Pharmacol Ther.* 17.2 (2012).

[122] John L. Lachin. “Mortality in Type 1 Diabetes in the DCCT/EDIC Versus the General Population”. In: *Diabetes Care* 39.8 (2016).

[123] H J Lamb et al. “Diastolic dysfunction in hypertensive heart disease is associated with altered myocardial metabolism.” In: *Circulation* 99.17 (1999), pp. 2261–7.

[124] R Lango et al. “Influence of L-carnitine and its derivatives on myocardial metabolism and function in ischemic heart disease and during cardiopulmonary bypass.” In: *Cardiovascular Research* 51.1 (2001), pp. 21–9.

[125] Christoffer Laustsen et al. “Assessment of early diabetic renal changes with hyperpolarized [1-13C]pyruvate”. In: *Diabetes/Metabolism Research and Reviews* 29.2 (2013), pp. 125–129.

[126] Lydia M Le Page et al. “Increasing Pyruvate Dehydrogenase Flux as a Treatment for Diabetic Cardiomyopathy: A Combined 13C Hyperpolarized Magnetic Resonance and Echocardiography Study.” In: *Diabetes* 64.8 (2015), pp. 2735–43.

[127] Lydia M. Le Page et al. “Simultaneous in vivo assessment of cardiac and hepatic metabolism in the diabetic rat using hyperpolarized MRS”. In: *NMR in Biomedicine* 29.12 (2016), pp. 1759–1767.

[128] Siang Ing Lee et al. “Cardiovascular disease and type 1 diabetes: prevalence, prediction and management in an ageing population.” In: *Therapeutic advances in chronic disease* 6.6 (2015), pp. 347–74.

[129] S. Lenzen. “The mechanisms of alloxan- and streptozotocin-induced diabetes”. In: *Diabetologia* 51.2 (2008), pp. 216–226.

[130] Jin-Lian Li et al. “Effects of L-carnitine against oxidative stress in human hepatocytes: involvement of peroxisome proliferator-activated receptor alpha”. In: *Journal of Biomedical Science* 19.1 (2012), p. 32.

[131] A J Liedtke et al. “Properties of carnitine incorporation in working swine hearts. Effects of coronary flow, ischemia, and excess fatty acids.” In: *Circulation Research* 50.6 (1982), pp. 767–74.

[132] Edgars Liepinsh et al. “Anti-diabetic effects of mildronate alone or in combination with metformin in obese Zucker rats”. In: *European Journal of Pharmacology* 658.2-3 (2011), pp. 277–283.

[133] Edgars Liepinsh et al. “Effects of long-term mildronate treatment on cardiac and liver functions in rats”. In: *Basic & Clinical Pharmacology & Toxicology* 105.6 (2009), pp. 387–394.

[134] Edgars Liepinsh et al. “Mildronate, an inhibitor of carnitine biosynthesis, induces an increase in gamma-butyrobetaine contents and cardioprotection in isolated rat heart infarction”. In: *Journal of Cardiovascular Pharmacology* 48.6 (2006), pp. 314–319.

[135] Edgars Liepinsh et al. “Mildronate decreases carnitine availability and up-regulates glucose uptake and related gene expression in the mouse heart”. In: *Life Sciences* 83.17-18 (2008), pp. 613–619.

[136] Edgars Liepinsh et al. “Mildronate treatment alters γ-butyrobetaine and L-carnitine concentrations in healthy volunteers”. In: *Journal of Pharmacy and Pharmacology* 63.9 (2011), pp. 1195–1201.

[137] Edgars Liepinsh et al. “Protective effects of mildronate in an experimental model of type 2 diabetes in Goto-Kakizaki rats”. In: *British Journal of Pharmacology* 157.8 (2009), pp. 1549–1556.

[138] Marcus Lind et al. “Glycaemic control and incidence of heart failure in 20 985 patients with type 1 diabetes: an observational study”. In: *The Lancet* 378.9786 (2011), pp. 140–146.

[139] T C Linn et al. “Alpha-keto acid dehydrogenase complexes. X. Regulation of the activity of the pyruvate dehydrogenase complex from beef kidney mitochondria by phosphorylation and dephosphorylation.” In: *Proceedings of the National Academy of Sciences of the United States of America* 62.1 (1969), pp. 234–41.

[140] Que Liu et al. “High levels of fatty acids delay the recoveryof intracellular pH and cardiac efficiency inpost-ischemic hearts by inhibiting glucose oxidation”. In: *Journal of the American College of Cardiology* 39.4 (2002), pp. 718–725.

[141] Xiao-Ying Liu et al. “Left ventricular deformation associated with cardiomyocyte Ca 2+ transients delay in early stage of low-dose of STZ and high-fat diet induced type 2 diabetic rats”. In: *BMC Cardiovasc Diord.* 16.41 (2016).

[142] Rajprasad Loganathan et al. “Cardiac dysfunction in the diabetic rat: quantitative evaluation using high resolution magnetic resonance imaging”. In: *Cardiovascular Diabetology* 5.1 (2006), pp. 5–7.

[143] Nicola Longo et al. “Disorders of carnitine transport and the carnitine cycle”. In: *American Journal of Medical Genetics Part C: Seminars in Medical Genetics* 142C.2 (2006), pp. 77–85.

[144] G D Lopaschuk and Rick L Barr. “Measurements of fatty acid and carbohydrate metabolism in the isolated working rat heart”. In: *Molecular and Cellular BiochemistryMol Cell Biochem* 172.172 (1997), pp. 137–147.

[145] G D. Lopaschuk and J R. Ussher. “Evolving concepts of myocardial energy metabolism”. In: *Circulation Research* 119.11 (2016), pp. 1173–1176.

[146] G D Lopaschuk et al. “Glucose and palmitate oxidation in isolated working rat hearts reperfused after a period of transient global ischemia.” In: *Circulation Research* 66.2 (1990), pp. 546–53.

[147] G D Lopaschuk et al. “Myocardial fatty acid metabolism in health and disease”. In: *Physiological Reviews* 90.1 (2010), pp. 207–258.

[148] H Löster. “Effects of L-carnitine and its derivatives-studies on isolated hearts”. In: *Monatshefte fur Chemie* 136 (2005), pp. 1443–1466.

[149] H Löster and M Punzel. “Effects of L-carnitine on mechanical recovery of isolated rat hearts in relation to the perfusion with glucose and palmitate.” In: *Molecular and cellular biochemistry* 185.1-2 (1998), pp. 65–75.

[150] W Lysiak et al. “Quantitation of the effect of L-carnitine on the levels of acid-soluble short-chain acyl-CoA and CoASH in rat heart and liver mitochondria.” In: *The Journal of biological chemistry* 263.3 (1988), pp. 1151–6.

[151] Eaton M Mackay et al. “The relation of fasting ketosis in the rat to the preceding diet and the liver fat”. In: *J. Biol. Chem* 141 (1941), pp. 889–896.

[152] J Maddahi et al. “Role of thallium-201 and PET imaging in evaluation of myocardial viability and management of patients with coronary artery disease and left ventricular dysfunction.” In: *Society of Nuclear Medicine* 35.4 (1994), pp. 707–15.

[153] Dimitrios Mamoulakis et al. “Carnitine deficiency in children and adolescents with type 1 diabetes”. In: *Journal of Diabetes and its Complications* 18.5 (2004), pp. 271–274.

[154] Latt S Mansor et al. “Cardiac metabolism in a new rat model of type 2 diabetes using high-fat diet with low dose streptozotocin”. In: *Cardiovascular Diabetology* 24.12 (2013).

[155] G la Marca et al. “Children who develop type 1 diabetes early in life show low levels of carnitine and amino acids at birth: does this finding shed light on the etiopathogenesis of the disease?” In: *Nutrition and Diabetes* 3.10 (2013), e94–e94.

[156] E Markworth, C Schwanstecher, and M Schwanstecher. “ATP4- mediates closure of pancreatic beta-cell ATP-sensitive potassium channels by interaction with 1 of 4 identical sites.” In: *Diabetes* 49.9 (2000), pp. 1413–8.

[157] S Marshak et al. “Impaired beta-cell functions induced by chronic exposure of cultured human pancreatic islets to high glucose.” In: *Diabetes* 48.6 (1999), pp. 1230–6.

[158] Dirk Mayer et al. “Application of hyperpolarized [1-13C]lactate for the in vivo investigation of cardiac metabolism”. In: *NMR in Biomedicine* 25.10 (2012), pp. 1119–1124.

[159] Pradip K Mazumder et al. “Impaired cardiac efficiency and increased fatty acid oxidation in insulin-resistant ob/ob mouse hearts.” In: *Diabetes* 53.9 (2004), pp. 2366–74.

[160] Stephen A. McClave et al. “Obesity, inflammation, and pharmaconutrition in critical illness”. In: *Nutrition* 30.4 (2014), pp. 492–494.

[161] J D Mcgarry et al. “A possible role for malonyl-CoA in the regulation of hepatic fatty acid oxidation and ketogenesis. A possible role for malonyl-CoA in the regulation of hepatic fatty acid oxidation and ketogenesis”. In: *J Clin Invest* 60.1 (1977), pp. 265–270.

[162] Jurgen M Meier et al. “Studies of the development of diabetic ketosis in the rat”. In: *J Lipid Res.* 13.2 (1972), pp. 228–233.

[163] Eva O Melin et al. “Abdominal obesity in type 1 diabetes associated with gender, cardiovascular risk factors and complications, and difficulties achieving treatment targets: a cross sectional study at a secondary care diabetes clinic”. In: *BMC Others* 14.5 (2018).

[164] Snehal Nitin Mestry et al. “Attenuation of diabetic nephropathy in streptozotocin-induced diabetic rats by Punica granatum Linn. leaves extract”. In: *Journal of Traditional and Complementary Medicine* 7.3 (2017), pp. 273–280.

[165] Jose L Miguel-Carrasco et al. “The role of inflammatory markers in the cardioprotective effect of L-carnitine in L-NAME-induced hypertension.” In: *American Journal of Hypertension* 21.11 (2008), pp. 1231–7.

[166] Takayuki Miki et al. “Diabetic cardiomyopathy: pathophysiology and clinical features.” In: *Heart failure reviews* 18.2 (2013), pp. 149–66.

[167] Geltrude Mingrone. “Carnitine in type 2 diabetes”. In: *Annals of the New York Academy of Sciences* 1033.1 (2004), pp. 99–107.

[168] Geltrude Mingrone et al. “L-Carnitine improves glucose disposal in type 2 diabetic patients”. In: *Journal of the American College of Nutrition* 18.1 (1999), pp. 77–82.

[169] Hidekazu Miyazaki et al. “Myocyte remodeling in streptozotocin-induced diabetic heart”. In: *Journal of Cardiac Failure* 5.3 (1999), p. 56.

[170] Stuart A Montgomery, L J Thal, and R Amrein. “Meta-analysis of double blind randomized controlled clinical trials of acetyl-L-carnitine versus placebo in the treatment of mild cognitive impairment and mild Alzheimer’s disease.” In: *International Clinical Psychopharmacology* 18.2 (2003), pp. 61–71.

[171] Cornelius von Morze et al. “Detection of localized changes in the metabolism of hyperpolarized gluconeogenic precursors 13 C-lactate and 13 C-pyruvate in kidney and liver.” In: *Magnetic Resonance in Medicine* 77.4 (2017), pp. 1429–1437.

[172] Cornelius von Morze et al. “Hyperpolarized [13C]ketobutyrate, a molecular analog of pyruvate with modified specificity for LDH isoforms.” In: *Magnetic Resonance in Medicine* 75.5 (2016), pp. 1894–1900.

[173] Katherine Motyl and Laura R Mccabe. “Streptozotocin, type I diabetes severity and bone”. In: *Biol Proced Online* 11 (2009), pp. 296–315.

[174] Y Murakami et al. “Myocardial oxygenation during high work states in hearts with postinfarction remodeling.” In: *Circulation* 99.7 (1999), pp. 942–8.

[175] M. Najafi et al. “Antiarrhythmic and arrhythmogenic effects of L-carnitine in ischemia and reperfusion”. In: *Bulletin of Experimental Biology and Medicine* 146.2 (2008), pp. 210–213.

[176] Katarzyna A Nalqcz et al. “Carnitine - A known compound, a novel function in neural cells”. In: *Acta Neurobiologiae Experimentalis* 56.2 (1996), pp. 597–609.

[177] Sarah J Nelson et al. “Metabolic imaging of patients with prostate cancer using hyperpolarized [1-^{13}C]pyruvate.” In: *Science Translational medicine* 5.198 (2013), 198ra108.

[178] S Neubauer et al. “Contributions of 31P-magnetic resonance spectroscopy to the understanding of dilated heart muscle disease.” In: *European Heart Journal* 16 Suppl O (1995), pp. 115–8.

[179] Stefan Neubauer. “The failing heart — An engine out of fuel”. In: *New England Journal of Medicine* 356.11 (2007), pp. 1140–1151.

[180] R Nishimura et al. “Mortality trends in type 1 diabetes. The Allegheny County (Pennsylvania) Registry 1965-1999.” In: *Diabetes Care* 24.5 (2001), pp. 823–7.

[181] Katerina Novakova et al. “Effect of l-carnitine supplementation on the body carnitine pool, skeletal muscle energy metabolism and physical performance in male vegetarians”. In: *European Journal of Nutrition* 55.1 (2016), pp. 207–217.

[182] Thomas J. Nowak and A. Gordon. Handford. *Essentials of pathophysiology: concepts and applications for health care professionals*. McGraw-Hill, 1999, p. 696.

[183] Christoph J Olbrlcht, Beate Geissinger, and Elisabeth Gutjahr. “Renal hypertrophy in streptozotocin diabetic rats: Role of proteolytic lysosomal enzymes with the technical assistance of”. In: *Laboratory Investigation* 41.4 (1992), pp. 966–972.

[184] A L Olson and J E Pessin. “Structure, function, and regulation of the mammalian facilitative glucose transporter gene family”. In: *Annual Review of Nutrition* 16.1 (1996), pp. 235–256.

[185] Trevor J Orchard et al. “Type 1 diabetes and coronary artery disease.” In: *Diabetes Care* 29.11 (2006), pp. 2528–38.

[186] Albert W. Overhauser. “Polarization of nuclei in metals”. In: *Physical Review* 92.2 (1953), pp. 411–415.

[187] R O A Ozório. “Dietary L-carnitine and energy and lipid metabolism in African catfish (Clarias gariepinus) juveniles”. PhD thesis. Wageningen University, 2001, pp. 1–144.

[188] I. Park, S.J. Nelson, and J.F. Talbott. “In vivo monitoring of rat spinal cord metabolism using hyperpolarized carbon-13 MR spectroscopic imaging”. In: *American Journal of Neuroradiology* 37.12 (2016), pp. 2407–2409.

[189] Jae Mo Park et al. “Volumetric spiral chemical shift imaging of hyperpolarized [2-13C]pyruvate in a rat c6 glioma model”. In: *Magnetic Resonance in Medicine* 75.3 (2016), pp. 973–984.

[190] Mamatha B Patil and Nishkal Prabhu A Burji. “Echocardiographic evaluation of diastolic dysfunction in asymptomatic type 2 diabetes mellitus.” In: *The Journal of the Association of Physicians of India* 60 (2012), pp. 23–6.

[191] D J Paulson and A L Shug. “Effects of carnitine on the ischemic arrested heart”. In: 77.4 (1982), pp. 460–463.

[192] Dennis J Paulson and M F Crass. “Endogenous triacylglycerol metabolism in diabetic heart”. In: 11.4 (1982), pp. 1084–1094.

[193] Dennis J. Paulson and Austin L. Shug. “Inhibition of the adenine nucleotide translocator by matrix-localized palmityl-CoA in rat heart mitochondria”. In: *Biochimica et Biophysica Acta* 766.1 (1984), pp. 70–76.

[194] Dennis J. Paulson et al. “Improvement of myocardial function in diabetic rats after treatment with L-carnitine”. In: *Metabolism* 33.4 (1984), pp. 358–363.

[195] Ewan R. Pearson et al. “Switching from insulin to oral sulfonylureas in patients with diabetes due to kir6.2 mutations”. In: *New England Journal of Medicine* 355.5 (2006), pp. 467–477.

[196] D Pennell et al. “Clinical indications for cardiovascular magnetic resonance (CMR): Consensus Panel report?” In: *European Heart Journal* 25.21 (2004), pp. 1940–1965.

[197] Isabelle Pham et al. “Evidence for a specific diabetic cardiomyopathy: An observational retrospective echocardiographic study in 656 asymptomatic type 2 diabetic patients.” In: *International Journal of Endocrinology* 2015 (2015), p. 743503.

[198] G M Pieper and W J Murray. “In vivo and in vitro intervention with L-carnitine prevents abnormal energy metabolism in isolated diabetic rat heart: chemical and phosphorus-31 NMR evidence.” In: *Biochemical Medicine and Metabolic Biology* 38.1 (1987), pp. 111–20.

[199] G M Pieper et al. “Salient effects of L-carnitine on adenine-nucleotide loss and coenzyme A acylation in the diabetic heart perfused with excess palmitic acid. A phosphorus-31 NMR and chemical extract study.” In: *Biochimica et Biophysica Acta* 803.4 (1984), pp. 241–9.

[200] Donald B Plewes and Walter Kucharczyk. “Review: MR physics for clinicians physics of MRI: A primer”. In: *Journal of Magnetic Resonance Imaging* 35.5 (2012).

[201] Serricchio M Pola P, Savi L, Grilli M, Flore R. “Carnitine in the therapy of dyslipidemic patients”. In: *Curr Ther Res* 27 (1980), pp. 208–16.

[202] M. Pooyandjoo et al. “The effect of (L-)carnitine on weight loss in adults: a systematic review and meta-analysis of randomized controlled trials”. In: *Obesity Reviews* 17.10 (2016), pp. 970–976.

[203] P. Pregant et al. “Vermindertes Plasmacarnitin bei Typ-I Diabetes mellitus”. In: *Klinische Wochenschrift* 69.12 (1991), pp. 511–516.

[204] M. Prentki, K. Tornheim, and B. E. Corkey. “Signal transduction mechanisms in nutrient-induced insulin secretion”. In: *Diabetologia* 40.0 (1997), S32–S41.

[205] Thomas Pulinilkunnil et al. “Evidence for rapid "metabolic switching" through lipoprotein lipase occupation of endothelial-binding sites”. In: *Journal of Molecular and Cellular Cardiology* 35 (2003), pp. 1093–1103.

[206] N Rakieten, M L Rakieten, and M V Nadkarni. “Studies on the diabetogenic action of streptozotocin (NSC-37917).” In: *Cancer Chemotherapy Reports* 29 (1963), pp. 91–8.

[207] P. J. Randle et al. “The glucose fatty-acid cycle its role in insulin sensitivity and the metabolic disturbances of diabetes mellitus”. In: *The Lancet* 281.7285 (1963), pp. 785–789.

[208] Gerald M Reaven et al. “Measurement of plasma glucose, free fatty acid, lactate, and insulin for 24 h in patients with NIDDM”. In: *Diabetes* 37.8 (1988), pp. 1020–1024.

[209] CJ Rebouche. *Modern nutrition in health and disease*. Ed. by Philadelphia: Lippincott. Lippincott Williams and Wilkins, 2006, pp. 537–544.

[210] Maria Sara Remedi et al. “Acute sulfonylurea therapy at disease onset can cause permanent remission of KATP-induced diabetes.” In: *Diabetes* 60.10 (2011), pp. 2515–22.

[211] Oliver J Rider and Damian J Tyler. “Clinical implications of dardiac hyperpolarized magnetic resonance imaging”. In: *Journal of Cardiovascular Magnetic Resonance* 15.1 (2013), p. 93.

[212] Brian Rodrigues and John H Mcneill. “Lack of effect of oral L-carnitin treatment on lipid metabolism and cardiac function in chronically diabetic rats in Chronically Diabetic Rats”. In: Opie 1970 (1989).

[213] Brian Rodrigues, Hong Xiang, and John H Mcneill. “Effect of L-carnitine treatment on lipid metabolism and cardiac performance in chronically diabetic rats”. In: *Diabetes* 37.October (1988), pp. 1358–1364.

[214] Maria Rohm et al. “Cardiac dysfunction and metabolic inflexibility in a mouse model of diabetes without dyslipidemia.” In: *Diabetes* 67.6 (2018), pp. 1057–1067.

[215] Thomas J. Rosol et al. *Endocrine system*. Elsevier, 2013, pp. 2391–2492.

[216] Jeffery Ross and Jack K. Goldman. “Effect of Streptozotocin-induced diabetes on kidney weight and compensatory hypertrophy in the rat”. In: *Endocrinology* 88.4 (1971), pp. 1079–1082.

[217] Ruth Cordiner. “Drug notes”. In: *Practical Diabetes* 33.9 (2016), pp. 330–331.

[218] J Sakamoto et al. “Contribution of malonyl-CoA decarboxylase to the high fatty acid oxidation rates seen in the diabetic heart.” In: *American Journal of Physiology. Heart and Circulatory Physiology* 278.4 (2000), H1196–204.

[219] Jorgen E. Schneider et al. “In vivo cardiac 1H-MRS in the mouse”. In: *Magnetic Resonance in Medicine* 52.5 (2004), pp. 1029–1035.

[220] Oliver Schnell et al. “Type 1 diabetes and cardiovascular disease”. In: *Cardiovascular Diabetology* 12.1 (2013), p. 156.

[221] B O Schönekess, M F Allard, and G D Lopaschuk. “Propionyl L-carnitine improvement of hypertrophied heart function is accompanied by an increase in carbohydrate oxidation.” In: *Circulation Research* 77.4 (1995), pp. 726–34.

[222] Marie A Schroeder et al. “Hyperpolarized magnetic resonance: a novel technique for the in vivo assessment of cardiovascular disease.” In: *Circulation* 124.14 (2011), pp. 1580–94.

[223] Marie A Schroeder et al. “In vivo assessment of pyruvate dehydrogenase flux in the heart using hyperpolarized carbon-13 magnetic resonance”. In: *Proc Natl Acad Sci USA* 105.33 (2008), pp. 12051–12056.

[224] Marie a. Schroeder et al. “The cycling of acetyl-coenzyme A through acetylcarnitine buffers cardiac substrate supply: A hyperpolarized 13C magnetic resonance study”. In: *Circulation: Cardiovascular Imaging* 5 (2012), pp. 201–209.

[225] Adam E. Schussheim and Howard L. Kantor. “Cardiac nuclear magnetic resonance spectroscopy”. In: *Coronary Artery Disease* 4.4 (1993), pp. 361–370.

[226] Aaron M Secrest et al. “Chapter 35: Mortality in Type 1 Diabetes”. In: *Diabetes in America* (2014), pp. 1–16.

[227] Robert A Sesti, Casilde; Simkhovich, Boris Z.;Kalvinsh, Ivars; Kloner. “Mildronate, a novel fatty acid oxidation inhibitor and antiaanginal agen, reduces myocardial infarct size without affecting hemodynamics.” In: *Journal of Cardiovascular Pharmacology* 47.3 (2006), pp. 493–499.

[228] Anne-Marie L Seymour et al. “In vivo assessment of cardiac metabolism and function in the abdominal aortic banding model of compensated cardiac hypertrophy”. In: *Cardiovascular Research* 106.2 (2015), pp. 249–260.

[229] B Shahouzehi et al. “Effect of L-carnitine administration on serum insulin and adiponectin levels, and AMPK, APPL1 and PPAR-gamma gene expression in STZ-induced diabetic rat liver”. In: *Biochem. J* 89.6 (2017).

[230] K Sharma and F N Ziyadeh. “Renal hypertrophy is associated with upregulation of TGF-beta 1 gene expression in diabetic BB rat and NOD mouse.” In: *The American Journal of Physiology* 267.6 Pt 2 (1994), F1094–01.

[231] A. S.P. Sharp et al. “Tissue Doppler E/E’ ratio is a powerful predictor of primary cardiac events in a hypertensive population: an ASCOT substudy”. In: *European Heart Journal* 31.6 (2010), pp. 747–752.

[232] A D Sherry, R L Nunnally, and R M Peshock. “Metabolic studies of pyruvate- and lactate-perfused guinea pig hearts by 13C NMR. Determination of substrate preference by glutamate isotopomer distribution.” In: *The Journal of Biological Chemistry* 260.16 (1985), pp. 9272–9.

[233] Tetsuya Shiomi et al. “Streptozotocin-induced hyperglycemia exacerbates left ventricular remodeling and failure after experimental myocardial infarction”. In: *Journal of the American College of Cardiology* 42.1 (2003), pp. 165–172.

[234] G. N. Shivu et al. “Relationship Between Coronary Microvascular Dysfunction and Cardiac Energetics Impairment in Type 1 Diabetes Mellitus”. In: *Circulation* 121.10 (2010), pp. 1209–1215.

[235] A Shug et al. “Protective Effects of Propionyl-L-Carnitine During Ischemia and Reperfusion”. In: *Cardiovascular Drugs Therapy* 5.1 (), pp. 77–83.

[236] A K Shukla and Utham Kumar. “Positron emission tomography: An overview.” In: *Journal of Medical Physics* 31.1 (2006), pp. 13–21.

[237] Labros S Sidossis et al. “Glucose plus insulin regulate fat oxidation by controlling the rate of fatty acid entry into the mitochondria”. In: *Journal of Clinical Investigation* 98.10 (1996), pp. 2244–2250.

[238] B Singh et al. “Determination of malonyl-coenzyme A in rat heart, kidney, and liver: a comparison between acetyl-coenzyme A and butyryl-coenzyme A as fatty acid synthase primers in the assay procedure.” In: *Analytical Biochemistry* 138.1 (1984), pp. 107–11.

[239] R B Singh and M Aslam. “L-carnitine administration in coronary artery disease and cardiomyopathy.” In: *The Journal of the Association of Physicians of India* 46.9 (1998), pp. 801–5.

[240] R B Singh et al. “A randomised, double-blind, placebo-controlled trial of L-carnitine in suspected acute myocardial infarction Moradabad-lO (UP) 244001 India”. In: *Postgraduate Medical Journal* 72.843 (1996), pp. 45–50.

[241] Nikolajs Sjakste, Aleksandrs Gutcaits, and Ivars Kalvinsh. “Mildronate: An antiischemic drug for neurological indications”. In: *CNS Drug Reviews* 11.2 (2006), pp. 151–168.

[242] Rebecca Smith-Bindman et al. “Radiation dose associated with common computed tomography examinations and the associated lifetime attributable risk of cancer.” In: *Archives of Internal Medicine* 169.22 (2009), pp. 2078–86.

[243] S S Soedamah-Muthu J H Fuller H E Mulnier V S Raleigh R A Lawrenson H M Colhoun. "All-cause mortality rates in patients with type 1 diabetes mellitus compared with a non-diabetic population from the UK general practice research database". In: *Diabetologia* 49 (2006), pp. 660–666.

[244] Sabita S Soedamah-Muthu et al. "High risk of cardiovascular disease in patients with type 1 diabetes in the U.K.: a cohort study using the general practice research database." In: *Diabetes care* 29.4 (2006), pp. 798–804.

[245] J. Sokolovska et al. "The influence of mildronate on peripheral neuropathy and some characteristics of glucose and lipid metabolism in rats with the streptozotocin model of diabetes mellitus". In: *Biochemistry (Moscow) Supplement Series B: Biomedical Chemistry* 6.2 (2012), pp. 177–184.

[246] Jelizaveta Sokolovska et al. "Correction of glycaemia and GLUT1 level by mildronate in rat streptozotocin diabetes mellitus model". In: *Cell Biochemistry and Function* 29.1 (2011), pp. 55–63.

[247] J Stamler et al. "Diabetes, other risk factors, and 12-yr cardiovascular mortality for men screened in the Multiple Risk Factor Intervention Trial." In: *Diabetes Care* 16.2 (1993), pp. 434–44.

[248] William C Stanley and Mario Marzilli. "Metabolic therapy in the treatment of ischaemic heart disease: the pharmacology of trimetazidine." In: *Fundamental and Clinical Pharmacology* 17.2 (2003), pp. 133–45.

[249] Francis B. Stephens et al. "Insulin stimulates L-carnitine accumulation in human skeletal muscle". In: *The FASEB Journal* 20.2 (2006), pp. 377–379.

[250] Michael Benjamin Stokes and Ross Roberts-Thomson. "The role of cardiac imaging in clinical practice." In: *Australian Prescriber* 40.4 (2017), pp. 151–155.

[251] Karin Strijbis, Frédéric M. Vaz, and Ben Distel. "Enzymology of the carnitine biosynthesis pathway". In: *IUBMB Life* 62.5 (2010), NA–NA.

[252] Satoru Sugiyama et al. "Reversal of ischemia-induced mitochondrial dysfunction after coronary reperfusion". In: *The American Journal of Cardiology* 49.4 (1982), p. 1014.

[253] Heinrich Taegtmeyer, Patrick McNulty, and Martin E Young. "Adaptation and maladaptation of the heart in diabetes: Part I: general concepts." In: *Circulation* 105.14 (2002), pp. 1727–33.

[254] Heinrich Taegtmeyer et al. "Assessing cardiac metabolism: A scientific statement from the american heart association." In: *Circulation Research* 118.10 (2016), pp. 1659–701.

[255] A G Tahiliani, G D Lopaschuk, and J H McNeill. "Effect of insulin treatment on long-term diabetes-induced alteration of myocardial function." In: *General Pharmacology* 15.6 (1984), pp. 545–7.

[256] N Tamamoğullari et al. "Carnitine deficiency in diabetes mellitus complications." In: *Journal of Diabetes and its Complications* 13.5-6 (1999), pp. 251–3.

[257] Ten Hove Michiel and Neubauer Stefan. "MR spectroscopy in heart failure—clinical and experimental findings". In: *Heart Failure Reviews* 12.1 (2007), pp. 48–57.

[258] Ryuya Terada et al. “Effects of propionyl-l-carnitine on cardiac dysfunction in streptozotocin-diabetic rats”. In: *European Journal of Pharmacology* 357.2-3 (1998), pp. 185–191.

[259] Damian J Tyler et al. “CINE-MR imaging of the normal and infarcted rat heart using an 11.7 T vertical bore MR system”. In: *Journal of Cardiovascular Magnetic Resonance* 8 (2006), pp. 327–333.

[260] K Ugurbil et al. “High resolution proton NMR studies of perfused rat hearts.” In: *FEBS letters* 167.1 (1984), pp. 73–8.

[261] John R. Ussher et al. “Stimulation of glucose oxidation protects against acute myocardial infarction and reperfusion injury”. In: *Cardiovascular Research* 94.2 (2012), pp. 359–369.

[262] Carmem P. Valgas da Silva et al. “L-carnitine supplementation impairs endothelium-dependent relaxation in mesenteric arteries from rats”. In: *Archives of Physiology and Biochemistry* 120.3 (2014), pp. 112–118.

[263] Vanhamme, van den Boogaart A, and Van Huffel S. “Improved method for accurate and efficient quantification of MRS data with use of prior knowledge”. In: *Journal of Magnetic Resonance* 129.1 (1997), pp. 35–43.

[264] Thomas C Vary and James R Neely. “A mechanism for reduced myocardial carnitine levels in diabetic animals”. In: *Am J Physiol* 12.2 (1982), pp. 5–158.

[265] Frédéric M Vaz and Ronald J A Wanders. “Carnitine biosynthesis in mammals.” In: *The Biochemical Journal* 361 (2002), pp. 417–429.

[266] Myrian Velasco et al. “Modulation of ionic channels and insulin secretion by drugs and hormones in pancreatic beta cells.” In: *Molecular Pharmacology* 90.3 (2016), pp. 341–57.

[267] Reinis Vilskersts et al. “Administration of L-carnitine and mildronate improves endothelial function and decreases mortality in hypertensive Dahl rats”. In: *Pharmacological Reports* 63.3 (2011), pp. 752–762.

[268] Reinis Vilskersts et al. “Methyl-γ-butyrobetaine decreases levels of acylcarnitines and attenuates the development of atherosclerosis”. In: *Vascular Pharmacology* 72 (2015), pp. 101–107.

[269] Reinis Vilskersts et al. “Mildronate, a regulator of energy metabolism, reduces atherosclerosis in apoE/LDLR-/- mice.” In: *Pharmacology* 83.5 (2009), pp. 287–93.

[270] Reinis Vilskersts et al. “Myocardial infarct size-limiting and anti-arrhythmic effects of mildronate orotate in the rat heart”. In: *Cardiovascular Drugs and Therapy* 23.4 (2009), pp. 281–288.

[271] Jerzy Walecki et al. “Usefulness of 1H MR spectroscopy in the evaluation of myocardial metabolism in patients with dilated idiopathic cardiomyopathy: pilot study.” In: *Academic Radiology* 10.10 (2003), pp. 1187–92.

[272] Benjamin T. Wall et al. “Chronic oral ingestion of L-carnitine and carbohydrate increases muscle carnitine content and alters muscle fuel metabolism during exercise in humans”. In: *The Journal of Physiology* 589.4 (2011), pp. 963–973.

[273] Yan-Jiang Wang et al. “Causes of death in STZ-induced rat models of diabetes mellitus.” In: *Journal of Sichuan University. Medical Science Edition* 45.4 (2014), pp. 691–5.

[274] Michael Wei et al. “The streptozotocin-diabetic rat as a model of the chronic complications of human diabetes”. In: *Heart, Lung and Circulation* 12.1 (2003), pp. 44–50.

[275] Caroline Weytjens et al. “Doppler myocardial imaging in the diagnosis of early systolic left ventricular dysfunction in diabetic rats”. In: ().

[276] Jens E Wilhjelm et al. *Medical diagnostic ultrasound-physical principles and imaging*. Tech. rep. 2013.

[277] Susan C. Winter et al. “Relative carnitine insufficiency in children with type I diabetes mellitus”. In: *Archives of Pediatrics and Adolescent Medicine* 143.11 (1989), p. 1337.

[278] Benjamin Wittels and Rubin Bressler. “Biochemical lesion of diphtheria toxin in the heart”. In: *Journal of Clinical Investigation* 43.4 (1964).

[279] World Health Organization. *Global report on diabetes*. Tech. rep. 2016, pp. 92–4.

[280] Yang Xiao et al. “TAX1BP1 overexpression attenuates cardiac dysfunction and remodeling in STZ-induced diabetic cardiomyopathy in mice by regulating autophagy”. In: *BBA - Molecular Basis of Disease* 1864 (2018), pp. 1728–1743.

[281] Zhonglin Xie et al. “Improvement of cardiac functions by chronic metformin treatment is associated with enhanced cardiac autophagy in diabetic OVE26 mice.” In: *Diabetes* 60.6 (2011), pp. 1770–8.

[282] Mei Xue et al. “L-carnitine attenuates cardiac dysfunction by ischemic insults through akt signaling pathway”. In: *Toxicological Sciences* 160.2 (2017), pp. 341–350.

[283] Hua Yang and James R. Wright. “Human β cells are exceedingly resistant to Streptozotocin in vivo”. In: *Endocrinology* 143.7 (2002), pp. 2491–2495.

[284] N L Young, D R Lopez, and D J McNamara. “Contributions of absorbed dietary cholesterol and cholesterol synthesized in small intestine to hypercholesterolemia in diabetic rats.” In: *Diabetes* 37.8 (1988), pp. 1151–6.

[285] Jun-jie Zhang et al. “L-carnitine ameliorated fasting-induced fatigue, hunger, and metabolic abnormalities in patients with metabolic syndrome: a randomized controlled study.” In: *Nutrition Journal* 13 (2014), p. 110.

[286] Liyan Zhang et al. “Cardiac diacylglycerol accumulation in high fat-fed mice is associated with impaired insulin-stimulated glucose oxidation”. In: *Cardiovascular Research* 89.1 (2011), pp. 148–156.